

THESIS

**HYDRAULIC ANALYSIS AND DOUBLE MASS CURVES
OF THE MIDDLE RIO GRANDE FROM COCHITI TO SAN MARCIAL,
NEW MEXICO**

Submitted by

Jason M. Albert

Department of Civil Engineering

In partial fulfillment of the requirements

For the Degree of Master of Science

Colorado State University

Fort Collins, Colorado

Fall 2004

COLORADO STATE UNIVERSITY

August 30, 2004

WE HEREBY RECOMMEND THAT THE THESIS PREPARED UNDER OUR SUPERVISION BY **JASON M. ALBERT** ENTITLED **HYDRAULIC ANALYSIS AND DOUBLE MASS CURVES OF THE MIDDLE RIO GRANDE FROM COCHITI TO SAN MARCIAL, NEW MEXICO** BE ACCEPTED AS FULFILLING IN PART REQUIREMENTS FOR THE DEGREE OF MASTER OF SCIENCE.

Committee on Graduate Work

Adviser

Department Head

ABSTRACT OF THESIS

HYDRAULIC ANALYSIS AND DOUBLE MASS CURVES OF THE MIDDLE RIO GRANDE FROM COCHITI TO SAN MARCIAL, NEW MEXICO

The Middle Rio Grande located in Central New Mexico is one of the most historically documented rivers in the United States. Since the early 20th century regulatory agencies have been interested and concerned with its management.

A Hydraulic Modeling Analysis (HMA) of the Corrales reach, located 34 miles downstream of Cochiti Dam, was conducted. An extensive collection of data was used to determine the temporal and spatial changes in the channel. General trends for the Corrales Reach include a decrease in width, width to depth ratio, energy grade line slope and wetted perimeter, and an increase in mean velocity and depth during the 1962-2001 time period. The reach degraded as much as 3 feet in some areas during this same time period while the sinuosity remained the same. Since 1918 the width of the reach decreased from 1275 feet to 474 ft in 2001. Bed material coarsened from Cochiti Dam to just upstream of Albuquerque and the bed is expected to armor in the near future due to the lack of incoming sediment.

A Double Mass Analysis (DMA) was also conducted on the Albuquerque Reach of the Middle Rio Grande. Data from four gaging stations (Albuquerque, Bernardo, San Acacia and San Marcial) were used to create the curves. The Albuquerque gage shows the greatest effects of Cochiti dam with a large decrease in sediment transport after 1973, the other three gages have slight decreases, 0 to 10%, in sediment load after

1973. However, the construction of Cochiti dam has not affected the suspended sediment transport, which remained constant at 2.8 M tons/year. Also, from the analysis it was estimated that the bed would degrade as much as 4 feet downstream from Cochiti Dam to San Marcial. The sediment due to degradation is estimated to contribute 65% of the transported sediment at the Albuquerque and Bernardo gages. At the San Acacia and San Marcial gages the majority of the transported sediment passing the gage is supplied by the Rio Puerco with the degradation of the bed contributing less than 8% of the sediment downstream of the Rio Puerco.

Jason Mark Albert
Civil Engineering Department
Colorado State University
Fort Collins, CO 80523
Fall 2004

ACKNOWLEDGEMENTS

First and Foremost I would like to thank my lord and savior Jesus Christ for the ability to conduct this research and write this thesis. I would also like to thank my Adviser Dr. Pierre Julien for his superb guidance I received from him through out my time here at CSU. Thanks to the U.S. Bureau of Reclamation for the opportunity to work on the Rio Grande. I would also like to thank my other committee members Dr. Brian Bledsoe of the Civil Engineering Department and Dr. Sara Rathburn of the Geosciences Department.

Thanks to all that have come before me on this project the amount of information you all provided helped immensely. The rest of the team needs to be thanked too, thank you Un, Max, Forrest, Mike, Susan, D.K. and Mark. Special thanks is needed for the Lil' Fella and Velleux. Lil' Fella thanks for everything; I thoroughly enjoyed your company at the bars and work, you are the nicest guy I have ever met. Velleux without you I wouldn't have done as well as I did, thank you for your suggestions, insight and friendship.

I would also like to thank other friends that have shown their support though out this long strange journey including Amy, John, Mark, Peaches I mean Kristoph, Ben, Billy, and Matt. Mark, you have been awesome not only for providing me with a roof over my head but also for being a great friend. Billy thanks for providing me with a friend to talk to when things got rough and one hell of week in the AK.

Finally I would like to thank my family especially my parents without you I wouldn't exist, thanks for everything including the money and loving support, I love you. I suppose I should also thank my siblings, Brian and Anthony, for my competitive nature.

In closing I would like to thank everyone who helped, thanks for keepin' it real.

TABLE OF CONTENTS

ABSTRACT OF THESIS	iii
ACKNOWLEDGEMENTS	v
TABLE OF CONTENTS	vi
LIST OF FIGURES.....	viii
LIST OF TABLES.....	xi
LIST OF SYMBOLS	xii
LIST OF ACRONYMNS	xiv
CHAPTER 1: INTRODUCTION.....	1
CHAPTER 2: LITERATURE REVIEW.....	5
2.1. Introduction.....	5
2.2. Hydraulic Modeling Analysis (HMA)	7
2.2.1. Site Background	7
2.2.2. Previous Studies of the Middle Rio Grande	9
2.2.3. Hydrology and Climate	12
2.3. Total Load Procedures	14
2.3.1. Background.....	14
2.3.2. The Modified Einstein Procedure.....	15
2.3.3. Modified Einstein Equations	16
2.3.4. Computer Programs that perform MEP analysis	24
2.4. Mass and Double Mass Curves.....	25
2.5. Summary	27
CHAPTER 3: HYDRAULIC MODELING ANALYSIS (HMA)	28
3.1. Introduction.....	28
3.2. Reach Background	29
3.2.1. Reach Definition	29
3.2.2. Subreach Definition	30
3.2.3. Available Data.....	31
3.2.4. Channel Forming Discharge (CFD)	32
3.3. Geomorphic Characterization.....	34
3.3.1. Channel Classification	34
3.3.2. Sinuosity	39
3.3.3. Longitudinal Profile	40
3.3.4. Channel Cross Sections	42
3.3.5. Channel Geometry.....	43
3.3.6. Width.....	45
3.3.7. Bed Material.....	45
3.4. Suspended Sediment and Water History.....	50
3.4.1. Single Mass Curves.....	50
3.4.2. Double Mass Curve	52
3.5. Sediment Transport Analysis.....	53
3.6. Discussion of Uncertainties	58
3.7. Summary	59
CHAPTER 4: Analysis of Mass and Double Mass Curves.....	62
4.1 Introduction.....	62
4.2 Reach Background	62
4.1.1. Reach Definition	62
4.2.1. Data for Analyses	63

4.2.	Data Analyses and Results.....	64
4.2.1.	Suspended Sediment Mass Curves	64
4.2.2.	Sediment Rating Curves for Periods Between Breaks in Slope	65
4.2.3.	Mass and Double Mass Curves.....	66
4.3.	Summary of Double Mass Curves	80
4.4.	Discussion	88
4.5.	Discussion of Uncertainties	91
CHAPTER 5: SUMMARY AND CONCLUSIONS.....		93
5.1.	Introduction	93
5.2.	Hydraulic Modeling Analysis (HMA)	93
5.3.	Double Mass Analysis (DMA).....	94
5.4.	Summary	96
REFERENCES.....		97
APPENDIX A: Location Maps and Aerial Photograph Data		103
APPENDIX B: Cross Section Survey Dates		110
APPENDIX C: Cross Sections		112
APPENDIX D: Annual Peak Mean Discharges		122
APPENDIX E: HEC-RAS Modeling Results		124
APPENDIX F: Bed Material Histograms and Statistics		126
APPENDIX G: MEP Input Data and Results		137
APPENDIX H: Mass and Double Mass Curves.....		149
APPENDIX I: BORAMEP Data.....		158
APPENDIX J: Total and Sand Load Rating Curves		181

LIST OF FIGURES

Figure 2-1 Map of New Mexico with gaging stations and Corrales Reach locations identified.....	6
Figure 2-2 Annual Suspended Sediment Yield in the Rio Grande at Otowi Gage (upstream of Cochiti Dam), Cochiti Gage (just downstream of Cochiti dam) and Albuquerque Gage (downstream of Cochiti Gage) from 1974 to 2000. Cochiti gage record ends in 1988.....	9
Figure 2-3 1995 Rio Grande spring runoff hydrograph	13
Figure 2-4 Correction for x in the logarithmic friction formula in terms of k_s/δ (Holmquist-Johnson 2004).....	18
Figure 2-5 Cumulative discharge vs. cumulative suspended sediment load at Rio Grande at Bernalillo and Rio Grande at Albuquerque (1956 – 1999 (Sixta et al. 2003a).....	26
Figure 3-1 River planform of the Corrales Reach indicating locations of CO-lines and subreaches, 1992.....	30
Figure 3-2 Annual peak daily-mean discharge at Rio Grande at Albuquerque (1943 – 2001).	33
Figure 3-3 Maximum mean daily annual discharge histograms on the Rio Grande at Albuquerque.....	34
Figure 3-4 Non-vegetated active channel of the Corrales Reach. 1918 planform from topographic survey. 1935, 1962, 1992 and 2001 planform from aerial photos.	36
Figure 3-5: Time series of sinuosity of the Corrales Reach as measured from the digitized aerial photos.....	39
Figure 3-6 Mean bed elevation profile of entire Corrales Reach. Distance downstream is measured from agg/deg 351.	41
Figure 3-7 Cross section CO-33 representing pre and post-dam conditions.	42
Figure 3-8 Reach-averaged main channel geometry from HEC-RAS® results for $Q = 5,000$ cfs. (a) mean velocity, (b) cross-section area, (c) average depth, (d) width-to-depth ratio, (e) wetted perimeter.	44
Figure 3-9 Reach averaged active channel width from digitized aerial photos (GIS).....	45
Figure 3-10 Histogram depicting the d_{50} and d_{84} change with time for CO-33.	47
Figure 3-11 Comparison of 1992 and 2001 bed material gradation curves for subreach 1.	48
Figure 3-12 Comparison of 1992 and 2001 bed material gradation curves for subreach 2.	48
Figure 3-13 Comparison of 1992 and 2001 bed material gradation curves for subreach 3.	49
Figure 3-14 2001 Bed-material samples used in the sediment transport and equilibrium	49
Figure 3-15 Discharge mass curve at Bernalillo and Albuquerque Gages (1942-2000). 51	
Figure 3-16 Suspended sediment mass curve at Bernalillo and Albuquerque Gages (1956-1999).....	52
Figure 3-17 Cumulative discharge vs. cumulative suspended sediment load at Rio Grande at Bernalillo and Rio Grande at Albuquerque (1956 - 1999).	53
Figure 3-18 Albuquerque Gage sand load rating curve for spring and summer.	56
Figure 4-1 Suspended sediment mass curve for San Marcial Gage.....	65
Figure 4-2 Total and Sand Load Rating curve from San Marcial Gage, 1982-1992	66
Figure 4-3 Mass Curves for Bernardo and Albuquerque Gages.....	67
Figure 4-4 Double mass curves for Bernalillo and Albuquerque gages.....	69
Figure 4-5 Mass Curves for the Bernardo Gage	70

Figure 4-6 Double mass curves for the Bernardo gage	72
Figure 4-7 Mass Curves for the San Acacia Gage.....	74
Figure 4-8 Double mass curves for the San Acacia gage	75
Figure 4-9 Mass Curves for the San Marcial Gage.....	77
Figure 4-10 Double mass curves for the San Marcial gage	79
Figure 4-11 Pre-dam loads and their relative locations on the Rio Grande.	84
Figure 4-12 Post-dam loads and there relative locations on the Rio Grande.....	84
Figure 4-13 Suspended mass curve for Bernalillo and Albuquerque gages, with pre and post-dam slopes.	89
Figure 4-14 Suspended mass curves of all gages examined.....	89
Figure A-1Corrales Reach subreach definitions.	106
Figure A-2 photo of subreach 1.....	107
Figure A-3Aerial photo of subreach 2.	108
Figure A-4 Aerial photo of subreach 3.	109
Figure C-1 Cross Section CO-33 representing pre-dam conditions.....	113
Figure C-2 Cross Section CO-33 representing post-dam conditions.	114
Figure C-3 Cross Section CO-33 representing pre and post-dam conditions.	115
Figure C-4 Cross Section CO-34 representing pre-dam conditions.....	116
Figure C-5 Cross Section CO-34 representing post-dam conditions.	117
Figure C-6 Cross Section CO-34 representing pre and post-dam conditions.	118
Figure C-7 Cross Section CO-35 representing pre and post-dam conditions.	119
Figure C-8 Cross Section CO-35 representing post-dam conditions.	120
Figure C-9 Cross Section CO-35 representing pre and post-dam conditions.	121
Figure D-1 Annual peak discharge in cfs at Bernalillo (1941-1969).	123
Figure E-1 Active channel widths from HEC-RAS modeling.....	125
Figure F-1 Histograms depicting the D_{50} and D_{84} change with time for CO-34 and CO-35 (Corrales Reach).	127
Figure F-2 Histograms depicting the D_{50} and D_{84} change with time for CA-1 and CA-2 (Corrales Reach).	128
Figure F-3 Histograms depicting the D_{50} and D_{84} change with time for CA-4 and CA-6 (Corrales Reach).	129
Figure F-4 Histograms depicting the D_{50} and D_{84} change with time for CA-8 and CA-10 (Corrales Reach).	130
Figure F-5 Histograms depicting the D_{50} and D_{84} change with time for CA-12 and CA-13 (Corrales Reach).	131
Figure F-6 1992 sediment size distribution curves for subreaches 1 and 2.....	132
Figure F-71992 sediment size distribution curves for subreach 3.....	133
Figure F-8 2001 sediment size distribution curves for subreaches 1 and 2.....	134
Figure F-9 2001 sediment size distribution curves for subreach 3.....	135
Figure H-1 Discharge mass curve for Bernardo and Albuquerque gages 1942-2000. .	150
Figure H-2 Suspended Sediment mass curve Bernardo and Albuquerque gages 1942- 1999.	150
Figure H-3 Double mass curve for Bernardo and Albuquerque gages 1942-1999.	151
Figure H-4 Discharge mass curve for Bernardo gage 1953-1997.....	152
Figure H-5 Suspended Sediment mass curve for Bernardo gage 1965-1995.	152
Figure H-6 Double mass curve for Bernardo gage 1965-1996.	153
Figure H-7 Discharge mass curve for San Acacia gage 1946-2000.	154
Figure H-8 Suspended Sediment mass curve for San Acacia gage 1959-1996.	154
Figure H-9 Double mass curve for San Acacia gage 1959-1996.....	155
Figure H-10 Discharge mass curve for San Marcial gage 1925-1997.	156
Figure H-11 Suspended Sediment mass curve for San Marcial Gage 1925-1997.	156

Figure H-12 Double mass curve for San Marcial 1925-1997.....	157
Figure H-13 Suspended Sediment mass curve for Rio Puerco.....	157
Figure J-1 Total load rating curves for the Albuquerque Gage 1968-1973.....	182
Figure J-2 Total load rating curves for the Albuquerque Gage 1973-1985.....	183
Figure J-3 Total load rating curves for the Albuquerque Gage 1985-1995.....	184
Figure J-4 Total load rating curves for the Albuquerque Gage 1995-2001.....	185
Figure J-5 Sand load rating curves for the Albuquerque Gage 1968-1973.....	186
Figure J-6 Sand load rating curves for the Albuquerque Gage 1973-1985.....	187
Figure J-7 Sand load rating curves for the Albuquerque Gage 1985-1995.....	188
Figure J-8 Sand load rating curves for the Albuquerque Gage 1995-2001.....	189
Figure J-9 Total load rating curves for the Bernardo Gage 1968-1973.....	190
Figure J-10 Total load rating curves for the Bernardo Gage 1973-1991.....	191
Figure J-11 Total load rating curves for the Bernardo Gage 1991-2001.....	192
Figure J-12 Sand load rating curves for the Bernardo Gage 1968-1973.....	193
Figure J-13 Sand load rating curves for the Bernardo Gage 1973-1991.....	194
Figure J-14 Sand load rating curves for the Bernardo Gage 1991-2001.....	195
Figure J-15 Total load rating curves for the San Acacia Gage 1969-1979.....	196
Figure J-16 Total load rating curves for the San Acacia Gage 1979-1997.....	197
Figure J-17 Total load rating curves for the San Acacia Gage 1997-2001.....	198
Figure J-18 Sand load rating curves for the San Acacia Gage 1969-1979.....	199
Figure J-19 Sand load rating curves for the San Acacia Gage 1979-1997.....	200
Figure J-20 Sand load rating curves for the San Acacia Gage 1997-2001.....	201
Figure J-21 Total load rating curves for the San Marcial Gage 1968-1982.....	202
Figure J-22 Total load rating curves for the San Marcial Gage 1982-1997.....	203
Figure J-23 Total load rating curves for the San Marcial Gage 1997-2001.....	204
Figure J-24 Sand load rating curves for the San Marcial Gage 1968-1982.....	205
Figure J-25 Sand load rating curves for the San Marcial Gage 1982-1997.....	206
Figure J-26 Sand load rating curves for the San Marcial Gage 1997-2001.....	207

LIST OF TABLES

Table 3-1 Periods of record for discharge and continuous suspended sediment data collection by the USGS.	31
Table 3-2 Periods of record for bed material particle size distribution data collected by the USGS.	32
Table 3-3 Surveyed dates for bed material particle size distribution data at CO-Lines and CA-Lines.....	32
Table 3-4 Channel pattern classification for 1962 and 1972.	37
Table 3-5 Channel pattern classification for 1992 and 2001.	38
Table 3-6 Percents of total load that behave as washload and bed material load at flows close to 5,000 cfs.	54
Table 3-7 Bed material transport capacity for the 1992 and 2001 slopes.	57
Table 3-8 Resulting slope predictions from sediment transport capacity equations for 2001.	58
Table 3-9: Summarized sediment transport results for 1992 and 2001.	61
Table 4-1 Periods of Record for discharge and continuous sediment data collected by the USGS.	63
Table 4-2 Mass curve slopes and r-squared values for trend lines for the Bernalillo and Albuquerque gages.	68
Table 4-3 Mass curve slopes and r-squared values for trend lines for the Bernardo gage.	71
Table 4-4 Mass curve slopes and r-squared values for trend lines for the San Acacia gage.	74
Table 4-5 Mass curve slopes and r-squared values for trend lines for the San Marcial gage.	78
Table A-1 Aerial Photograph Data (Source: Richard et al. 2001).	104
Table A-2 Aerial photograph dates and mean daily discharge on those days.	105
Table B-1 Surveyed dates for the CO and CA lines collected by the US Bureau of Reclamation.	111
Table E-1 Reach-Averaged HEC-RAS Results.....	125
Table F-1 Median grain size statistics from the bed material samples at Bernalillo gage, CO-lines, CA-lines and CR-lines.	136
Table G-1 MEP input data for Albuquerque gage.	138
Table G-2 MEP results for Albuquerque gage and bed material load estimations.....	147
Table I-1 BORMEP data for the Bernalillo and Albuquerque gages.	159
Table I-2 BORMEP data for the Bernardo gage.	166
Table I-3 BORMEP data for the San Acacia gage.	170
Table I-4 BORMEP data for the San Marcial gage.	176

LIST OF SYMBOLS

A – channel cross-sectional area
a – limit of integration
A' – fraction of flow depth not sampled
A'' – mathematical abbreviation
b – limit of integration
B* - constant equal to 0.143
Conc – suspended sediment concentration
d_i – geometric mean for each size class
d_n' – vertical distance not sampled
d_s' – vertical distance sampled
d_s – material grain size (particle diameter)
d₁₀ – effective size (particle diameter corresponding to 10% finer)
d₃₅ – effective size (particle diameter corresponding to 35% finer)
d₅₀ – effective size (particle diameter corresponding to 50% finer)
d₈₄ – effective size (particle diameter corresponding to 84% finer)
F – mathematical abbreviation
Fr – Froude number
g – acceleration due to gravity
H – hydraulic depth (= A/Tw)
h – flow depth
i_B – fraction of bed material in a given size range
i_s – fraction of suspended material in a given size range
I₁' – mathematical abbreviation that contains J₁' and A'
I₂' – mathematical abbreviation
J₁' – mathematical abbreviation that contains A'
J₁' – mathematical abbreviation that contains A''
J₂' – mathematical abbreviation that contains A'
k_s – effective roughness
L – channel length along centerline
n – Manning's roughness coefficient
P – sinuosity
P' – mathematical abbreviation
p – probability that a particle will be entrained in the flow
Q – flow discharge
Q_B – bed load for each size fraction
q_B – unit bed load for a given size fraction
Q_s – measured suspended load
Q'_s – suspended load
Q'_{s total} – total sampled suspended load
Q_{s total suspended} – total load due to suspended sediment
Q_{s total bed} – total load due to bed-load
Q_{s total} – total load
R – hydraulic radius
S – channel slope
S_f – friction slope
Tw – active channel top width
U* - shear velocity
V - flow velocity

V_{avg} – average stream velocity
 W – active channel width
 WP – wetted perimeter
 x – dimensionless parameter
 Z – theoretical exponent for vertical distribution of sediment
 δ - laminar sublayer thickness
 ν - kinematic viscosity
 ϕ_* - half of the intensity of the bed-load transport
 γ - specific weight of water
 γ_s – specific weight of sediment
 η_0 - constant equal to 0.5
 ρ - density of water
 ω - fall velocity
 ψ – shear intensity for all particle sizes

LIST OF ACRONYMNS

CA – Calabacillas survey lines
cfs – cubic-feet-per-second (ft³/s)
CO – Cochiti survey lines
CR – Corrales survey lines
DMA – Double Mass Analysis
GIS – Geographic Information Systems
HEC-RAS® – Hydraulic Engineering Center – River Analysis System
HMA – Hydraulic Modeling Analysis
LFCC – Low Flow Conveyance Channel
M – million
MBE – Mean Bed Elevation
MEP – Modified Einstein Procedure
NRCS – National Resources Conservation Service
RM – River Mile
USACE – United States Army Corps of Engineers
USBR – United States Bureau of Reclamation
USGS – United States Geological Survey
WSE – Water Surface Elevation

CHAPTER 1: INTRODUCTION

The Middle Rio Grande is located in central New Mexico and spans about 143 miles from White Rock Canyon to the San Marcial Constriction at the headwaters of the Elephant Butte Reservoir (Lagasse 1994). Historically, the Middle Rio Grande was characterized as an aggrading sand bed channel with extensive lateral bank movement. Because of the flood and safety hazards posed by channel movements, regulatory agencies such as the U.S. Bureau of Reclamation (USBR) and U.S. Army Corps of Engineers (USACE) initiated efforts to reduce these risks in the 1920's. Efforts included the construction of numerous diversion structures, levees and dams, and culminated with the construction of Cochiti Dam, which closed in November 1973. This dam caused significant geomorphologic changes downstream.

The main focus of this study is to analyze the impacts of the changes in the river due to the closure of the dam, with the goal of forecasting future river conditions. Forecasting how the river channel is expected to change will help with management issues by letting agencies know how to focus restoration efforts. Restoration efforts in this region are particularly important due to the specific habitat needs of local endangered species such as the silvery minnow and the southwestern willow flycatcher. In attaining the objective of forecasting the expected changes of the river, an approach was taken to focus research efforts on two main areas: 1) hydraulic modeling analysis (HMA); and 2) create mass and double mass curves using the Modified Einstein Procedure (MEP) analysis.

HMA was conducted on a subreach of the Middle Rio Grande known as the Corrales reach; this subreach spans 10.3 miles from the Corrales Flood Channel to the Montano Bridge. Mass and double mass analysis was performed on the entire Albuquerque reach which spans from Albuquerque to Elephant Butte reservoir near San Marcial.

Objectives of the HMA were to analyze historic data to estimate past and potential future conditions of the reach. To meet these objectives, numerous analyses were performed such as the identification of spatial and temporal trends in channel geometry by evaluation of cross section data. Also, planform classifications were performed through analyses of aerial photos and channel geometry data. Temporal trends in water and sediment discharge and concentration were analyzed using U.S. Geological Survey (USGS) gaging station data. In addition, temporal trends in bed material were identified through analyses of gradation curves and histograms. Finally, the equilibrium state of the river was evaluated through applications of hydraulic geometry methods, empirical width-time relationships and sediment transport analyses using a Modified Einstein Procedure (MEP).

MEP analysis was performed on the Albuquerque Reach of the Middle Rio Grande at four USGS gaging stations; Albuquerque, Bernardo, San Acacia, and San Marcial gages, using a program developed by the USBR, BORAMEP. After the MEP analysis was completed mass and double mass curves were developed using the data from each station. Daily values of the sand and total loads were estimated by creating rating curves of discharge versus the MEP values for sand and total loads. The total load is defined as all sediment sizes transported through a cross section regardless of their source, and sand load is defined as the portion of the total load with sediment sizes greater than 0.0625 mm. Once the daily loads were determined cumulative values for sand, total and suspended load were plotted versus time to create the mass curves.

Double mass curves were then created using cumulative values of load versus cumulative values of discharge.

Mass and double mass curves were created for all four USGS stations studied using the same methodology and computer programs. Objectives of this analysis were to identify and analyze historical sediment trends in the river via breaks in slope. By analyzing the plotted trends it is possible to determine how various changes affect the river, and then predict how the river will react in the future if similar changes occur. One major change that affected the Albuquerque Reach was the closure of Cochiti Dam in 1973. Decreases in sediment loads were expected because the dam traps nearly 99% of the incoming sediment. Because the Albuquerque Reach is a significant distance downstream from the dam, the effects of the dam would not be as significant at the downstream locations.

Another use of mass curves is to identify sources or sinks of sediment. By comparing the mass curve slopes of upstream and downstream gages the difference in sediment loads per year can be discerned. If this difference is significant then a large sediment source or sink may exist between the two gages. In the Albuquerque Reach a major sediment source located is the Rio Puerco located between the Bernardo and San Acacia gages.

This thesis has been developed in five chapters. An introduction is presented in Chapter 1. Chapter 2 is the literature review performed for the HMA, the MEP and for the double mass curve analysis. The literature review for the HMA includes an historical background, the climate of the area and previous studies performed on the Middle Rio Grande. The mass and double mass literature review was conducted to better understand the various applications and usefulness of this type of analysis. Since the mass and double mass analysis requires the use of the MEP, the MEP was also researched to understand how the total load is determined and what tools could be used

to determine the total load. Analyses performed and results obtained from the HMA are presented in Chapter 3. Chapter 4 is the MEP analysis and the development of mass and double mass curves and the methodology behind them. Chapter 5 contains a summary of the results and conclusions.

CHAPTER 2: LITERATURE REVIEW

2.1. Introduction

The headwaters of the Rio Grande is located in central southern Colorado, from there the river flows south through New Mexico (Figure 2-1) then southwest between Texas and Mexico until it reaches the Gulf of Mexico (Rittenhouse 1944). Located in central New Mexico the Middle Rio Grande is a 143-mile long reach, that spans from White Rock Canyon to Elephant Butte Reservoir (Lagasse 1994). The southern most reach of the Middle Rio Grande is the reach of interest for this study. This reach, known as the Albuquerque Reach, starts at the mouth of the Arroyo Tongue and spans to the Elephant Butte Reservoir near San Marcial, New Mexico (Crawford et al. 1993). Hydraulic modeling analyses were performed on a subreach of the Middle Rio Grande known as the Corrales reach. The Corrales reach begins at the Corrales Flood Channel and spans 10.3 miles to the Montano Bridge. The total load, mass and double mass analyses were performed on the entire Albuquerque Reach, from the Albuquerque gaging station to the San Marcial gaging station. To aid the development of these analyses a literature review was performed. Figure 2-1 contains a location map of the study reach.

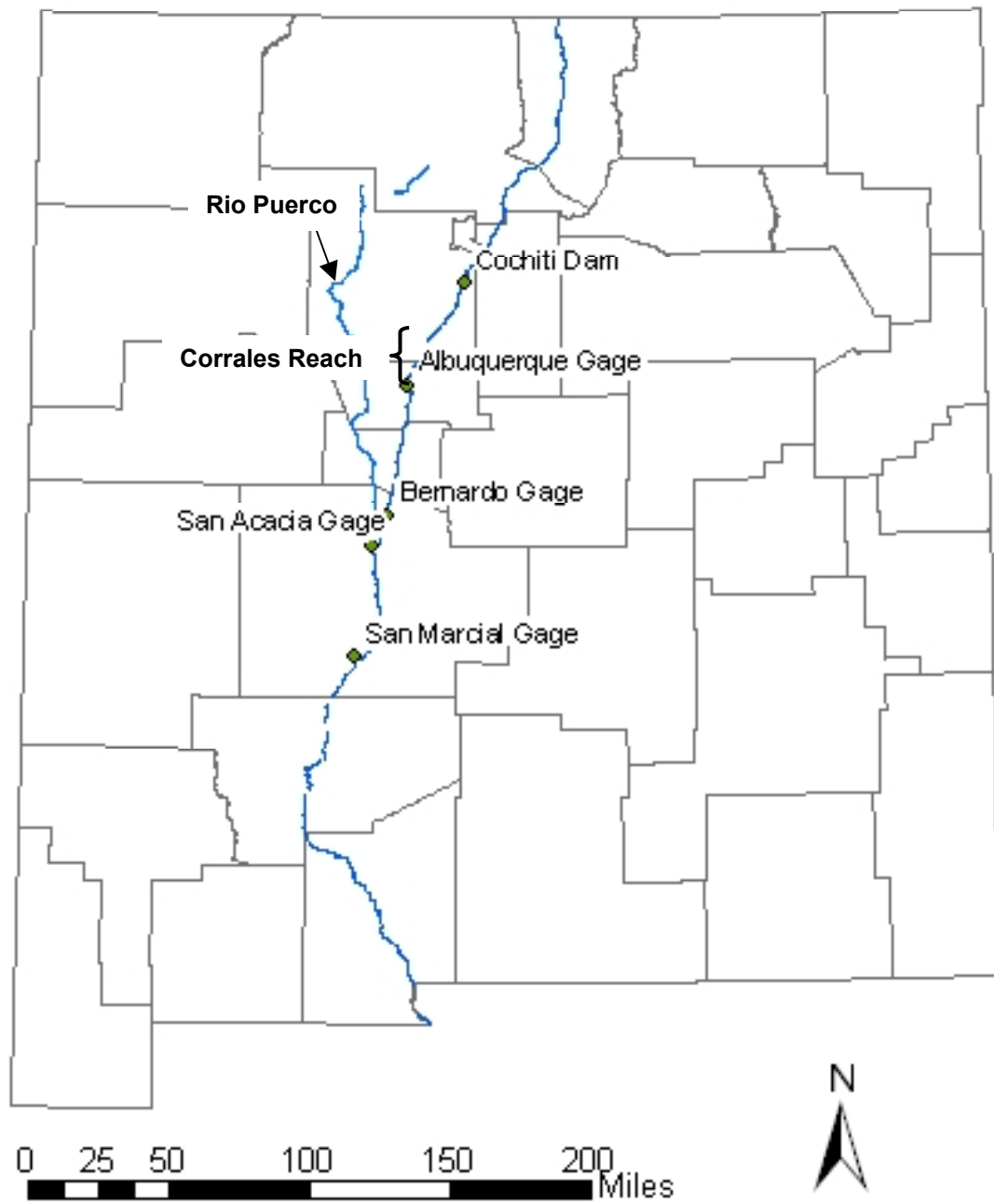


Figure 2-1 Map of New Mexico with gaging stations and Corrales Reach locations identified.

2.2. Hydraulic Modeling Analysis (HMA)

2.2.1. Site Background

The Middle Rio Grande has been inhabited and cultivated for centuries before the Spaniards arrived in 1539. Native Americans in this area were already cultivating the land and soon every community along the river built their own irrigation ditch (Burkholder 1929). This irrigation trend continued once Anglo-Americans settled into this area in the late 1800's. By the 1880's about 124,000 acres of land were cultivated, the most ever recorded for this area (Lagasse 1980). At the same time the amount of land cultivated reached its peak, an increase in the amount of sediment brought into the Rio Grande occurred. Arroyo cutting in the Southwestern US is thought to be the mechanism that introduced the increase of sediment (Lagasse 1980). Increased sediment produced an aggrading river and in turn the aggradation of the river caused flooding, waterlogged lands, and failing irrigation systems (Scurlock 1998). Irrigated lands were reduced to 40,000 acres by 1925 as an effect of the aggrading bed (Leon 1998).

During the 1920's construction of a number of dams, levees, diversion structures and channelization works were created in efforts to save irrigated lands and reduce flood risks (Scurlock 1998). In 1925, the Middle Rio Grande Conservatory District was organized. The purpose of this organization was to improve drainage, irrigation and flood control for approximately 128,000 acres of land in the Middle Valley (Woodson and Martin 1962). A floodway was the basic flood control element for the Middle Rio Grande; it was constructed in 1935 (Woodson 1961). This floodway had an average width of 1,500 feet between the levees, and the levees were approximately 8 feet high (Lagasse 1980). The designed flow of the floodway was 40,000 cfs. In the vicinity of the city of Albuquerque extra height was added to the levees to pass a design flow of 75,000 cfs (Woodson and Martin 1962).

Levees were breached in 25 places along the river due to a major flood in 1941 that had a mean daily discharge of 22,500 cfs for a 2-month duration (Woodson and Martin 1962). These high flows caused extensive flood damage and as much as 50,000 acres were inundated (Scurlock 1998). As a direct result of the flooding in 1941 the Corps of Engineers and the Bureau of Reclamation, along with various other federal, State and local agencies, recommended the Comprehensive Plan of Improvement for the Rio Grande in New Mexico in 1948 (Pemberton 1964). A system of reservoirs (Abiquiu, Jemez, Cochiti, Galisteo) on the Rio Grande and its tributaries, along with the rehabilitation of the floodway, were called for in the Comprehensive Plan (Woodson and Martin 1962). The reconstructed floodway would have a reduced capacity from 40,000 cfs to 20,000 cfs, and in the area surrounding Albuquerque a reduction from 75,000 cfs to 42,000 cfs was made (Leon 1998).

The Comprehensive Plan included many efforts to stabilize the banks. The efforts were culminated in 1973 with Cochiti Dam located near Cochiti Pueblo on the main stem of the river (Lagasse 1980). Cochiti Dam's purpose was to provide flood control and to reduce sediment transport. A 50,000 acre-feet reservoir behind the dam traps nearly all the sediment entering the Cochiti Reservoir. Sediment trapping is done to prevent the aggradational trend and induce degradation via clear water scour on the Middle Rio Grande (Lagasse 1980). Degradation was expected to extend as far downstream as the Rio Puerco, along with bed coarsening over time, which would prevent further degradation (Sixta 2004)

Clear water scour induced by trapping nearly all the sediment (99%) at the Cochiti Reservoir has caused degradation and an armored bed in many places along the Middle Rio Grande (Sixta 2004). Since the dam was complete in 1973 there is virtually no suspended sediment recorded at the Cochiti gaging station, this is shown in Figure 2-2. In Figure 2-2 the Otowi Gage is upstream of the dam and the Albuquerque gage is

downstream of it, the suspended sediment recorded at the Albuquerque gage is due to erosion of the banks, bed, and sediment input from tributaries such as the Jemez River, Galisteo Creek, Arroyo Tonque, etc. (Albert et al. 2003).

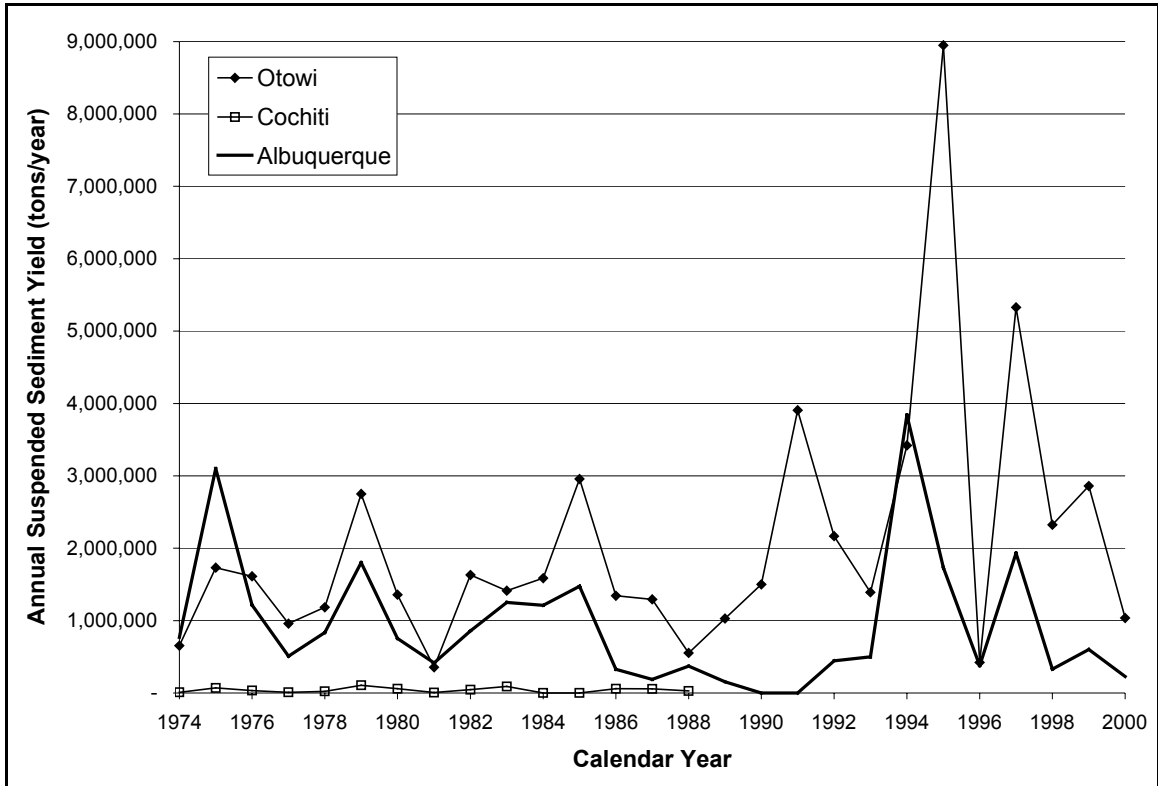


Figure 2-2 Annual Suspended Sediment Yield in the Rio Grande at Otowi Gage (upstream of Cochiti Dam), Cochiti Gage (just downstream of Cochiti dam) and Albuquerque Gage (downstream of Cochiti Gage) from 1974 to 2000. Cochiti gage record ends in 1988

2.2.2. Previous Studies of the Middle Rio Grande

The Middle Rio Grande has been one of the most historically documented rivers in the United States; the longest running gaging station in the U.S. is located on the Rio Grande at Embudo (Graf 1994). A number of papers have been written and studies conducted to better understand the river. This literature review focuses on those studies and papers that were completed after the closure of Cochiti Dam in 1973.

Lagasse (1980) performed a geomorphic analysis of the Middle Rio Grande before and after the construction of the Cochiti Dam, 1971 to 1975. The reach of the

river he studied stretched from Cochiti Dam to Isleta Diversion Dam. This study indicates that the river's response to the construction of Cochiti dam has been dominated by the inflow of arroyos and tributaries (Leon 1998). Also seen in this study reach the portion of the river from the dam to the Jemez River confluence approached a stable condition sooner than that downstream of the confluence, this is due to the development of an armor layer and local base controls established by arroyos and tributaries (Leon 1998). Lagasse (1980) also found that just upstream of the Isleta Diversion Dam the bed aggraded, this indicates that large sediment loads were being transported from the upstream portion on the reach (Bauer 2000)

In Lagasse's 1980 geomorphic analysis, the changes in the channel due to the construction of the dam were documented through a qualitative analysis of planform, profile, cross section and sediment data (Leon 1998). The hydraulic modeling analysis used this Lagasse's study and similar methodology as a guide for some of the same analysis.

Graf (1994) conducted research about the transport of plutonium in the Northern Rio Grande. In part of his study aerial photos of the river from 1940 to 1980 were analyzed. These photos indicate that the river was wide, shallow and braided before the early 1940's. Decreased flows that were induced due to the Comprehensive Plan, led to the development of a single thread channel and a larger floodplain (Bauer 2000). The change from a braided to a single channel river is often due to the closure of dams. However, it can also be because of regional hydroclimatic influences. Evidence of this can be seen upstream of the dam where the river also reduced in size. Instability increased as the Rio Grande narrowed. In unconfined sections of the river, lateral migration occurred, and in some places the river changed its horizontal position as much as 0.6 miles. This happened when channel of the river would plug with sediment and the water would flow over its poorly consolidated banks to create a new channel (Graf 1994)

Besides assisting in establishing the Middle Rio Grande as a single thread river, the reduction in peak flows has also complicated the hydraulics at the confluences of tributaries to the main stem (Bauer 2000). Many times the sediment transported by these tributaries to the Rio Grande exceeds the rivers capacity to transport the sediment (Crawford et al. 1993).

An example of problems caused by incoming sediment can be seen at and downstream of the confluence of the Rio Puerco. The Rio Puerco is not as stable as the Rio Grande and over the past 3000 years this tributary has aggraded and at least three major channels have been cut and filled. This process is a result of fluctuating incoming sediment levels to the Rio Grande (Crawford et al. 1993). Currently the Rio Puerco contributes more than twice the amount of suspended sediment that is carried past Albuquerque, this sediment is deposited upstream of the San Marcial gaging station (Bauer, 2000).

Morphological changes in the Cochiti Reach since 1918 have been documented by Sanchez and Baird (1997). In this study a narrowing trend was observed. However this trend has not accelerated since the completion of Cochiti Dam. While the sinuosity of the river increased after the construction of the dam, it did not reach the peak value observed in 1949 (Sixta 2004). Another morphologic study was conducted by Mosley (1998) on the Santa Ana Reach. This reach extends from the Angostura Diversion Dam to the Highway 44 Bridge in Bernalillo. It was shown that the reach changed from a braided to a meandering riffle/pool channel with a high width to depth ratio that is dominated by gravel material. After the construction of the dam the width to depth ratio decreased.

Many other studies have observed these same trends in reaches of along the Middle Rio Grande. Reports written for the USBR document these trends. The Research conducted in these reports was performed at Colorado State University under the

tutelage of Dr. P. Y. Julien and through funding by the USBR. The reaches researched to date include the following:

- Rio Puerco Reach (Richard et al. 2001). This reach spans 10 miles from just downstream of the mouth of the Rio Puerco (agg/deg 1101) to the San Acacia Diversion dam (agg/deg 1206).
- Corrales Reach (Leon and Julien 2001b), updated by Albert et al. (2003). This reach spans 10.3 miles from the Corrales Flood Channel (agg/deg 351) to the Montano Bridge (agg/deg 462).
- Bernalillo Bridge Reach (Leon and Julien 2001a), updated by Sixta et al. (2003a). This reach spans 5.1 miles from New Mexico Highway 44 (agg/deg 298) to cross-section CO-33 (agg/deg 351).
- San Felipe Reach (Sixta et al. 2003b). This reach spans 6.2 miles from the mouth of the Arroyo Tonque (agg/deg 174) to the Angostura Diversion Dam (agg/deg 236).

2.2.3. Hydrology and Climate

Water flows through a system of basins where surface and ground water are interrelated, thus making the hydrology of the Middle Rio Grande valley very complex (Lagasse 1980). Two different flows are encountered in the Middle Rio Grande due to seasonal precipitation variations. During the spring and early summer (April through June) flows are due to snowmelt and rain from the mountains. During the mid-summer and early fall (July to October) flows are caused by heavy local rains on one or more tributary areas (Rittenhouse 1944). The spring and early summer hydrograph exhibits a gradual rise to a moderate discharge then this discharge is maintained for about 2 months. Peak flows during this period are usually short term with high volumes of runoff (Leon 1998). Summer and fall flows are characterized by a sharp hydrograph with

relatively small volumes of runoff. Flows exceeding 5000 cfs are considered to be flood flow for this reach (Woodson 1961).

Figure 2-3 illustrates a typical spring hydrograph in the Middle Rio Grande. The Otowi stream gage station is located upstream of Cochiti Dam. The location of pertinent USGS gaging stations along the Middle Rio Grande can be seen in Figure 2-1. Attenuation of the spring runoff peak between Otowi and the gages located downstream of the dam is evident in the hydrographs (Figure 2-3). Peak outflows from Cochiti can historically occur as little as 62 days after, or as much as 225 days prior to the peak inflows to the reservoir (Bullard and Lane 1993).

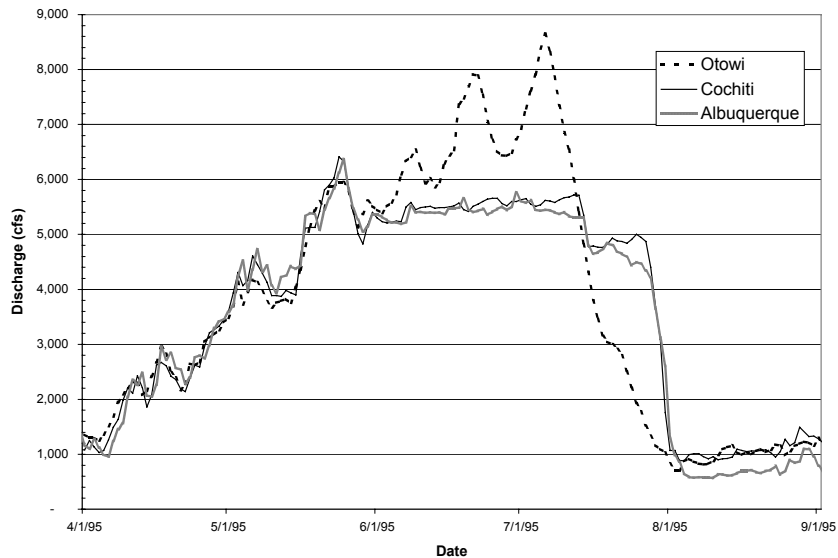


Figure 2-3 1995 Rio Grande spring runoff hydrograph

Along with flood regulations changes in the climate also have a strong effect on the flow regime of the Rio Grande. Richard (2001) saw that the magnitude of the annual peak flows declined since 1895, before the main dams were constructed in the Rio Grande. A dry period is seen, from the Cochiti Gage data, from about 1943 to 1978 (Richard 2001). In addition to the declining peak flows, the peak flows prior to Cochiti

Dam construction, 1948 to 1973, and the peak flows post construction, 1974 to 1996 are not statistically different (Richard 2001).

Molnar (2001) evaluated the Rio Puerco's trends in streamflow and precipitation. The Rio Puerco is one of the largest tributary arroyos of the Rio Grande, it is located downstream of the Cochiti Reach. Molnar's (2001) study concluded, at the annual time scale from 1948 to 1997, that a statistically significant increasing trend in the basin occurred. Increases in non-summer precipitation, especially in the frequency and intensity of moderate rainfall events, cause the increasing trend. Also seen in this study was a strong relationship between the long-term precipitation trends in the basin and sea surface temperature anomalies in the Northern Pacific.

Molnar (2001) also found that the annual maximum precipitation events seem to produce lower annual maximum runoff events in the last 50 years, this is due to vegetation cover and the hydraulic characteristics of the basin. This type of study has not been conducted on any other sub-basin in the Middle Rio Grande but it is likely that the same trends take place in the surrounding area (Sixta 2004).

2.3. Total Load Procedures

2.3.1. Background

In 1950 one of the most famous methods to estimate the total sediment load was introduced by Hans Albert Einstein. His procedure known as the Einstein Procedure was a labor intensive and time-consuming process. Because the Einstein procedure is so strenuous, alternative methods using the same basic methodology were proposed. Colby and Hembree presented one of these methods in 1955. They called their procedure the Modified Einstein Procedure (MEP). This procedure is computationally simpler and it uses parameters more readily available from actual stream measurements

(Burkham and Dawdy 1980). Over the years Colby and Hembree's original procedure has been scrutinized and updated to have it apply more readily to more rivers.

2.3.2. The Modified Einstein Procedure

Einstein (1950) defined bed load and suspended load as follows; bed particles moving the bed layer, in which the bed layer is defined as two grain diameters thick; particles moving outside the bed layer, respectively. The sum of the bed load and suspended load is the total load calculated using Einstein's procedure. Computations using Einstein's procedure are for a representative channel cross section and an average energy slope (Burkham and Dawdy 1980). Identifying a reach of sufficient length to establish an overall energy slope, then averaging the necessary parameters such as wetted perimeter and area determine a representative cross section. Once a representative cross section is determined the rest of the analysis is broken into three parts; (1) equations pertinent to suspended load, (2) equations pertinent to bedload, and (3) equations pertinent to the transition between bedload and suspended load (Burkham 1980).

In 1955, Colby and Hembree introduced the Modified Einstein Procedure (MEP). This new method introduced a method of calculating the total load using data from a single cross section. Data needed to conduct the MEP is stream discharge, mean velocity cross-sectional area, width, mean value of depths at verticals where suspended sediment samples were collected, the measured sediment discharge concentration, the size distribution of the measured load, the size distribution of bed material at a cross-section, and the water temperature (Simons et al. 1976).

The MEP is based on Einstein's (1950) original method, however the two methods serve different purposes (Simons et al. 1976). Einstein's procedure is mainly used for design purposes, it estimates bed material discharges for different river discharges based on channel cross section and sediment bed samples in a selected

river reach. While, the MEP estimates the total sediment discharge for a given water discharge from the measured depth-integrated suspended sediment samples, the streamflow measurements, the bed material samples, and the water temperature for the specific discharge at the cross section (Simons et al. 1976). Therefore, the MEP cannot be used for design or predictive purposes (Stevens 1985).

Principal advantages of the MEP as compared to the Einstein's procedure is that it uses readily available data, requires no point-integrated samples or energy gradients, can be applied to only one cross section, and computes the sediment discharge of all sizes of particles not just the discharge of particles in the size range that is found in the bed (Colby and Hembree 1955). Another major advantage to the MEP is computationally simpler and thus less time consuming.

However, there are some disadvantages to the MEP. Since, the MEP involves the extrapolation of measured suspended sediment discharge and computed bed load discharge it is intended to be used at sites where the bed material is less than 16 mm and only if a significant portion of the measured suspended sediment discharge is comprised of the same size as particles found in the bed material (Stevens 1985).

2.3.3. Modified Einstein Equations

Essential steps and fundamental equations used by the Bureau of Reclamation in applying the modified Einstein procedure for calculating total sediment load are presented below (Holmquist-Johnson 2004). This same procedure was used for the analysis presented in Chapter 4.

1) Compute the measured suspended load (Q_s):

$$Q_s = 0.0027 Q Conc \text{ (tons/day)} \quad (2-1)$$

Where:

Q = discharge (cfs);

Conc = suspended sediment concentration (mg/l).

2) Compute the product of the hydraulic radius and friction slope assuming $x = 1$:

2a) First, compute the value of $\sqrt{(RS_f)}$ using the Einstein Equation:

$$\sqrt{(RS_f)} = \frac{V_{avg}}{32.63 \log \left[12.27 \frac{h}{k_s} x \right]} \quad (2-2)$$

Where:

V_{avg} = average stream velocity (ft/s);

h = flow depth (ft);

x = dimensionless parameter; and

k_s = effective roughness.

2b) Compute the shear velocity (U_*):

$$U_* = \sqrt{g(RS_f)} \quad (2-3)$$

Where:

g = acceleration due to gravity (ft/s²);

R = hydraulic radius (ft);

S_f = friction slope (ft/ft); and

(RS_f) = slope-hydraulic radius function.

2c) Compute the laminar sublayer thickness δ :

$$\delta = \frac{11.6\nu}{U_*} \quad (2-4)$$

Where:

ν = kinematic viscosity (ft²/s).

2d) Recheck x to make sure that the initial guess is valid. Check Figure 2-4 (Einstein's Plate #3) for a value of x given k_s / δ or use the equation to determine the

value of x . This procedure is iterative and repeats until initial and final estimates of x converge.

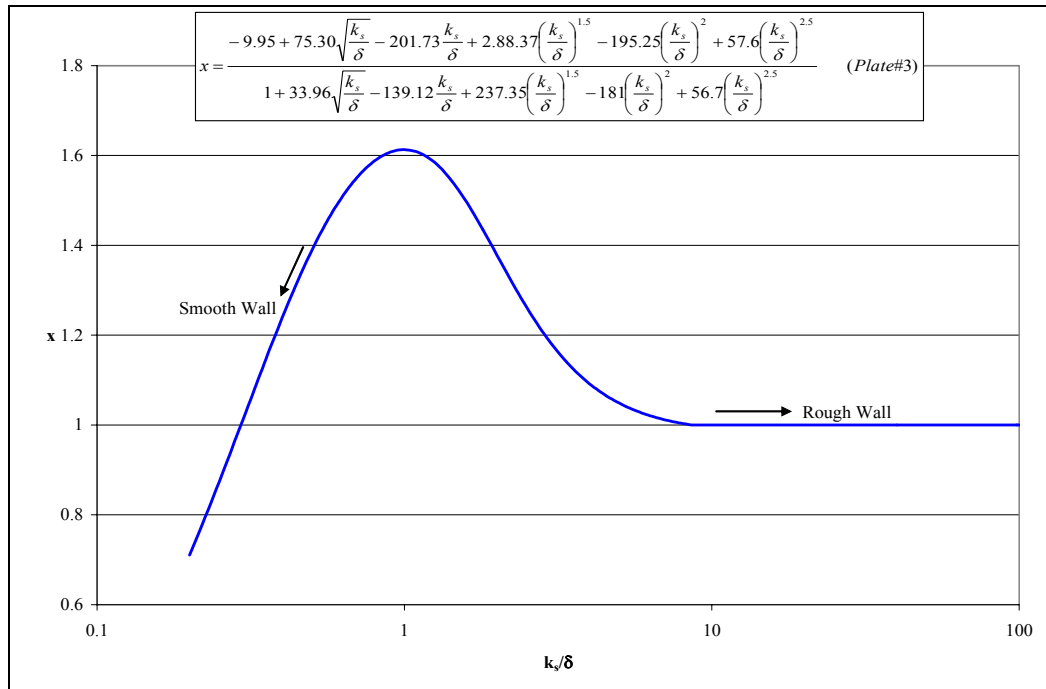


Figure 2-4 Correction for x in the logarithmic friction formula in terms of k_s/δ (Holmquist-Johnson 2004).

3) Compute the value of P' :

$$P' = 2.303 \log \left[30.2 \frac{hx}{k_s} \right] \quad (2-5)$$

Where:

x = dimensionless parameter

P' = mathematic abbreviation for equation 2-5.

4) Compute the fraction of the flow depth not sampled (A'):

$$A' = \frac{d'_n}{d'_s} \quad (2-6)$$

Where:

d'_n = vertical distance not sampled; and

d'_s = vertical distance sampled

5) Compute the sediment discharge Q'_s through the sampled zone. This is calculated using a percentage of the flow sampled determined from the appropriate equation for the value of A' and P' (Holmquist-Johnson 2004).

$$Q'_{s\text{total}} = Q_s * \% \text{ flow sampled} \quad (2-7)$$

For $P'=4$, % flow sampled=

$$\frac{100 - 2941.79A'^2 + 265357.48A'^4 + 64219.08A'^6 - 325482.24A'^8}{1 - 29.38A'^2 + 2621.48A'^4 + 5407.23A'^6 + 157.44A'^8 + 1272.32A'^{10}} \quad (2-8)$$

For $P'=8$, % flow sampled=

$$\frac{100 + 30991.16A'^2 + 21184.18A'^4 + 211800.14A'^6 - 263775.36A'^8}{1 + 325.87A'^2 + 1201.21A'^4 + 1872.11A'^6 + 5759.38A'^8 - 2976.45A'^{10}} \quad (2-9)$$

For $P'=11$, % flow sampled=

$$\frac{100.19 + 31425.83A'^2 - 54359.86A'^4 + 1566703.2A'^6 - 1543898.1A'^8}{1 + 336.12A'^2 + 444.29A'^4 + 15662.05A'^6 + 18936.5A'^8 - 5820.32A'^{10}} \quad (2-10)$$

For $P'=14$, % flow sampled=

$$\frac{100.31 + 45744.98A'^2 + 103307.39A'^4 + 635604.51A'^6 - 784215.44A'^8}{1 + 485A'^2 + 2934.57A'^4 + 7640.27A'^6 + 11737.99A'^8 - 3015.81A'^{10}} \quad (2-11)$$

6) Compute the bed-load for each size fraction:

6a) Step one in computing the bedload is to calculate the shear intensity (ψ) for all particle sizes. ψ is calculated using the greater of the following two equations for all size classes.

$$\psi = 1.65 \left(\frac{d_{35}}{RS_f} \right) \text{ or } 0.66 \left(\frac{d_i}{RS_f} \right) \quad (2-12)$$

Where:

d_{35} = particle size at which 35 percent of the bed material by weight is finer (ft); and

d_i = the geometric mean for each size class (ft).

6b) Compute half of the intensity of the bed-load transport (ϕ) using the following equation.

$$\phi_* = \frac{0.023p}{(1-p)} \quad (2-13)$$

Where p is the probability that a sediment particle will be entrained in the flow and is calculated using the following equation (Yang,1996):

$$p = 1 - \frac{1}{\sqrt{\pi}} \int_a^b e^{-t^2} dt \quad (2-14)$$

Where:

$$a = -\frac{B_*}{\psi} - \frac{1}{\eta_0}; \text{ and}$$

$$b = \frac{B_*}{\psi} - \frac{1}{\eta_0}.$$

B_* is equal to a value of 0.143 and η_0 is equal to a value of 0.5.

6c) Compute the unit bed-load for each size fraction using the following equation:

$$i_B q_B = 1200 d_i^{3/2} i_B \frac{\phi_*}{2} \quad (2-15)$$

Where:

i_B = fraction of bed material in a given size range; and

$\phi_*/2$ = intensity of bedload transport for individual grain size.

6d) Compute the bed-load for each size fraction in Tons/Day by multiplying by the conversion factor 43.2 and the channel width.

$$i_B Q_B = i_B q_B (43.2W) \quad (2-16)$$

Where:

$i_B q_B$ = sediment discharge through the bed layer (lb/s per foot of width)

; and

W = channel width (ft).

7) Compute Suspended Load (Q'_s) for each size fraction by multiplying the total sampled suspended load ($Q'_{s\ total}$) by the suspended load fractions for the sample.

$$Q'_s = i_s Q'_{s\ total} \quad (2-17)$$

Where:

i_s = fraction of suspended material in a given size range; and

$Q'_{s\ total}$ = total suspended sediment load (tons/day).

8) Compute the theoretical exponent for vertical distribution of sediment (Z). Colby and Hembree's (1955) original method determined Z (termed Z' in the initial calculations) by trial and error using a figure (Plate 8) for a selected reference size. For the other size ranges values of Z were then computed in proportion to the 0.7 power of the fall velocities of the geometric mean (Lara 1966). However, Plate 8 was based solely on data from the Niobrara River near Cody, Nebraska. A subsequent study by the USBR in 1966 (Computation of Z 's for use in the Modified Einstein Procedure) determined that using the regression line in Plate 8 produced errors on the order of 20% for the total load. Therefore, the following process determines the Z -values only by trial and error.

8a) Compute the ratio $\frac{Q'_s}{i_B q_B}$ for all size classes with suspended load transport.

8b) Size classes that have calculated values for the ratio of the suspended load to the bed-load are used as the reference ranges for Z -value computations. However, since silt sized particles, less than or equal to 0.0625 mm, are not found in appreciable quantities in the bed and are considered washload, ratios in this size range are not used.

The ratio of suspended load to bed-load is set equal to a function with the parameters I_1'', J_1'', J_1', J_2' (USBR1955):

$$\frac{Q_s'}{i_B Q_B} = \frac{I_1''}{J_1''} (PJ_1' + J_2') \quad (2-18)$$

Where:

I_1'' = mathematical abbreviation that contains J_1'' and A'' ;

J_1'' = mathematical abbreviation that contains A'' ;

J_1' = mathematical abbreviation that contains A' ;

J_2' = mathematical abbreviation that contains A' ; and

In the original MEP to explicitly solve the integral form of the equations for I_1'', J_1'', J_1', J_2' , these values were read from plates 9-11(USBR 1955). However, advances in computer technology since 1955 allows for a numerical solution of these integrals which results in a more precise answer to the parameters. The dependent variables for these parameters are A' and A'' . A' has previously been computed. A'' is calculated for each size class using the following:

$$A'' = \frac{2d_i}{h} \quad (2-19)$$

An initial Z-value must be assumed for each size class then the following equations are used to determine the parameters contained in plates 9-11. The following equation is used in order to provide an the initial guess of the Z-value (from Einstein's Plate #8):

$$Z_{guess} = -0.1465 \ln \left(\frac{Q_s'}{i_B Q_B} \right) + 1.0844 \quad (2-20)$$

Using the initial guess for the Z-values and the equations given below for I_1'', J_1'', J_1', J_2' , a trial and error process is carried out for each size class to determine the correct Z-value.

$$I_1'' = 0.216 \frac{A''^{(z-1)}}{(1-A'')^z} J_1'' \quad (2-21)$$

$$J_1' = \int_{A'}^1 \left(\frac{1-y}{y} \right)^z dy \quad (2-22)$$

$$J_1'' = \int_{A''}^1 \left(\frac{1-y}{y} \right)^z \log_e(y) dy \quad (2-23)$$

$$-J_2' = \int_{A'}^1 \left(\frac{1-y}{y} \right)^z \log_e(y) dy \quad (2-24)$$

$$-J_2'' = \int_{A''}^1 \left(\frac{1-y}{y} \right)^z \log_e(y) dy \quad (2-25)$$

8c) Once the Z-values have been determined for the suspended load, Z and the fall velocity, ω , are plotted on a log-log plot for each size class. A power function equation is then developed such that $Z = a \omega^b$. Z-values for the bed-load are then computed using this relationship. The fall velocity is computed using Rubey's Equation.

$$\omega = F \left[d_i g \left(\frac{\gamma_s - \gamma}{\gamma} \right) \right]^{1/2} \quad (2-26)$$

Where:

γ_s = specific weight of sediment (lb/ft³); and

γ = specific weight of water (lb/ft³).

$$F = \left[\frac{2}{3} + \frac{36\nu^2}{g d^3 \left(\frac{\gamma_s}{\gamma} - 1 \right)} \right]^{\frac{1}{2}} - \left[\frac{36\nu^2}{g d^3 \left(\frac{\gamma_s}{\gamma} - 1 \right)} \right]^{\frac{1}{2}} \quad (2-27)$$

9) Compute the total sediment load.

9a) Calculate the total load due to suspended sediment using the following:

$$Q_{S_{total\ suspended}} = Q_s' \frac{(P J_1'' + J_2'')}{(P J_1' + J_2')} \quad (2-28)$$

9b) The total load for the remaining size classes are calculated using the computed bed-load. Using the Z-values calculated with the power function from step 8c, calculate I_1'' and $-I_2''$ using the following equations:

$$I_1'' = 0.216 \frac{A''^{(z-1)}}{(1-A'')^z} J_1'' \quad (2-29)$$

$$-I_2'' = 0.216 \frac{A''^{(z-1)}}{(1-A'')^z} J_2'' \quad (2-30)$$

Then, compute the value $(P' I_1'' + I_2'' + 1)$ and multiply by the computed bed-load for that size class to compute the total load due to bed-load.

$$Q_{S_{total\ bed}} = i_B Q_B (P' I_1'' + I_2'' + 1) \quad (2-31)$$

9c) The total load is then the sum of the total suspended and total bed load.

$$Q_{S_{total}} = Q_{S_{total\ suspended}} + Q_{S_{total\ bed}} \quad (2-32)$$

2.3.4. Computer Programs that perform MEP analysis

Due its complexity and popularity, many computer programs were created to calculate the total sediment load using the MEP. Two of the more popular MEP programs are PSANDS and MODEIN. However, these programs are becoming increasingly outdated and difficult to use for large data sets. A new program, was

created by the USBR to facilitate the use of the MEP. This new program created by Holmquist-Johnson (2004) is BORAMEP. One of the main advantages of using BORAMEP is that it provides the user the capability to calculate the total load for numerous samples as opposed to one sample at a time. Other advances such as explicitly solving the I and J integrals and calculating the Z values for each size fraction using the procedure presented previously make this program ideal for the analysis presented in this thesis.

2.4. Mass and Double Mass Curves

Mass and double mass curves are very basic analysis tools. A mass curve is a plot of cumulative values against time; a double mass curve is a plot of cumulative values of one variable against the cumulation of another quantity during the same time period (Searcy and Hardison 1960). The theory behind double mass curves is that by plotting the cumulation of two quantities the data will plot as a straight line, and the slope of this line will represent the constant of proportionality between the two quantities. A break in slope indicates a change in the constant of proportionality (Searcy and Hardison 1960).

Mass and double mass curves can be applied to numerous types of hydraulic and hydrological data. The purpose of these curves is to check the consistency of data over time and to identify changes in trends by changes in the slope. Mass and double mass analysis are often used to adjust precipitation records. Precipitation data can be very inconsistent due to nonrepresentative factors, such as change in location or exposure of the rain gage (Chow 1964). Even though the double mass analysis is typically performed on precipitation data, this type of analysis can be performed on many types of data such as sediment transport (Hindall 1991), reservoir sedimentation (Yang

et al. 2002), and aquifer drawdown (Ruteledge 1985). Figure 2-5 presents an example of a double mass curve of flow and sediment load for the Rio Grande.

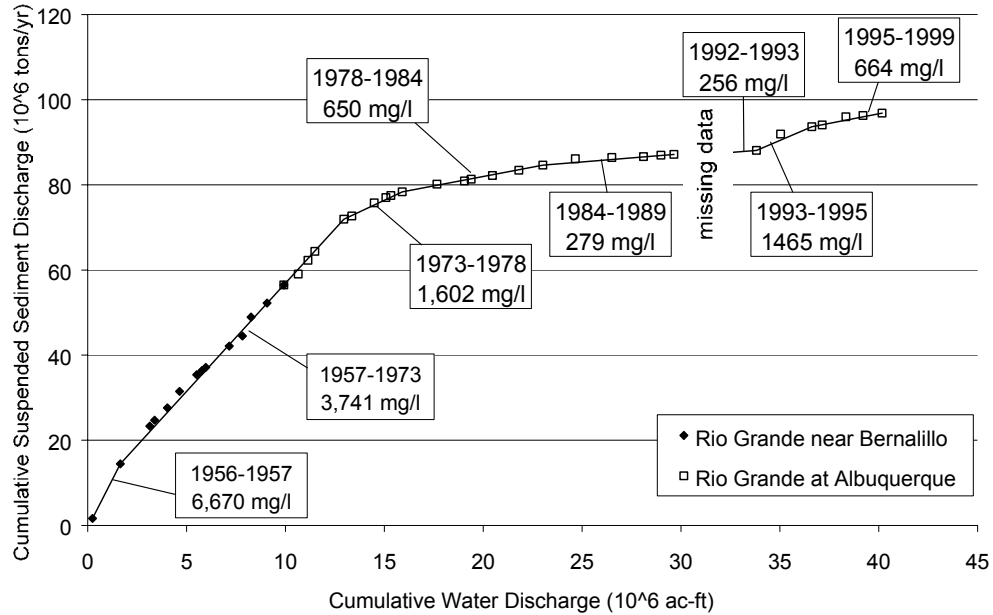


Figure 2-5 Cumulative discharge vs. cumulative suspended sediment load at Rio Grande at Bernalillo and Rio Grande at Albuquerque (1956 – 1999 (Sixta et al. 2003a)).

Breaks in slopes within curves on the plots can be caused by many factors. A change in flow magnitudes, construction, urbanization, increase/decrease in vegetation, climate changes, and anything else that can effect sediment influx and discharge into a data collecting gage can cause slope breaks in sediment DMCs. If the DMC doesn't have any breaks in slope it means that the correlation between the two plotted values has not been changed or affected significantly over the years. However, slope breaks are common in DMCs and help provide added information about the relationship between the two variables.

The most significant information that a break in slope provides is an estimate of the time at which a change occurred (Searcy and Hardison 1960). Once the date is known in which the change occurred one can study the historical record of the gaging

station and or river to see if any anthropogenic changes to the river or sampling methods have been documented. If no changes have been documented, it can be concluded that the change in slope is due natural causes. It is a general rule to ignore breaks in slope that persist for less than 5 years, if the break continues for more than five years it is considered a trend and should be investigated further (Searcy and Hardison 1960).

2.5. Summary

Being one of only two rivers in the world with a perched degrading bed the Rio Grande is very fascinating (Pers. Comm. Baird 2003). By performing this literature review some significant information was exposed about the MRG including location, climate, history and hydrology. Also analyses used in this thesis were examined for their applicability and dependability to the Middle Rio Grande. Many studies have been conducted on the Middle Rio Grande. By using previous studies and conducting additional analysis, prediction of the future conditions of the river can be made. In turn this can provide better restoration efforts. Some analysis that can be done to determine the historic and future trends in the river is double mass analysis. Performing this analysis will show how the sediment load has changed overtime and provides insight on future sediment conditions.

CHAPTER 3: HYDRAULIC MODELING ANALYSIS (HMA)

3.1. Introduction

The objective of this work is to analyze historical data and estimate potential conditions of the river channel. Prediction of future equilibrium conditions of the Corrales Reach will facilitate the identification of sites that are more conducive to restoration efforts.

In order to achieve this objective, the following analyses were performed:

- Identification of spatial and temporal trends in channel geometry through the analysis of cross-section survey data.
- Planform classification through analysis of aerial photos and channel geometry data.
- Analysis of temporal trends in water and sediment discharge and sediment concentration using United States Geological Survey (USGS) gaging station data.
- Identification of temporal trends in bed material through the analysis of gradation curves and histograms.
- Evaluation of the equilibrium state of the river through the application of hydraulic geometry methods, empirical width-time relationships and sediment transport analyses.

3.2. Reach Background

3.2.1. Reach Definition

The Corrales Reach of the Middle Rio Grande spans 10.3 miles from the Corrales Flood Channel to the Montano Bridge. It spans from Aggradation/Degradation (agg/deg) line 351 to agg/deg line 462 (Appendix A, Figure A-1). Aggradation/Degradation lines are cross section survey lines that are spaced approximately every 500 feet apart and are photogrammetrically surveyed. Also included in the Corrales Reach are Cochiti (CO) range lines, which are cross sections that were field surveyed in this reach by the US Bureau of Reclamation. There are three CO-lines located in the study reach (Figure 3-1). CO-33 is the first upstream cross section of the study reach (agg/deg 351), CO-34 coincides with agg/deg 407 and CO-35 corresponds to the agg/deg line 453. Calabacillas (CA) range lines were also field surveyed and established just upstream and downstream from Paseo del Norte. In addition to the CO and CA lines, 14 Corrales (CR) range lines were established throughout the reach.

Maps generated utilizing a Geographic Information System (GIS) depicting the locations of the agg/deg lines, CO-lines and CA-lines can be seen in Appendix A. Also included in this appendix (Figures A-2 to A-4) are aerial photographs of the Corrales Reach showing the locations of the CO-lines along with pertinent geographic features. A description of the photo and flow data (Table A-1 and A-2) for the dates that the aerial photos were taken are also include in the appendix.

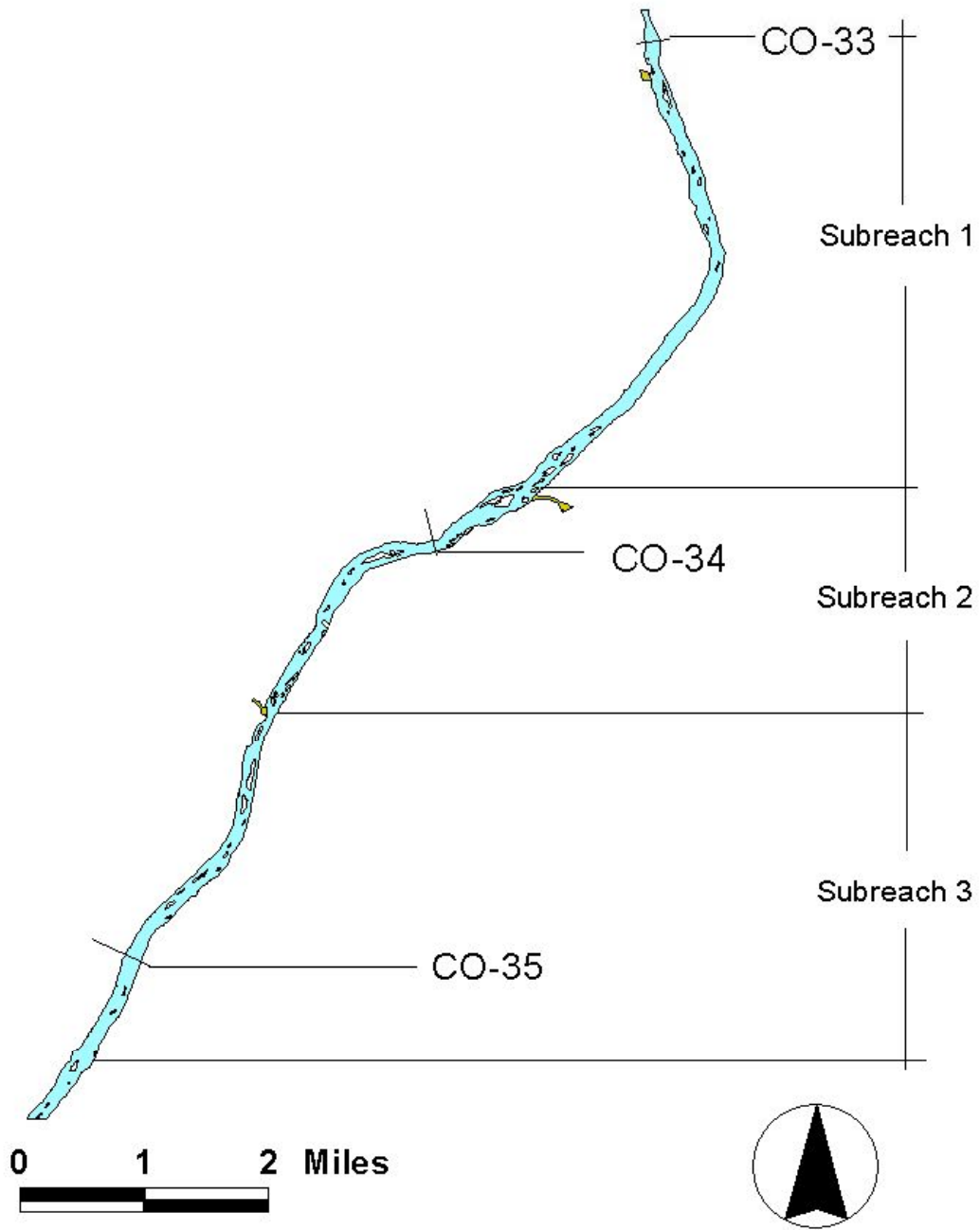


Figure 3-1 River planform of the Corrales Reach indicating locations of CO-lines and subreaches, 1992.

3.2.2. Subreach Definition

The Corrales Reach was subdivided into three subreaches to facilitate the characterization of the reach. The entire reach exhibits similar channel characteristics,

such as width, planform and profile. Subreach delineation was based largely on water and sediment inputs to the reach from tributaries and diversion channels. Subreach 1 is 4.1 miles long and spans from cross section CO-33 (Agg/Deg 351) to the AMAFCA North Diversion Drain (Agg/Deg 397). Subreach 2 is 3.0 miles long and spans from the AMAFCA North Diversion Drain to Arroyo de las Calabacillas (Agg/Deg 428), just upstream from Paseo del Norte Bridge. Subreach 3 is 3.2 miles long and extends from the Arroyo de las Calabacillas to Montano Bridge (Agg/deg 462).

3.2.3. Available Data

The sources of data utilized in the HMA included gaging station data, database data and sets of digitized aerial photos. From these data, numerous geomorphic analyses were performed in the pursuit of finding reach trends.

There is one U.S. Geological Survey (USGS) gaging station (Bernalillo - # 08329500) located about 1.8 miles upstream from Corrales Reach, however this station was decommissioned in 1969. In addition, there is a gaging station located downstream of the study reach. Rio Grande at Albuquerque (#08330000) gaging station is about 6.2 miles downstream from Montano Bridge. Both of these gaging stations were utilized primarily in this study. Table 3-1 summarizes the available water discharge and suspended sediment data from the USGS gages.

Table 3-1 Periods of record for discharge and continuous suspended sediment data collection by the USGS.

<i>Stations</i>	<i>Mean Daily</i>	<i>Continuous</i>
	<i>Discharge</i>	<i>Suspended Sediment</i>
	Period of Record	Period of Record
Rio Grande near Bernalillo	1942-1968	1956-1969
Rio Grande at Albuquerque	1942-2001	1969-1989 1992-1999

Bed material particle size distribution data were collected at the USGS gaging stations at Bernalillo and Albuquerque. Table 3-2 summarizes the periods of record for

the bed material data from the above-mentioned USGS gages. Additionally, the USBR collected periodic bed material samples at the CO, CR and CA-lines. Table 3-3 lists the bed material surveyed dates at the CO-lines, CA-lines and CR-lines.

Table 3-2 Periods of record for bed material particle size distribution data collected by the USGS.

<i>Stations</i>	<i>Bed Material Particle Size</i>
	<i>Distributions</i>
	Period of Record
Rio Grande near Bernalillo	1961, 1966 - 1969
Rio Grande at Albuquerque	1969 - 2001

Table 3-3 Surveyed dates for bed material particle size distribution data at CO-Lines and CA-Lines.

<i>Stations</i>	<i>Bed Material Particle Size</i>
	<i>Distributions</i>
	Surveyed Date
CO-33	1970 - 1982, 1992, 1995, 2001
CO-34	1970 - 1972, 1974, 1975, 2001
CO-35	1970 - 1972, 1974, 1975, 1992, 1995, 2001
CA-1	1988-1993, 1995, 1996, 2001
CA-6 and CA-12	1988-1996, 2001
CA-2 to CA-5, CA-7 to CA-11 and CA-13	1988-1996
CR-355, 361, 367, 372, 378, 382, 388, 394, 400, 413, 443, 448, 458, 462	2001

The survey dates for the CO, CA, and CR-lines that lie within the Corrales Reach are summarized in Table B-1 (Appendix B). CO-line plots representing two surveys, one pre-Cochiti Dam (1973) and one post-Cochiti Dam are included in Appendix C. A more detailed discussion of these plots as they relate to the closure of Cochiti Dam is discussed later in this chapter.

3.2.4. Channel Forming Discharge (CFD)

Reclamation's Albuquerque office determined the channel forming discharge from discharge/frequency analysis in the Santa Ana Reach. The Corrales reach is 5.10 miles downstream from the Santa Ana Restoration Project. The two year instantaneous

peak discharge of 5000 cfs used as the channel maintenance discharge in the Santa Ana Geomorphic Analysis (Mosley and Boelman 1998) is also utilized in this work.

Figure 3-2 shows the annual maximum daily mean discharges recorded by the USGS at the Albuquerque gaging station. Since 1958, there haven't been any flows recorded at Albuquerque exceeding 10,000 cfs. Since flow regulation began at the Abiquiu Dam on the Rio Chama in 1963 and at the Cochiti Dam on the Rio Grande in 1973, the regulated two-year flow has decreased to 5,650 cfs (Bullard and Lane 1993). Figure 3-3 shows annual peak flow histograms before and after 1958. Most of the flows are between 3,000 cfs and 7,000 cfs after 1958. Annual peak daily-mean discharge plot at the Bernalillo Gage is included in Appendix C.

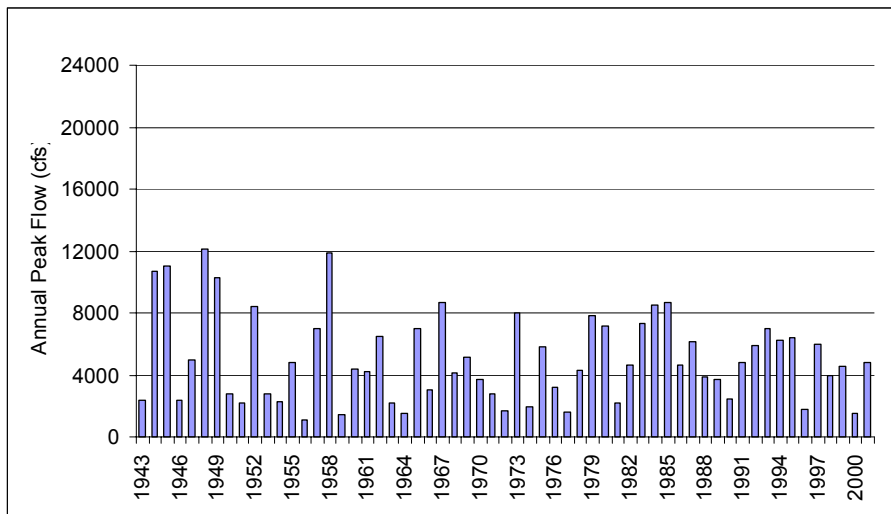


Figure 3-2 Annual peak daily-mean discharge at Rio Grande at Albuquerque (1943 – 2001).

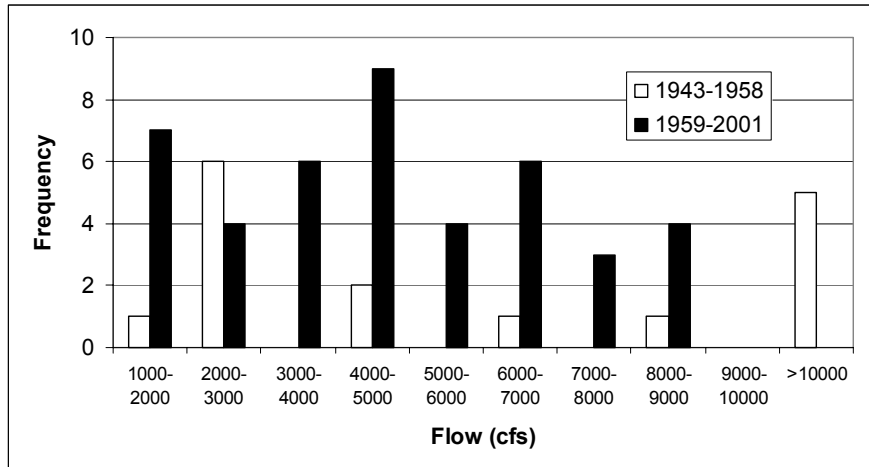


Figure 3-3 Maximum mean daily annual discharge histograms on the Rio Grande at Albuquerque.

3.3. Geomorphic Characterization

3.3.1. Channel Classification

Current channel pattern was qualitatively described from the 2001 set of aerial photos. In addition, qualitative descriptions of the non-vegetated channel planform were performed from the GIS coverages from 1918 to 2001.

Several channel classification methods were applied to the study reach to characterize the spatial and temporal trends of the channel planform. These methods are based on different concepts, such as slope-discharge relationships, channel morphology and unit stream power. Using a channel forming discharge of 5,000 cfs along with various parameters from HEC-RAS[®] and d_{50} values from gradation curves as inputs, the following methods were analyzed for the study reach: Leopold and Wolman (1957), Lane (1957, from Richardson et al. 2001), Henderson (1963, from Henderson 1966), Ackers and Charlton (1970, from Ackers 1982), Schumm and Khan (1972), Rosgen (1996), Parker (1976), van den Berg (1995), Knighton and Nanson (1993) and Chang (1979).

Figure 3-4 was produced from GIS coverages of the Corrales Reach and represents the changes in river planform that occurred in the non-vegetated active channel in 1918, 1935, 1962, 1992 and 2001. It is evident that the study reach planform has not experienced significant changes since 1962. The 1992 and 2001 planforms are comparable and represent a single thread channel with visible islands at low flow. The floodway construction between 1930 and 1936 do not seem to have halted the channel-narrowing trend observed since 1918 but it may have exacerbated the channel narrowing. Conversely, rehabilitation of the floodway by the 1950's might be responsible for stabilization of the width of the channel, as shown in Figure 3-4.

The current channel pattern description is based on observation of the 2001 set of aerial photos, which were taken during the winter season (Appendix A). At flows below bankfull (<5,000 cfs), the Corrales Reach exhibits a multi-channel pattern. Formation of sediment bars at low flow is also evident in the aerial photos (Appendix A) as well as in the cross section plot of CO-35 (Appendix B).

The values of the input parameters for the different channel classification methods applied to the 1962, 1972, 1992 and 2001 surveys of the Corrales Reach are in Table 3-4. These methods produced descriptions of the channel that range from straight to meandering and braided (Tables 3-4 and 3-5). The discrepancy among classification methods is likely due to the fact that this stretch of the Rio Grande is not in a state of equilibrium, and the classification methods were designed under the assumption that the river is in state of equilibrium. Equilibrium for this study means that the channel geometry of the river is not changing with time.

Channel patterns predicted by each method, yield results with little variation between subreaches for all the three periods. The lack of variation might be due to the constant channel-forming discharge used in the computation (5,000 cfs), little variation in bed material and channel width, etc.

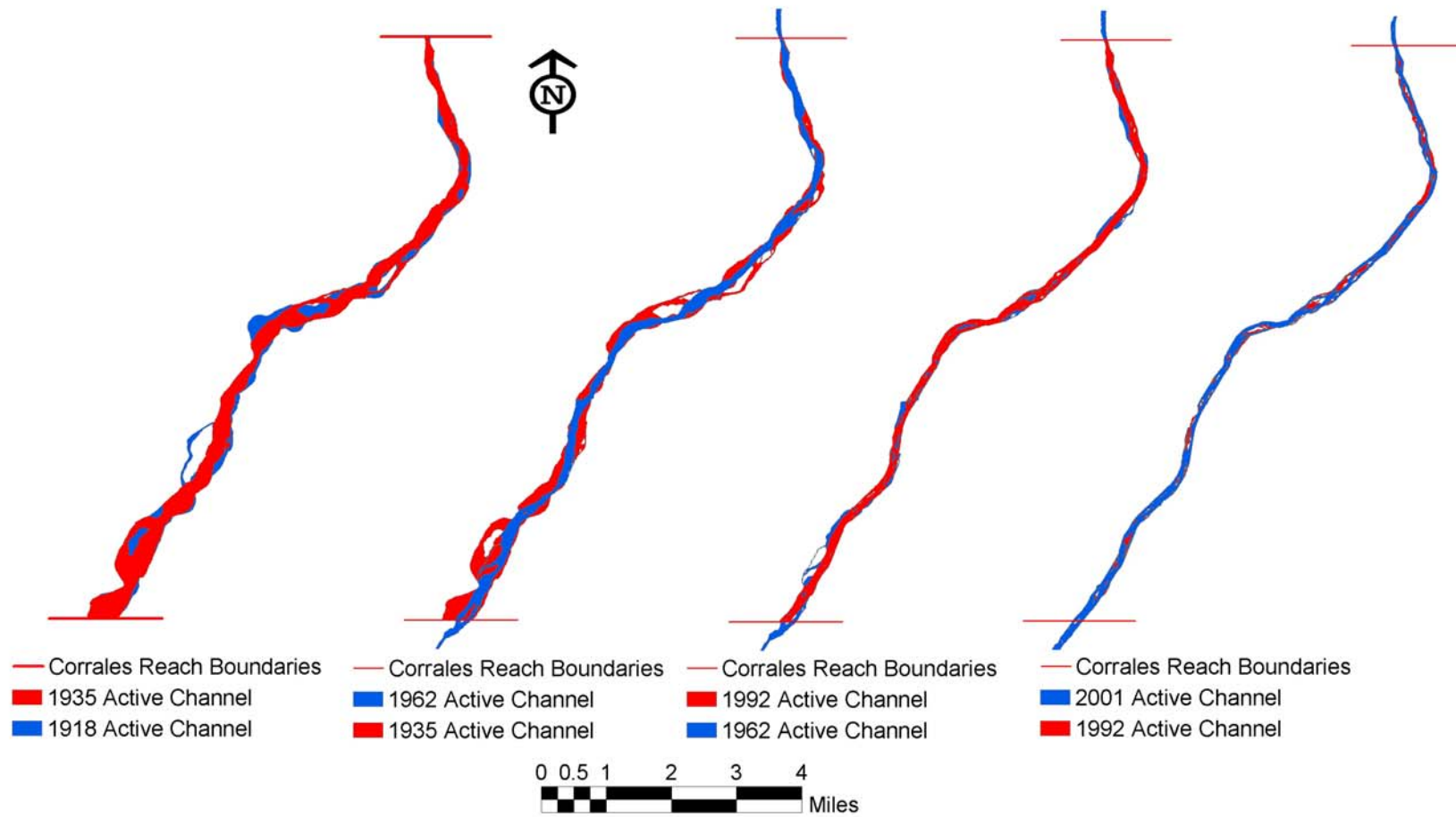


Figure 3-4 Non-vegetated active channel of the Corrales Reach. 1918 planform from topographic survey. 1935, 1962, 1992 and 2001 planform from aerial photos.

Table 3-4 Channel pattern classification for 1962 and 1972.

Reach #	Slope-discharge					Channel Morphology		Stream Power		
	Leopold and Wolman	Lane	Henderson	Ackers & Charlton		Schumm & Khan	Rosgen	Parker	van den Berg	Chang
				Comparing with channel slope	Comparing with valley slope					
1962										
1	Straight	Intermediate	Braided	Meandering	Meandering	Straight	D5c-	Meandering	Low stream power low sinosity single-thread and narrow channel	from meandering to steep braided
2	Straight	Intermediate	Braided	Meandering	Meandering	Straight	D5	Meandering	Low stream power low sinosity single-thread and narrow channel	from meandering to steep braided
3	Straight	Intermediate	Braided	Meandering	Meandering	Straight	D5	Meandering	Low stream power low sinosity single-thread and narrow channel	from meandering to steep braided
Total	Straight	Intermediate	Braided	Meandering	Meandering	Straight	D5c-	Meandering	Low stream power low sinosity single-thread and narrow channel	from meandering to steep braided
1972										
1	Straight	Intermediate	Braided	Meandering	Meandering	Straight	D5c-	Meandering	Low stream power low sinosity single-thread and narrow channel	from meandering to steep braided
2	Straight	Intermediate	Braided	Meandering	Meandering	Straight	D5	Meandering	Low stream power low sinosity single-thread and narrow channel	from meandering to steep braided
3	Straight	Intermediate	Braided	Meandering	Meandering	Straight	D5	Meandering	Low stream power single thread narrow channel	from meandering to steep braided
Total	Straight	Intermediate	Braided	Meandering	Meandering	Straight	D5	Meandering	Low stream power low sinosity single-thread and narrow channel	from meandering to steep braided

Table 3-5 Channel pattern classification for 1992 and 2001.

Reach #	Slope-discharge					Channel Morphology		Stream Power		
	Leopold and Wolman	Lane	Henderson	Ackers & Charlton		Schumm & Khan	Rosgen	Parker	van den Berg	Chang
				Comparing with channel slope	Comparing with valley slope					
1992										
1	Straight	Intermediate	Braided	Meandering	Meandering	Straight	D5	Meandering	Low stream power single thread narrow channel	from meandering to steep braided
2	Straight	Intermediate	Braided	Meandering	Meandering	Straight	D5	Meandering	Low stream power single thread narrow channel	from meandering to steep braided
3	Straight	Intermediate	Braided	Meandering	Meandering	Straight	D5c-	Meandering	Low stream power single thread narrow channel	from meandering to steep braided
Total	Straight	Intermediate	Braided	Meandering	Meandering	Straight	D5	Meandering	Low stream power single thread narrow channel	from meandering to steep braided
2001										
1	Straight	Intermediate	Braided	Meandering	Meandering	Straight	D5c-	Meandering	Low stream power single thread narrow channel	from meandering to steep braided
2	Straight	Intermediate	Braided	Meandering	Meandering	Straight	D5c-	Meandering	Low stream power single thread narrow channel	from meandering to steep braided
3	Straight	Intermediate	Braided	Meandering	Meandering	Straight	D5c-	Meandering	Low stream power single thread narrow channel	from meandering to steep braided
Total	Straight	Intermediate	Braided	Meandering	Meandering	Straight	D5c-	Meandering	Low stream power single thread narrow channel	from meandering to steep braided

3.3.2. Sinuosity

The sinuosity of the study reach and the subreaches were estimated as the ratio of the channel thalweg length to the valley length. Reclamation's GIS and Remote Sensing Group in Denver, CO digitized the channel thalweg and measured valley lengths from aerial photos and topographic maps. The thalweg length was used as the active channel length in the sinuosity computations. Identification of the channel length is subject to the quality of the photos and surveys.

The sinuosity of Corrales Reach remained close to 1.15 from 1918 to 1949. After 1949, the sinuosity increased and remained between 1.15 and 1.20 (Figure 3-5). Subreach 1 maintained its sinuosity close to 1.2 for the entire study period. However, it has been above 1.2 since 1949. Subreach 2 has had a more variable sinuosity than the other reaches, fluctuating between 1.15 and 1.21. Subreach 3 increased its sinuosity consistently from 1.05 to around 1.11, but has the lowest sinuosity of all the reaches. Channels are classified as straight if the sinuosity is near one.

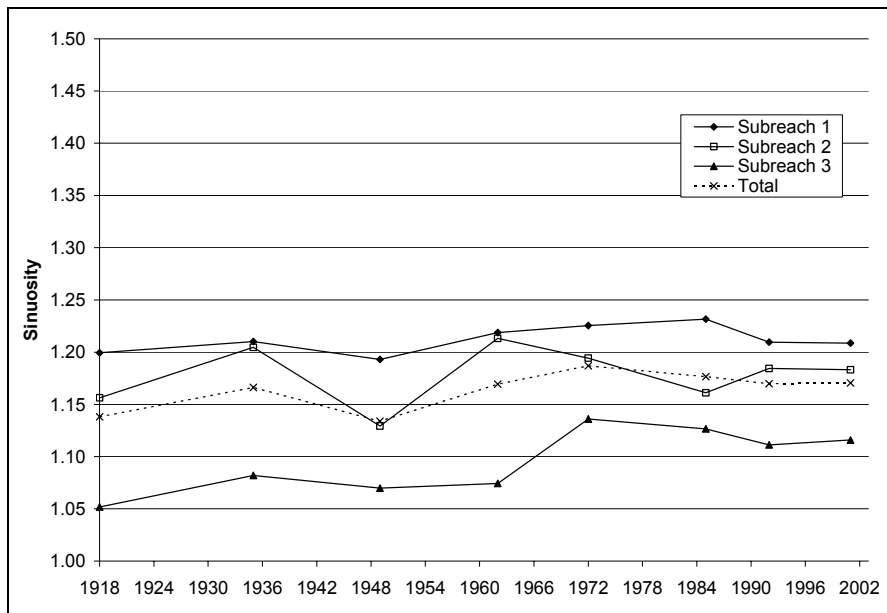


Figure 3-5: Time series of sinuosity of the Corrales Reach as measured from the digitized aerial photos.

3.3.3. Longitudinal Profile

Longitudinal profiles were plotted for the study reach and the subreaches for the years of 1962, 1972, 1992 and 2001. The profiles for the first three sets of years were generated from the agg/deg data. The longitudinal profile for 2001 was generated from the CO, CR and CA-line data and plotted together with the agg/deg line longitudinal profiles. All profiles were generated using the same methodology. Parameters calculated from the U.S. Army Corps of Engineers' Hydrologic Engineering Center-River Analysis System (HEC-RAS[®]) version 3.1 program (USACE 1998) were utilized in this methodology. The HEC-RAS[®] runs that were executed using the channel forming discharge of 5,000 cfs. To calculate the mean bed elevation (MBE), the following equation was used:

$$MBE = WSE - \frac{A}{Tw} = WSE - h$$

In this equation, WSE represents the water surface elevation (ft), A represents the channel area (ft²), Tw represents the channel top width (ft) and h represents the hydraulic depth (ft), which is seen to be equivalent to the area-to-top width ratio.

Longitudinal profiles of the mean bed elevation for the entire reach and subreaches are presented in Figure 3-6. The majority of the reach aggraded between 1962 and 1972. The entire reach degraded from 1972 to 1992. The reach-averaged aggradation from 1962 to 1972 is approximately 0.1 feet, and the reach-average degradation from 1972 to 1992 is approximately 2.5 feet. The net change in mean bed elevation between 1962 and 1992 is approximately 2.4 feet of degradation. From 1992 to 2001 the bed aggraded as much as 3 feet. Subreach 1 degraded slightly (less than one foot on average), subreach 2 aggraded slightly (less than one foot on average) and subreach 3 aggraded significantly (upwards of 3 feet) (Figure 3-6).

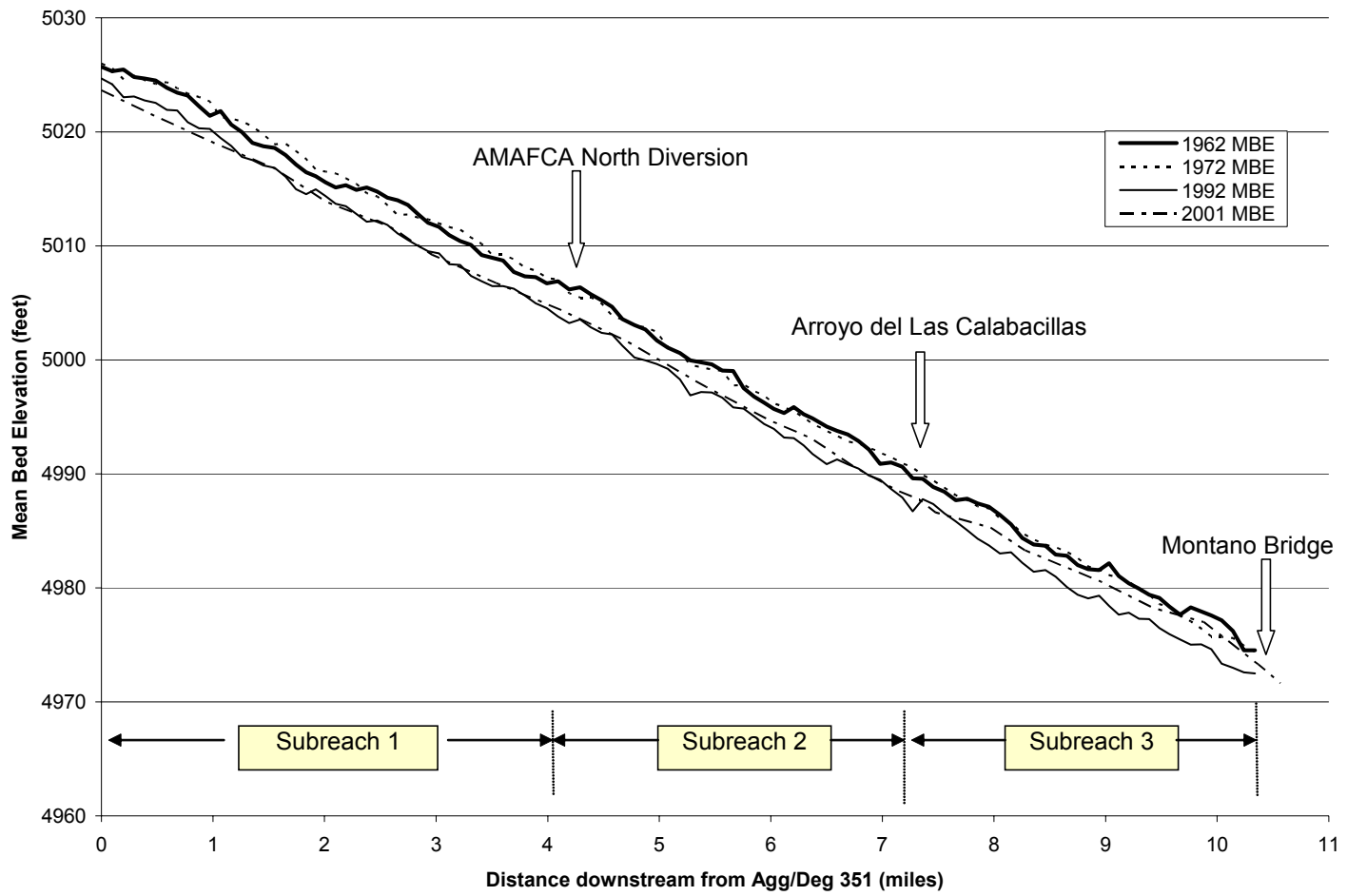


Figure 3-6 Mean bed elevation profile of entire Corrales Reach. Distance downstream is measured from agg/deg 351.

3.3.4. Channel Cross Sections

Each of the three cross sections from the CO-line surveys was plotted for two different survey dates. These dates were chosen based on the closure of Cochiti Dam in 1973. One of the dates represents pre-dam conditions and one of the dates represents post-dam conditions. Survey dates were chosen to view the impacts of the dam on the channel.

The cross section for CO-33 representing the channel conditions in 1971 and 1998 is graphically displayed in Figure 3-7. The 1971 cross-section represents the pre-dam conditions, while the 1998 cross-section represents post-dam conditions. It can be seen that as much as five feet of degradation has occurred since the closure of Cochiti Dam. These results are consistent with the trend of the longitudinal profiles (Figure 3-6). Similar results can be seen in the other two cross sections. All CO-line cross-sections are attached in Appendix B.

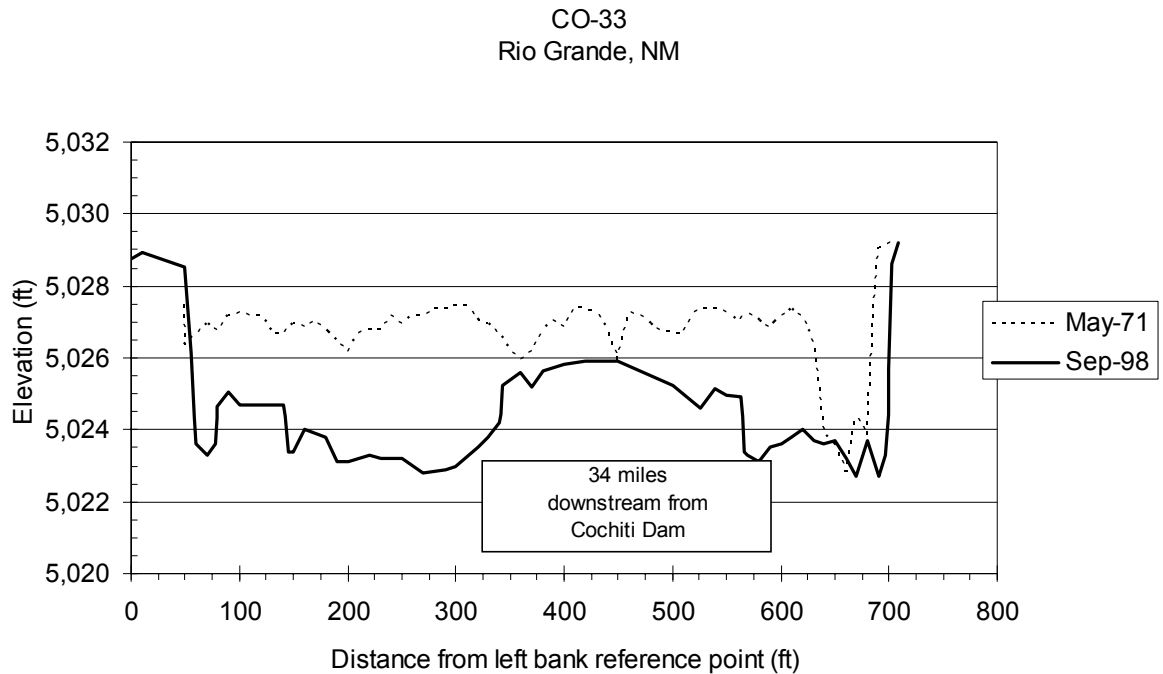


Figure 3-7 Cross section CO-33 representing pre and post-dam conditions.

3.3.5. Channel Geometry

Two methods were used to describe the channel geometry characteristics of the study reach: 1) HEC-RAS[®] model and; 2) digitized aerial photo interpretation. HEC-RAS[®] was used to model the channel geometry of the study reach with the available agg/deg line data for 1962, 1972 and 1992 and CO, CR and CA-line data for 2001. A total of 109 agg/deg cross sections spaced approximately 500 feet apart were modeled for the 1962, 1972 and 1992 model. The model for 2001 was performed using 3 CO-lines, 14 CR lines and 7 CA-lines spaced from approximately 800 to 4,000 feet apart. A channel forming discharge of 5,000 cfs was routed through the reach. A Manning's n value of 0.02 was used for the channel and 0.1 for the floodplain for all simulations. All HEC-RAS[®] results for each of the simulated years are summarized in Appendix E. Digitized aerial photos were used for active channel delineation as well as to measure the non-vegetated channel width at each agg/deg line. The measurements were executed through the use of ArcGIS v. 8.2.

The resulting channel geometry parameters at each cross section were then averaged over the entire reach using a weighting factor equal to the sum of one half of the distances to each of the adjacent upstream and downstream cross sections.

The following channel geometry parameters were computed:

Wetted Perimeter = WP
Wetted Cross Section Area = A
Mean Flow Velocity = $V = Q/A$
Where Q = Flow discharge
Top Width = Tw
Hydraulic Depth = $H = A/W$
Width-to-Depth ratio = WDR
Froude Number $Fr = V/(gh)^{0.5}$

The temporal changes in channel geometry as calculated from HEC-RAS[®] under a channel forming discharge of 5000 cfs are summarized in Figure 3-8. The changes in channel geometry generally show similar trends for all subreaches from 1962 to 1992,

which are increases in mean velocity, width-to-depth ratio and wetted perimeter, and decreases in cross section area and average depth from 1962 to 1972. From 1972 to 1992 the opposite trends are observed, that being an increase in cross section area and average depth and decrease in velocity, width-to-depth ratio and wetted perimeter. Subreaches 1 and 2 continue to follow similar trends from 1992 to 2001, which is an increase in velocity and depth, and a decrease in flow area, width-depth ratio and wetted perimeter. Subreach 3 experiences an increase in velocity, average depth, width-to-depth ratio and wetted perimeter and a decrease in flow area from 1992 to 2001.

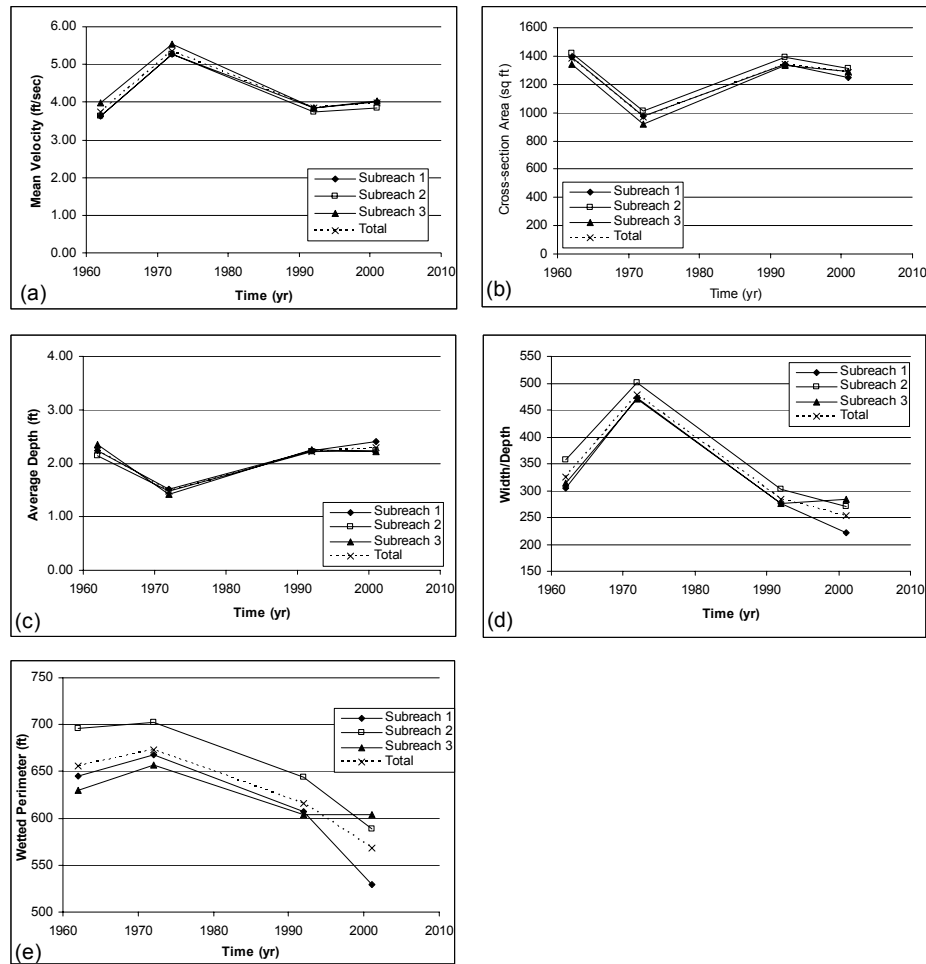


Figure 3-8 Reach-averaged main channel geometry from HEC-RAS® results for Q = 5,000 cfs. (a) mean velocity, (b) cross-section area, (c) average depth, (d) width-to-depth ratio, (e) wetted perimeter.

3.3.6. Width

Active channel width time series from the digitized vegetation boundaries are presented in Figure 3-9. All of the reaches exhibit declining width with time. Maximum decreases in channel width occurred from 1918 to 1962. All the subreaches achieved nearly the same width after 1962. From 1962 to 1972, the channel width increased slightly. After 1972, channel width began to decline again at a slower rate than that prior to 1962. The main-channel widths predicted by the HEC-RAS® model at 5,000 cfs exhibit similar trends observed in Figure 3-9 for the 1962 to 2001 time period (Appendix E).

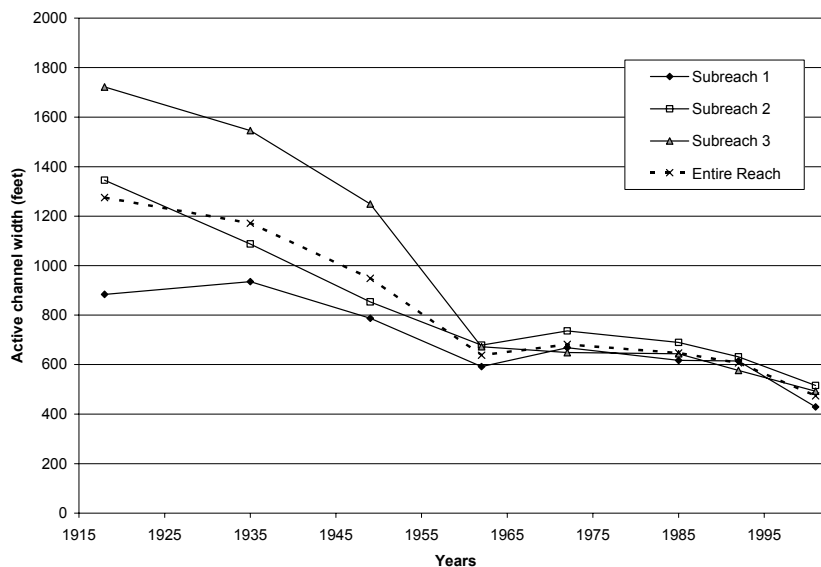


Figure 3-9 Reach averaged active channel width from digitized aerial photos (GIS).

3.3.7. Bed Material

Characterization of the spatial and temporal variability of median bed material size (d_{50}) was performed for each subreach. Median grain sizes were computed for 1962, 1972, 1992 and 2001 from USGS gaging stations, CO-line, CR-line and CA-line data. Apparent temporal and spatial trends were noted through the generation of bed material gradation curves. In addition, histograms were generated using the d_{50} and d_{84}

sizes at each of the three cross sections from the CO-line surveys and from 8 CA-lines. These histograms were generated using the available data for dates as far back as 1970 (see Table 3-2).

Several samples were collected across each cross section. The average of the median bed material sizes (d_{50}) of all the samples collected in the bed of the channel at each station were calculated to characterize the bed material of the reach. These averages were input into the channel classification methods (see Table 3-4 and 3-5). In addition, different statistics such as minimum, maximum and standard deviation of the median bed material sizes were computed for each of the locations and dates see Appendix F. These statistics were used to further analyze the bed material trends occurring in the subreaches.

The median grain sizes from the bed material samples at the Bernalillo gage and CO lines are comprised of fine sand for all the subreaches for 1962 and 1972. In 1992, the median size material ranged from medium sand to coarse gravel in subreach 1, fine sand to coarse gravel in subreach 2 and medium sand to coarse gravel in subreach 3. The median grain size in 2001 consisted of medium sand to medium gravel in subreach 1, medium sand to very coarse sand in subreach 2 and medium sand to coarse sand in subreach 3.

In general, the grain size coarsens with time from 1962 to 1992. This trend is likely due to sediment detention by Cochiti Dam and tributary sediment detention structures, which leads to clear-water scour. However, the coarsening of the bed does not account for the finer material observed in 2001. The finer material found is likely due to the time of year in which the sediment was collected. The 2001 data were collected in early April and late August when low flows are common which are not likely to transport the sand off the bed. Conversely, the 1992 data were collected in July when high flows

are more likely to be observed (Figure 2-2). High flows are likely to transport the smaller sand particles downstream, leaving behind the coarser gravels.

A histogram showing how the d_{50} and d_{84} sizes change with time for CO-33 is shown in Figure 3-10. A combination of pebble count data and sediment distribution data was used to create this histogram. It can be seen that both the d_{50} and d_{84} values coarsen after 1974, which roughly corresponds to the closure of Cochiti Dam. Similar trends can be seen in the other cross sections. Histograms for the remaining two CO-lines and for eight CA-lines (CA-1, 2, 4, 6, 8, 10, 12, and 13) are attached in Appendix F.

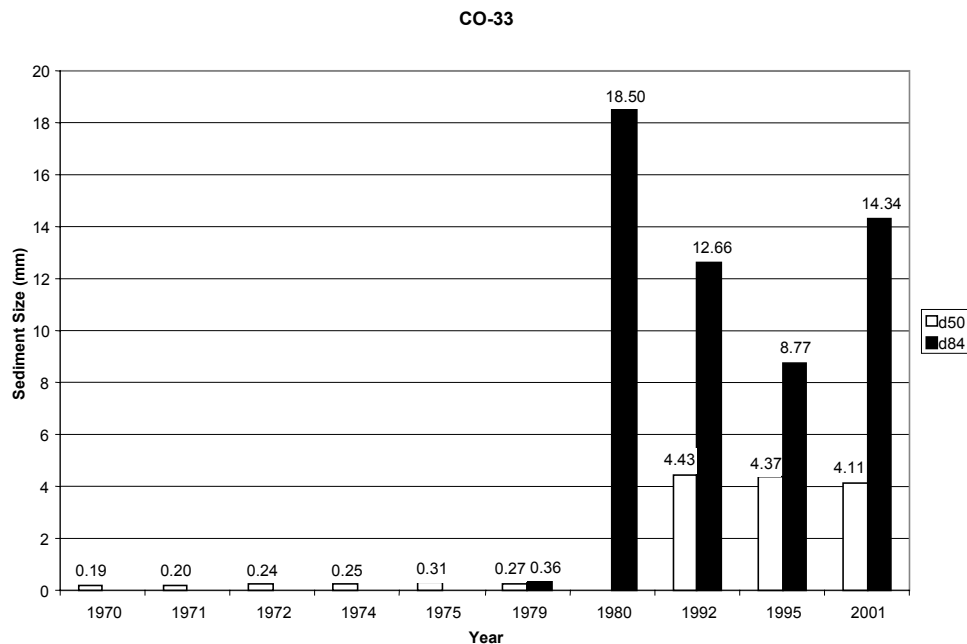


Figure 3-10 Histogram depicting the d_{50} and d_{84} change with time for CO-33.

All of the median grain sizes (d_{50}) are in the sand range for 1961 and 1972. Some of the samples contain median grain sizes in the gravel range in 1992. Gravel sediment particles were surveyed at both high (3,260 cfs) and low (517 cfs) flows. However, a slight shift from coarser to finer material can be observed in the material distribution curves for all three subreaches from 1992 to 2001 (Figures 3-11 to 3-13). Figures 3-11 to 3-13 show the averaged bed material distribution of all of the bed

material data collected for the entire subreach, see Appendix F for the complete set of individual distribution curves.

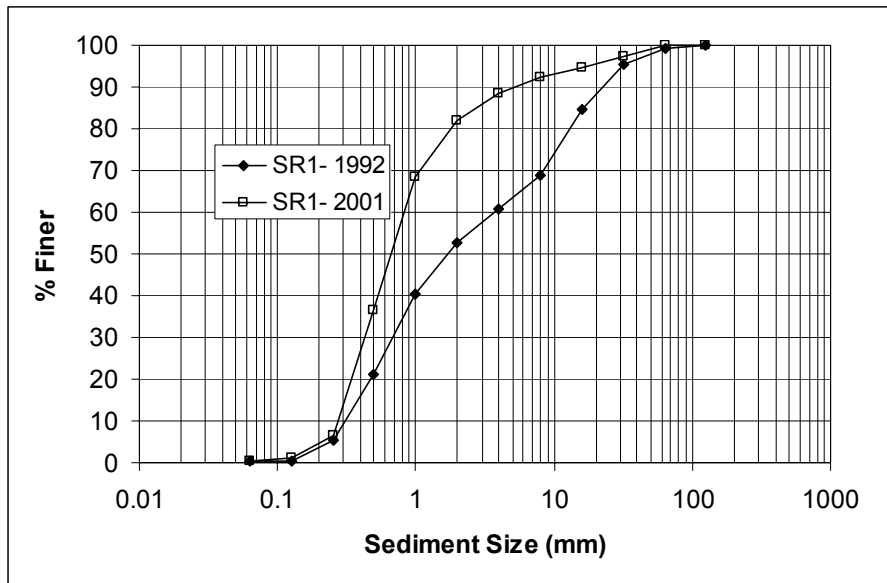


Figure 3-11 Comparison of 1992 and 2001 bed material gradation curves for subreach 1.

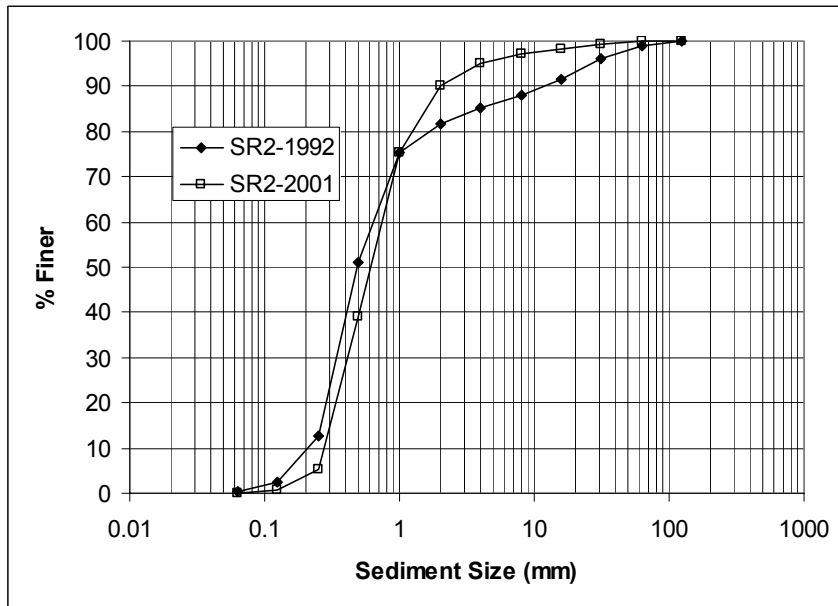


Figure 3-12 Comparison of 1992 and 2001 bed material gradation curves for subreach 2.

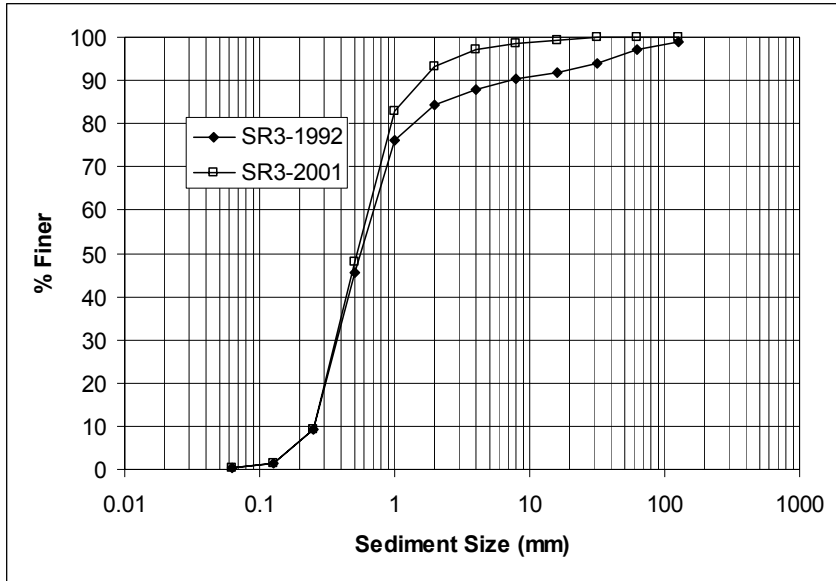


Figure 3-13 Comparison of 1992 and 2001 bed material gradation curves for subreach 3.

Figure 3-14 shows the averaged bed material size distribution curves for each subreach and the entire reach for 2001. These curves were used as input for the 2001 sediment transport discussed later in this chapter. The 1992 gradation curves in Figures 3-11 to 3-13 were also used in the sediment transport analysis for that year.

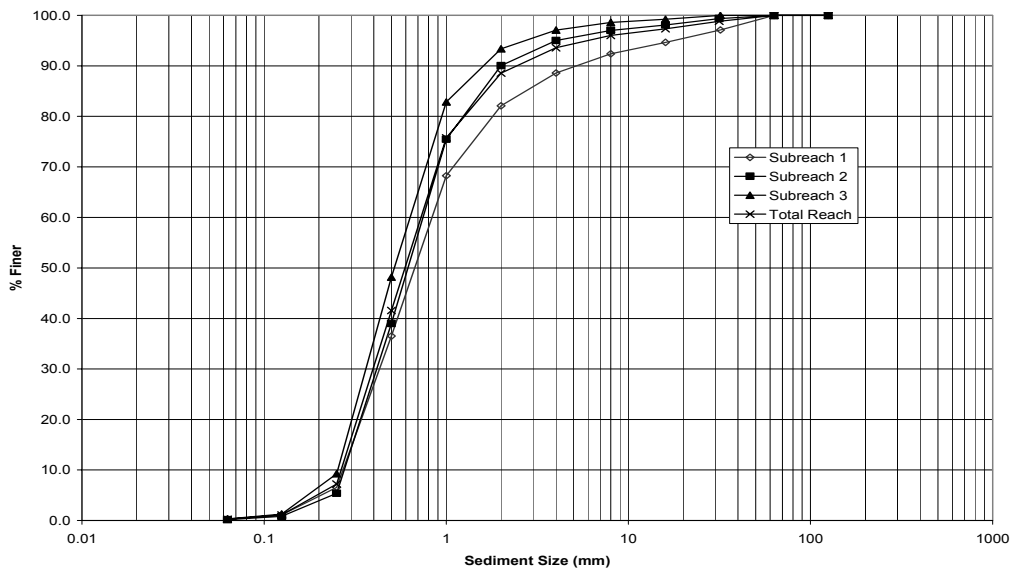


Figure 3-14 2001 Bed-material samples used in the sediment transport and equilibrium

3.4. Suspended Sediment and Water History

Water and sediment flow trends in the Corrales Reach were analyzed through the development of single mass curves and double mass curves. Not enough suspended sediment data were available to generate difference-mass curves and perform a sediment continuity analysis of the reach.

The following curves were developed for the Bernalillo and Albuquerque gages, for the entire period of record:

- Mass curve of water discharge (acre-feet/year) from 1942 to 2000.
- Mass curve of sediment discharge (tons/year) from 1956 to 1999.
- Double mass curve with water and sediment discharge for trends in sediment concentration (mg/l) from 1956 to 1999.

The slopes of each curve and the time periods of breaks in the curves were also estimated.

3.4.1. Single Mass Curves

3.4.1.1. Discharge Mass Curve

The discharge mass curve for Bernalillo and Albuquerque gages (Figure 3-15) have similar trends, indicating that there is not significant water input from the ephemeral tributaries between the two gages. There are three breaks in slope in the discharge mass curve (1942-1978, 1978 - 1987 and 1987 – 2000 periods), with an increase in annual discharge rate from 1978 to 1987 and a slight decrease from 1987 to 2000 (Figure 3-15). The drier water discharge period (1942-1978) at Bernalillo and Albuquerque Gages coincides with the drier water period at Cochiti Gage, as identified by Richard (2001). These slope breaks in the mass curve represent changes in water

regime in the river. Changes may be due to changes in climate and/or flood management or regulation in the Rio Grande Basin.

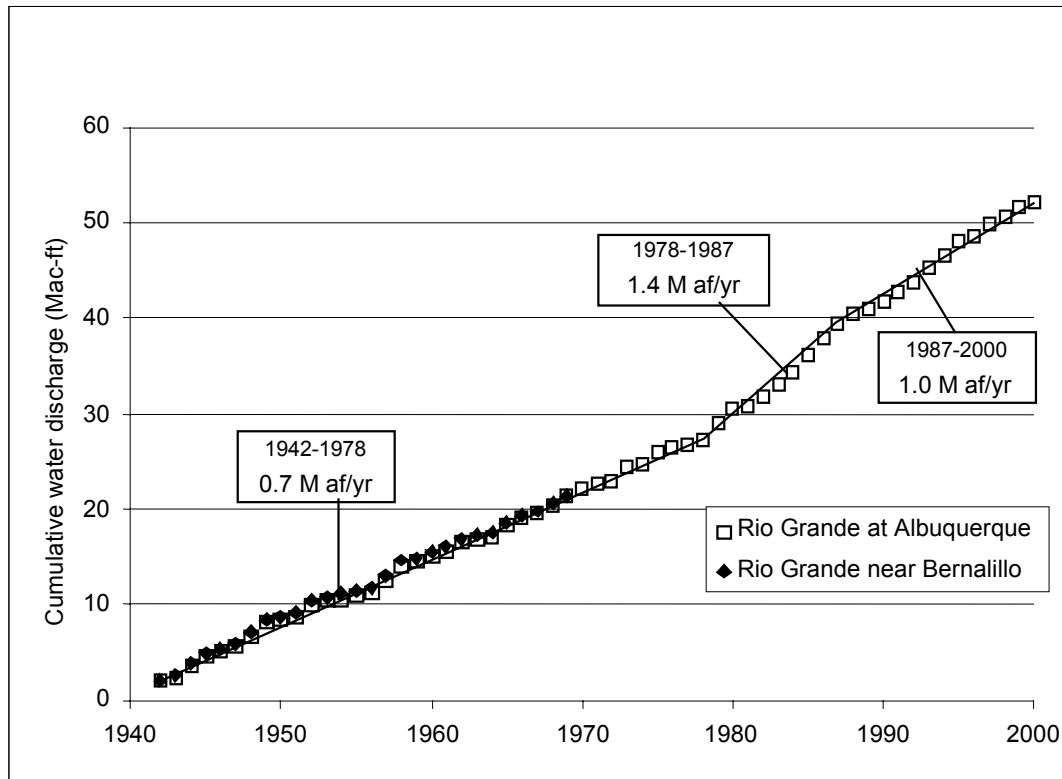


Figure 3-15 Discharge mass curve at Bernalillo and Albuquerque Gages (1942-2000).

3.4.1.2. Suspended Sediment Mass Curve

The suspended sediment mass curve for Bernalillo and Albuquerque shows nine slope breaks (Figure 3-16). In general, the slopes are steeper from 1956 to 1973 than after 1973. The slope values range from 2.3 to 10.8 M tons per year between 1956 and 1973. After 1973, the slope values are between 0.25 to 2.79 M tons per year. This change in sediment rate in 1973 coincides with the closure of Cochiti Dam. There was an increase of suspended sediment discharge from 1993 to 1995 (2.79 M tons/yr) with respect to the 1978-1993 discharges (1.11 M tons/yr and 0.25 M tons/yr). However, the 1995-1999 suspended sediment discharge has decreased to 0.8 M tons/yr and is comparable to the 1978-1985 sediment discharge (1.11 M tons/yr).

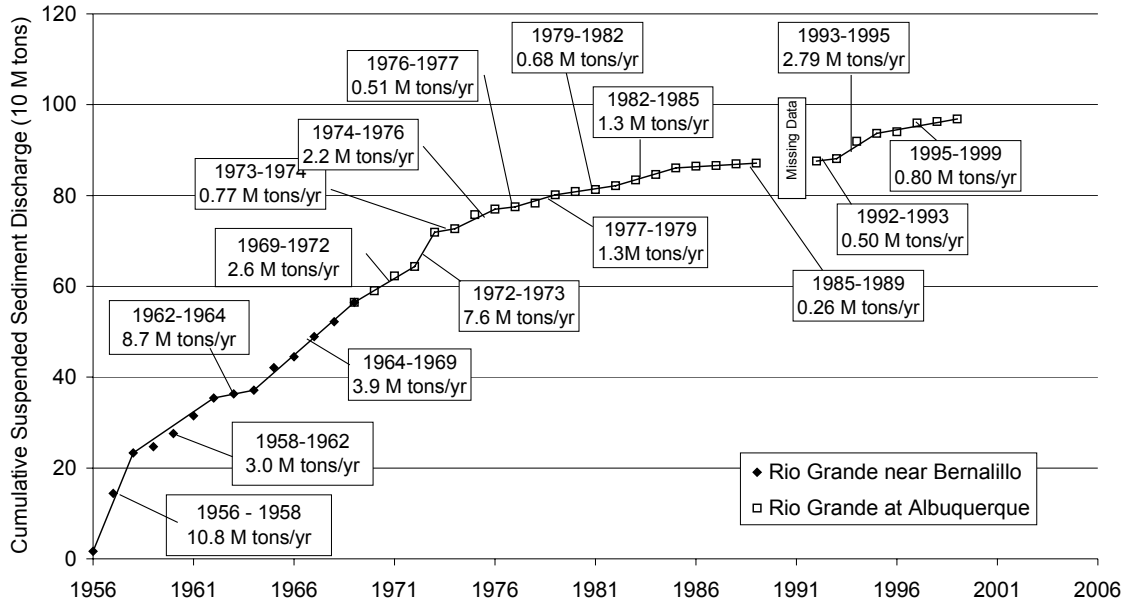


Figure 3-16 Suspended sediment mass curve at Bernalillo and Albuquerque Gages (1956-1999).

3.4.2. Double Mass Curve

The double mass curve of cumulative water discharge versus cumulative sediment discharge shows the changes of suspended sediment concentration with time. Figure 3-17 shows higher concentrations of suspended sediment from 1956 to 1973 with average concentration varying from 3,741 mg/l to 6,670 mg/l. After 1973, the concentration does not exceed 1,602 mg/l. In general, the double mass curve shows a similar trend as the suspended sediment single mass curve. An average concentration of 664 mg/l has persisted from 1995 to 1999 and is close to the 1978-1984 average concentration (650 mg/l). Table 3-6 summarizes the suspended sediment concentrations at Bernalillo and Albuquerque Gages between 1956 and 1999.

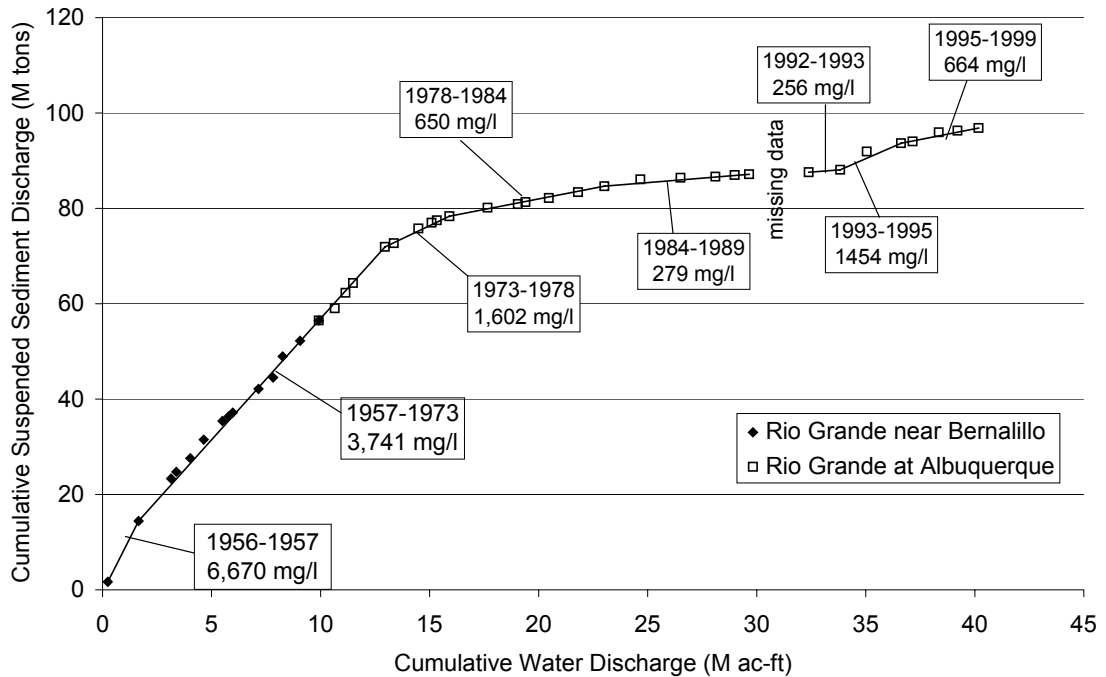


Figure 3-17 Cumulative discharge vs. cumulative suspended sediment load at Rio Grande at Bernalillo and Rio Grande at Albuquerque (1956 - 1999).

3.5. Sediment Transport Analysis

A sediment transport analysis was performed to compare the subreach transport capacity with: 1) the incoming sand load ($0.0625 \text{ mm} < d_s < 2 \text{ mm}$); and 2) the incoming bed material load ($0.30 \text{ mm} < d_s < 2 \text{ mm}$).

Field observations performed by the USBR indicate that sand size particles are mobile at all flows greater than 300 cfs as bedload material, and become suspended at flows greater than 3,000 cfs (Massong 2001). According to these field observations, it is believed that the bed material load is comparable to the sand load (0.0625 mm and 2 mm) (Massong 2001).

However, very fine and fine sand size particles (0.0625 mm to 0.25 mm) are not found in large quantities in the bed (d_{10} of bed material = 0.27 mm (Figure 3-14)) at flows close to 5,000 cfs, which suggest that they behave as washload (Appendix G, Table 3-

6). In addition, the amount of sand particles in suspension finer than 0.27 mm (d_{10} of the bed material) is approximately 65% or more at flows close to 5,000 cfs (Table 3-6, Appendix G). As a result, the bed material load comprises only the sediment particles coarser than 0.27 mm at flows close to 5,000 cfs.

Table 3-6 Percents of total load that behave as washload and bed material load at flows close to 5,000 cfs.

Date	Inst. Discharge (cfs)	% washload	% bed material load
5/22/1978	4260	53	47
4/23/1979	4980	82	18
7/9/1979	6040	78	22
4/28/1980	4730	53	47
5/24/1982	4280	81	19
6/7/1982	4570	79	21
4/24/1984	4270	86	14
5/8/1984	4440	77	23
6/13/1994	5030	97	3
6/27/1994	4860	66	34
5/5/1995	3980	64	36
6/6/1995	4960	44	56
7/3/1995	5620	30	70
6/3/1997	5040	29	71
5/24/1999	4080	65	35
Average =	4743	66	34

Total sediment input to the reach was estimated using the Modified Einstein Procedure (MEP) (Colby and Hembree 1955 USBR 1955). Cross-section geometry measurements, suspended sediment and bed material samples at the Albuquerque Gage from 1978 to 1999 were used for the purpose of estimating the incoming total sediment load and sand-load to the reach using the MEP. The Albuquerque Gage is located downstream from the study reach. As a result, the total load might be slightly over estimated because sediment is probably mined from the bed and banks between the study reach and the gage. The data were subdivided by separating snowmelt and summer flows. The snowmelt period was defined as April to July based on interpretation of the mean-daily discharge record for the Albuquerque gaging station from 1978 to

1999. Linear regression functions were fit to the MEP results to develop sand load rating curves.

The bed material transport capacity of the subreaches was estimated for 1992 and 2001 using the following sediment transport equations: Laursen, Engelund and Hansen, Ackers and White (d_{50} and d_{35}), Yang – Sand (d_{50} and size fraction), Einstein and Toffaleti (Stevens and Yang 1989, Julien 1998). The bed material gradation analysis indicates that the median grain sizes of all the subreaches are fine to medium sand and therefore, most of the bed material transport relationships are appropriate to use. The input data to the sediment transport equations are the reach-averaged channel geometry values resulting from HEC-RAS[®] run at 5,000 cfs (Appendix E).

The transport capacity equations are functions of the slope of the channel. Therefore, the channel slope was adjusted to produce a transport capacity that approximated the incoming bed material load. An adjusted slope was obtained from each sediment transport equation.

Figure 3-18 presents the spring and summer sand load rating curves at the Albuquerque Gage. Using a channel forming discharge of 5,000 cfs, the estimated MEP sand load at the Albuquerque gaging station is 17,600 tons/day. It is evident that the variability of the data points around the regression line is about one order of magnitude (Figure 3-18). As a result, the real sand load could considerably vary from the estimated value.

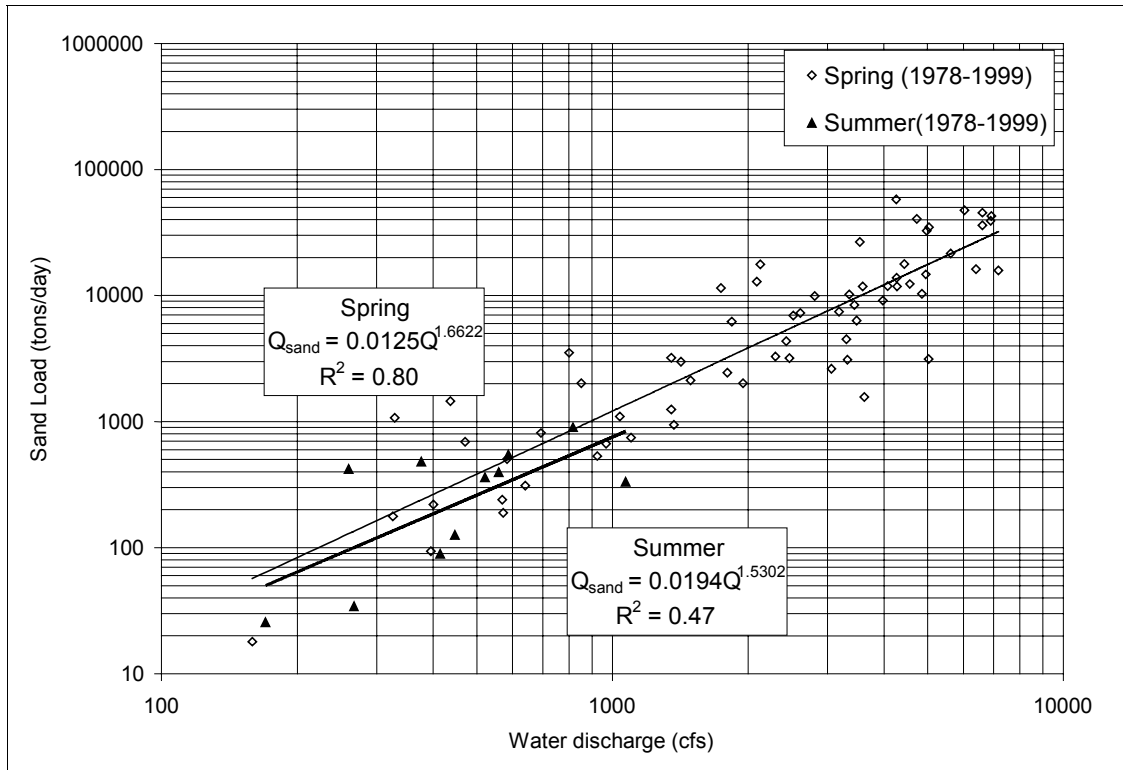


Figure 3-18 Albuquerque Gage sand load rating curve for spring and summer.

Table 3-8 lists the bed material transport capacity estimates for the 1992 and 2001 subreach slopes. The different equation results varied widely for each subreach. In general, subreaches 1 and 3 exhibit similar trends from 1992 to 2001. For these two subreaches, all of the transport equations, with the exception of Laursen and Toffaleti, predict a larger capacity in 2001. This corresponds with the finer material observed in 2001. Subreach 2 generally exhibits the opposite trend whereby having higher sediment transport capacities in 1992 with the same slope. To account for this phenomenon, the grain size distribution curve for this subreach (Figure 3-12) is referred to. It can be seen that half of the subreach bed material got coarser while the other half got finer from 1992 to 2001. No sediment transport capacity exceeds 16,000 tons/day. The sediment transport equations are comparable for some years and slopes, but for the most part significantly different capacities are calculated by each equation (Table 3-8).

The average bed material load transport capacity in 1992 is lower than the average transport capacity in 2001 for subreaches 1 and 3. The average bed material load transport capacity in 1992 is higher than the average transport capacity in 2001 for subreach 2. Again, this trend is seen to be different from subreaches 1 and 3, likely due to the subreach being in a transitional state. All transport capacities are lower than the incoming sand load (17,600 tons/day). This would indicate aggradation in all subreaches, which is not in agreement with the observed degradation of subreach 1, but is in agreement with the observed aggradation of subreaches 2 and 3 that occurred between 1992 and 2001 (Figure 3-4).

In general, the washload is comprised of the fine particles not found in large quantities in the bed ($d_s < d_{10}$) (Julien 1998). The d_{10} of the bed material is on average 0.27 mm (Figure 3-14). The percent of material in suspension finer than 0.27 mm is roughly 66 percent at flows close to 5,000 cfs (Table 3-7), which suggests that very fine and fine sand particles behave as washload. As a result, the incoming bed material load is approximately 6,000 tons/day, which represents 34 percent of the sand load (Appendix G). This methodology for the bed material load estimation is carried out under the assumption that the silt load is small enough to be neglected.

Table 3-7 Bed material transport capacity in tons/day for the 1992 and 2001 slopes.

Bed-material Transport Equations	Existing Slopes					
	S= 0.0010 Subreach 1 1992	S= 0.0009 Subreach 1 2001	S=0.0010 Subreach 2 1992	S= 0.0010 Subreach 2 2001	S=0.0009 Subreach 3 1992	S= 0.0010 Subreach 3 2001
Laursen	7,904	5,455	12,125	5,444	8,757	7,472
Engelund & Hansen	3,913	8,978	13,486	10,687	11,211	13,806
Ackers and White (d50)	3,901	8,448	11,132	9,147	10,559	12,188
Ackers and White (d35)	7,850	10,941	14,100	11,704	12,998	15,309
Yang Sand (d50)	7,828	8,106	9,604	8,919	8,400	10,594
Yang Sand (size fraction)	14,030	10,672	14,216	11,023	11,024	13,258
Einstein	1,001	5,248	6,476	6,993	6,589	9,093
Toffaletti	8,354	8,334	17,813	7,657	13,430	12,322
Average =	6,848	8,273	12,369	8,947	10,371	11,755

The slopes of each subreach were adjusted to match the capacity with the incoming bed material load (5,982 tons/day). The resulting slope predictions for each method and subreach are summarized in Table 3-9. Ackers and White (d_{50}) and Ackers and White (d_{35}) produced very small slopes for all subreaches. Laursen's method produced slopes closest to the 2001 slopes for all subreaches. All other equations predicted slopes that were flatter than the 2001 slopes with the exception of Einstein's equation for subreach 1.

Table 3-8 Resulting slope predictions from sediment transport capacity equations for 2001.

Bed-material Transport Equations	Subreach 1 Q = 5000 cfs		Subreach 2 Q = 5000 cfs		Subreach 3 Q = 5000 cfs	
	Capacity	Slope	Capacity	Slope	Capacity	Slope
Laursen	5,956	0.001	5,875	0.0011	6,207	0.0008
Engelund & Hansen	6,158	0.0007	6,259	0.0007	6,417	0.0006
Ackers & White (d_{50})	5,968	0.0003	5,982	0.0003	6,264	0.0002
Ackers & White (d_{35})	5,589	0.0002	5,380	0.0002	6,520	0.0002
Yang Sand (d_{50})	5,982	0.0007	5,763	0.0007	5,584	0.0006
Yang Sand (size fraction)	5,286	0.0005	5,898	0.0006	5,500	0.0005
Einstein	6,081	0.0012	5,882	0.0007	5,977	0.0004
Toffaletti	6,660	0.0005	6,248	0.0005	9,244	0.0005

3.6. Discussion of Uncertainties

Although it would be desired to use data that are without uncertainties, it is not possible. Data used in the HMA includes discharge, survey, bed material, and suspended sediment. To an extent all of these data contain uncertainties.

Survey data collected by the USBR seem to have the least amount of uncertainties. Many of the cross sections analyzed were physically measured while the other cross sections used were photogramatically surveyed. The photogramatically cross sectioned surveys were calibrated and checked against physically measured cross sections and are a very accurate representation of the cross section.

Another very accurate set of data is the discharge data collected daily by the USGS. In order to ensure the accuracy of these data the rating curves are calibrated

periodically and the records are checked against surrounding stations (Carter and Davidian 1968).

The bed material data seem to exhibit a large range of values for grain sizes at different areas along the reach. Bed material data was collected using pebble counts and discrete point samples throughout the reach. These data were collected periodically throughout the year, which could explain the variability of the sizes. The Rio Grande has high discharge periods in the spring due to snowmelt. For the entire reach the variability of the d_{50} ranges from 12.44 mm to 0.36 mm, with the d_{50} decreasing downstream (Appendix F). Overall the bed material data used in this analysis is good, trends seen in these data are consistent with trends upstream and downstream of the study reach.

Suspended sediment data used in the mass and double mass curves are discussed in Chapter 4.

In summary the data used in this chapter is good. Trends expected with the closure of a dam are seen clearly. The most dependable data used are the survey data then the discharge data and the bed material data, the least dependable is the suspended sediment data. However, all data used is good, some just exhibit more variability than others.

3.7. Summary

This work pertains to the hydraulic modeling analysis of the Corrales Reach of the Middle Rio Grande, which spans 10.3 miles from the Corrales Flood Channel (agg/deg 351) to the Montano Bridge (agg/deg 462). This chapter characterizes the historic conditions of the study reach and evaluates potential future equilibrium conditions. The general trend of the study reach includes a decrease in width, width-to-depth ratio, area, water surface slope, energy-grade line slope and wetted perimeter and an increase in mean velocity and depth during the 1962 to 2001 time period.

Most of the reach aggraded approximately 0.1 feet from 1962 to 1972 and degraded about 2.5 feet between 1972 and 1992. Degradation during the 1972 to 1992 time period exceeded the aggradation that occurred between 1962 and 1972. Therefore, the net change has been degradation between 1962 and 1992. From 1992 to 2001 the bed degraded slightly in subreach 1 and aggraded in subreaches 2 and 3. Maximum aggradation for this time period was about 2.0 feet, which occurred in subreach 3.

The main conclusions for this hydraulic modeling analysis on the Corrales Reach are as follows:

1. The median bed material size in the Corrales Reach comprises of fine sand in 1962 and 1972, fine sand to coarse gravel in 1992, and medium sand to coarse gravel in 2001. Recent field observations indicate that the bed material is characterized by a bimodal distribution (Massong 2001).
2. The active channel width of the study reach decreased from 1,275 feet in 1918 to 474 feet in 2001. The largest change in width occurred from 1918 to 1962. A slight increase in channel width occurred during the 1962 to 1972 time period as a result of the aggradational trend of the river bed. Bed degradation after 1972 induced a small narrowing trend of the channel. The channel width was essentially stable from 1972 to 1992, with a width of approximately 650 feet. From 1992 to 2001 the channel narrowed significantly from 607 feet to 474 feet.
3. Planform geometry of the entire reach is a straight, single-thread channel for 1962 and 1972 and straight, multi channel for 1992 and 2001 at a bankfull discharge of 5,000 cfs. The channel sinuosity ranges increased slightly from 1.14 to 1.17 throughout the entire period analyzed. These values are indicative of a nearly straight channel.

4. At flows close to 5,000 cfs, very fine and fine sand particles ($d_s < 0.0625$ mm) behave as washload. The bed material load is approximately 34% of the sand load (17,600 tons/day). Therefore, the incoming bed material load is approximately 6,000 tons/day.

5. The bed material transport capacity of the subreaches was estimated for 1992 and 2001 using the following sediment transport equations: Laursen, Engelund and Hansen, Ackers and White (d_{50} and d_{35}), Yang – Sand (d_{50} and size fraction), Einstein and Toffaleti (Stevens and Yang 1989, Julien 1998). Laursen’s equation most closely resembles the 2001 conditions, for both slope and transport capacity of the three subreaches, suggesting a slight increase of slope in subreach 1 and 2 and a slight decrease in subreach 3 is necessary to reach a state of equilibrium. The transport capacity results for each subreach are summarized in 3-9; more details can be seen in Tables 3-7 and 3-8.

Table 3-9: Summarized sediment transport results for 1992 and 2001.

Year	Subreach	BML average (tons/day)	Minimum BML (tons/day)	Maximum BML (tons/day)
1992	1	6,848	1,001	14,030
	2	12,369	6,476	17,813
	3	10,371	6,589	13,430
2001	1	8,273	5,248	10,941
	2	8,947	5,444	11,704
	3	11,755	7,472	15,309

CHAPTER 4: Analysis of Mass and Double Mass Curves

4.1 Introduction

Mass curves and double mass curves provide useful information about the history of a river. Applying this type of analysis to the Middle Rio Grande provides information regarding how the river's sediment trends have changed over time. Also, by applying these approaches to an extended portion of a river one can identify the part of the river where the most sediment is flowing into the river. Since Cochiti Dam was constructed in 1973 major changes to the Rio Grande have occurred. However, the effects become less noticeable with distance downstream.

4.2 Reach Background

4.1.1. Reach Definition

Mass and double mass curve analyses were applied to the Albuquerque Reach of the Middle Rio Grande (Figure 2-1). This study reach is 115 river miles long and extends from the Albuquerque gage, River Mile (RM) 183.4, to the San Marcial Gage, RM 68.5. Despite its length, this portion of the river has only one major tributary, the Rio Puerco. This tributary is located between the Bernardo and San Acacia gaging stations. A significant amount of sediment is transported into the reach from the Rio Puerco. A number of smaller arroyos also flow into the river. However, these arroyos only flow at certain times of the year and are relatively small and insignificant to the river.

4.2.1. Data for Analyses

Data used for these analyses included daily suspended sediment and discharge data from four active USGS gages and one discontinued USGS gage. The active gages are Rio Grande at Albuquerque (#08330000), Rio Grande Floodway near Bernardo (#08332010), Rio Grande at San Acacia (#08355000), and Rio Grande at San Marcial (#08358500). These final two stations include data from the floodway and the conveyance channel. The discontinued gage is the Bernalillo gage (#08329500), which operated from 1941 to 1969 (Table 4-1). The Bernalillo gage was located just upstream of the Albuquerque gage, and was discontinued in 1969. However, the data from this gage provides useful information for long-term sediment trend analyses. Table 4.1 shows the daily data used for each gage.

Table 4-1 Periods of Record for discharge and continuous sediment data collected by the USGS

Stations	Mean Daily Discharge	Continuous Suspended Sediment Discharge
	Period of Record	Period of Record
Rio Grande near Bernalillo	1941-1968	1956-1969
Rio Grande at Albuquerque	1942-2002	1969-1989 1992-1999
Rio Grande Floodway near Bernardo	1957-2002	1965-1995
Rio Grande at San Acacia	1958-2002	1959-1996
Rio Grande at San Marcial	1899-2002	1925-1997

Along with the daily suspended sediment and discharge data for each of these gaging stations, the USGS provided additional gage data needed to perform the MEP, dating back to early 1969. The MEP data includes size fractions of the bed material and suspended sediment, mean velocity, depth, width, and temperature. Data used for MEP analysis were collected sporadically throughout the year, some months MEP data were collected three times a month, while other months only one or zero sets of data were collected. In addition to the sporadic data many of the samples were insufficient and the

MEP could not be conducted on these samples. Despite the setbacks in the data sufficient, sediment-rating curves could be created.

4.2. Data Analyses and Results

Mass and double mass curve analyses of the lower Middle Rio Grande required daily sediment and discharge data. However, daily total and sand loads are only obtainable when enough data are available to perform the MEP. To obtain daily values for these loads, rating curves were created and the data were reconstituted. The procedures used in the analysis and the results obtained are outlined below.

4.2.1. Suspended Sediment Mass Curves

Suspended sediment mass curves were created for each gaging station. A representative curve is presented in Figure 4-1, and the additional curves are provided in appendix H. Generating these mass curves was a relatively simple process. The first step was to locate the daily suspended sediment data from the USGS for each site. This was done using the database created by Leon (1998). The second step was to calculate yearly totals of suspended sediment discharge. Finally, the yearly sediment discharges were added in succession, paired with the corresponding years, and then plotted. Breaks in slopes were then identified according to the guidelines outlined by Searcy and Hardirson (1960).

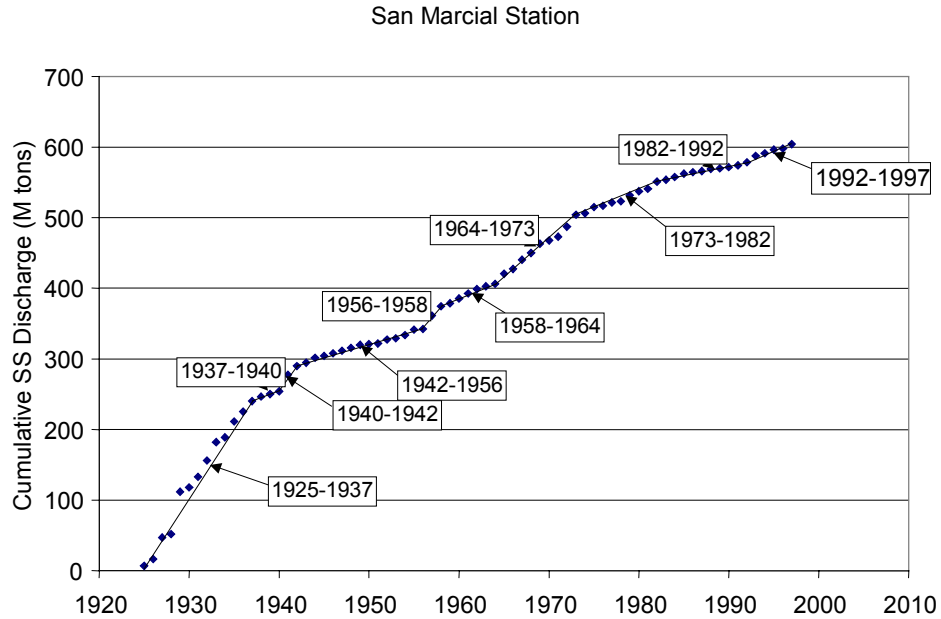


Figure 4-1 Suspended sediment mass curve for San Marcial Gage

Breaks in slope were used to identify changing trends. For all suspended sediment mass curves created, clear breaks in slope were seen in 1973. These breaks in slope were expected because the construction of Cochiti Dam was completed in 1973. It was also expected that the slopes after 1973 would be less than the slopes prior to 1973 because the incoming sediment is trapped at the dam. Further discussion of the impact of Cochiti Dam closure is presented in section 4.2.3.

4.2.2. Sediment Rating Curves for Periods Between Breaks in Slope

Before any rating curves could be created the total and sand load had to be determined using the MEP. Data used by BORAMEP are provided in Appendix I. The definition of the total load calculated by BORAMEP is all sediment sizes transported through a cross section regardless of their source. Sand load is defined as the portion of the total load with a sediment size larger than 0.625 mm. Output values provided by BORAMEP were compared to previous studies to confirm the program was providing accurate data. Using the output values from BORAMEP total and sand load rating

curves were developed. An example of a typical rating curve is Figure 4-2. Time frames used on these rating curves were determined from the breaks in slope of the suspended sediment mass curves Figure 4-1. Once the rating curves were created, a best fit power function for the sand and total load was determined using Excel. These equations were then used to reconstitute sand load and total load data used in the mass and double mass curves. In total 23 sand and total rating curves were created and can be located in Appendix J.

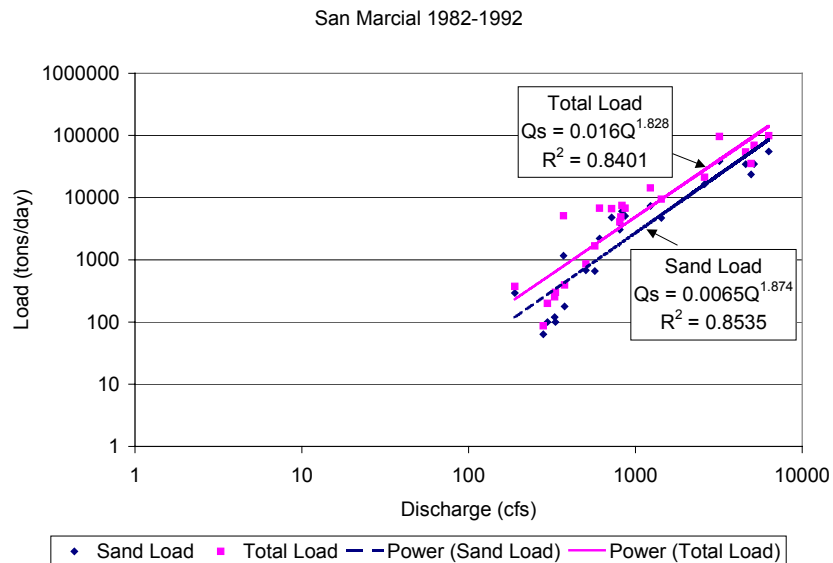


Figure 4-2 Total and Sand Load Rating curve from San Marcial Gage, 1982-1992

4.2.3. Mass and Double Mass Curves

4.2.3.1. Bernalillo and Albuquerque Gages

Data from the Bernalillo and Albuquerque gages were combined in the mass and double mass analysis. These two gaging stations are located very close to each other the Albuquerque gage is just downstream of the Bernalillo gage. Because, at the Bernalillo Gage, suspended sediment data was collected prior to 1969 and no suspended sediment data was collected at the Albuquerque gage prior to 1969, the data

for these two gages were combined. This is reasonable since, prior to the closure of the Bernalillo gage, the flow records for these two gages are almost identical.

Mass curves were created for the gaging station to study the trends in the river and how they have changed over time. Figure 4-3 shows the mass curves for the suspended sediment, total, and sand loads on the primary x-axis, on the secondary x-axis are cumulative values of discharge. Discharge values were added to the mass curves to show that the trends in discharge have not changed significantly after the construction of the dam. A mass curve for the complete period of record can be seen in Appendix H.

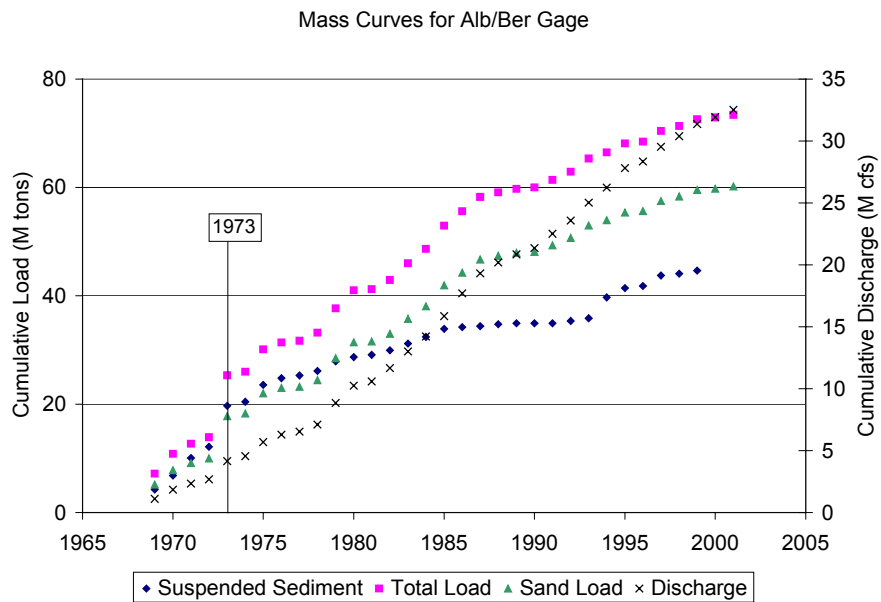


Figure 4-3 Mass Curves for Bernardo and Albuquerque Gages

From the mass curve it can be seen that the sediment loads have been relatively steady since 1973 meaning that when a trend line was determined for this data the r squared value was very close to one. Slopes of the trend lines along with their r-squared values, pre and post 1973, are presented in Table 4-2. Since the slopes of the line are so consistent after 1973 it can be concluded that there has not been a lot of changes to the river that have affected the sediment since the construction of the dam in 1973.

Table 4-2 Mass curve slopes and r-squared values for trend lines for the Bernalillo and Albuquerque gages.

	Pre 1973		Post 1973	
	Slope	r-squared	Slope	r-squared
Sand Load (M tons/year)	2.7375	0.8400	1.6061	0.9715
Suspended Load (M tons/year)	3.4362	0.9711	0.9551	0.9724
Total Load (M tons/year)	3.9398	0.8308	1.8142	0.9703

In addition to the lack of changes in the river, the slopes of the plots also reveal that the sediment being transported by the river has decreased since the closure of Cochiti Dam. This is expected since the dam traps nearly all the sediment coming into it. Prior to the building of the dam the total load's yearly accumulation was over 2 times larger than the value post 1973. Similar trends are seen in the sand and suspended sediment loads; pre dam values are nearly two times and four times larger than the post dam conditions respectively.

Another observation made when examining the mass curves is that the sand load makes up more of the total load after the dam was built. Prior to construction the suspended sediment and sand loads were very close to one another with the suspended load slightly larger. After construction of the dam was completed, the suspended load was still larger for six more years, until 1979, at this time the sand load increased and the suspended load decreased. Because the dam discharges clear water downstream, the bed degraded and coarsened as mentioned in Chapter 3. However, this process did not occur immediately after the dam was completed. It took six years before the sand load was larger than the suspended load. Reasoning for this is that the clear water scour downstream of the dam starts directly downstream of the dam then moves downstream slowly, relatively speaking. Looking at the mass curve it can be seen that the dam's effects were not seen in the transported sediment significantly until 1979.

Double mass curves for this station can be seen in Figure 4-4. These curves show the correlation between the different loads and discharge. It can be seen that there was a significant change in 1973, which was the building of the Cochiti Dam. Cochiti Dam affected the river in many ways but it did not change the annual discharge of the river significantly. This can be seen in the mass curve (Figure 4-3). Because the dam did not significantly change the trend in discharge, the changes in slope on the double mass curve are due to changes in sediment loads.

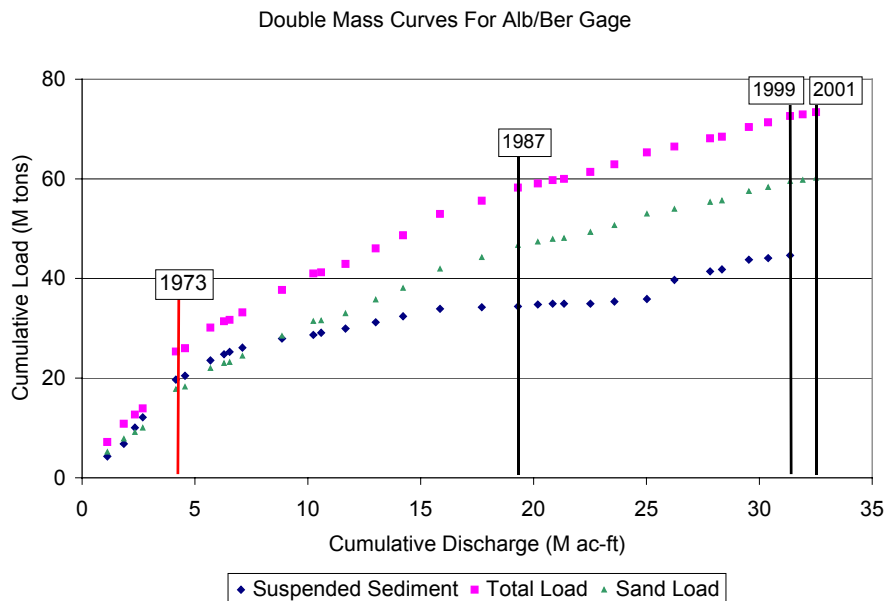


Figure 4-4 Double mass curves for Bernalillo and Albuquerque gages.

By analyzing the double mass curve the decrease in suspended sediment is clear. While the sand load and total load continue to rise the suspended sediment load seems to flatten out after 1985, which may be due to the lack of incoming sediment, as mentioned previously. Also from previous studies by Sixta et al. (2003b), the upstream portion of the Middle Rio Grande has armored therefore very little fine sediment, which is normally suspended, would be transported from the upstream sections.

4.2.3.2. Bernardo Gage

Downstream of the Albuquerque gage is the Bernardo gage. Located farther downstream it is expected that the effects of the dam are not as noticeable as they were at the Albuquerque Gage. Mass curves created for the Bernardo station are shown in Figure 4-5. Again the discharge is presented on the secondary x-axis. The mass curve shows that low flows occurred prior to 1973. Mass curves for the complete record of data can be found in Appendix H.

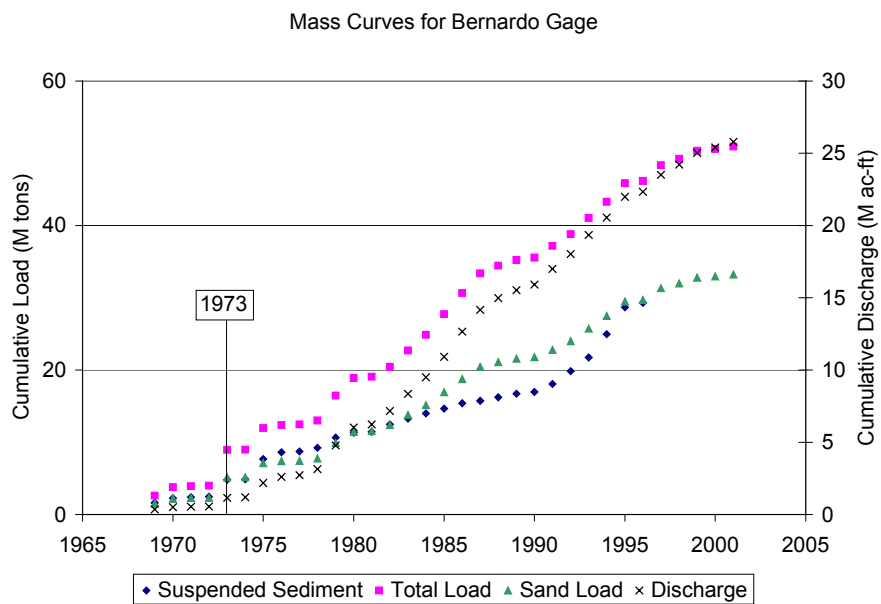


Figure 4-5 Mass Curves for the Bernardo Gage

Like the Albuquerque gage mass curve the suspended sediment was larger than the sand load until a little while after the closure of the dam. Also seen is an increase in suspended sediment after 1991. This could have been caused by a number of things; construction along the banks of the river, increased bed scour from upstream locations, increased bank erosion, etc. Since the river has not changed its planform significantly and the discharge has not increased enough to provide enough energy to increase the bed scour the reason for the increased suspended sediment is more than likely

anthropogenic. However, since average conditions are used over a large area there could be areas where erosion occurs.

The mass curves slopes pre and post 1973 were also examined. Table 4-3 shows these values. R-squared values for total and sand load are low prior to 1973 because only four years of data were available to determine the trend line. An increase in total load and sand load and a decrease in suspended load are seen.

Table 4-3 Mass curve slopes and r-squared values for trend lines for the Bernardo gage.

	Pre 1973		Post 1973	
	Slope	r-squared	Slope	r-squared
Sand Load (M tons/year)	0.7371	0.6811	1.1079	0.9913
Suspended Load (M tons/year)	0.9739	0.9435	0.9048	0.9184
Total Load (M tons/year)	1.2857	0.6805	1.6700	0.9900

A decrease in all types of loads was expected because of the trapping of the sediment by the dam. There could be many reasons why the loads increased after the closure of the dam such as; increased incoming sediment from overland flow and/or tributaries, bed scour upstream of the station, increased flows etc. As mentioned previously only four years of data were used in the determination of the slope for the sand and total loads. These values were determined using sediment rating curves with discharge as the independent variable in the equation. So, an increase in discharge will show an increase in sand and total loads. Because the suspended load decreased after 1973 it is likely with more sand and total load data prior to 1973 these would also decrease. The most logical reason for the increase in total and sand loads is the low flows that occurred from 1969 to 1973.

As for the other potential reasons for the increased loads post dam construction, increased loads due to tributaries is very unlikely because of the lack of major tributaries

or arroyos between Albuquerque and Bernardo. Scour from the upstream portion of the river is also unlikely because the load being transported prior to the dam was very large and by trapping most of the incoming sediment clear water scour would occur at the downstream of the dam. This clear water scour may have increased the sediment loads for a few years after the dam was built. However, studies show that downstream of the dam is armored thus the sediment being supplied and transported through these areas are low (Sixta et al. 2003b).

Double mass curves for the Bernardo gage are presented in Figure 4-6. These curves show a large decrease in the proportionality of discharge and load after 1973. A result like this was expected. Low flows prior to 1973, as shown in the discharge mass curve, still transported large sediment loads hence the slope of the double mass curve is large. Prior to 1973, the suspended sediment was large and the closure of the dam trapped all of it thus depleting the sediment supply. This decrease in supply is seen; the slopes of the double mass curves decrease even though the discharge increases therefore less sediment is being transported during larger flows.

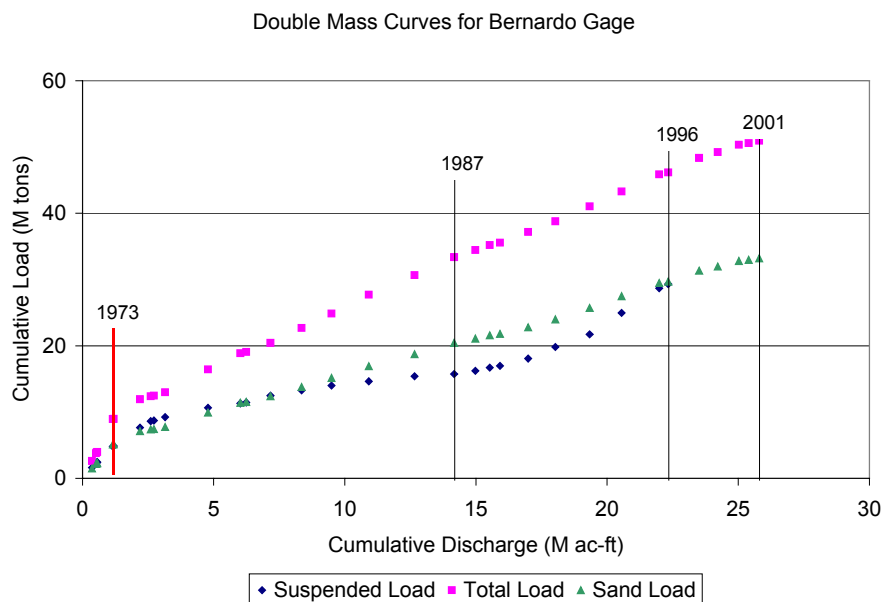


Figure 4-6 Double mass curves for the Bernardo gage

Examining the mass and double mass curves one can see that the suspended sediment and sand load are almost the same. This could be an indication that the dam has less affect on this data than the Albuquerque gage data. However Cochiti Dam does have a large effect as can be seen be the decrease in proportionality after 1973.

4.2.3.3. San Acacia Gage

Data from the San Acacia gage yielded anomalous results. At this site the suspended sediment loads were larger than the total load. This is not physically possible; by definition part of the total load is the suspended load. Reasons for this anomaly is more than likely the way the different loads were determined. The USGS determines the suspended sediment by taking a point sample then calculating the suspended sediment using an equation calibrated for the cross-section from which the sample was taken (Porterfield 1972). It is possible for the calculated suspended sediment load to exceed the total load using this method (Pers. Comm. P. Julien 2004). Despite the obvious errors mass and double mass analysis was still carried out because sediment trends could be identified but not quantified. Mass curves for the San Acacia gage are shown in Figure 4-7. This figure illustrates the point mentioned previously that the suspended sediment is larger than the total load.

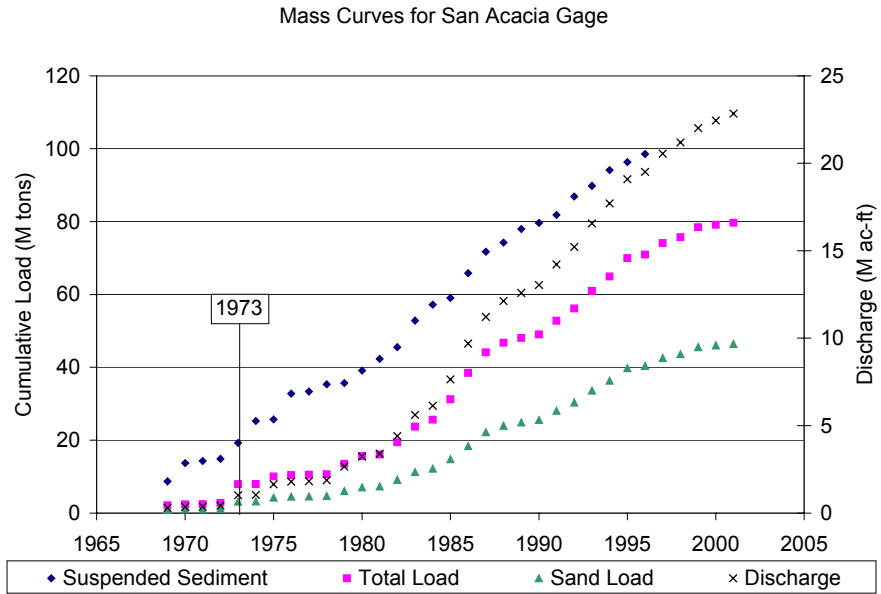


Figure 4-7 Mass Curves for the San Acacia Gage

By examining the mass curve we see that the slope of the line has not change significantly since 1969. When the slopes were calculated for pre dam conditions they show that the slopes for sand and total load are a lot smaller than the post dam slopes (Table 4-4). However, when a trendline is determined for all of the total and sand load data the slopes are 2.8 and 1.6 with r-squared values of 0.97 and 0.95, respectively. Like the Bernardo gage, the lack of data prior to 1969 does not give accurate results for pre dam conditions.

Table 4-4 Mass curve slopes and r-squared values for trend lines for the San Acacia gage.

	Pre 1973		Post 1973	
	Slope	r-squared	Slope	r-squared
Sand Load (M tons/year)	0.4666	0.6109	1.8041	0.9695
Suspended Load (M tons/year)	3.7782	0.9476	3.5750	0.9904
Total Load (M tons/year)	1.1989	0.5899	3.0173	0.9761

Between the Bernardo gage and San Acacia one of the largest tributaries of the Rio Grande, the Rio Puerco, is located. The Rio Puerco discharges a significant amount of sediment into the river (Richard et al. 2001). Because of this the sediment load per year should be significantly larger than the upstream stations. Also, because of the sediment from the Rio Puerco the effects of the dam are not as noticeable. Pre and post dam slopes of the suspended load show a slight decrease. This slight decrease is more than likely a result of the closure of the dam, but this a very small change and could be due to any number of reasons.

Double mass curves also show very little of the dam's effects (Figure 4-8). Total and sand load data show a straight line for the duration of the curves. This means that the constant of proportionality between discharge and sediment load did not change after the construction Cochiti dam. The suspended sediment double mass curve does have a change after the construction of the dam but not for a number of years. There is a distinct change in slope around 1981 and 1982. After that the slope is almost parallel to the total load curve.

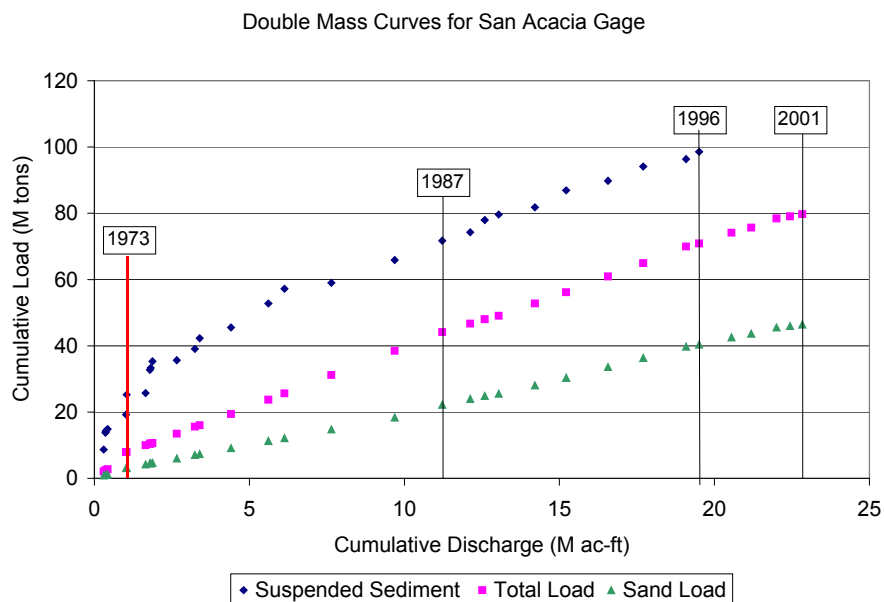


Figure 4-8 Double mass curves for the San Acacia gage

Many things could have caused this break in slope such as changes in sampling techniques, changes to the station itself, and the lag time before the dam's effects reached the station. Looking at the historical flow data for this site, a low flow conveyance channel (LFCC) was constructed in 1958. A number of LFCC's were constructed along the middle Rio Grande to increase water delivery to Elephant Butte Reservoir. These structures were in use continuously from their construction through the early 80's (Pers. Comm. D. Baird 2004). According to USGS discharge data, the LFCC at the San Acacia is still used sporadically today but continuous use of it ended in the early 80's. Discontinued use of the LFCC increased flows through the station as seen in the discharge mass curve in Figure 4-7. The increased flows are probably the cause of the break in slope. Looking at the suspended sediment mass curve the amount of sediment transported per year is constant over the duration of the study so an increase in discharge would decrease the slope of the double mass curve.

Even though increased flows attributable to discontinued use of the LFCC's are the most probable cause of the break in slope, other changes may also be significant. The San Acacia gage is very far down stream from Cochiti Dam so the effects of the dam may not be seen for years, but these effects were seen almost immediately at the upstream stations.

4.2.3.4. San Marcial Gage

San Marcial gaging station is located just upstream of the Elephant Butte Reservoir and is the furthest station downstream from Cochiti Dam. Mass curves created using data from this station are presented in Figure 4-9. Like the San Acacia station the San Marcial station has a LFCC. However, continuous use of the LFCC stopped in 1977. This stoppage of use does not show a significant change in the discharge meaning the mass curve does not have a clear break in slope at 1977.

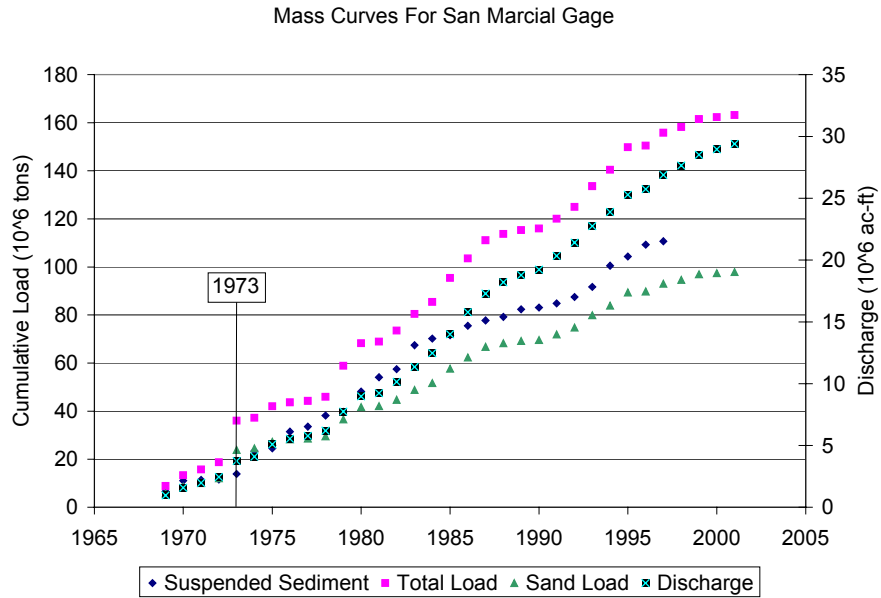


Figure 4-9 Mass Curves for the San Marcial Gage

Also seen in the mass curves is the suspended sediment is larger than the sand load. The Rio Puerco supplies a significant load of fine sediment upstream of the San Acacia gage so the suspended sediment should be larger than the sand load. At the San Acacia gage the suspended sediment load was larger than the sand load too but it was also larger than the total load. Since one or both of the analyses contained errors conclusions cannot be made by comparing them.

Table 4-5 shows the comparison of slopes pre and post dam. Like the previous three stations pre dam slopes for the sand and total load only used four years of data but the trendline determined fit the data better than the previous three stations. Comparing pre and post 1973 slopes, there is a slight decrease in the sand and total load slopes and a very slight increase in the suspended load slope. A slight decrease in the slopes would be expected due to the impacts of Cochiti Dam.

Table 4-5 Mass curve slopes and r-squared values for trend lines for the San Marcial gage.

	Pre 1973		Post 1973	
	Slope	r-squared	Slope	r-squared
Sand Load (M tons/year)	3.9587	0.8063	2.9595	0.9891
Suspended Load (M tons/year)	3.7970	0.9806	3.8360	0.9800
Total Load (M tons/year)	5.9818	0.8224	5.0915	0.9881

At the San Acacia gage the expected effects of the dam were not seen but they are seen quite clearly in these double mass curves, Figure 4-10. In 1973 there is a change in slope that indicates a decrease in the total and sand loads. Between 1972 and 1973 the suspended sediment transport rate decreased to much less than the sand load. This is probably due to the construction of the dam. With a large amount of sediment incoming from the Rio Puerco and being so far downstream of Cochiti Dam a break in slope should be hard to identify. Even though the break in slope is easy to locate it is not a large change, this is consistent with the fact of large sediment loads and distance downstream of the dam.

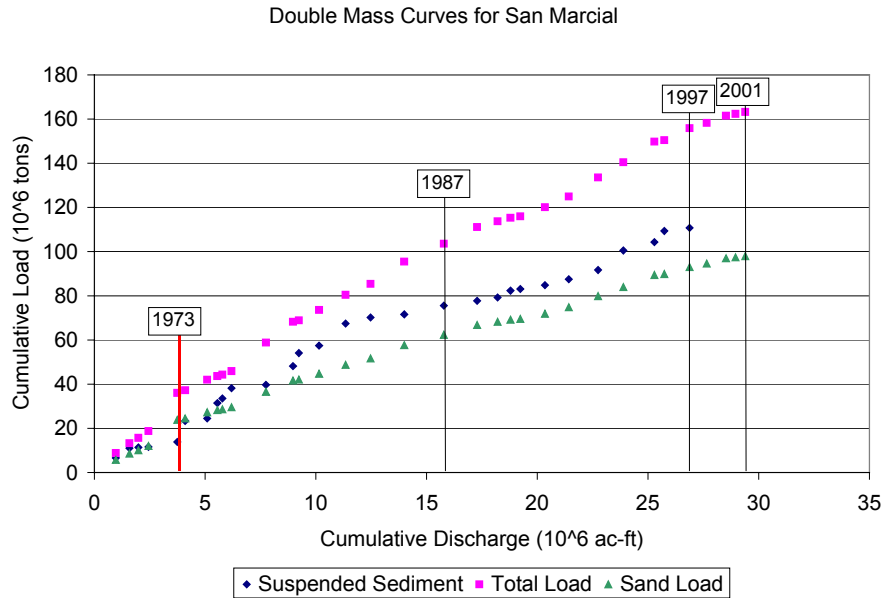


Figure 4-10 Double mass curves for the San Marcial gage

The suspended load double mass curve seems quite erratic from 1973 to 1981. During this period of time the LFCC was being used less frequently so the increased flow through the floodway may have increased the suspended sediment transport but there is not a significant change in the discharge mass curve that indicates a large change in discharge. Since a lot of suspended sediment comes from the Rio Puerco it is more likely that the erratic behavior of the suspended sediment is due changes or inconsistent flow conditions of the Rio Puerco.

Some interesting observations were seen at the San Marcial station, many of which were not seen at the upstream gages. Large sediment loads from the Rio Puerco and the distance away from the dam is the cause for these different observations. The San Acacia gage should have had similar results as the San Marcial station but there was an error in the data at the San Acacia Gage.

4.3. Summary of Double Mass Curves

Mass and double mass analyses were utilized to obtain information about the Albuquerque Reach's responses to the construction of Cochiti Dam. This analysis was applied to four current USGS gages, Rio Grande at Albuquerque, Rio Grande Floodway near Bernardo, Rio Grande at San Acacia, and Rio Grande at San Marcial. These four gages were chosen because they have a continuous daily suspended sediment record. Along with the USGS gage daily data, MEP data was also used from these four stations to calculate the total and sand loads. With these total and sand loads rating curves were created, daily values were then determined using these rating curves. After all of the daily data was determined mass and double mass curves were created.

Since the MEP data only dated back to 1969 the total and sand load mass and double mass curves used discharge data from 1969 to 2002. Mass and double mass curves for discharge and suspended sediment were created for the entire period of record at the station, these can be found in appendix J and H respectively.

Bernalillo and Albuquerque gage data are combined to create the mass and double mass curves seen in Figures 4-3 and 4-4. Analyses of these curves reveal that Cochiti Dam has had a large impact on the river at this station. A large break in slope at 1973 in both the mass and double mass curves indicate this. After 1973 the slopes of the mass curves did not change much, since the slopes have not changed it can be concluded that there has not been a lot of changes to the river that has affected the sediment since 1973.

Also seen in the mass curves is the decrease in sediment transported since 1973. Of the three loads scrutinized the suspended load decreased the most. Prior to the construction of Cochiti Dam the suspended sediment load was larger than sand load but after the dam was constructed the sand load is larger than the suspended load

because the dam traps a significant amount of sediment flowing into the reach. However, this was not seen immediately after the closure of the dam but six years later. Being located 40 miles downstream of the dam the affects of the dam on the suspended sediment and sand load due to clear water discharge took a while to reach the station.

Double mass curves at the Albuquerque station reveal much of the same things the mass curves did. They show the relationship between the loads and discharge, this relationship clearly changes in 1973. Since the discharge mass curve does not show any significant changes over time the break in slope of the mass curves is due to a change in sediment being transported.

Downstream of the Albuquerque gage is the second of the stations used in the analysis, the Bernardo gage. Since there are not any significant tributaries or arroyos between the Albuquerque gage and the Bernardo gage many of the same trends are seen at the Bernardo gage. However when comparing the slopes of the mass curves pre and post dam the sand and total load slopes slightly increased after 1973 while the suspended sediment load slope decreased as expected.

The reason for the increase in sand and total load is probably a combination of lack of data prior to 1973 and low flows from 1969 to 1973. Only four years of data were available to determine the slopes of the mass curves for the sand and total loads and the trendline did not fit the data very well. Since the sand and total loads were also determined using the discharge, lower discharges would provide lower loads. It can be seen in the mass curves, Figure 4-5, that the flow rates from 1969 to 1973 were quite low so the reason for the increased slopes is small discharges.

Other reasons such as sediment from incoming tributaries or overland flow and bed scour upstream from the station are not likely the cause of this. As mentioned previously there are not any significant tributaries or arroyos upstream of the Bernardo gage so not a lot of sediment is coming from the tributaries or arroyos. Increased bed

scour upstream as a cause of the increased slope is unlikely. Cochiti Dam traps most of the incoming sediment, which causes clearwater scour downstream of the dam. This scour may have increased the sediment loads but this would only occur for a short period of time until the supply of sediment has been exhausted as seen by the armoring of the bed.

Double mass analysis indicates a change in proportionality between discharge and sediment load in 1973, as expected. Also seen from both the mass and double mass analysis is the fact that the suspended load and sand load are nearly identical for the duration of the study. This indicates that the dam's effects are lesser here than upstream.

The San Acacia gaging station was the third station downstream of Cochiti Dam that was studied. Errors in data provided very strange results at this station. Analysis of the data shows that the suspended sediment is larger than the total load, which is not physically possible. This type of error is not uncommon and mass and double mass analysis was still carried out.

Looking at the mass curves one can see that the slope of the curves do not change significantly over the duration of the study. However when slopes pre and post 1973 are compared they indicate a significant increase. This is due to the lack of data pre 1973. Analysis done on the complete set of data shows that the slope is essentially constant.

Double mass curves at this station show very little of the dam's effects; there isn't a clear break in slope in 1973. Being so far downstream of the dam and having a large supply of sediment incoming from the Rio Puerco is the reason for this. Even though the dam's effects are not seen at this station there is a break in slope in the suspended sediment curve in 1981 or 1982. Around this time the LFCC stopped being used continuously thus increasing the flows through the floodway. Since the slope of the

suspended sediment mass curve remained constant an increase in discharge is the reason for the break in slope.

Farthest downstream of Cochiti Dam and just upstream of Elephant Butte Reservoir is the San Marcial station, the final station studied. Examining the mass curves from this station, Figure 4-9, little change in discharge is seen since 1969. Even though, like the San Acacia gage, the LFCC stopped being used continuously in 1977. Also seen in the mass curves is the fact that the suspended sediment is larger than sand load. Fine sediment from the Rio Puerco is the cause for the large amount of suspended sediment. Comparing the slopes of the mass curves the sand and total load slopes decrease slightly while the suspended sediment load remained essentially constant. Because of the effects of the dam a slight decrease was expected.

Double mass curves for the San Marcial gage indicate a break in slope in 1973, see Figure 4-10. These breaks in slope were not seen in any of the curves at the San Acacia gage. Because of the incoming sediment from the Rio Puerco and the large distance from Cochiti Dam the slope of the double mass curve should be constant over the period of study. Even though this is not the case the change in slope is clear but very small indicating the dam has some effect on this station but very little, as expected.

Another observation seen at the San Marcial gage is erratic suspended sediment concentrations from 1973 to 1981. According to the station records during this time the LFCC was being used off and on to divert water. However since the discharge mass curve does not show a change in discharge over this time the erratic behavior is due to changes in the suspended sediment. Since the Rio Puerco brings in a large amount of sediment, changes in the flow in the Rio Puerco are the probable cause of the erratic suspended sediment data.

Comparison of all the stations data can indicate where sediment is coming from and how the dam affects each station. A comparison of the different loads is presented

in Figures 4-11 and 4-12. Mass curve slopes were used to estimate the total, suspended and sand loads. Pre and post 1973 loads were determined for all stations for all data in addition the Rio Puerco suspended load was also determined. The San Marcial gage is unique in that it has a large amount of suspended sediment data prior to 1973. By examining the suspended sediment mass curve a very large break in slope was seen in 1941, so the slope pre 1941 was also determined. A large flood in 1941 that had severe effects on the river is the cause of the change in the suspended sediment load; the load previous to the flood was 16.8 M tons/year.

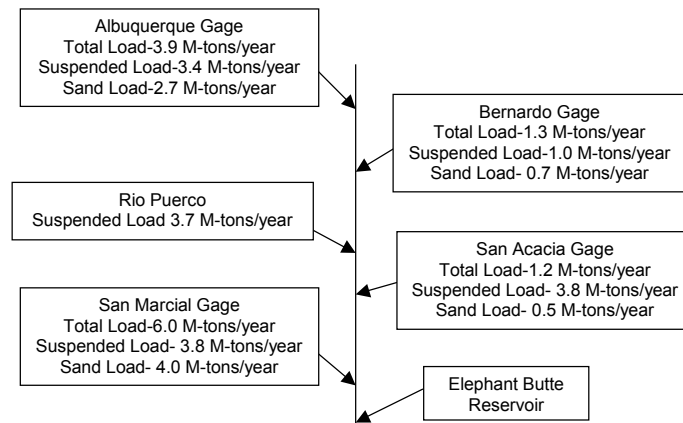


Figure 4-11 Pre-dam loads and their relative locations on the Rio Grande.

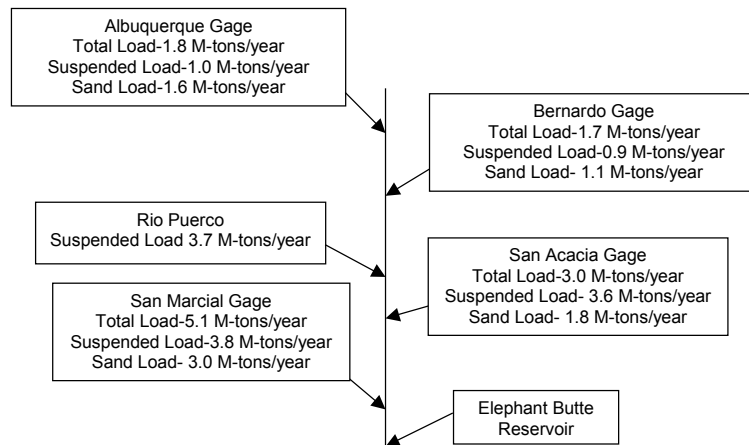


Figure 4-12 Post-dam loads and there relative locations on the Rio Grande.

It was expected, before any analysis was carried out, that the Albuquerque and Bernardo gages would have almost the same amount of sediment transported due to the lack of tributaries and arroyos between the gages. While the sediment transported through the San Acacia and San Marcial gages would be larger than the two upstream gages because of the Rio Puerco. However, these trends were not seen for the different loads at all of the gages.

Prior to 1973 the slopes of the sand and total load do not convey an accurate interpretation of the trends of the river because only 4 years of data was used to determine the slopes. In order to identify an actual trend the slope must be constant over 5 years (Searcy and Hardison 1960). This may explain the reasons for the large total and sand loads at the Albuquerque and San Marcial gages and the small loads at the other two gages. In order to analyze the sediment budget prior to 1973 the suspended sediment should be examined.

The suspended sediment values for the Bernardo, San Acacia and San Marcial seem to be accurate meaning there is a significant increase in the suspended sediment downstream of the Rio Puerco, 2.8 M tons/year. However, at the Albuquerque gage prior to 1973 the suspended sediment transported seems to be very large, only 0.4 M tons/year smaller than the suspended sediment at the San Marcial gage. Evidence suggests that the Albuquerque gage data is more accurate than the Bernardo gage data, because it follows trends expected after the construction of a dam. Because the river was very sediment laden prior to the construction of Cochiti Dam the sediment being transferred was nearing the rivers transport capacity. Only a small amount of sediment from the Rio Puerco could be transported because of the limiting capacity, it is highly unlikely that the Rio Grande could transfer and additional 3.7 M tons/year prior to 1973 (Baird Pers. Comm. 2003). This explains the small difference in the suspended sediment loads between the Albuquerque and San Marcial gages. As mentioned previously errors

in suspended sediment measurements are not uncommon and since the data of the Bernardo gage were only collected for eight years prior to 1973 calibration of the measurement techniques are the probable cause for the discrepancy.

Trends for the data post 1973 were expected to show a decrease in sediment transport. This is seen at all of the gages for suspended load but these trends were not seen in the sand and total loads. Mentioned previously is the lack of data for the sand and total loads prior to 1969 so the comparison of the slopes pre and post dam cannot give dependable results.

Comparing the values for the sand and total loads at each gage the results seem to vary. For the two upstream gages, Albuquerque and Bernardo, the results seem reasonable, the total and suspended loads do not change from gage to gage but the sand load at the Albuquerque gage is 0.5 M tons/year larger than the sand load at Bernardo. Being closer to the dam and the fact that the bed upstream of Albuquerque is armored, the Albuquerque gage has coarser sediment transported passed the gage. Between the two gages the bed is made of finer particles that will be transported before the sand particles thus the sand load at Bernardo is smaller than the sand load at Albuquerque.

Some peculiar results are obtained at the San Acacia gage. The total load is less than the suspended load, which is not physically possible. Since both procedures, MEP and suspended sediment sampling, are very complicated and error prone it is not unusual for this to occur. Comparing the values for each there is only a difference of 0.6 M tons/year, which is small in terms of sediment transport. Results obtained seem to make more sense when it is noted that the Rio Grande downstream of the Rio Puerco is very sediment laden and the majority of the total load should be in suspension thus the suspended load and total load should have almost the same value.

At the San Marcial gage the total load seems to be too large. Between San Acacia and San Marcial there are no major tributaries so a 2.1 M tons/year increase in sediment is highly unlikely. Again complications due to the MEP are the probable cause for the difference between the two gages. In order to get the best idea of what is occurring after 1973 the suspended sediment loads should be examined.

Comparing the suspended sediment loads of all four gages post 1973 the expected results are seen. Albuquerque and Bernardo gages have about the same amount of sediment being transported past each gage. A significant increase in suspended sediment is seen from Bernardo to San Acacia due to the Rio Puerco, which supplies an estimated 3.7 M tons/year of suspended sediment into the Rio Grande. At the San Marcial gage a slight increase is seen in suspended sediment.

Prior to the construction of Cochiti Dam the Middle Rio Grande was a very sediment laden river. Because of the large amount of sediment being transferred the capacity of river to transport any additional sediment was very low, thus incoming sediment from the Rio Puerco did not affect the suspended sediment by a large amount. After 1973 the sediment transport trends of the Rio Grande has changed significantly. A large decrease in sediment occurred at the two upstream gages due to the dam. At the downstream gages the suspended sediment remained about the same but the source of the sediment is the Rio Puerco. Even though the sediment trends changed due to Cochiti dam the transport capacity has appeared to remain constant at an estimated rate of 3.8 M tons/year. This result makes sense since the channel geometry (Figures 3-4, 3-6, and 3-8) and flow conditions (see Figures 4-3, 4-5, 4-7, and 4-9) have not changed drastically since 1973.

4.4. Discussion

A combination of the analyses from Chapters 3 and 4 can provide valuable information on how the river has behaved. In Chapter 3 HMA was performed on the Corrales Reach. Analysis of this reach showed that since 1973 the bed of the Middle Rio Grande has degraded on average about 2.4 ft while the width of the river has remained essentially constant at around 600 ft (Figures 3-6 and 3-9). This indicates that the majority of the sediment eroded is derived from the bed and not from the banks. It is also known that the bed of the Rio Grande from Cochiti Dam to Albuquerque has degraded up to 4 feet and armored since 1973 (Sixta et al. 2003a). By knowing the amount of sediment coming into the reach via mass curve analysis (Chapter 4), and the fact that the upstream portion of the bed has degraded and armored, one can estimate how much sediment is coming from the bed of the river and how fast the degradation front will travel downstream.

A significant change in the suspended mass curve is also observed at the Albuquerque gage after the closure of the dam in 1973, Figure 4-13. By comparing the pre and post dam slopes of this mass curve the average difference in suspended sediment transport can be quantified. The difference in suspended sediment transport at the Albuquerque gage was estimated to be 2.6 M tons/yr (Figure 4-13). This decrease is a direct result of the closure of the dam. The difference in suspended sediment transport was not nearly as noticeable at the other gage because they are further downstream of the dam, Figure 4-11, 4-12 and 4-14. These downstream gages still receive enough suspended sediment from the degrading bed upstream and tributaries to keep the dam's effects to a minimum.

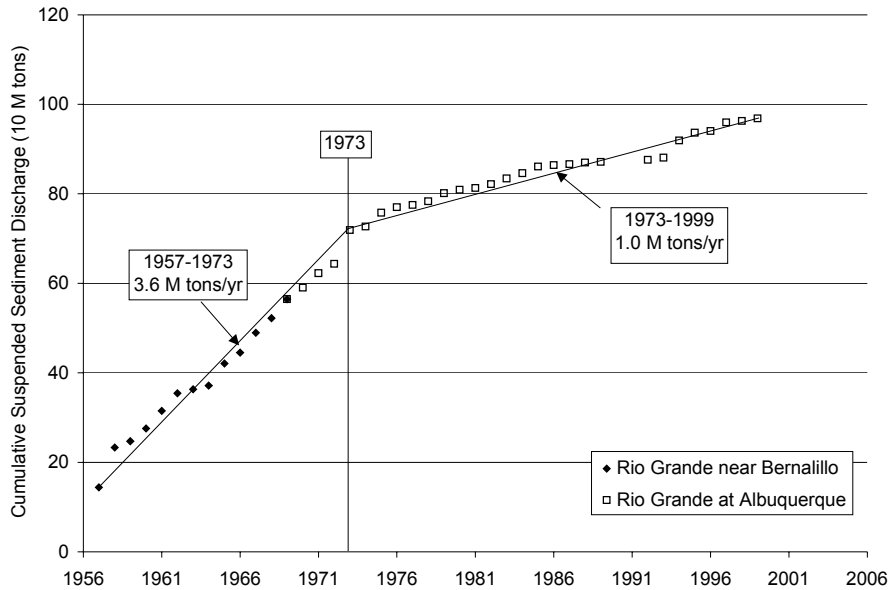


Figure 4-13 Suspended mass curve for Bernalillo and Albuquerque gages, with pre and post-dam slopes.

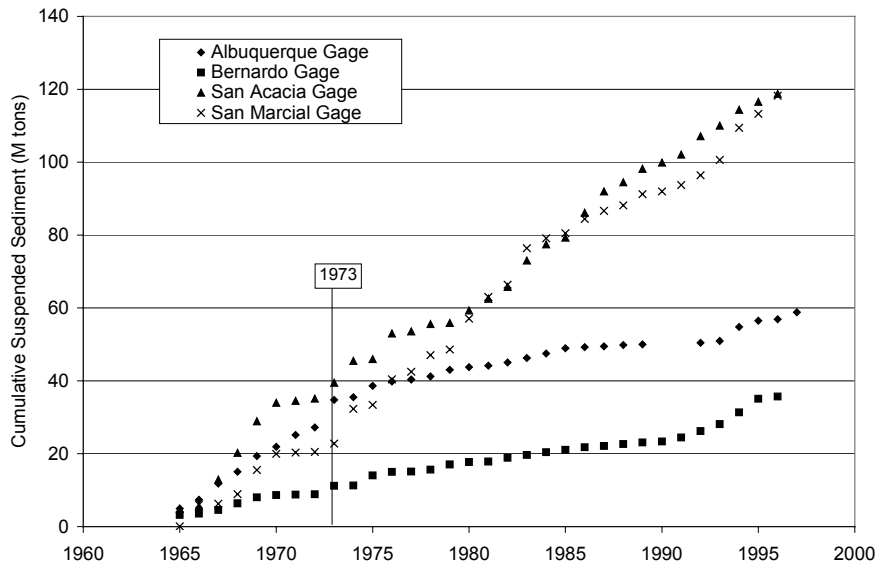


Figure 4-14 Suspended mass curves of all gages examined.

Figure 4-14 shows all four suspended sediment mass curves. Comparing the curves to each other it appears that all of them are very similar from 1965 to 1973, with the exception of the Bernardo gage. After the dam was built the Albuquerque gage curve flattens out while the other two continue to climb at almost the same rate. Examining

aerial photos of the study reach there is only one large tributary, the Rio Puerco. Assuming that there is very little or no sediment from overland flow and smaller arroyos and tributaries the amount of sediment supplied by the Rio Puerco is about 3.7 M tons/year.

The average rate at which the bed degradation front moves downstream can be estimated from: 1) the difference in pre and post dam suspended sediment transport rates, 2) the average depth of degradation, 3) the average active channel width; and 4) the average bulk density of bed sediments. As determined from Figure 4-13, the average difference in pre- and post-dam suspended sediment transport rates is approximately 2.6 M tons/year. Since 1973 the bed of the river from the dam to Bernalillo has degraded about 3.5 ft on average (Sixta et al. 2003b). The average width of the river upstream of the Albuquerque gage is about 400 ft. A typical bulk density for river sediments is approximately 100 lbs/ft³ (0.05 tons/ft³) (for quartz materials with an in-situ porosity of 0.6). Combining these values, the degradation front moves downstream at an estimated rate of 7 miles/year. Over the period 1973 to 2001, the degradation front is estimated to have progressed approximately 197 miles downstream of Cochiti dam. Evidence suggests this to be true, as much as 4 feet of degradation has occurred just upstream of the San Acacia gage (Richard 2001). An estimation of the total volume of sediment transported due to degradation is 275,800 ft³. Most of this sediment will be deposited in Elephant Butte reservoir just downstream of San Marcial. Elephant Butte Reservoir has a total capacity of 2,106,423 acre-ft (9.2*10¹⁰ ft³) so the sediment from degradation will not affect the life of this reservoir significantly.

Since, San Acacia gage is downstream of the Rio Puerco it appears that the front of degradation and the amount of degradation due to the dam is not affected by the large amount of sediment from the Rio Puerco. The amount of sediment from the degradation of the bed can be again estimated from the length of the reach, the active channel width,

the average depth of degradation and the average bulk density of bed sediments. Using the same numbers mentioned previously and the distance of 14.6 miles, the distance between the Bernardo and San Acacia gages. The approximate amount of sediment from the bed is 5.4 million tons which comes out to 190,000 tons/year for the period of 1973 to 2001. This is a very small amount compared to the total of 3.7 M tons/year from the Rio Puerco. However when the same analysis is performed on the 49-mile reach from Cochiti Dam to the Albuquerque gage the approximate amount of suspended sediment from the bed is 647,000 tons/year, which is 65% of the incoming sediment according to Figure 4-13.

Looking at the big picture of the river from Cochiti Dam to Elephant Butte Reservoir the reach has degraded due to the construction of the dam. However this amount of degradation does not provide a significant amount of sediment to cause concern for the reservoir. Also observed is the fact that almost 65% of the incoming sediment at the Albuquerque and Bernardo gages, post dam, is due to the degradation of the bed. However the sediment due to the degradation of the bed is very small compared to the incoming sediment of the Rio Puerco. Most of the suspended sediment at the San Acacia and San Marcial gages is from the Rio Puerco.

4.5. Discussion of Uncertainties

Data used in the mass and double mass analysis seem to contain a lot of variability. Most notably, at the San Acacia gage where the total load is less than the suspended load. Many uncertainties in the collection and calculation of the suspended sediment and MEP data used are the reasons for these anomalies.

Daily suspended sediment data collected by the USGS are known to vary from the actual. Suspended sediment is calculated daily using USGS procedures outlined by Porterfield (1972). Inadequacies in data could be caused by any number of factors most

common is that too few samples were collected to cover the natural variation in concentration (Porterfield 1972). Many studies have been conducted on the accuracy of these data but none have been definitive. However since trends observed in the suspended sediment loads are consistent with what would be expected in this reach the data used are very good.

The rating curves used in the determination of the total and sand loads were created using MEP results. A large amount of data is needed to conduct the MEP. All of these data used contain some uncertainties. The MEP is complex and is prone to variability due to the nature of the procedure, see Chapter 2. Examining the rating curves (Figures 3-18, 4-2 and Appendix J) one can see that the range of variability varies from a very small amount to more than one order of magnitude. The variability seen in the rating curves is exaggerated once all of the daily values are determined and summed to create mass curves. Because of the combination of a large amount of data and the very complicated MEP a large amount of variability can be expected.

Variability in the results of this chapter is the direct results of uncertainty in data and the complexity of the MEP. Although it is difficult to quantify the degree of uncertainty of the results, the accuracy of the suspended sediment data is more reliable than the MEP results.

CHAPTER 5: SUMMARY AND CONCLUSIONS

5.1. Introduction

Two separate analyses were performed on the Middle Rio Grande for this thesis: a Hydraulic Modeling Analysis (HMA) and a Double Mass Analysis (DMA). These analyses were performed to examine the behavior of the river and to predict how the river will respond to changes. The HMA was performed on Corrales Reach of the Middle Rio Grande, this reach spans 10.3 miles from the Corrales Flood Channel to the Montano Bridge. Mass and double mass curves are calculated for the entire Albuquerque Reach, from Albuquerque to San Marcial. Ultimately the HMA and DMA analyses will help in restoration and management of the river system.

5.2. Hydraulic Modeling Analysis (HMA)

Using data that included cross sections, discharge, suspended sediment, bed material particle size, and aerial photos a model was created utilizing HEC-RAS[®] 3.0 to aid in the analysis of the Corrales Reach. General trends from the analysis show a decrease in width, width-to-depth ratio, cross sectional area and an increase in mean velocity and flow depth during the 1962 to 2001 time period. More comprehensive conclusions consist of:

- An aggradation of 0.1 feet from 1962 to 1972 and a severe degradation of 2.5 feet from 1972 to 1992 while the bed elevation changed very little in

subreaches 1 and 2 from 1992 to 2001 while subreach 3 aggraded as much as 2 feet. Clear water scour due to the construction of Cochiti Dam is the reason for the change in trends from aggradation to degradation.

- Bed material coarsened from fine sand in 1962 and 1972 to a mixture of fine sand and coarse gravel in 1992, and medium sand to coarse gravel in 2001.
- From 1918 to 2001 the active channel width decreased from 1275 feet to 474 feet, the largest decrease in width occurred from 1918 to 1962. An increase in width was seen from 1962 to 1972 due to the aggradational trend of the bed. From 1972 to 1992 the width remained stable at about 605 feet, then the width decreased to 474 feet from 1992 to 2001.
- In 1962 and 1972 the planform geometry was characterized as a straight single thread channel then changed to a straight multi channel pattern in 1992 and 2001 for a channel forming discharge of 5000 cfs. Sinuosity ranged from 1.14 to 1.17 (Figure 3-5) for the entire study reach indicating a nearly straight channel for the duration from 1918 to 2001.
- For all three subreaches the bed material transport capacity was estimated using a variety of transport equations (Tables 3-7 and 3-8). Of the equations used in this analysis Laursen's provided the best results for 2001, for both slope and transport capacity, for all three subreaches. In order to reach a state of equilibrium Laursen's equation suggests a slight increase in slope for subreaches 1 and 2 and a slight decrease for subreach 3

5.3. Double Mass Analysis (DMA)

Data from four USGS gaging stations (Albuquerque, Bernardo, San Acacia and San Marcial) were used to create mass and double mass curves. Pre and post dam

slopes of each mass curve were determined to examine the effects that Cochiti Dam has had on the sediment transport. Also observed was the effect of the Rio Puerco on the mass curves.

At the Albuquerque gage the decrease in sediment transport before and after 1973 was very identifiable but the other gages only show a slight changes in sediment transport. Also seen at the Albuquerque gage the incoming sediment load before 1973 was 3.4 M tons/year and the load after 1973 was 1.0 M tons/year. For the other three stations there was not a large decrease in sediment transport after 1973 because the dam's effects on the river decreased with downstream distance traveled.

Despite the large amount of degradation throughout the reach the average bed slope and cross sectional flow area are largely unchanged since 1973, also the flow conditions have not changed. Thus the sediment transport capacity should be constant before and after 1973. By comparing sediment transport rates pre and post 1973 shows that the suspended sediment transport capacity has not changed notably. The source of the sediment has changed however; prior to 1973 the majority of the suspended sediment was transported from upstream of the Rio Puerco after 1973 the Rio Puerco introduces a large amount suspended sediment into the river.

In addition to observing how the sediment loads change over time a comparison of sediment transport rates allows a sediment budget analysis, in term of how much sediment is coming in to the reach or being deposited. It was estimated that the amount of sediment provided from the bed upstream of the Albuquerque gage is ~647,000 tons/year and makes up about 65% of the incoming sediment. From Bernardo to San Acacia the sediment from the bed was estimated to be ~190,000 tons/year, this is a very small amount compared to the amount of sediment incoming from the Rio Puerco (~3.7 M tons/year).

By looking at an overview of the Rio Grande from Cochiti Dam to the Elephant Butte Reservoir many interesting observations were obtained.

The main conclusions of the DMA are:

1. The effects of Cochiti Dam on the reduced sediment load are less noticeable the further downstream traveled as seen when comparing the Albuquerque gage results to those of the other three gages.
2. The incoming sediment load after 1973 to the Albuquerque and Bernardo gages is largely made up of material that was degraded from the river bed upstream.
3. Sediment volume from the river bed degradation does not significantly affect the sediment budget at the San Acacia and San Marcial gages contributing only approximately 8% of the suspended sediment.
4. After the construction of Cochiti Dam the suspended sediment transport capacity of the river below the Rio Puerco has remained nearly constant at 3.8 M tons/year.

5.4. Summary

Overall these analyses conducted on the Middle Rio Grande provide us with a better understanding of how and why the river has changed. Applying this knowledge to restoration efforts will provide an idea of what the Rio Grande will behave like in the future. Also if changes are made to the river these analyses can aid in the prediction of how the river will react to the changes.

REFERENCES

- Ackers, P. (1982). Meandering Channels and the Influence of Bed Material. In: Gravel Bed Rivers. Fluvial Processes, Engineering and Management. Hey, R. D., Bathurst, J. C., and Thorne, C. R. (eds). John Wiley and Sons Ltd, pp. 389-414.
- Albert, J, Sixta, M, Leon, C., and Julien, P. (2003b). Corrales Reach. Corrales Flood Channel to Montano Bridge. Hydraulic Modeling Analysis. 1962 - 2001. Middle Rio Grande, New Mexico. Prepared for U.S. Bureau of Reclamation. Albuquerque, New Mexico. Colorado State University, Fort Collins, CO.
- Baird, D. C. (2003). Personal Communication. Senior Hydraulic Engineer. Representing U.S. Bureau of Reclamation. Technical Services Division. River Analysis Team. Albuquerque, NM. Colorado State University, Fort Collins, CO.
- Baird, D. C. (2004). Personal Communication. Senior Hydraulic Engineer. Representing U.S. Bureau of Reclamation. Technical Services Division. River Analysis Team. Albuquerque, NM. Colorado State University, Fort Collins, CO.
- Bauer, T. R. (2000). Morphology of the Middle Rio Grande from Bernalillo Bridge to the San Acacia Diversion Dam, New Mexico. M.S. Thesis. Colorado State University, Fort Collins, CO. 308 pp.
- Bullard, K. L. and Lane, W. L. (1993). Middle Rio Grande Peak Flow Frequency Study. U.S. Department of Interior, Bureau of Reclamation, Albuquerque, NM.
- Burkham, D.E., and Dawdy, D.R. (1980). General Study of the Modified Einstein Method of Computing Total Sediment Discharge. USGS Water Supply Paper 2066. pp. 99
- Burkholder, J.L., Report of Chief Engineer. Middle Rio Grande Conservancy District. Albuquerque, New Mexico. Dated March 19, 1929.
- Carter, R. W., and Dvididian, J. (1968). General Procedure for Gaging Streams: Geologic Survey Techniques of Water-Resources Investigations of the United States Geologic Survey: Book 3. Chapter A6. 13 pp.

- Chang, H. H. (1979). Minimum Stream Power and River Channel Patterns. *Journal of Hydrology*. 41:303-327.
- Chow, V. T. (1964). Handbook of Applied Hydrology. McGraw-Hill Book Company Inc. New York, NY.
- Colby, B. R. and Hembree, C. H. (1955). Computations of Total Sediment Discharge Niobrara River near Cody, Nebraska. Geological Survey Water-Supply Paper 1357. pp. 187.
- Crawford, Clifford S., Cully, Anne C., Leutheuser, Rob, Sifuentes, Mark S., White, Larry H., Wilber, James P., (1993) "Middle Rio Grande Ecosystem: Bosque Biological Management Plan." U.S. Fish and Wildlife Service, Albuquerque, New Mexico.
- Einstein, H.A. (1950). The bed-load function for sediment transportation in open channel flows. U.S. Department of Agriculture, Soil Conservation Service, Technical Bulletin No. 1026. pp. 71.
- Graf, W. L. (1994). Plutonium and the Rio Grande. Environmental Change and Contamination in the Nuclear Age. Oxford University Press, New York.
- Henderson, F. M. (1966). Open Channel Flow. Macmillan Publishing Co., Inc., New York, NY. 522 pp.
- Hindall, S. M. (1991). Temporal Trends in Fluvial-Sediment in Ohio, 1950-1987. *Journal of soil and Water Conservation*. 46:4:311-313.
- Holmquist-Johnson, Chris. (2004). Bureau of Reclamation Automated Modified Einstein Procedure (BORAMEP) Program for Computing Total Sediment Discharge-DRAFT. U.S. Department of the Interior, Bureau of Reclamation, Denver, CO. pp.29.
- Julien, P. Y. (1998). Erosion and Sedimentation. Cambridge University Press, Cambridge, U.K.
- Julien, P. Y. (2004) Personal Communication. Professor. Colorado State University, Fort Collins, CO.
- Knighton, A. D. and Nanson, G. C. (1993). Anastomosis and the Continuum of Channel Pattern. *Earth Surface Processes and Landforms*. 18:613-625.

- Lagasse, P. F. (1980). An Assessment of the Response of the Rio Grande to Dam Construction - Cochiti to Isleta Reach. U.S. Army Corps of Engineers. Albuquerque, NM.
- Lagasse, P. F. (1994). Variable Response of the Rio Grande to Dam Construction. In: The Variability of Large Alluvial Rivers. ASCE Press, New York, NY.
- Lara, J. (1966). Computation of "Z's" for use in the Modified Einstein Procedure. U.S. Department of the Interior, Bureau of Reclamation, Office of Chief Engineer.
- Leon, C. (1998). Morphology of the Middle Rio Grande from Cochiti Dam to Bernalillo Bridge, New Mexico. M.S. Thesis. Colorado State University, Fort Collins, CO. 210 pp.
- Leon, C. and Julien, P. (2001a). Bernalillo Bridge Reach. Highway 44 Bridge to Corrales Flood Channel Outfall. Hydraulic Modeling Analysis. 1962 - 1992. Middle Rio Grande, New Mexico. Prepared for U.S. Bureau of Reclamation. Albuquerque, New Mexico. Colorado State University, Fort Collins, CO. 85 pp.
- Leon, C. and Julien, P. (2001b). Hydraulic Modeling on the Middle Rio Grande, NM. Corrales Reach. Corrales Flood Channel to Montano Bridge. Prepared for U.S. Bureau of Reclamation. Albuquerque, New Mexico. Colorado State University, Fort Collins, CO. 83 pp.
- Leopold, L. B. and Wolman, M. G. (1957). River Channel Patterns: Braided, Meandering and Straight. USGS Professional Paper 282-B. 85 pp.
- Massong, T. (2001). Personal Communication. Geomorphologist. Representing U.S. Bureau of Reclamation. Environmental and Lands Division. Albuquerque, NM.
- Molnár, P. (2001). Precipitation and Erosion Dynamics in the Rio Puerco Basin. Ph.D. Dissertation. Colorado State University, Fort Collins, CO. 258 pp.
- Mosley, H. and Boelman, S. (1998). Santa Ana Reach. Geomorphic Report - DRAFT. U.S. Bureau of Reclamation, Albuquerque, NM.
- Parker, G. (1976). On the Cause and Characteristic Scales of Meandering and Braiding in Rivers. *Journal of Fluid Mechanics*. 76:part 3:457-480.

- Pemberton, E. L. (1964). Sediment Investigations - Middle Rio Grande. In: Proceedings of the American Society of Civil Engineers. *Journal of the Hydraulic Division*. 90:HY2:pp. 163-185.
- Porterfield, G. (1972). Computation of Fluvial-Sediment Discharge: Geologic Survey techniques of Water-Resources Investigations of the United States Geologic Survey: Book 3. Chapter C3. 66 pp.
- Richard, G. (2001). Quantification and Prediction of Lateral Channel Adjustments Downstream from Cochiti Dam, Rio Grande, NM. Ph.D. Dissertation. Colorado State University, Fort Collins, CO. 229 pp.
- Richard, G., Leon, C., and Julien, P. (2001). Hydraulic Modeling on the Middle Rio Grande, New Mexico. Rio Puerco Reach. Prepared for U.S. Bureau of Reclamation. Albuquerque, New Mexico. Colorado State University, Fort Collins, CO. 76 pp.
- Richardson, E. V., Simons, D. B., and Lagasse, P. F. (2001). River Engineering for Highway Encroachments: Highways in the River Environment. DRAFT. U.S. Department of Transportation, FHA, Washington, D.C.
- Rittenhouse, G. (1944). Sources of Modern Sands in the Middle Rio Grande Valley, New Mexico. *Journal of Geology*. 52:145-183.
- Rosgen, D. (1996). Applied River Morphology. Wildland Hydrology, Pagosa Springs, CO.
- Ruteledge, A.T. (1985). Use of Double Mass Curves to Determine Drawdown in a long term Aquifer Test in North Central Volusia County. Florida HSSS, Water Resources Investigations Report 84-4309. pp 29
- Sanchez, V. and Baird, D. (1997). River Channel Changes Downstream of Cochiti Dam. Middle Rio Grande, New Mexico. In: Proceedings of the Conference of Management of Landscapes Disturbed by Channel Incision. University of Mississippi, Oxford, MS.
- Schumm, S. A. and Khan, H. R. (1972). Experimental Study of Channel Patterns. *Geological Society of America Bulletin*. 83:1755-1770.

- Scurlock, D. (1998). From the Rio to the Sierra. An Environmental History of the Middle Rio Grande Basin. General Technical Report RMRS-GTR5. USDA, Forest Service, Rocky Mountain Research Station, Fort Collins. 440 pp.
- Searcy, J. K. and Hardison C. H. (1960). Double Mass Curves. U.S. Geological Survey, Water-Supply Paper 1541-B. pp. 66.
- Simons, D. B., and Senturk, F. (1976). Sediment Transport Technology. Water Resources Publications, Fort Collins, CO. pp. 807.
- Sixta, M. (2004). Hydraulic Modeling and Meander Migration of the Middle Rio Grande, New Mexico. M.S. Thesis. Colorado State University, Fort Collins, CO. 260 pp.
- Sixta, M., Albert, J., Leon, C., and Julien, P. (2003a). Bernalillo Bridge Reach. Highway 44 Bridge to Corrales Flood Channel Outfall. Hydraulic Modeling Analysis. 1962 - 2001. Middle Rio Grande, New Mexico. Prepared for U.S. Bureau of Reclamation. Albuquerque, New Mexico. Colorado State University, Fort Collins, CO. 87 pp.
- Sixta, M., Albert, J., Leon, C., and Julien, P. (2003c). San Felipe Reach. Arroyo Tonque to Angostura Diversion Dam. Hydraulic Modeling Analysis. 1962 - 1998. Middle Rio Grande, New Mexico. Prepared for U.S. Bureau of Reclamation. Albuquerque, New Mexico. Colorado State University, Fort Collins, CO. 85 pp.
- Stevens, H. H. and Yang, C. T. (1989). Summary and Use of Selected Fluvial Sediment-Discharge Formulas. USGS Water Resources Investigations Report 80-4026. 62 pp.
- Stevens, H. H. (1985). Computer Program for the Computation of Total Sediment Discharge by the Modified Einstein Procedure. U.S. Geological Survey, Water-Resources Investigations Report 85-4047. pp. 14.
- US Army Corps of Engineers (1998). Hydrologic Engineering Center-River Analysis System User's Manual. Version 2.2. Hydrologic Engineering Center, Davis, CA.
- US Bureau of Reclamation (1955). Step Method for Computing Total Sediment Load by the Modified Einstein Procedure. Prepared by the Sedimentation Section, Hydrology Branch. pp. 18.
- van den Berg, J. H. (1995). Prediction of Alluvial Channel Pattern of Perennial Rivers. *Geomorphology*. 12:259-279.

- Woodson, R. C. (1961). Stabilization of the Middle Rio Grande in New Mexico. In: Proceedings of the American Society of Civil Engineers. Journal of the Waterways and Harbor Division. 87:No. WW4:pp. 1-15.
- Woodson, R. C. and Martin, J. T. (1962). The Rio Grande comprehensive plan in New Mexico and its effects on the river regime through the middle valley. In: Control of Alluvial Rivers by Steel Jetties, American Society of Civil Engineers Proceedings. Carlson, E. J. and Dodge E. A. eds. *Journal of the Waterways and Harbor Division*. American Society of Civil Engineers, NY, NY, 88:pp. 53-81.
- Yang, C. T. (1996). Sediment Transport: Theory and Practice. McGraw-Hill Companies Inc. New York.
- Yang, S., Zhao, Q., and Belkin, I. M. (2002). Temporal Variation in the Sediment Load of the Yangtze River and the Influences of Human Activities. *Journal of Hydrology*.263:56-71.

APPENDIX A:
Location Maps and Aerial Photograph Data
(Corrales Reach)

Aerial Photograph Data
Aerial Photographs
Location Maps

Table A-1 Aerial Photograph Data (Source: Richard et al. 2001).

Aerial Photographs digitized in the Rio Grande Geomorphology Study, v. 1 by the USBR, Remote Sensing and Geographic Information Group, Denver, CO:

- 1) 1918 – Scale: 1:12,000, Hand drafted linens (39 sheets), USBR Albuquerque Area Office. Surveyed in 1918, published in 1922.
- 2) 1935 – Scale: 1:8,000. Black and white photography, USBR Albuquerque Area Office. Flown in 1935, published 1936.
- 3) 1949 – Scale 1:5,000. Photo-mosaic. J. Ammann Photogrammetric Engineers, San Antonio, TX. USBR Albuquerque Area Office.
- 4) March 15, 1962 – Scale: 1:4,800. Photo-mosaic. Abram Aerial Survey Corp. Lansing, MI. USBR Albuquerque Area Office.
- 5) April 1972 – Scale: 1:4,800. Photo-mosaic. Limbaugh Engineers, Inc., Albuquerque, NM. USBR Albuquerque Area Office.
- 6) March 31, 1985 – Scale: 1:4,800. Orthophoto. M&I Consulting Engineers, Fort Collins, CO. Aero-Metric Engineering, Sheboygan, MN. USBR Albuquerque Area Office.
- 7) February 24, 1992 – Scale: 1:4,800. Orthophoto. Koogle and Poules Engineering, Albuquerque, NM. USBR Albuquerque Area Office.
- 8) Winter 2001 – Scale: 1:4,800. Ratio-rectified photo-mosaic. Pacific Western Technologies, Ltd. USBR Albuquerque Area Office.

Table A-2 Aerial photograph dates and mean daily discharge on those days.

Aerial Photograph Dates	Mean Daily Discharge at San Felipe (cfs)	Mean Daily Discharge at Bernalillo (cfs)	Mean Daily Discharge at Albuquerque (cfs)
February 24, 1992	314	No data	159
March 31, 1985	570	No data	109
April 1972	Mean = 564 Max = 894 Min = 400	No data	Mean = 705 Max = 2540 Min = 116
March 15, 1962	722	493	No data
1949 (unknown date)	Mean = 1806 Max = 10500 Min = 316	Extreme low flow (from meta-data file)	No data
1935 (unknown date)	Mean = 1555 Max = 8000 Min = 310	Annual data from Otowi: Mean = 1,520 Max = 7,490 Min = 350	No data
1918 (unknown date)	No data	No data	No data

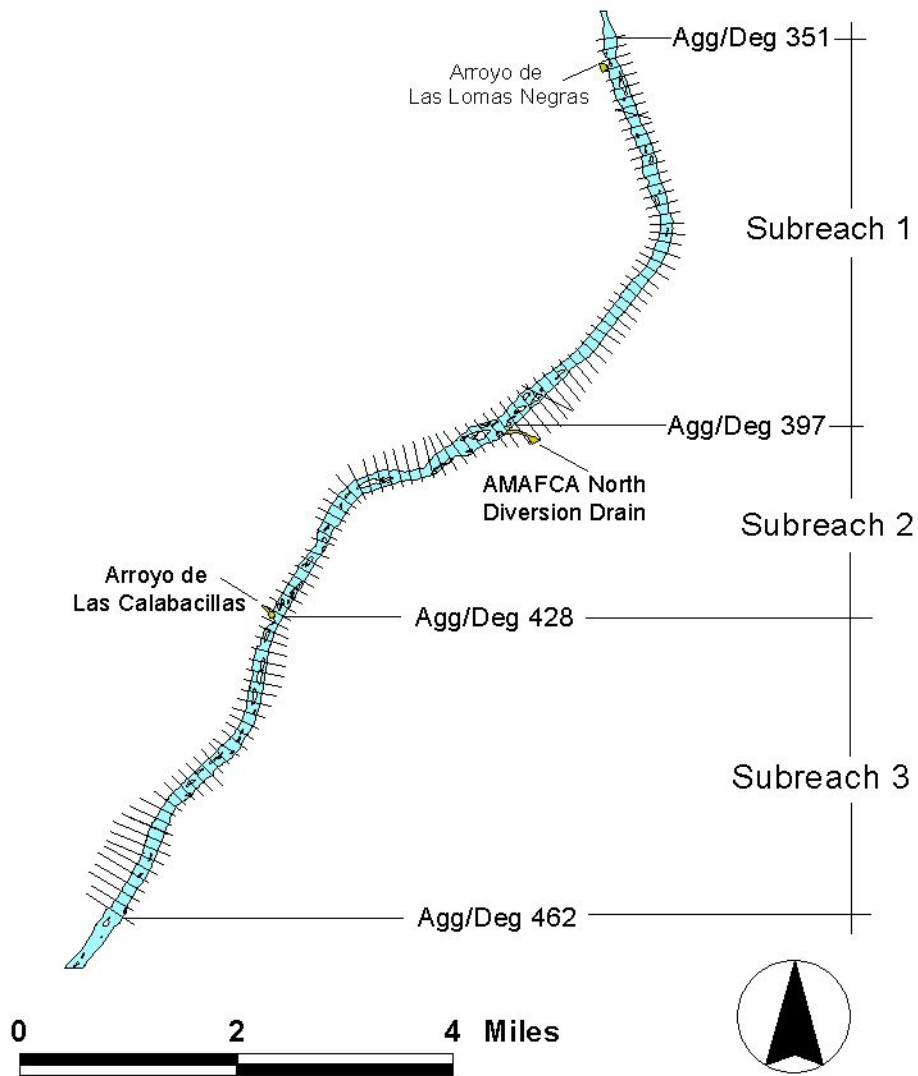


Figure A-1 Corrales Reach subreach definitions.



Figure A-2 photo of subreach 1.

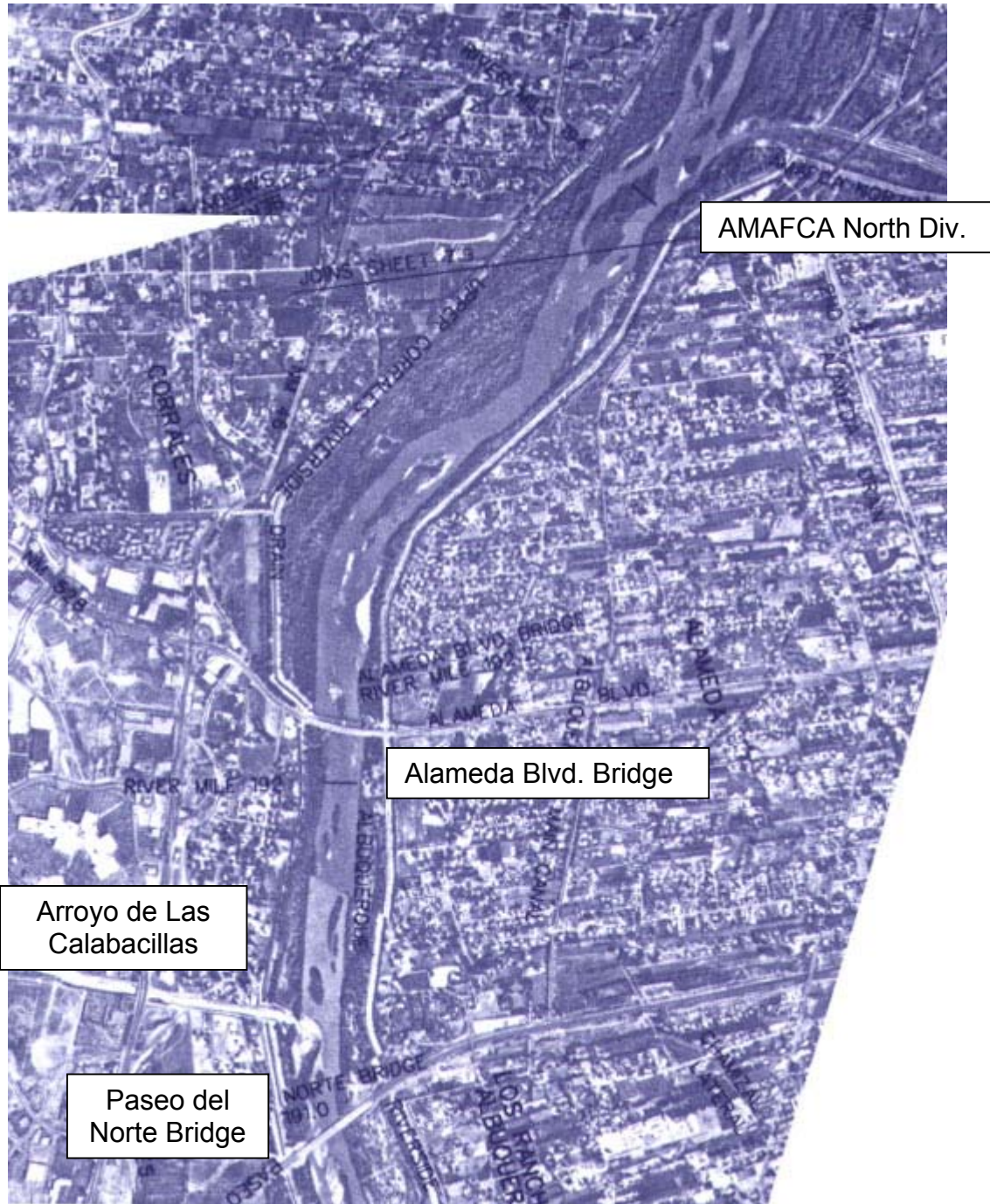


Figure A-3 Aerial photo of subreach 2.



Figure A-4 Aerial photo of subreach 3.

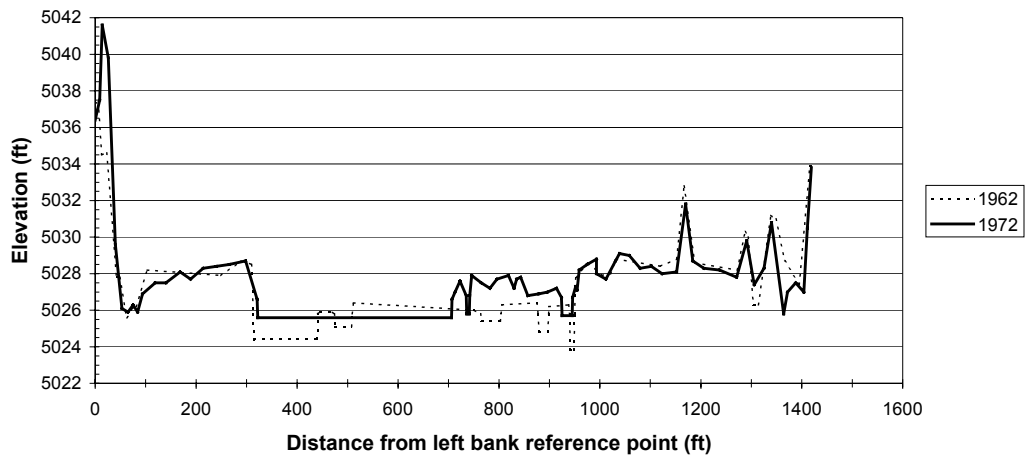
**APPENDIX B:
Cross Section Survey Dates
(Corrales Reach)**

Table B-1 Surveyed dates for the CO and CA lines collected by the US Bureau of Reclamation.

Date	Cross section															
	CO-33	CO-34	CO-35	CA-1	CA-2	CA-3	CA-4	CA-5	CA-6	CA-7	CA-8	CA-9	CA-10	CA-11	CA-12	CA-13
May-70			x													
May-71	x	x	x													
Sep-71		x	x													
Mar-72	x	x	x													
Nov-72	x	x	x													
May-73		x														
Jun-73	x	x	x													
May-74	x	x	x													
Sep-74	x	x	x													
Nov-74	x		x													
May-75			x													
Jul-75	x	x														
Nov-75	x	x	x													
Apr-79	x	x	x													
May-79	x															
Jul-79	x	x	x													
Jan-80	x	x	x													
Oct-82		x	x													
Nov-83	x	x	x													
Dec-86		x	x													
Nov-88				x	x	x	x									
Dec-88								x	x	x	x	x	x	x	x	x
Oct-89				x	x	x	x	x	x	x	x	x	x	x	x	x
Jul-90				x	x	x	x	x	x	x	x	x	x	x	x	x
Jun-91				x	x	x	x	x	x	x	x	x	x	x	x	x
Jun-92				x	x	x	x	x	x	x	x	x	x	x	x	x
Jul-92	x	x	x													
Apr-93				x	x	x	x	x	x	x	x	x	x	x	x	x
Jun-93 A				x	x	x	x	x	x	x	x	x	x	x	x	x
Jun-93 B				x	x	x	x	x	x	x	x	x	x	x	x	x
May-94 A					x	x	x	x	x	x	x					
May-94 B					x	x	x	x	x	x	x					
Jun-94 A					x	x	x	x	x	x	x	x	x	x	x	x
Jun-94 B												x	x	x	x	x
May-95						x	x	x	x	x	x	x	x	x	x	x
Jun-95				x	x	x	x	x	x	x	x	x	x	x	x	x
Jul-95				x	x	x	x	x	x	x	x	x	x	x	x	x
Aug-95	x	x	x													
Mar-96				x	x	x	x	x	x	x	x	x	x	x	x	x
May-96 A					x											
May-96 B					x											
Jun-96				x	x	x	x	x	x	x	x	x	x	x	x	x
Sep-98	x	x	x													
Apr-01	x	x	x	x	x		x		x			x			x	x
Aug-01	x	x	x						x						x	

**APPENDIX C:
Cross Sections
(Corrales Reach)**

AggDeg-351 / CO-33
Rio Grande, NM



CO-33 Pre-Dam
Rio Grande, NM

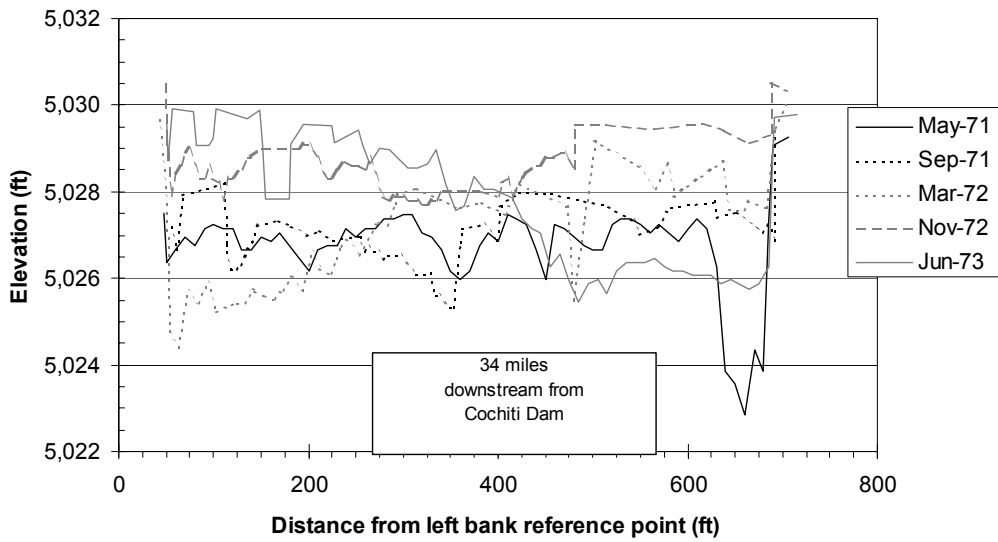
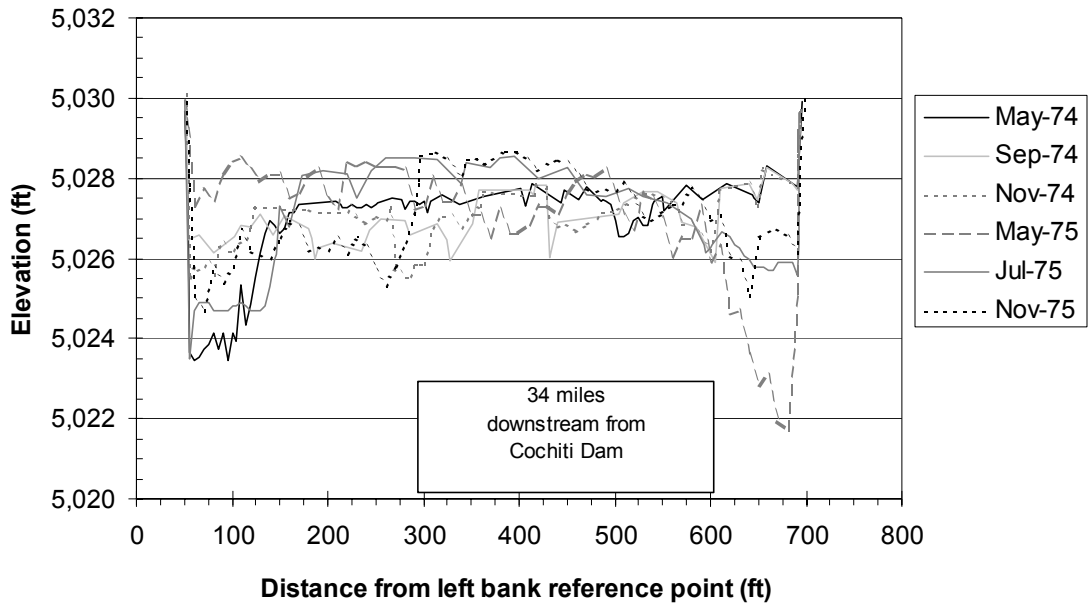


Figure C-1 Cross Section CO-33 representing pre-dam conditions.

CO-33 Post-Dam
Rio Grande, NM



CO-33 (1979-98)
Rio Grande, NM

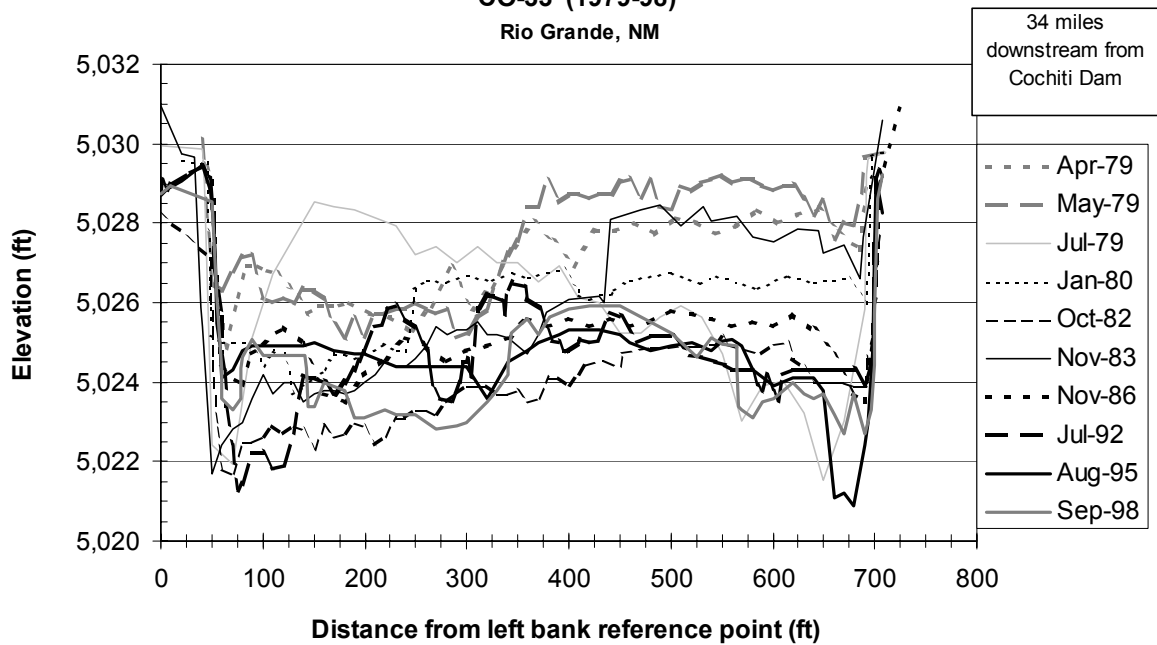


Figure C-2 Cross Section CO-33 representing post-dam conditions.

CO-33
Rio Grande, NM

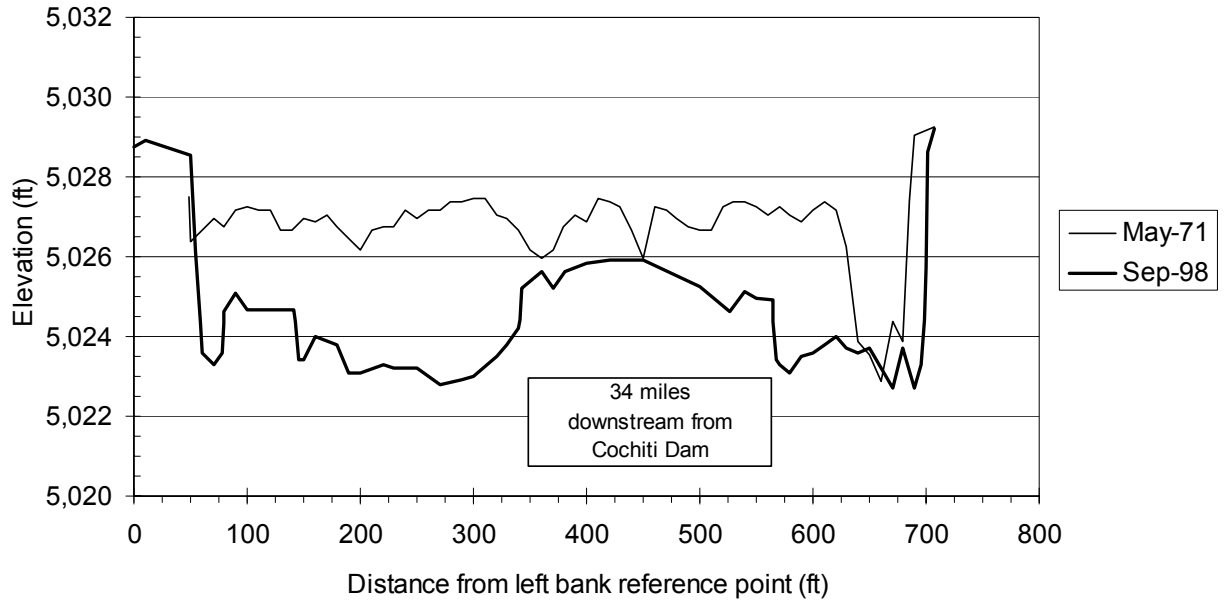
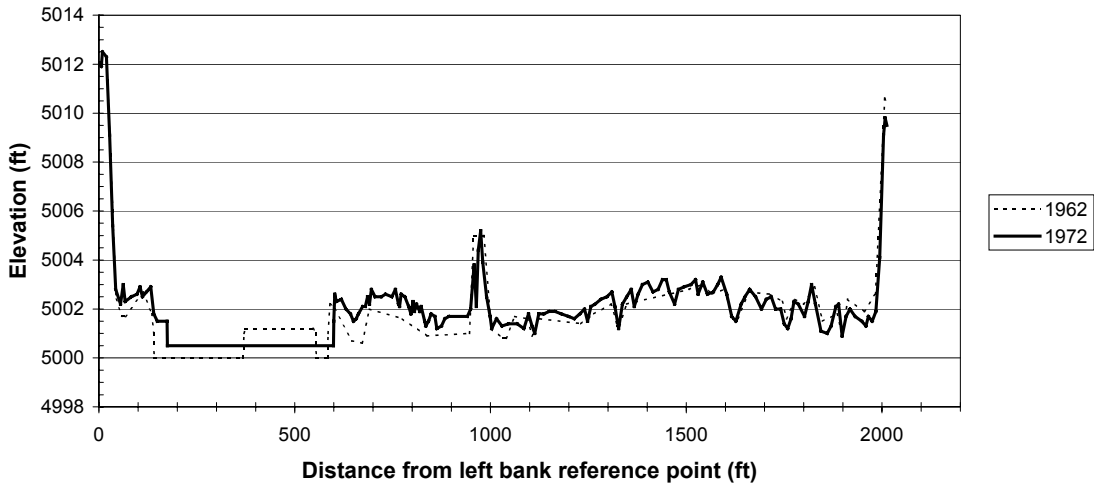


Figure C-3 Cross Section CO-33 representing pre and post-dam conditions.

AggDeg-407 / CO34
Rio Grande, NM



CO-34 Pre-Dam
Rio Grande, NM

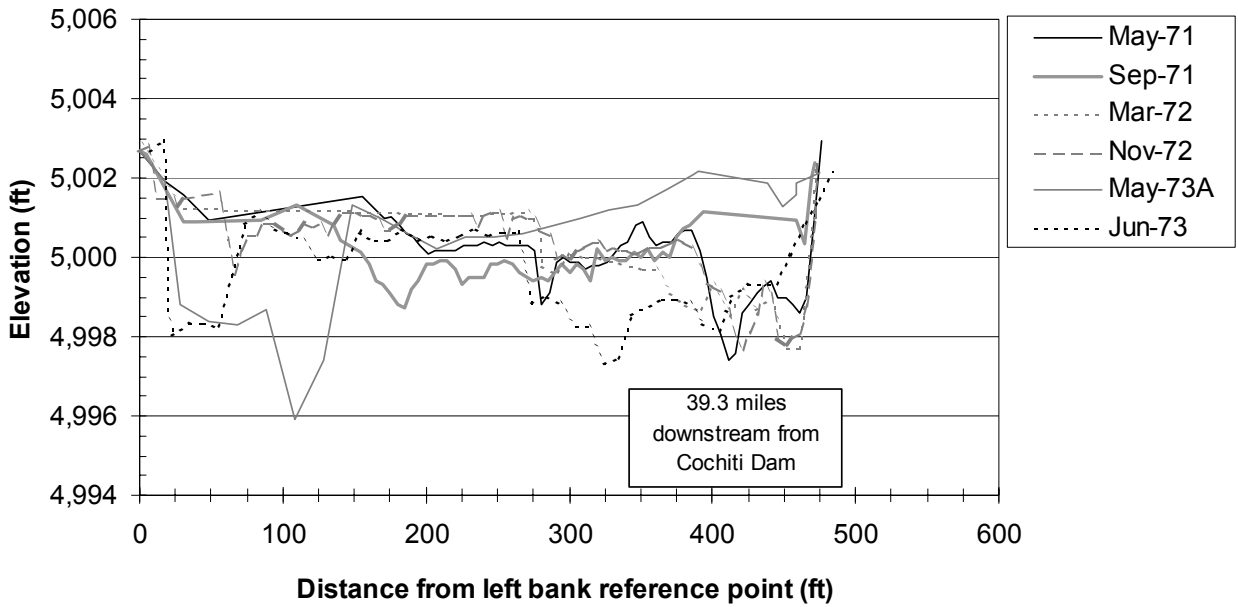
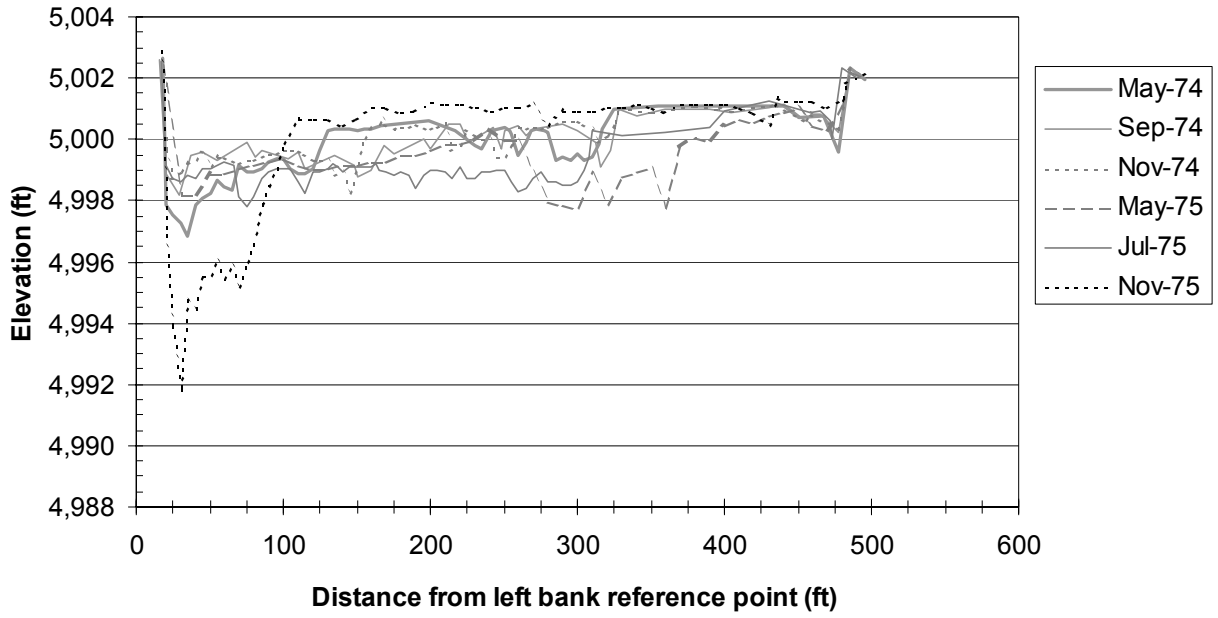


Figure C-4 Cross Section CO-34 representing pre-dam conditions.

CO-34 Post-Dam
Rio Grande, NM



CO-34 (1979-98)
Rio Grande, NM

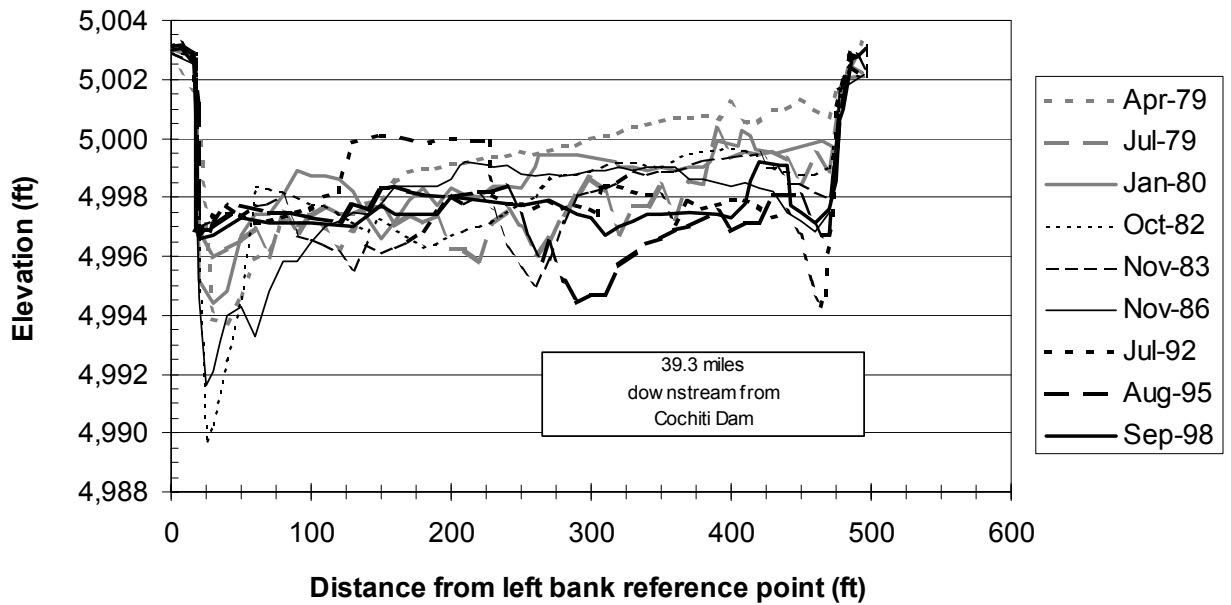


Figure C-5 Cross Section CO-34 representing post-dam conditions.

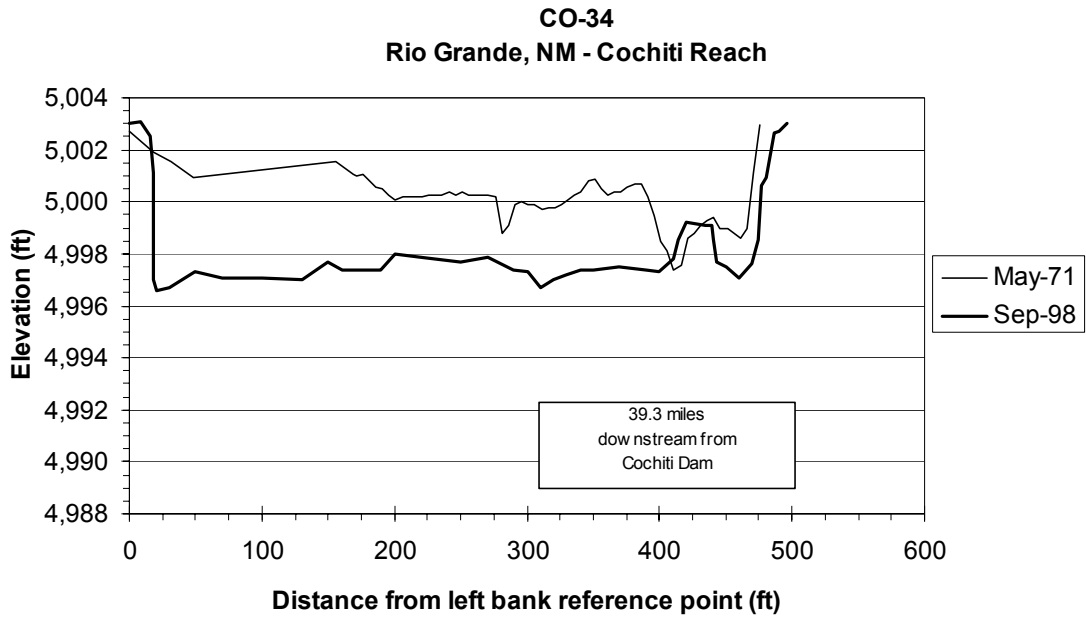
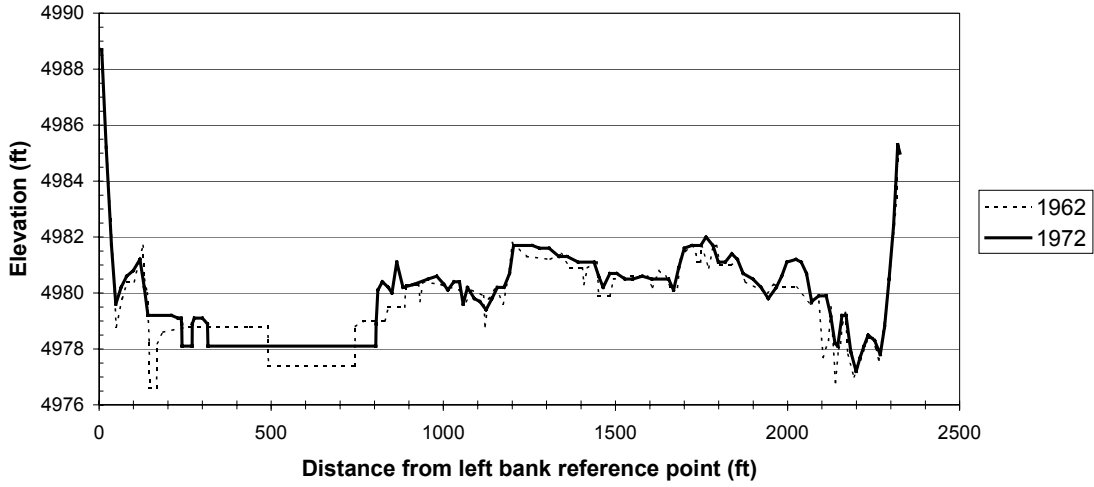


Figure C-6 Cross Section CO-34 representing pre and post-dam conditions.

AggDeg-453 / CO-35
Rio Grande, NM



CO-35 Pre-Dam
Rio Grande, NM

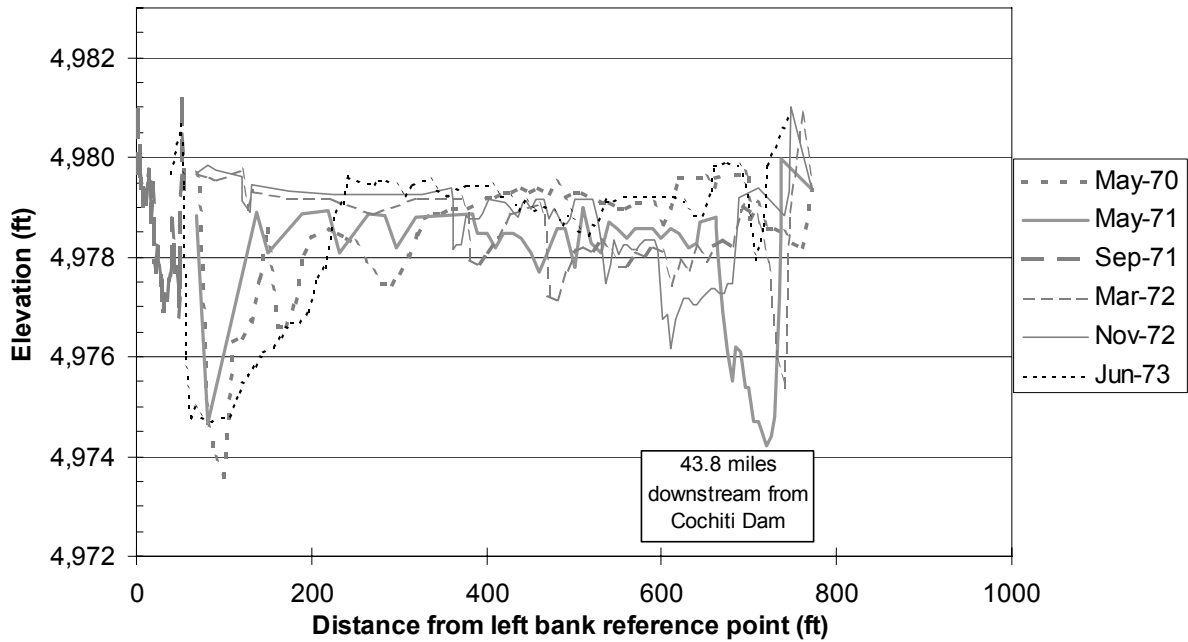
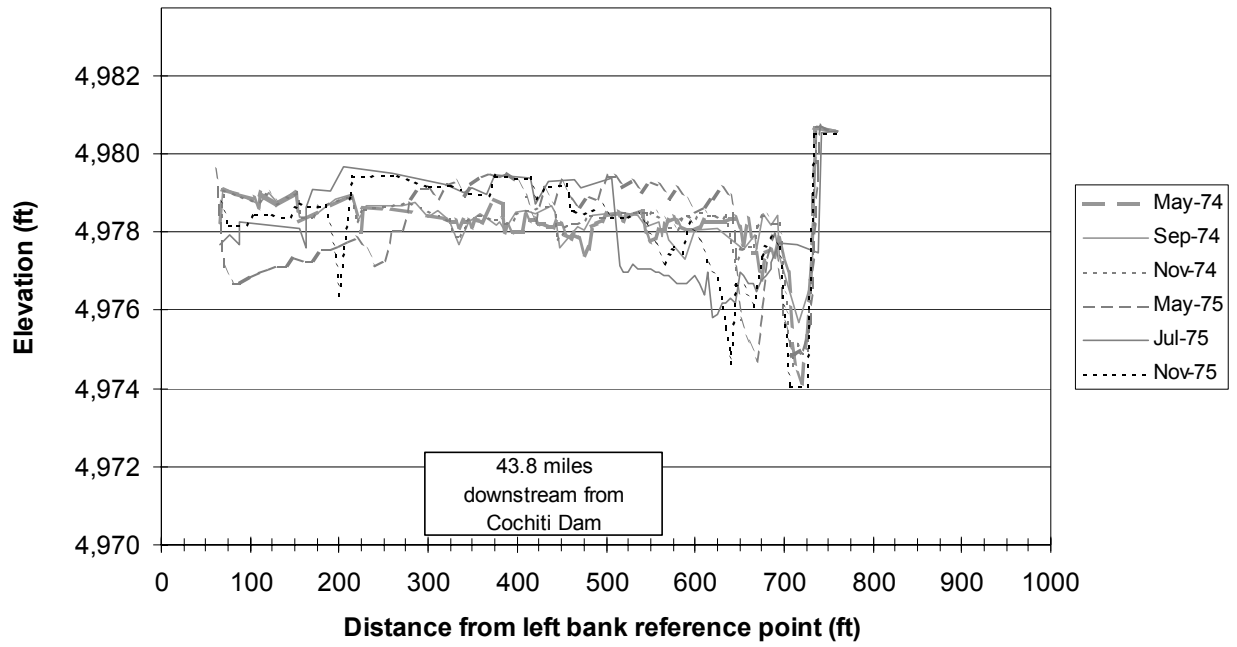


Figure C-7 Cross Section CO-35 representing pre and post-dam conditions.

CO-35 Post-Dam
Rio Grande, NM



CO-35 (1979-1995)
Rio Grande, NM

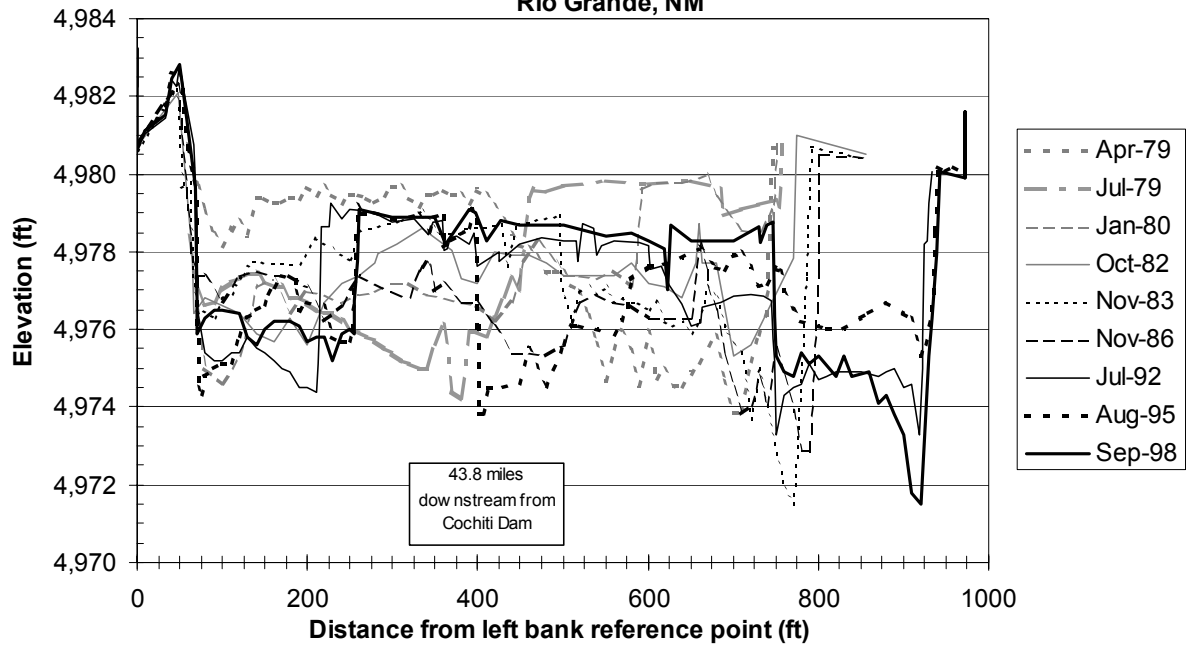


Figure C-8 Cross Section CO-35 representing post-dam conditions.

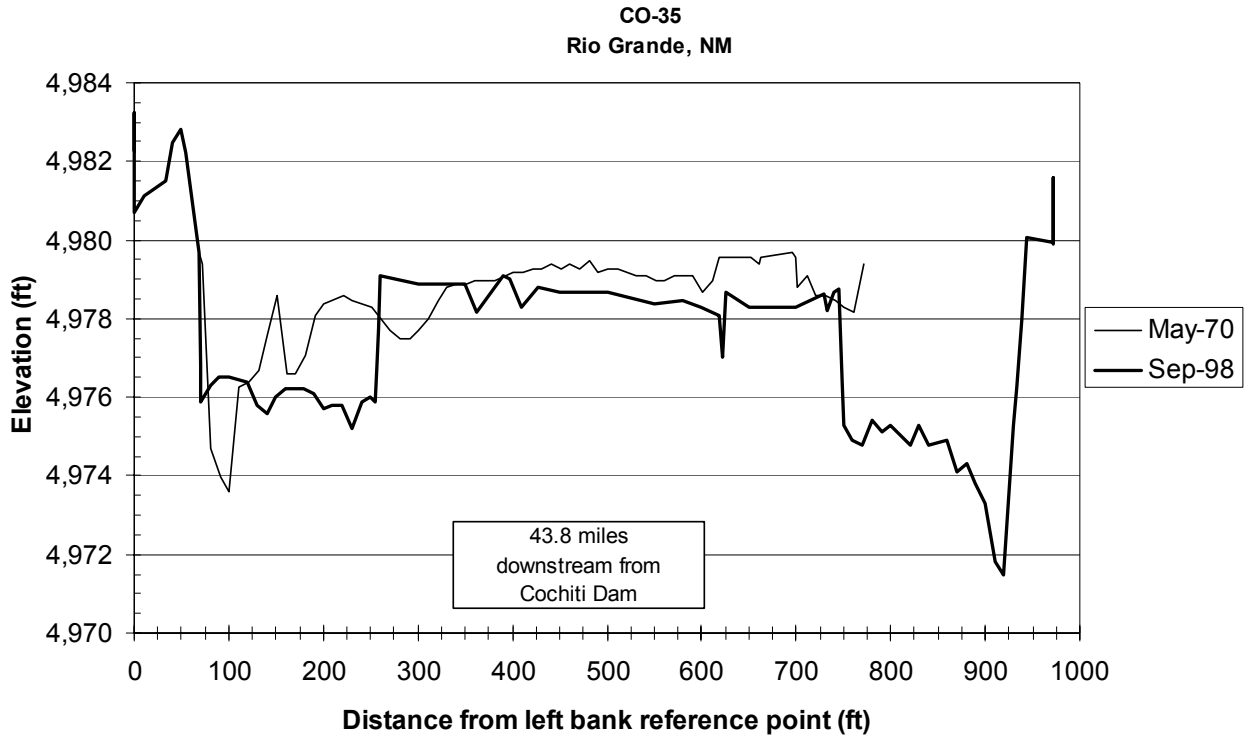


Figure C-9 Cross Section CO-35 representing pre and post-dam conditions.

**APPENDIX D:
Annual Peak Mean Discharges**

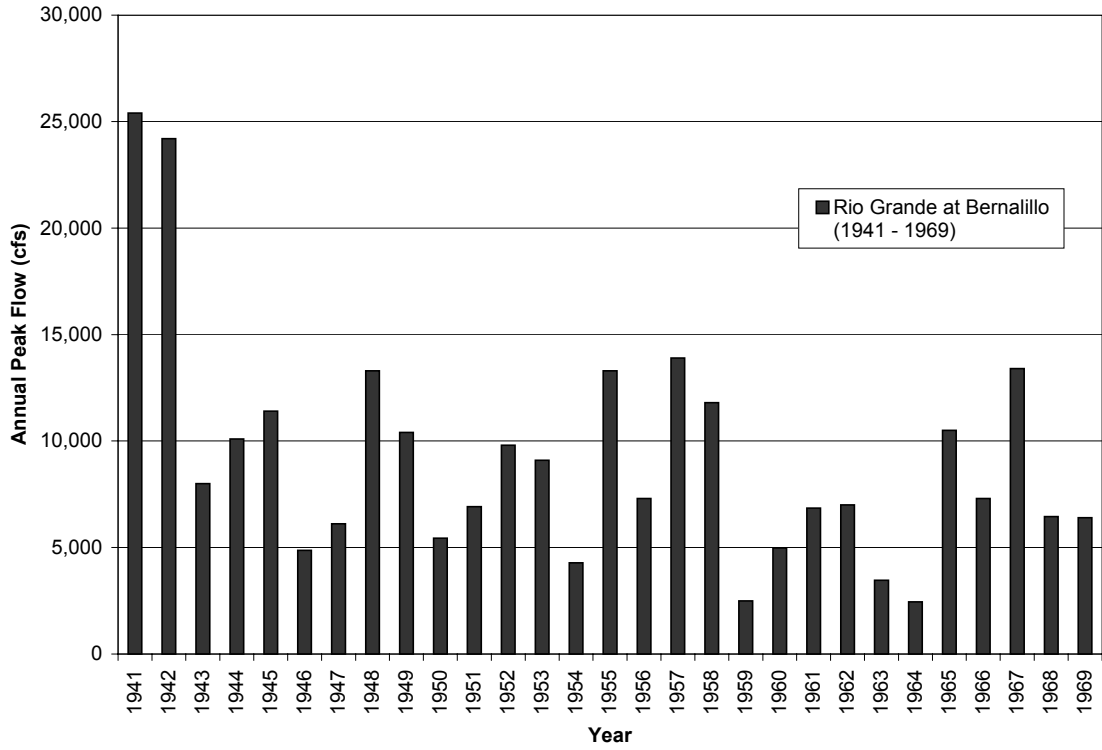


Figure D-1 Annual peak discharge in cfs at Bernalillo (1941-1969).

**APPENDIX E:
HEC-RAS Modeling Results**

Table E-1 Reach-Averaged HEC-RAS Results

Subreach 1									
Year	Width	EG Slope	Velocity	Area	Depth	W/D	WP	WS slope	MBE
1962	641	0.0009	3.62	1395	2.24	306	645	0.0009	5016
1972	665	0.0008	5.28	978	1.52	472	668	0.0009	5016
1992	603	0.0010	3.85	1338	2.23	276	607	0.0010	5014
2001	524	0.0009	4.01	1252	2.41	222.3	529	0.0009	5013

Subreach 2									
Year	Width	EG Slope	Velocity	Area	Depth	W/D	WP	WS slope	MBE
1962	692	0.0011	3.62	1420	2.14	358	695	0.0010	4998
1972	698	0.0008	5.27	1008	1.48	500	702	0.0010	4998
1992	640	0.0010	3.75	1389	2.21	303	644	0.0009	4996
2001	584	0.0009	3.86	1311	2.24	270.1	589	0.0009	4995

Subreach 3									
Year	Width	EG Slope	Velocity	Area	Depth	W/D	WP	WS slope	MBE
1962	627	0.0011	3.97	1341	2.35	315	630	0.0010	4982
1972	653	0.0009	5.53	922	1.41	470	656	0.0010	4982
1992	599	0.0010	3.85	1332	2.25	276	604	0.0010	4980
2001	598	0.0012	4.03	1293	2.22	284.2	604	0.0010	4980

Total									
Year	Width	EG Slope	Velocity	Area	Depth	W/D	WP	WS slope	MBE
1962	652	0.0010	3.73	1384	2.24	325	656	0.0009	
1972	670	0.0009	5.35	969	1.47	479	674	0.0009	
1992	612	0.0010	3.84	1344	2.22	285	616	0.0010	
2001	563	0.0010	3.97	1281	2.30	254.3	568	0.0009	

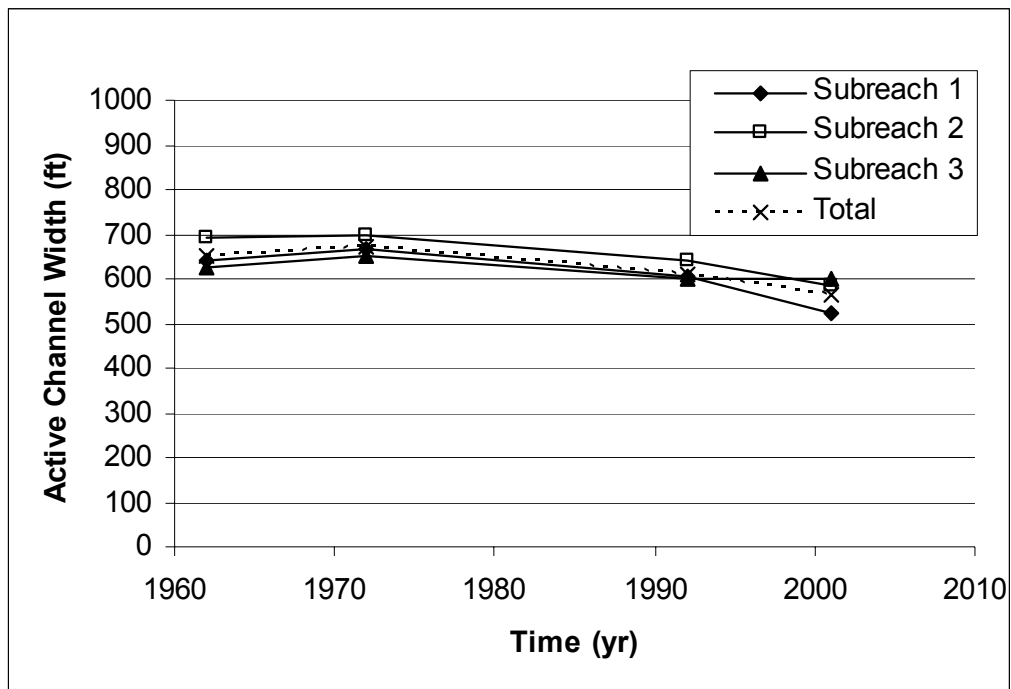
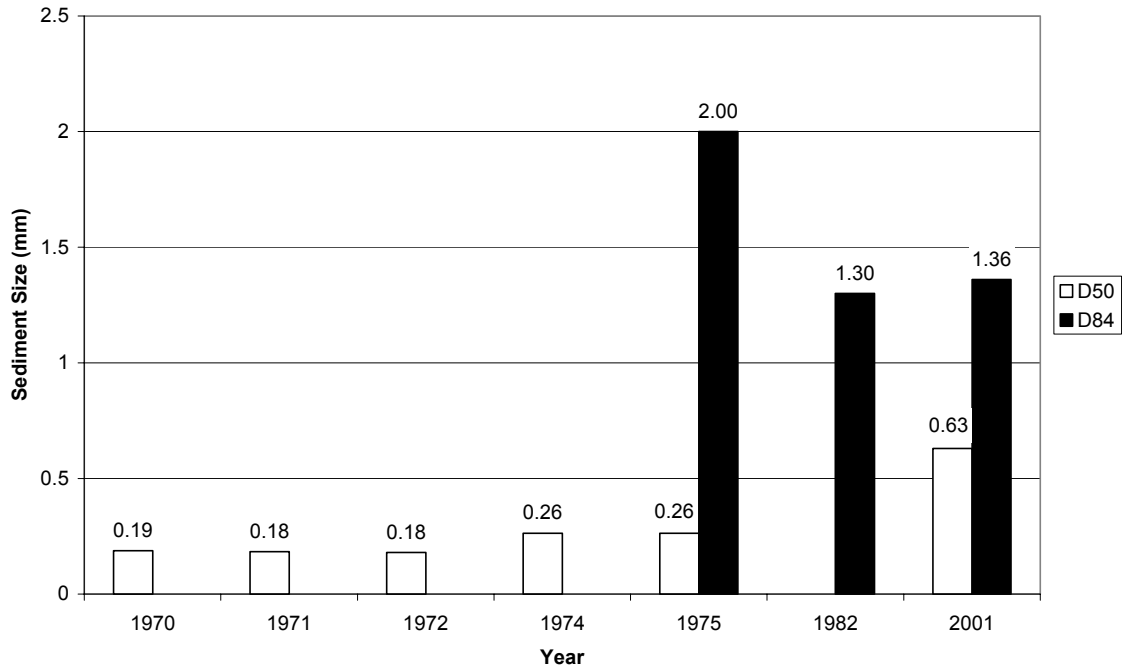


Figure E-1 Active channel widths from HEC-RAS modeling.

APPENDIX F:
Bed Material Histograms and Statistics
(Corrales Reach)

CO-34



CO-35

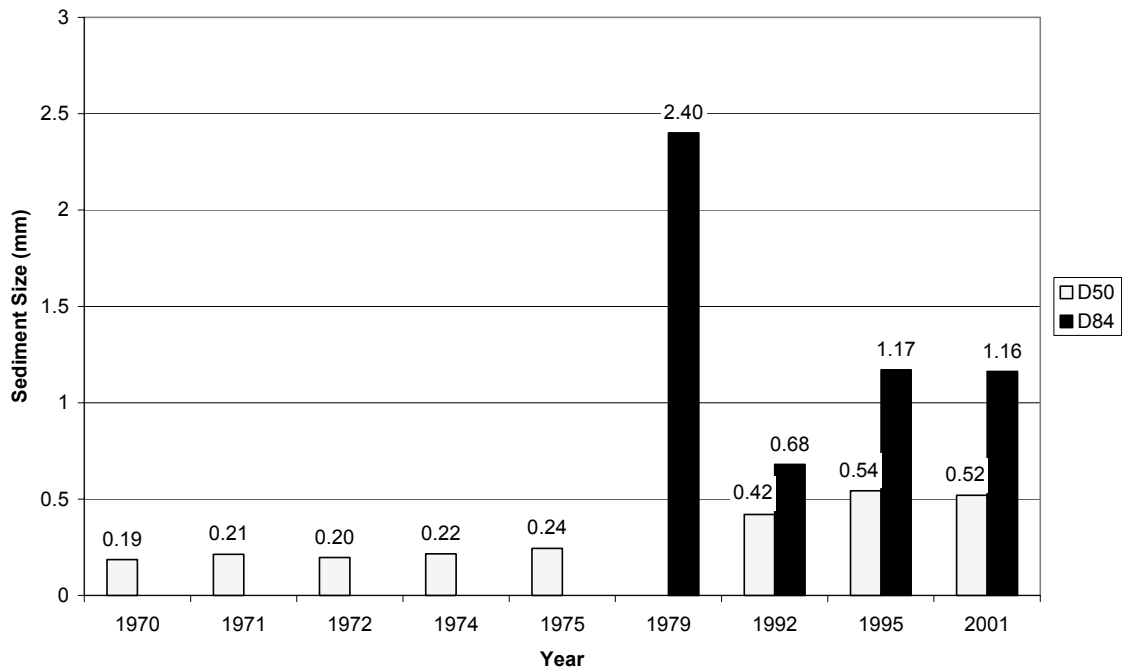


Figure F-1 Histograms depicting the D_{50} and D_{84} change with time for CO-34 and CO-35 (Corrales Reach).

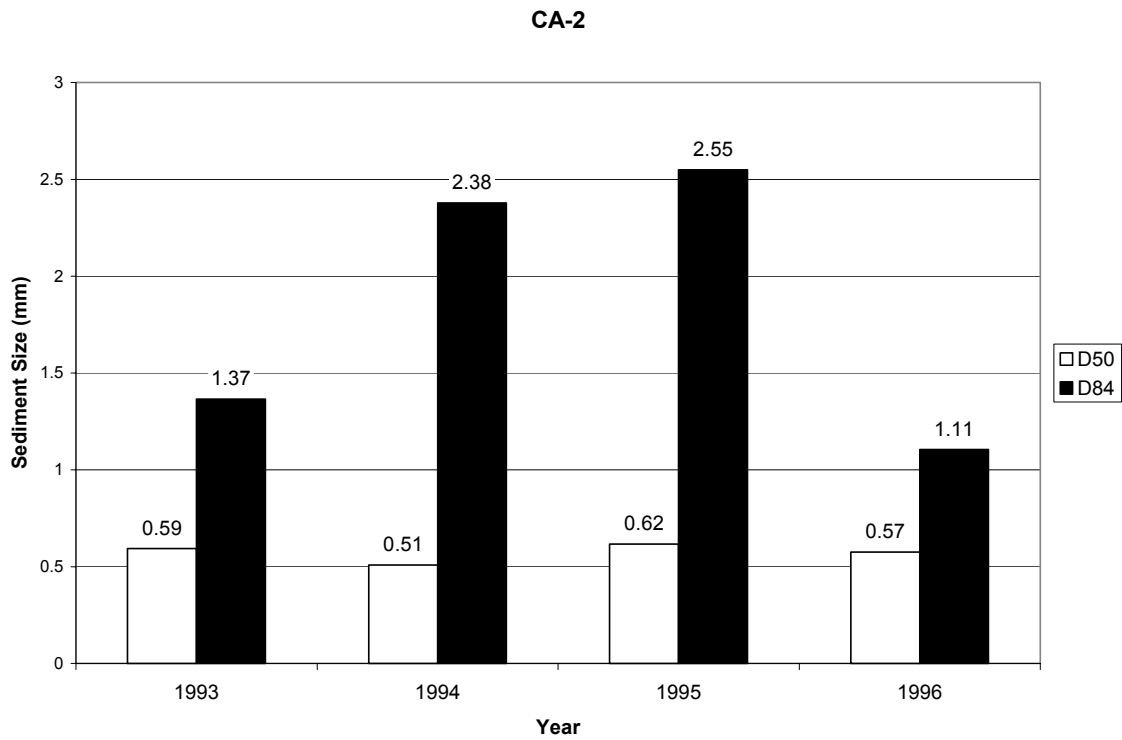
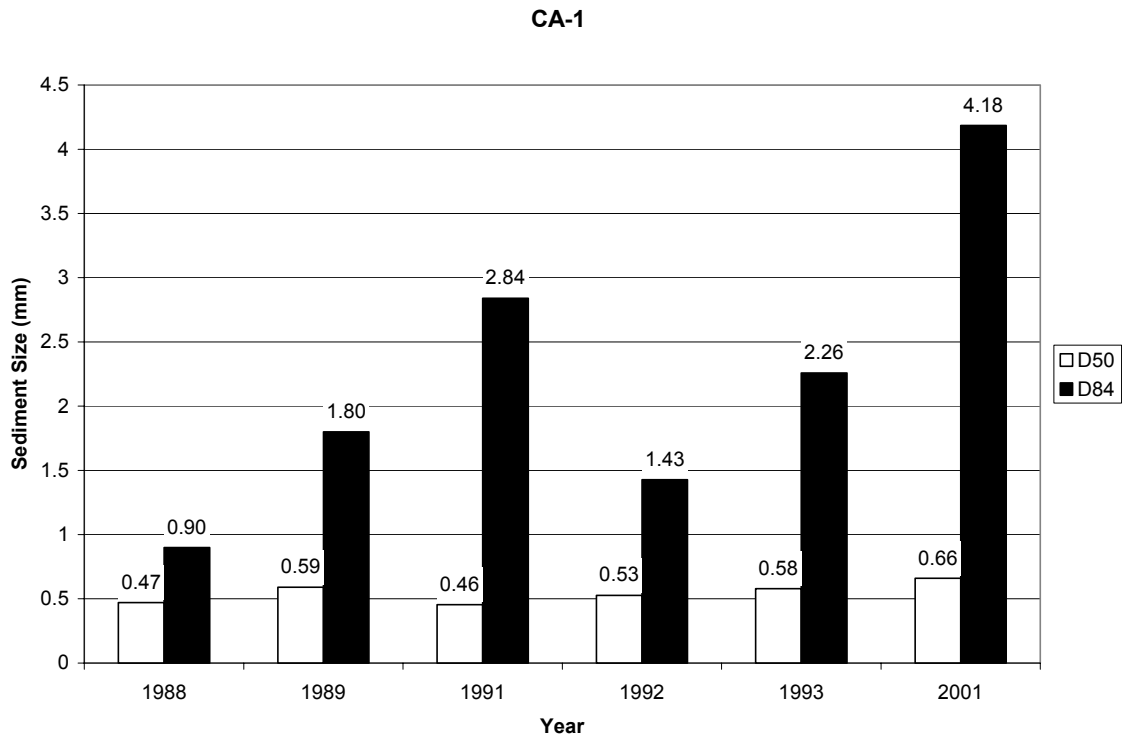
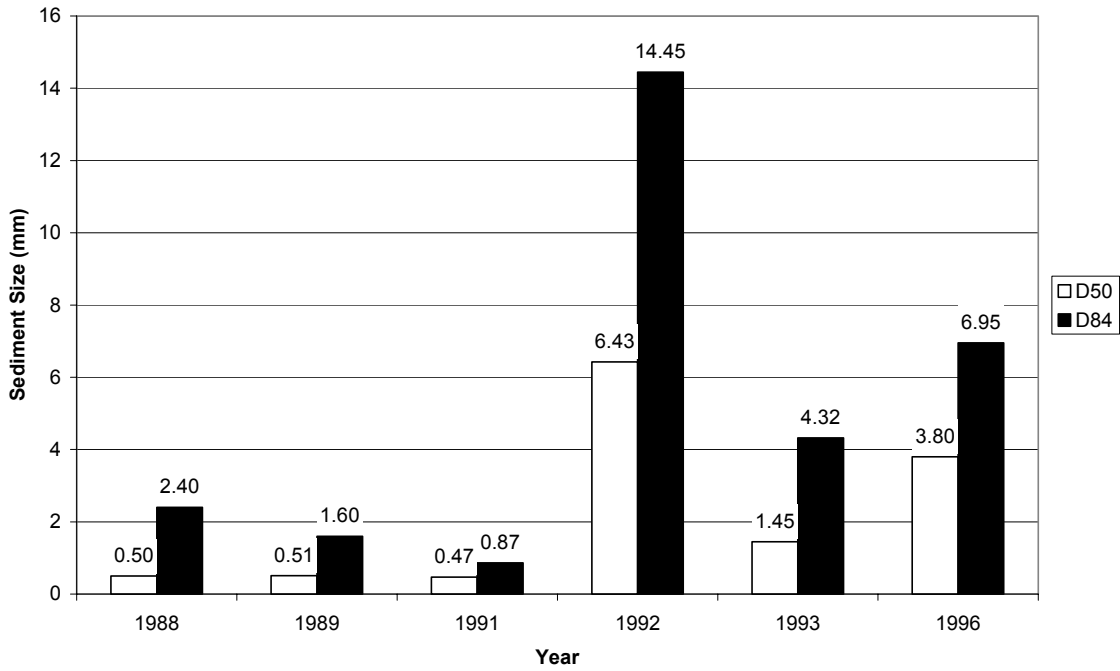


Figure F-2 Histograms depicting the D_{50} and D_{84} change with time for CA-1 and CA-2 (Corrales Reach).

CA-4



CA-6

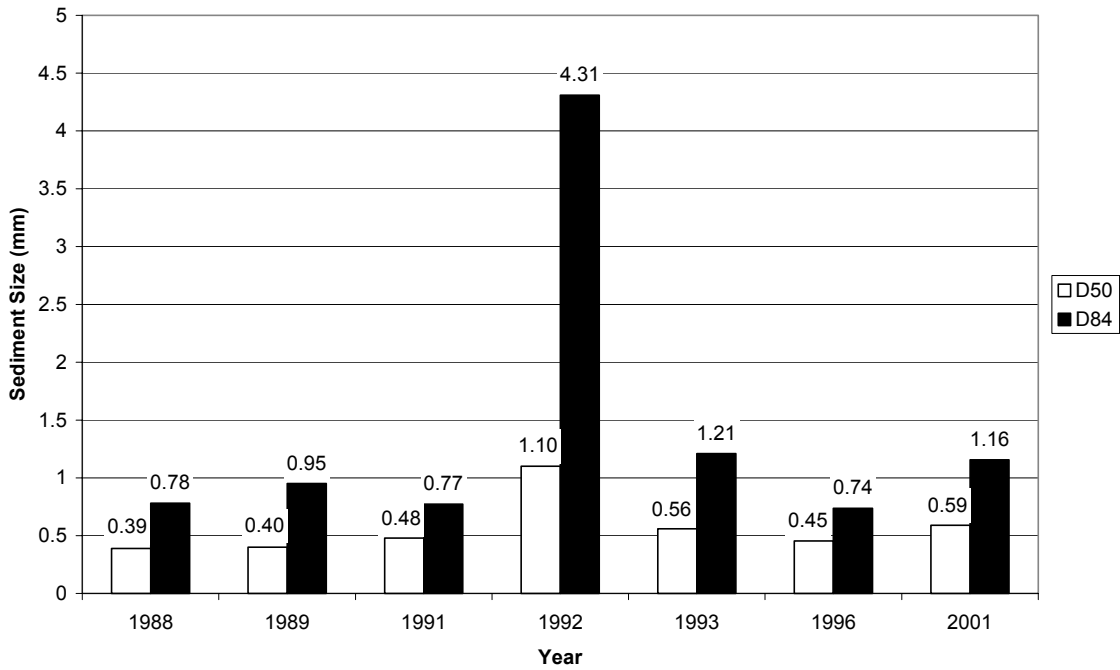


Figure F-3 Histograms depicting the D₅₀ and D₈₄ change with time for CA-4 and CA-6 (Corrales Reach).

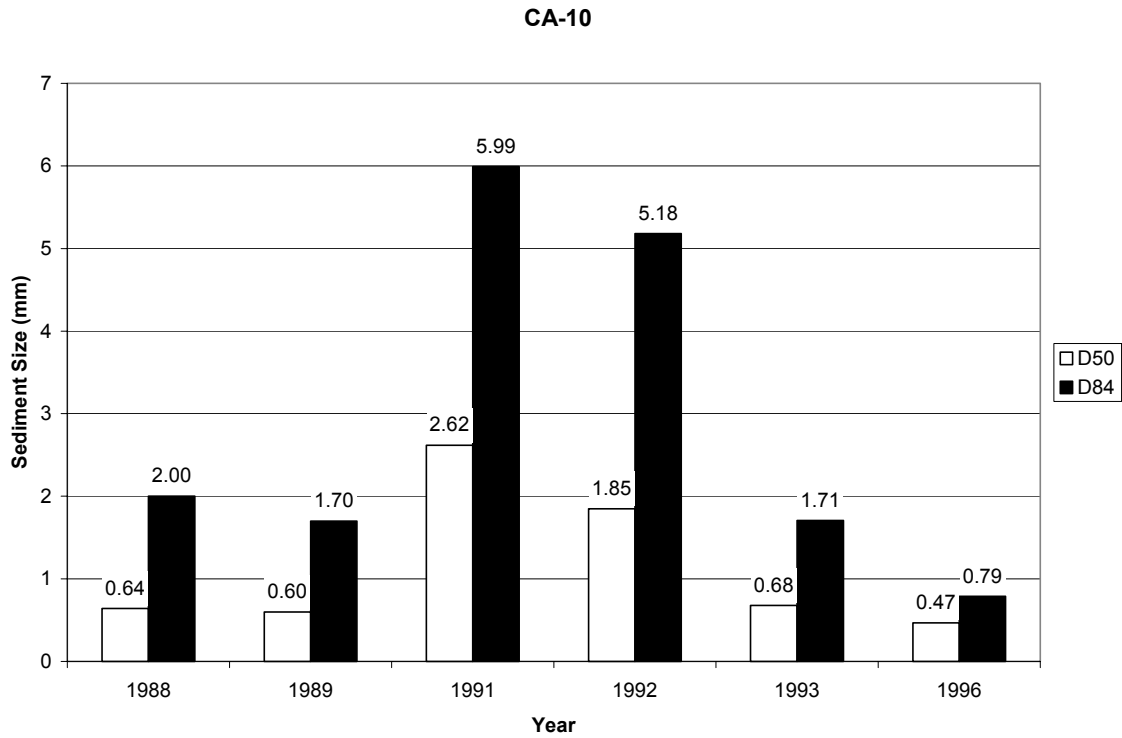
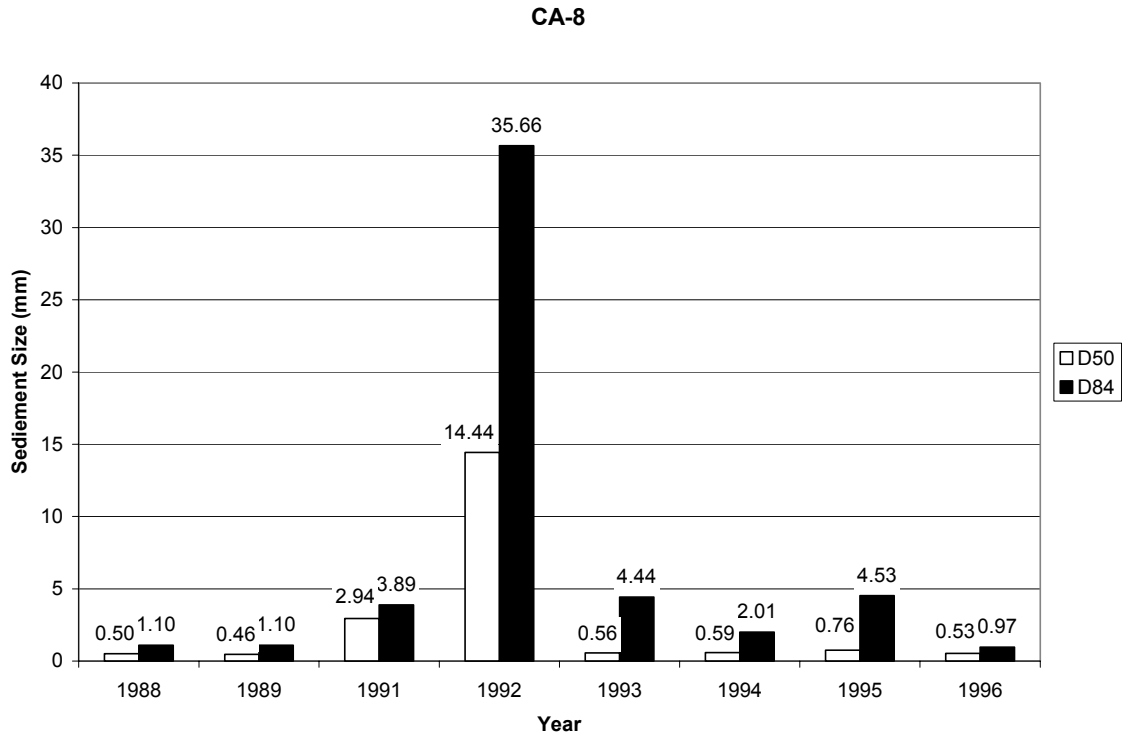
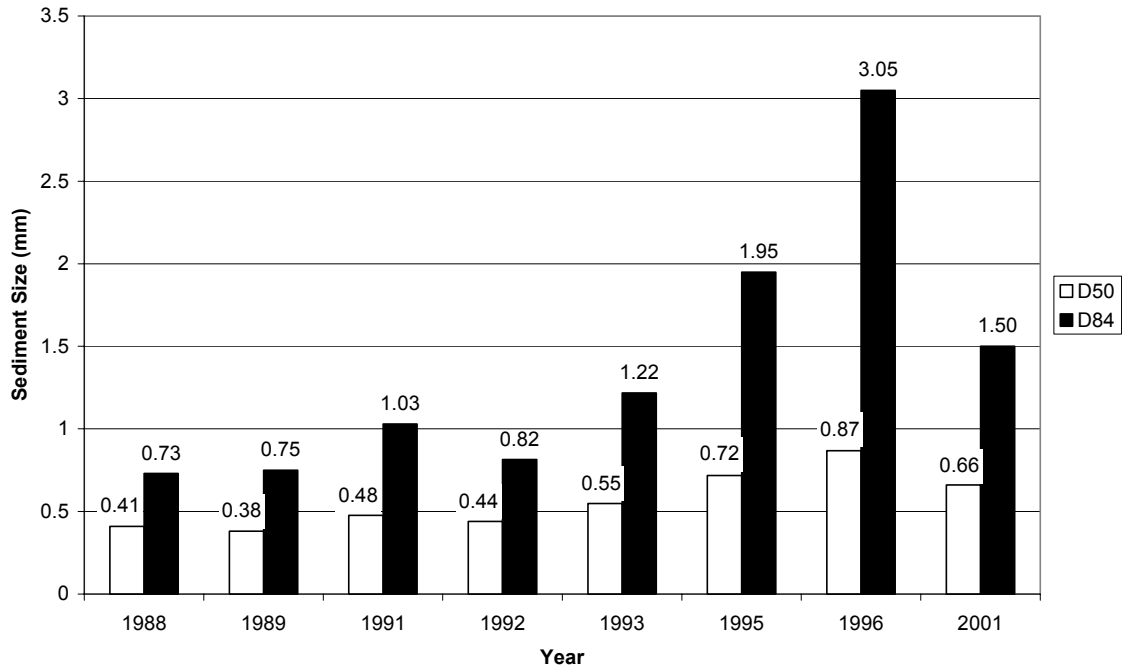


Figure F-4 Histograms depicting the D_{50} and D_{84} change with time for CA-8 and CA-10 (Corrales Reach).

CA-12



CA-13

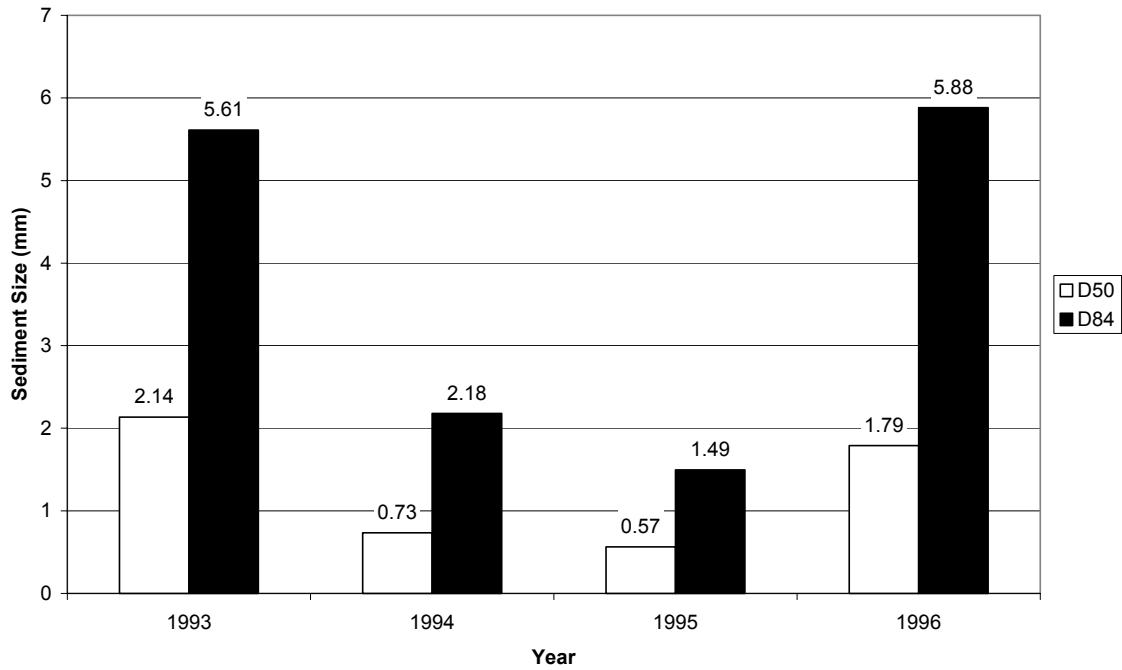


Figure F-5 Histograms depicting the D_{50} and D_{84} change with time for CA-12 and CA-13 (Corrales Reach).

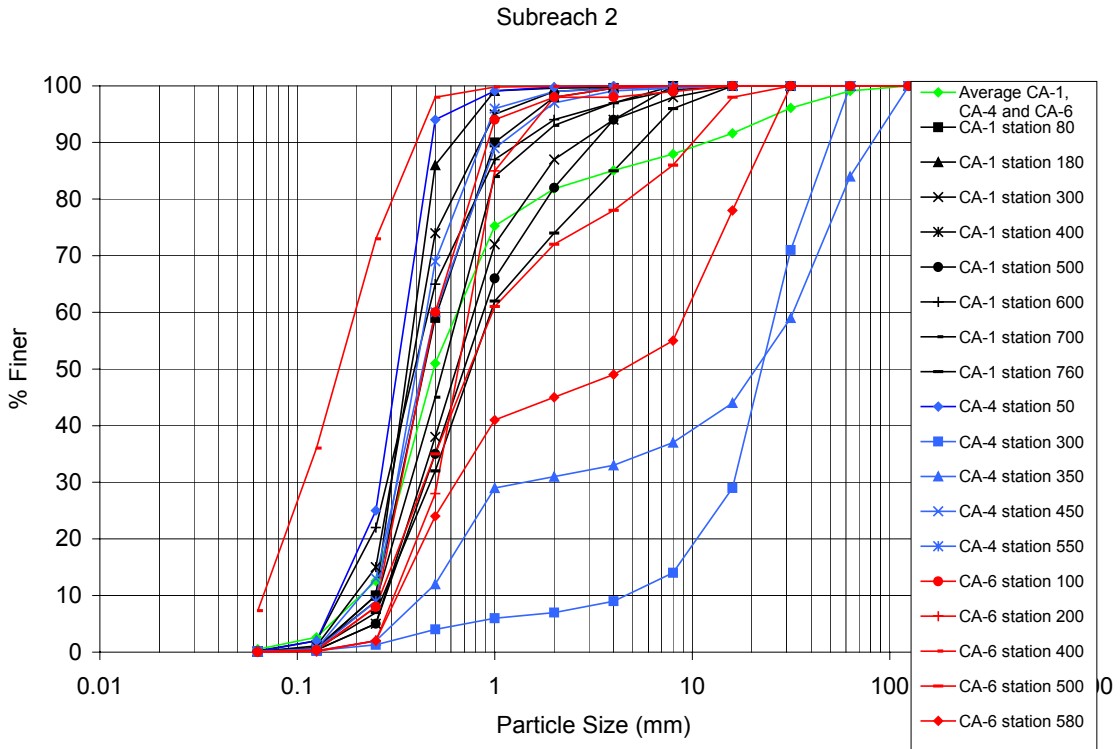
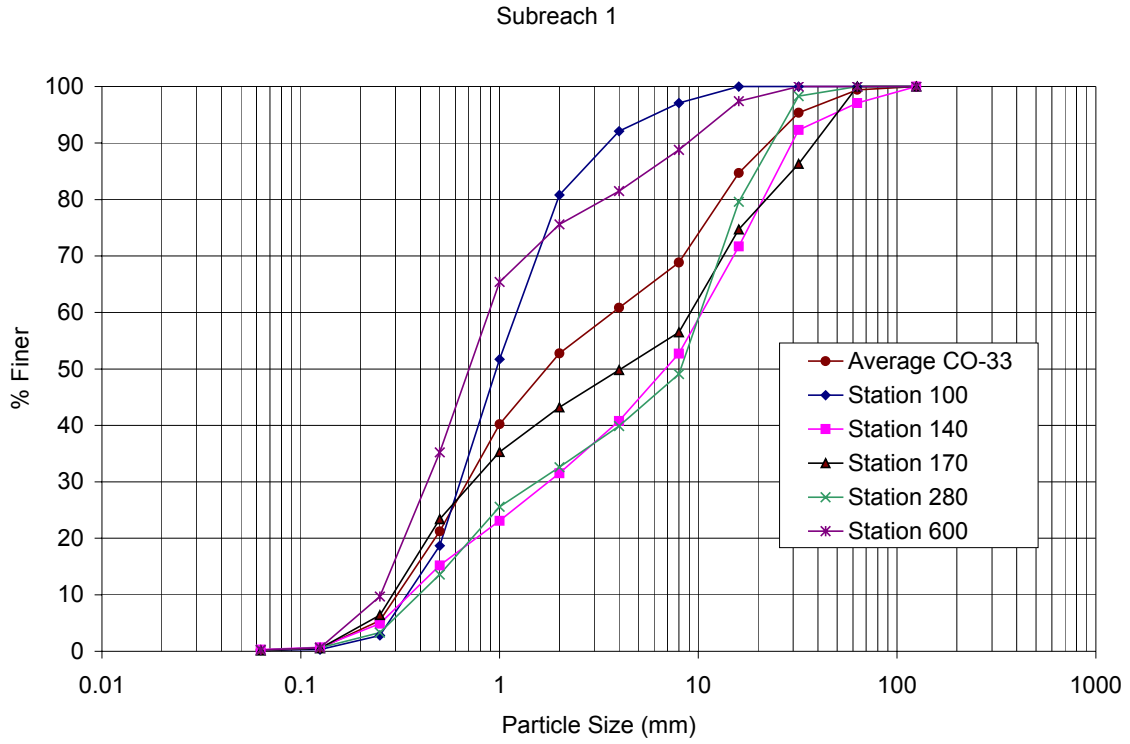


Figure F-6 1992 sediment size distribution curves for subreaches 1 and 2.

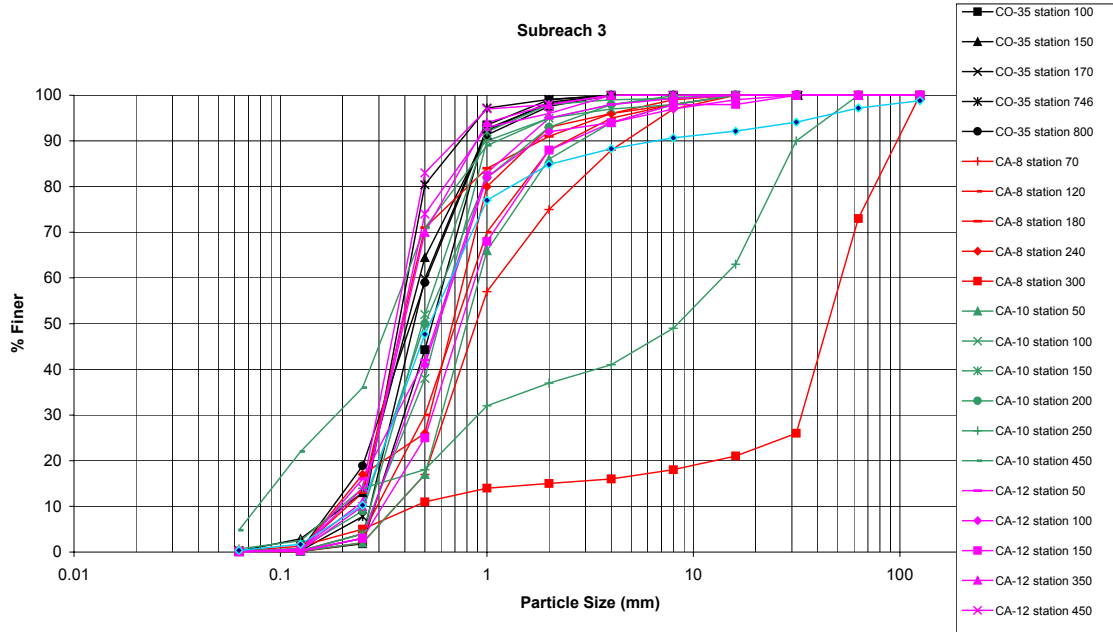


Figure F-71992 sediment size distribution curves for subreach 3.

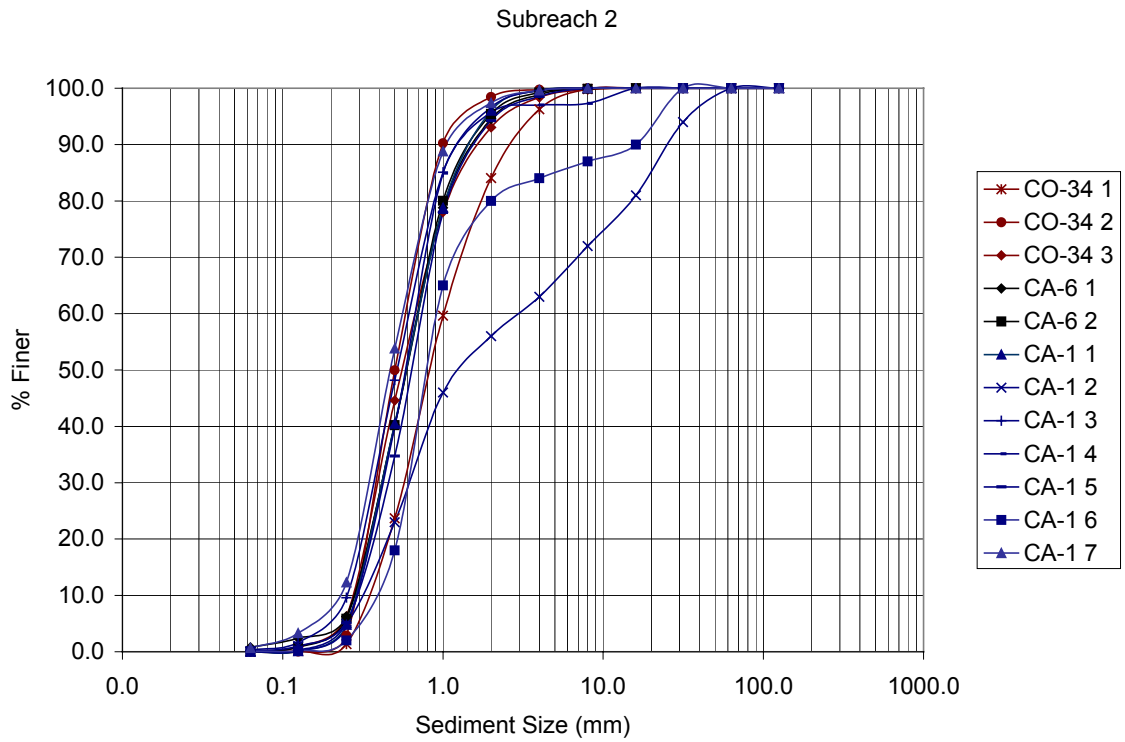
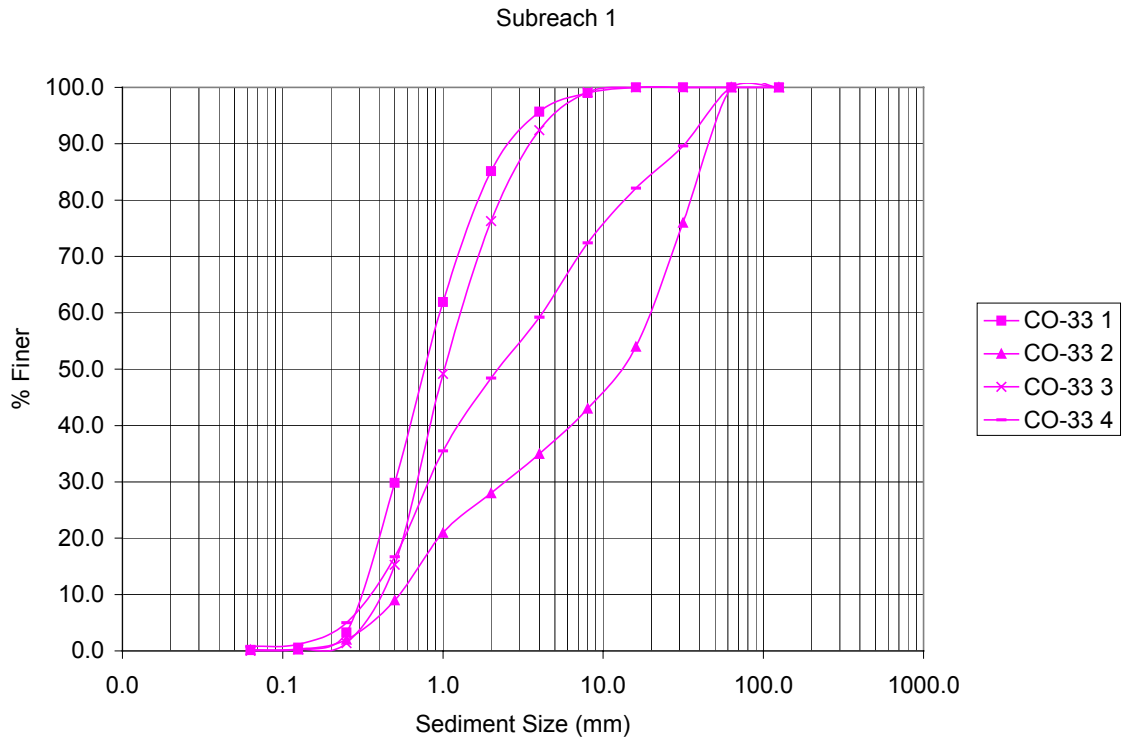


Figure F-8 2001 sediment size distribution curves for subreaches 1 and 2.

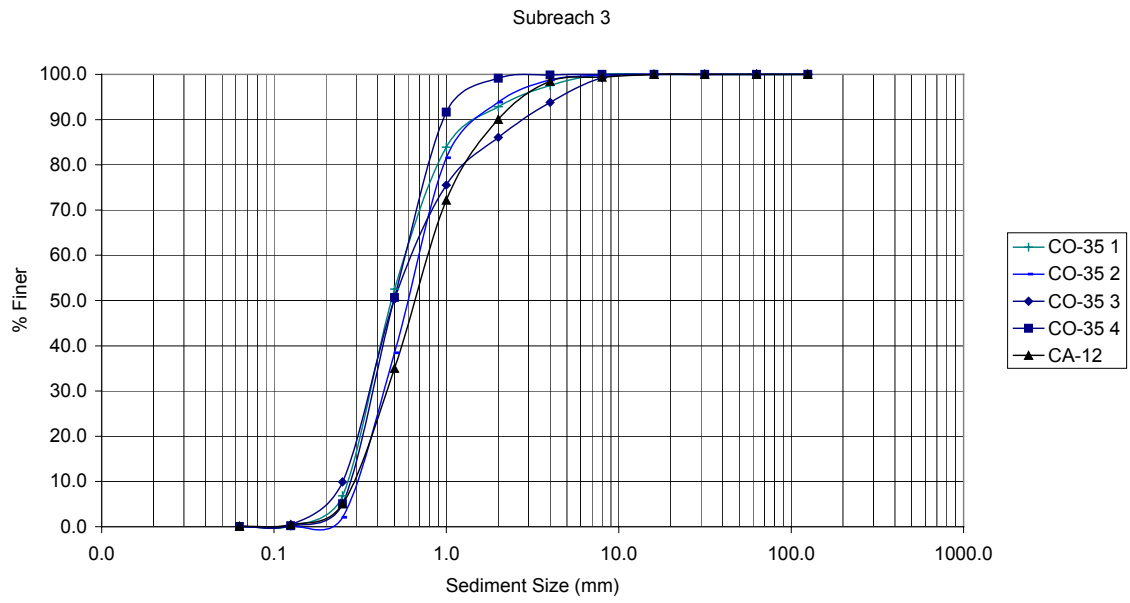


Figure F-9 2001 sediment size distribution curves for subreach 3.

Table F-1 Median grain size statistics from the bed material samples at Bernalillo gage, CO-lines, CA-lines and CR-lines.

Reach	Year	Station	Number of Observations	Range of flow discharges (cfs)	d ₅₀					
					Minimum value (mm)	Maximum value (mm)	Mean value (mm)	Standard deviation (mm)	# of d50 in the sand range	# of d50 in the gravel range
Entire reach	1961	Bernalillo Gage	3	2140-3850	0.20	0.22	0.21	0.01	3	0
Subreach 1	1972	CO-33	2	996-1010	0.21	0.27	0.24	0.05	2	0
Subreach 2	1972	CO-34	2	607-1010	0.179	0.181	0.180	0.001	2	0
Subreach 3	1972	CO-35	2	685-1250	0.179	0.249	0.21	0.050	2	0
Subreach 1	1992	CO-33	5	517	0.70	16.05	5.73	6.29	2	3
Subreach 2	1992	CA-1	8	3260	0.40	0.76	0.53	0.15	8	0
Subreach 2	1992	CA-4	5	3260	0.31	22.45	8.9	11.7	3	2
Subreach 2	1992	CA-6	5	3030	0.16	4.49	1.30	1.80	4	1
Average Subreach 2	1992	CA-1,CA-4, CA-6	18	3030-3260	0.16	22.45	3.07	6.85	15	3
Subreach 3	1992	CO-35	5	575	0.340	0.460	0.45	0.05	5	
Subreach 3	1992	CA-8	6	3030	0.4	44.93	14.44	21.41	4	2
Subreach 3	1992	CA-10	6	3030	0.33	8.4	1.85	3.21	5	1
Subreach 3	1992	CA-12	6	2610	0.36	0.75	0.51	0.15	6	0
Average Subreach 3	1992	CO-35, CA-8, CA-10, CA-12	23	575-3030	0.33	44.93	4.48	11.98	20	3
Subreach 1	2001	CO-33	4	422-892	0.78	12.44	4.11	5.59	2	2
Subreach 1	2001	CR-355	1	2130	0.56	0.56	0.56	0	1	0
Subreach 1	2001	CR-361	1	2410	0.5	0.5	0.5	0	1	0
Subreach 1	2001	CR-367	1	2410	0.54	0.54	0.54	0	1	0
Subreach 1	2001	CR-372	1	2410	0.72	0.72	0.72	0	1	0
Subreach 1	2001	CR-378	1	2410	0.57	0.57	0.57	0	1	0
Subreach 1	2001	CR-382	1	2410	0.48	0.48	0.48	0	1	0
Subreach 1	2001	CR-388	1	2460	0.45	0.45	0.45	0	1	0
Subreach 1	2001	CR-394	1	2460	0.53	0.53	0.53	0	1	0
Average Subreach 1	2001	CO-33, CR-355, 361, 367, 372, 378, 382, 388, 394	12	422-2460	0.45	12.44	1.73	3.41	10	2
Subreach 2	2001	CO-34	3	422-952	0.5	0.84	0.63	0.18	3	0
Subreach 2	2001	CA-1	2	824-892	0.59	1.32	0.92	0.52	2	0
Subreach 2	2001	CA-2	1	892	0.51	0.51	0.51	0	1	0
Subreach 2	2001	CA-6	2	438	0.59	0.59	0.59	0	2	0
Subreach 2	2001	CR-400	1	2600	0.49	0.49	0.49	0	1	0
Subreach 2	2001	CR-413	1	2600	0.69	0.69	0.69	0	1	0
Average Subreach 2	2001	CO-34, CA-1, 2, 6, CR-400, 413	10	422-2600	0.49	1.32	0.67	0.25	10	0
Subreach 3	2001	CO-35	4	438-952	0.49	0.59	0.52	0.050	4	0
Subreach 3	2001	CA-9	1	824	0.57	0.57	0.57	0	1	0
Subreach 3	2001	CA-12	3	438-952	0.63	0.81	0.7	0.1	3	0
Subreach 3	2001	CA-13	1	1050	0.47	0.47	0.47	0	1	0
Subreach 3	2001	CR-443	1	1050	0.36	0.36	0.36	0	1	0
Subreach 3	2001	CR-448	1	1050	0.48	0.48	0.48	0	1	0
Subreach 3	2001	CR-458	1	1050	0.46	0.46	0.46	0	1	0
Subreach 3	2001	CR-462	1	1050	0.38	0.38	0.38	0	1	0
Average Subreach 3	2001	CO-35, CA-9, 12, 13, CR-443, 448, 458, 462	13	438-1050	0.36	0.81	0.53	0.12	13	0

**APPENDIX G:
MEP Input Data and Results
(Corrales Reach)**

Table G-1 MEP Input data for Albuquerque gage.

Year	Month	Day	Velocity (ft/s)	Temp (degrees)	Temp (F)	Depth (feet)	Inst. Discharge (cfs)	Computed Area (sq-ft)	Width (feet)	Concentration in ppm	Avr. Depth of SS sampler
1978	4	10	1.9	9.5	49.1	1.2	326	181.2	151	408	0.9
1978	4	24	1.8	12.5	54.5	1.1	329	180.4	164	696	0.8
1978	5	8	2.3	16.5	61.7	2.3	1420	607.2	264	925	2
1978	5	22	4.4	18	64.4	3	4260	960	320	4020	2.7
1978	5	30	2.9	19	66.2	3.2	2520	864	270	942	2.9
1978	6	5	3.1	19	66.2	3.3	2810	920.7	279	1079	3
1978	6	26	2.4	20	68	2.2	1350	556.6	253	637	1.9
1978	7	24	2	25	77	1.7	1040	511.7	301	2526	1.4
1979	4	2	3	10	50	2.2	1840	605	275	781	1.9
1979	4	23	4.4	15	59	4	4980	1140	285	2107	3.7
1979	5	29	4.8	18	64.4	5	6610	1375	275	1997	4.7
1979	6	18	4.9	17.5	63.5	4.9	6920	1421	290	1818	4.6
1979	7	9	4.6	20	68	4.3	6040	1298.6	302	2027	4
1980	4	7	1.9	11	51.8	1.6	926	496	310	126	1.3
1980	4	28	4.7	12.5	54.5	3.2	4730	1008	315	2117	2.9
1980	5	12	4.5	13	55.4	4.7	6900	1527.5	325	1688	4.4
1980	6	9	4.8	17	62.6	4.3	6610	1376	320	1518	4
1981	4	20	1.9	17	62.6	1.4	641	336	240	68	1.1
1981	6	22	1.8	23	73.4	1.3	694	390	300	390	1
1981	7	27	1.8	27	80.6	1.1	584	308	280	685	0.8
1981	8	24	2	23	73.4	0.77	260	130.9	170	0	0.47
1982	4	26	2.6	12	53.6	2.4	1740	672	280	1658	2.1
1982	5	3	3.2	15	59	3.5	3350	1050	300	1129	3.2
1982	5	24	3.4	17.5	63.5	3.6	4280	1260	350	897	3.3
1982	6	7	3.7	13.5	56.3	3.6	4570	1224	340	678	3.3
1982	6	21	3.1	18	64.4	3.3	3480	1105.5	335	492	3

Table G-1 MEP Input data for Albuquerque gage.

Year	Month	Day	Velocity (ft/s)	Temp (degrees)	Temp (F)	Depth (feet)	Inst. Discharge (cfs)	Computed Area (sq-ft)	Width (feet)	Concentration in ppm	Avr. Depth of SS sampler
1982	7	7	2.3	21	69.8	2.5	1100	462.5	185	167	2.2
1982	7	26	1.5	24	75.2	1.6	159	102.4	64	69	1.3
1984	4	3	2.7	3	37.4	1.7	1350	493	290	107	1.4
1984	4	24	3.6	16	60.8	3.2	4270	1152	360	831	2.9
1984	5	8	4	12	53.6	3.2	4440	1088	340	904	2.9
1984	7	10	1.7	23.5	74.3	1.6	396	232	145	144	1.3
1985	5	15	5	15	59	3.8	7170	1444	380	434	3.5
1985	6	17	3.2	20.5	68.9	3	3620	1110	370	84	2.7
1986	5	6	3.1	15	59	2.1	2430	787.5	375	241	1.8
1986	5	20	3	16.5	61.7	2.1	2300	774.9	369	223	1.8
1986	6	3	3.6	12	53.6	2.6	3440	954.2	367	387	2.3
1988	5	11	2.53	20.5	68.9	1.9	1800	712.5	375	337	1.6
1990	5	8	2.77	16.5	61.7	2.3	1950	713	310	142	2
1990	7	2	2.05	24.5	76.1	1.1	570	270.6	246	102	0.8
1991	4	4	2.89	10	50	2.3	1490	506	220	262	2
1991	4	10	3.33	12	53.6	2.4	2130	650.4	271	2157	2.1
1991	4	22	3.44	13.5	56.3	2.6	3060	878.8	338	174	2.3
1991	6	3	3.79	-999999		3.1	3590	957.9	309	669	2.8
1991	7	2	3.32	15	59	2.1	2470	756	360	300	1.8
1991	7	10	1.44	-999999		0.99	401	280.17	283	218	0.69
1992	6	18	2.93	19.5	67.1	2.9	2610	899	310	550	2.6
1992	6	29	1.64	24	75.2	1.9	853	535.8	282	851	1.6
1992	7	31	2.03	23.5	74.3	1.4	801	397.6	284	1299	1.1
1994	4	1	2.47	9.5	49.1	1.9	1370	551	290	151	1.6
1994	5	2	3.36	-999999		3.1	3300	985.8	318	317	2.8
1994	6	13	3.67	17.9	64.22	4.2	5030	1386	330	143	3.9
1994	6	27	3.68	22.9	73.22	4	4860	1308	327	382	3.7

Table G-1 MEP Input data for Albuquerque gage.

Year	Month	Day	Velocity (ft/s)	Temp (degrees)	Temp (F)	Depth (feet)	Inst. Discharge (cfs)	Computed Area (sq-ft)	Width (feet)	Concentration in ppm	Avr. Depth of SS sampler
1995	5	5	3.26	13.5	56.3	3.8	3980	1204.6	317	641	3.5
1995	5	24	4.13	17	62.6	4.8	6400	1540.8	321	668	4.5
1995	6	6	3.94	-999999		3.8	4960	1261.6	332	682	3.5
1995	7	3	3.99	16.5	61.7	4.4	5620	1416.8	322	992	4.1
1996	4	5	1.95	8.3	46.94	1.7	437	219.3	129	919	1.4
1996	5	3	1.99	15.4	59.72	2	471	238	119	367	1.7
1996	6	20	1.78	19.2	66.56	1.2	572	319.2	266	86	0.9
1997	4	4	2.87	10	50	2.2	2090	721.6	328	1498	1.9
1997	6	3	3.52	16.5	61.7	4.2	5040	1411.2	336	1818	3.9
1998	5	5	3.25	13.5	56.3	3	3180	990	330	534	2.7
1998	6	3	3.13	18	64.4	3.4	3540	1118.6	329	2177	3.1
1999	4	27	2.23	12	53.6	1.6	969	428.8	268	164	1.3
1999	5	24	3.49	15.5	59.9	3.4	4080	1166.2	343	648	3.1
1978	8	7	1.9	22.5	72.5	1.4	817	421.4	301	785	1.1
1978	8	22	1.8	21	69.8	1.1	559	304.7	277	476	0.8
1979	8	13	1.9	21.5	70.7	1.4	588	308	220	514	1.1
1979	9	10	2.3	20	68	1.3	521	234	180	137	1
1980	8	18	1.4	22.5	72.5	0.89	377	267	300	436	0.59
1980	9	15	1.6	21.5	70.7	0.96	447	279.36	291	229	0.66
1990	8	6	1.6	18	64.4	1	415	258	258	157	0.7
1990	9	4	1.4	17.5	63.5	0.8	267	189.6	237	79	0.5
1992	8	31	2.1	21.5	70.7	1.8	1070	514.8	286	343	1.5
1993	8	13	2.08	20	68	1.6	536	262.4	164	179	1.3
1994	8	4	1.64	22.2	71.96	1.8	588	358.2	199	1658	1.5
1994	9	30	1.73	17.2	62.96	1.4	383	225.4	161	108	1.1
1997	9	2	1.95	20.5	68.9	1.5	774	381	254	445	1.2
1999	9	17	2.32	19	66.2	1.8	1080	477	265	152	1.5

Table G-1 MEP Input data for Albuquerque gage.

Year	Month	Day	SED-BED- SIEVE- % <0.062 mm	SED-BED- SIEVE- % <0.125 mm	SED-BED- SIEVE- % <0.25 mm	SED-BED- SIEVE- % <0.5 mm	SED-BED- SIEVE- % <1 mm	SED-BED- SIEVE- % <2 mm	SED-BED- SIEVE-% < 4 mm	SED-BED- SIEVE-% < 8 mm	SED-BED- SIEVE- %< 16 mm
1978	4	10					92	95	97	98	100
1978	4	24									
1978	5	8	1	3	36	84	98	100			
1978	5	22	1	3	36	90	100				
1978	5	30	0	4	45	90	99	100			
1978	6	5	0	1	28	86	98	100			
1978	6	26					64	67	72	82	96
1978	7	24	1	3	49	88	95	100			
1979	4	2	0	2	44	89	97	100			
1979	4	23					81	86	88	91	95
1979	5	29					70	82	87	89	92
1979	6	18					66	72	76	80	84
1979	7	9					82	90	93	95	98
1980	4	7					86	91	93	95	97
1980	4	28					79	85	88	91	97
1980	5	12					79	82	84	85	91
1980	6	9					77	81	83	86	89
1981	4	20					90	93	96	98	100
1981	6	22					88	91	92	94	96
1981	7	27					97	99	99	99	100
1981	8	24					96	98	99	100	
1982	4	26					97	99	99	100	
1982	5	3					99	100			
1982	5	24					89	97	99	100	
1982	6	7					86	91	94	96	99
1982	6	21					86	94	96	96	96

Table G-1 MEP Input data for Albuquerque gage.

Year	Month	Day	SED-BED- SIEVE- % <0.062 mm	SED-BED- SIEVE- % <0.125 mm	SED-BED- SIEVE- % <0.25 mm	SED-BED- SIEVE- % <0.5 mm	SED-BED- SIEVE- % <1 mm	SED-BED- SIEVE- % <2 mm	SED-BED- SIEVE-% < 4 mm	SED-BED- SIEVE-% < 8 mm	SED-BED- SIEVE- %< 16 mm
1982	7	7					87	93	97	99	100
1982	7	26					82	93	97	100	
1984	4	3					68	72	75	80	91
1984	4	24	0	1	55	99	100				
1984	5	8					98	99	99	99	100
1984	7	10					79	92	97	100	
1985	5	15	15	57	96	100					
1985	6	17					98	98	98	99	100
1986	5	6					85	87	89	91	94
1986	5	20					73	83	90	97	100
1986	6	3					97	98	99	100	
1988	5	11	19	40	54	86	99	100			
1990	5	8	9	18	28	66	93	98	99	100	
1990	7	2	0	1	17	82	97	99	100	100	
1991	4	4	0	1	20	77	96	99	99	100	
1991	4	10		0	2	39	90	98	100		
1991	4	22	8	11	22	81	98	99	100		
1991	6	3	0	3	23	77	97	100	100		
1991	7	2	1	4	16	72	97	100			
1991	7	10		0	11	60	94	99	100		
1992	6	18	23	75	97	100					
1992	6	29		0	12	68	91	99	100		
1992	7	31	0	3	17	44	70	79	83	88	100
1994	4	1		0	6	40	72	87	96	99	100
1994	5	2	0	1	10	48	79	92	97	99	100
1994	6	13	3	35	99	100					
1994	6	27	0	1	14	63	94	99	100		

Table G-1 MEP Input data for Albuquerque gage.

Year	Month	Day	SED-BED- SIEVE- % <0.062 mm	SED-BED- SIEVE- % <0.125 mm	SED-BED- SIEVE- % <0.25 mm	SED-BED- SIEVE- % <0.5 mm	SED-BED- SIEVE- % <1 mm	SED-BED- SIEVE- % <2 mm	SED-BED- SIEVE-% < 4 mm	SED-BED- SIEVE-% < 8 mm	SED-BED- SIEVE- %< 16 mm
1995	5	5		0	7	67	92	96	97	99	100
1995	5	24		0	8	60	89	97	99	100	
1995	6	6		0	4	39	71	78	82	86	90
1995	7	3		0	10	86	99	100	100		
1996	4	5	0	1	12	56	87	92	93	94	94
1996	5	3	1	4	15	61	92	98	100		
1996	6	20		0	12	60	82	88	90	92	98
1997	4	4	4	7	16	69	95	99	99	100	
1997	6	3		0	7	49	80	89	100	96	97
1998	5	5	1	3	13	66	92	97	98	99	100
1998	6	3	0	1	10	58	89	95	98	100	
1999	4	27		0	7	56	91	99	100		
1999	5	24		0	12	60	88	95	98	100	
1978	8	7					97	99	100		
1978	8	22					94	98	100		
1979	8	13			30	79	97	98	100		
1979	9	10	0	1	34	85	97	98		99	99
1980	8	18	1	1	27	66	72	74		79	85
1980	9	15					85	90	93	95	97
1990	8	6	0	1	10	57	78	89	95	99	100
1990	9	4	0	1	17	65	91	98	99	100	
1992	8	31	0	1	13	73	96	99	99	100	
1993	8	13	0	1	10	54	83	87	90	94	100
1994	8	4	1	3	18	68	93	98	100		
1994	9	30		0	11	56	84	93	98	100	
1997	9	2	0	1	6	53	85	93	96	97	100
1999	9	17	0	1	6	48	84	95	98	98	100

Table G-1 MEP Input data for Albuquerque gage.

Year	Month	Day	SED-BED- SIEVE-% < 32 mm
1978	4	10	
1978	4	24	
1978	5	8	
1978	5	22	
1978	5	30	
1978	6	5	
1978	6	26	100
1978	7	24	
1979	4	2	
1979	4	23	100
1979	5	29	100
1979	6	18	100
1979	7	9	100
1980	4	7	100
1980	4	28	100
1980	5	12	100
1980	6	9	100
1981	4	20	
1981	6	22	100
1981	7	27	
1981	8	24	
1982	4	26	
1982	5	3	
1982	5	24	
1982	6	7	100
1982	6	21	100

Table G-1 MEP Input data for Albuquerque gage.

Year	Month	Day	SED-BED- SIEVE-% < 32 mm
1982	7	7	
1982	7	26	
1984	4	3	100
1984	4	24	
1984	5	8	
1984	7	10	
1985	5	15	
1985	6	17	
1986	5	6	100
1986	5	20	
1986	6	3	
1988	5	11	
1990	5	8	
1990	7	2	
1991	4	4	
1991	4	10	
1991	4	22	
1991	6	3	
1991	7	2	
1991	7	10	
1992	6	18	
1992	6	29	
1992	7	31	
1994	4	1	
1994	5	2	
1994	6	13	
1994	6	27	

Table G-1 MEP Input data for Albuquerque gage.

Year	Month	Day	SED-BED- SIEVE-% < 32 mm
1995	5	5	
1995	5	24	
1995	6	6	100
1995	7	3	
1996	4	5	100
1996	5	3	
1996	6	20	100
1997	4	4	
1997	6	3	100
1998	5	5	
1998	6	3	
1999	4	27	
1999	5	24	
1978	8	7	
1978	8	22	
1979	8	13	
1979	9	10	100
1980	8	18	100
1980	9	15	100
1990	8	6	
1990	9	4	
1992	8	31	
1993	8	13	
1994	8	4	
1994	9	30	
1997	9	2	
1999	9	17	

Table G-1 MEP Input data for Albuquerque gage.

Year	Month	Day	0.002	0.004	0.008	0.016	0.062	0.125	0.25	0.5	1	2
			SED-SUSP-FALL-D-% <.002mm	SED-SUSP-FALL-D-% <0.004 mm	SED-SUSP-FALL-D-% <0.008 mm	SED-SUSP-FALL-D-% <0.016 mm	SED-SUSP-FALL-D-% <0.062m m	SED-SUSP-FALL-D-% <0.125 mm	SED-SUSP-FALL-D-% <0.25 mm	SED-SUSP-FALL-D-% <0.500 mm	SED-SUSP-FALL-D-% <1 mm	SED-SUSP-Sieve-D-% <2 mm
1978	4	10	55	63		74	85	88	98	100		
1978	4	24	15	17		20	24	26	56	94	96	96
1978	5	8	32	34		39	59	69	87	100		
1978	5	22	9	10		13	24	33	53	83	98	
1978	5	30	19	21		25	44	56	89	100		
1978	6	5	11	12		16	32	42	76	100		
1978	6	26					31	45	79	95	100	
1978	7	24	40	48		85	94	96	100			
1979	4	2					29	48	90	100		
1979	4	23	6	7		9	22	42	82	100		
1979	5	29	7	8		10	17	32	77	100		
1979	6	18	4	5		6	13	27	72	96	100	
1979	7	9	1	1		2	6	19	78	98	100	
1980	4	7					29	38	84	100		
1980	4	28	4	5		5	12	19	53	83	99	
1980	5	12	8	8		10	17	28	70	96	100	
1980	6	9	3	4	4	5	9	16	68	94	100	
1981	4	20	22	26	30	35	50	59	82	99	100	
1981	6	22	18	22		38	53	56	65	96	100	
1981	7	27	39	48		76	90	92	97	100		
1981	8	24	44	55		74	94	94	98	100		
1982	4	26	3	4		5	13	15	33	87	100	
1982	5	3	9	13		17	48	61	81	97	100	
1982	5	24	6	8		11	35	48	81	99	100	
1982	6	7	5	7		9	27	43	79	98	100	
1982	6	21	4	6		8	22	39	81	100		

Table G-1 MEP Input data for Albuquerque gage.

Year	Month	Day	SED-SUSP-FALL-D-% <.002mm	SED-SUSP-FALL-D-% <0.004 mm	SED-SUSP-FALL-D-% <0.008 mm	SED-SUSP-FALL-D-% <0.016 mm	SED-SUSP-FALL-D-% <0.062m m	SED-SUSP-FALL-D-% <0.125 mm	SED-SUSP-FALL-D-% <0.25 mm	SED-SUSP-FALL-D-% <0.500 mm	SED-SUSP-FALL-D-% <1 mm	SED-SUSP-Sieve-D-% <2 mm
1982	7	7					38	41	88	98	100	
1982	7	26					76	85	94	100		
1984	4	3					51	58	79	100		
1984	4	24					31	53	86	100		
1984	5	8					25	39	77	98	100	
1984	7	10					80	81	87	98	100	
1985	5	15					42	75	100			
1985	6	17					58	87	99	100		
1986	5	6					20	31	77	100		
1986	5	20					21	33	74	98	100	
1986	6	3					16	27	85	100		
1988	5	11	58	71		88	96	100				
1990	5	8					74	91	100			
1990	7	2					81	93	99	100		
1991	4	4					41	50	86	100		
1991	4	10					10	13	19	78	100	
1991	4	22					77	90	96	100		
1991	6	3					23	37	67	92	94	96
1991	7	2					67	79	93	100		
1991	7	10					47	48	54	85	100	
1992	6	18					11	22	41	78	84	92
1992	6	29					7	8	20	84	93	100
1992	7	31					12	12	20	79	96	100
1994	4	1					41	52	82	100		
1994	5	2					38	47	70	99	100	
1994	6	13					57	94	97	100		
1994	6	27					21	34	66	100		

Table G-1 MEP Input data for Albuquerque gage.

Year	Month	Day	SED-SUSP-FALL-D-% <.002mm	SED-SUSP-FALL-D-% <0.004 mm	SED-SUSP-FALL-D-% <0.008 mm	SED-SUSP-FALL-D-% <0.016 mm	SED-SUSP-FALL-D-% <0.062m m	SED-SUSP-FALL-D-% <0.125 mm	SED-SUSP-FALL-D-% <0.25 mm	SED-SUSP-FALL-D-% <0.500 mm	SED-SUSP-FALL-D-% <1 mm	SED-SUSP-Sieve-D-% <2 mm
1995	5	5					29	41	64	100		
1995	5	24					25	40	64	95	100	
1995	6	6					14	17	44	75	100	
1995	7	3					12	15	30	68	83	95
1996	4	5					3	4	9	54	90	100
1996	5	3					9	10	13	74	100	
1996	6	20					64	66	83	100		
1997	4	4					22	23	35	74	100	
1997	6	3					9	13	29	81	95	99
1998	5	5					31	45	68	97	98	100
1998	6	3					5	15	48	82	97	100
1999	4	27	31	36	42	49	61	72	93	100		
1999	5	24	12	14	17	19	28	36	65	99	100	
1978	8	7	36	52		70	84	88	99	100		
1978	8	22	42	53		75						
1979	8	13	34	44		59	65	67	74	81	99	
1979	9	10					77	82	98	100		
1980	8	18	16	18		22	27	27	36	96	100	
1980	9	15	46	57		79	91	93	98	100		
1990	8	6					74	86	97	100		
1990	9	4					84	90	96	100		
1992	8	31					81	89	95	100		
1993	8	13					82	83	94	100		
1994	8	4	60	76	89	94	98	99	99	100		
1994	9	30					85	88	96	100		
1997	9	2					94	95	98	100		
1999	9	17					74	77	90	100		

Table G-2 MEP Results for Albuquerque gage and bed-material load estimations.

Date	Inst. Discharge (cfs)	MEP results			d10 bed material	%	% bed material load	Bed material load (t/day)
		Total load	Sand load	Gravel load				
4/10/1978	326	498	177.8	0	0.16	92	8	40
4/24/1978	329	1319.9	1075.3	71.7	0.15	31	69	911
5/8/1978	1420	5186.7	2984.6	0	0.14	71	29	1504
5/22/1978	4260	69639	58058	0	0.15	36	64	44569
5/30/1978	2520	9891.2	6931.3	0	0.14	60	40	3956
6/5/1978	2810	12581	9882.1	0	0.17	51	49	6165
6/26/1978	1350	3967.6	3206.7	6.9	0.14	50	50	1984
7/24/1978	1040	7854.2	1099.4	0	0.14	96	4	314
4/2/1979	1840	7402.1	6199.2	0	0.14	54	46	3405
4/23/1979	4980	46704	32668	63.2	0.14	47	53	24753
5/29/1979	6610	56805	45329	589.6	0.17	50	50	28403
6/18/1979	6920	47924	42714	718	0.17	42	58	27796
7/9/1979	6040	50108	47521	465.8	0.15	31	69	34575
4/7/1980	926	632.5	535	0	0.18	60	40	253
4/28/1980	4730	44564	40624	586	0.2	41	59	26292
5/12/1980	6900	101837	39079	130.8	0.13	32	68	69249
6/9/1980	6610	94408	36005	170.2	0.14	22	78	73638
4/20/1981	641	382.7	311.3	0	0.15	62	38	145
6/22/1981	694	1223	813.7	0	0.15	58	42	514
7/27/1981	584	1527.7	506.4	0	0.15	94	6	92
4/26/1982	1740	12908	11471	0	0.16	21	79	10197
5/3/1982	3350	15378	10183	0	0.13	62	38	5843
5/24/1982	4280	15494	11801	15	0.12	47	53	8212
6/7/1982	4570	14723	12313	52	0.17	55	45	6625
6/21/1982	3480	7363.3	6331.5	6.8	0.25	81	19	1399
7/7/1982	1100	944.3	746.8	0.2	0.18	60	40	378
7/26/1982	159	42.4	18	0	0.19	90	10	4
4/3/1984	1350	1600.6	1250.6	12	0.048		100	1601
4/24/1984	4270	16901	13835	0	0.12	52	48	8113
5/8/1984	4440	20624	17746	0	0.14	43	57	11756
7/10/1984	396	232.4	93.8	0	0.19	84	16	37
5/15/1985	7170	21146	15793	0	0.039		100	21146
6/17/1985	3620	2060	1568.9	0	0.26	99	1	21
5/6/1986	2430	4713.4	4334.6	10.2	0.16	41	59	2781
5/20/1986	2300	3625.9	3274	37.7	0.2	60	40	1450
6/3/1986	3440	9018.5	8383	11.4	0.15	40	60	5411
6/30/1986	3320	5074.7	3089.8	0	0.24	95	5	254
5/11/1988	1800	6156.2	2448.1	0	0.046	94	6	369
5/8/1990	1950	2721.4	2022.2	1.7	0.065	74	26	708
7/2/1990	570	380	240.4	0	0.19	95	5	19
4/4/1991	1490	2590.6	2128.5	0	0.18	69	31	803
4/10/1991	2130	18968	17698	20.9	0.3	35	65	12329
4/22/1991	3060	4027	2628.7	9	0.1	86	14	564
6/3/1991	3590	15610	11825	2152	0.16	45	55	8585
7/2/1991	2470	4588.4	3182.9	0	0.18	85	15	688

Table G-2 MEP Results for Albuquerque gage and bed-material load estimations.

Date	Inst. Discharge (cfs)	MEP results			d10 bed material	%	% bed material load	Bed material load (t/day)
		Total load	Sand load	Gravel load				
7/10/1991	401	335.8	220.7	0	0.24	53	47	158
6/18/1992	2610	9164.3	7276.8	985.4	0.042		100	9164
6/29/1992	853	2162.6	2024.2	0	0.24	19	81	1752
7/31/1992	801	3884.5	3509.8	1.5	0.18	15	85	3302
4/1/1994	1370	1191.1	947.9	7.6	0.29	84	16	191
5/2/1994	3300	5670.8	4495.7	48.1	0.25	70	30	1701
6/13/1994	5030	4493.5	3129.8	0	0.074	67	33	1483
6/27/1994	4860	11452	10332	18	0.2	54	46	5268
5/5/1995	3980	11194	9148.1	6.1	0.26	65	35	3918
5/24/1995	6400	19249	16235	63.7	0.26	65	35	6737
6/6/1995	4960	16226	14724	200.5	0.29	45	55	8924
7/3/1995	5620	25603	21573	2069.4	0.26	31	69	17666
4/5/1996	437	1494.9	1454.8	0	0.21	6	94	1405
5/3/1996	471	734.3	691.2	0	0.19	12	88	646
6/20/1996	572	282.8	189.4	0	0.22	80	20	57
4/4/1997	2090	14853	12855	0	0.16	28	72	10694
6/3/1997	5040	54394	34814	247.4	0.26	30	70	38076
5/5/1998	3180	8875.1	7447.3	6.5	0.20	62	38	3373
6/3/1998	3540	27598	26511	47	0.25	48	52	14351
4/27/1999	969	1031.9	669.6	0.1	0.25	93	7	72
5/24/1999	4080	14002	11851	152.6	0.21	60	40	5601
8/7/1978	817	2504.4	902.9	0	0.13	90	10	250
8/22/1978	559	1075.7	397.8	0	0.14	94	6	65
8/13/1979	588	1160.1	549.9	0	0.16	69	31	360
9/10/1979	521	539.3	362.4	0	0.16	87	13	70
8/18/1980	377	633.5	483.1	0	0.16	30	70	443
9/15/1980	447	393.6	126.2	0				
8/24/1981	260	1484.8	421.6	0	0.14	95	5	74
8/6/1990	415	220.6	89.1	0	0.25	97	3	7
9/4/1990	267	84.8	34.4	0	0.18			
8/31/1992	1070	1153.8	333.8	0	0.21	94	6	69
8/13/1993	536	413.4	191.6	0	0.25	94	6	25
8/4/1994	588	2807.3	179.4	0	0.18	99	1	28
9/30/1994	383	155.1	55	0	0.12	87	13	20
9/2/1997	774	1355.1	335.1	0	0.27	98	2	27
9/17/1999	1080	980.3	615.3	0.7	0.27	91	9	88
Average (spring)					0.175	57		
Average (summer)					0.187	87		

**APPENDIX H:
Mass and Double Mass Curves**

**Suspended Mass Curves
Discharge Mass Curves
Double Mass Curves (Suspended Sediment verse Discharge)**

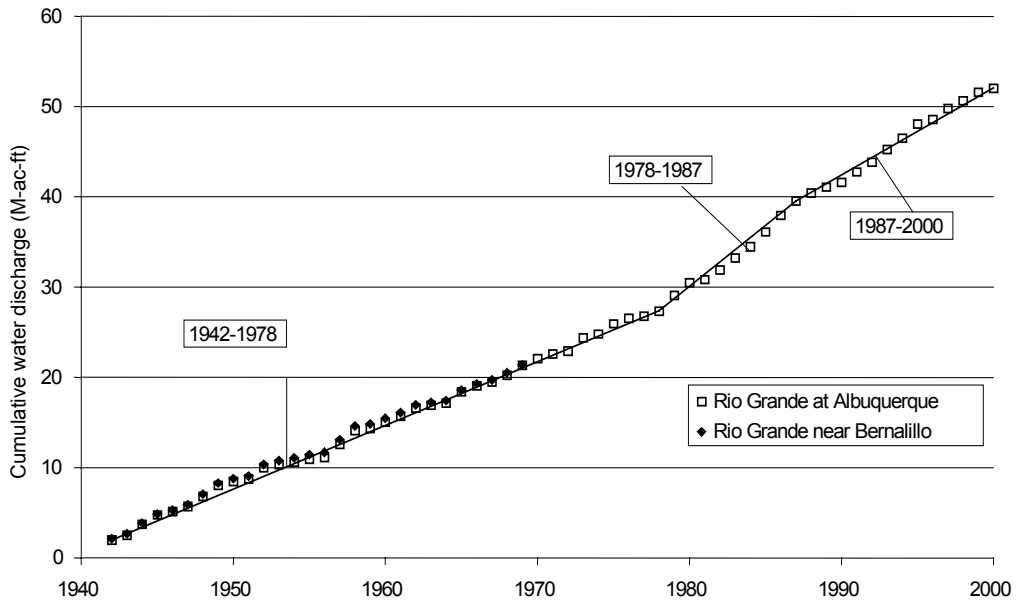


Figure H-1 Discharge mass curve for Bernardo and Albuquerque gages 1942-2000.

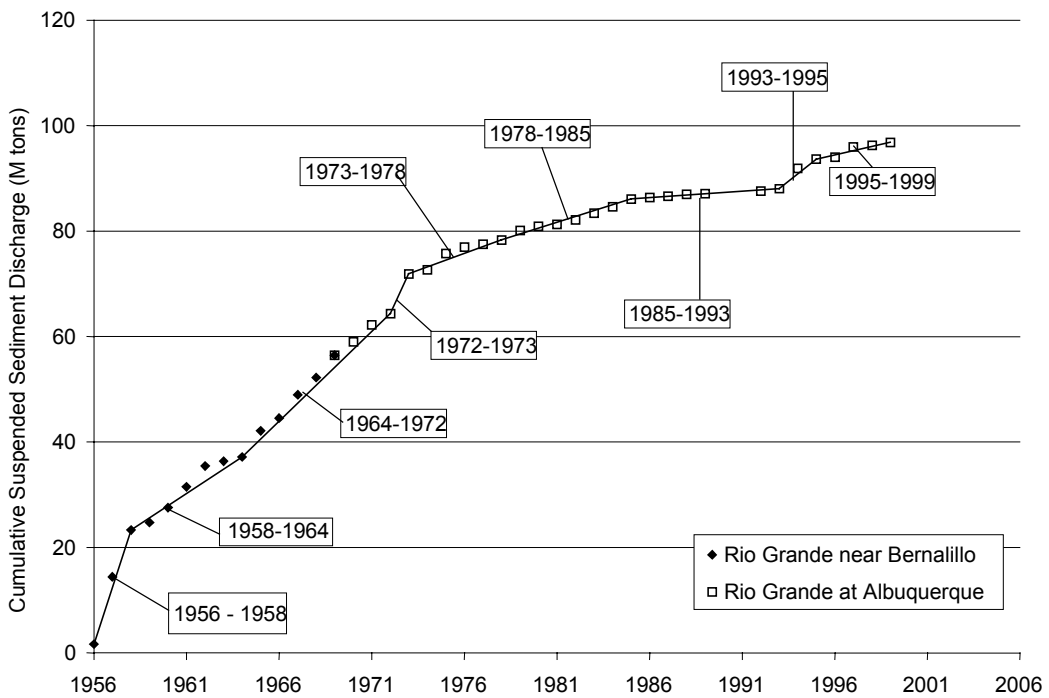


Figure H-2 Suspended Sediment mass curve Bernardo and Albuquerque gages 1942-1999.

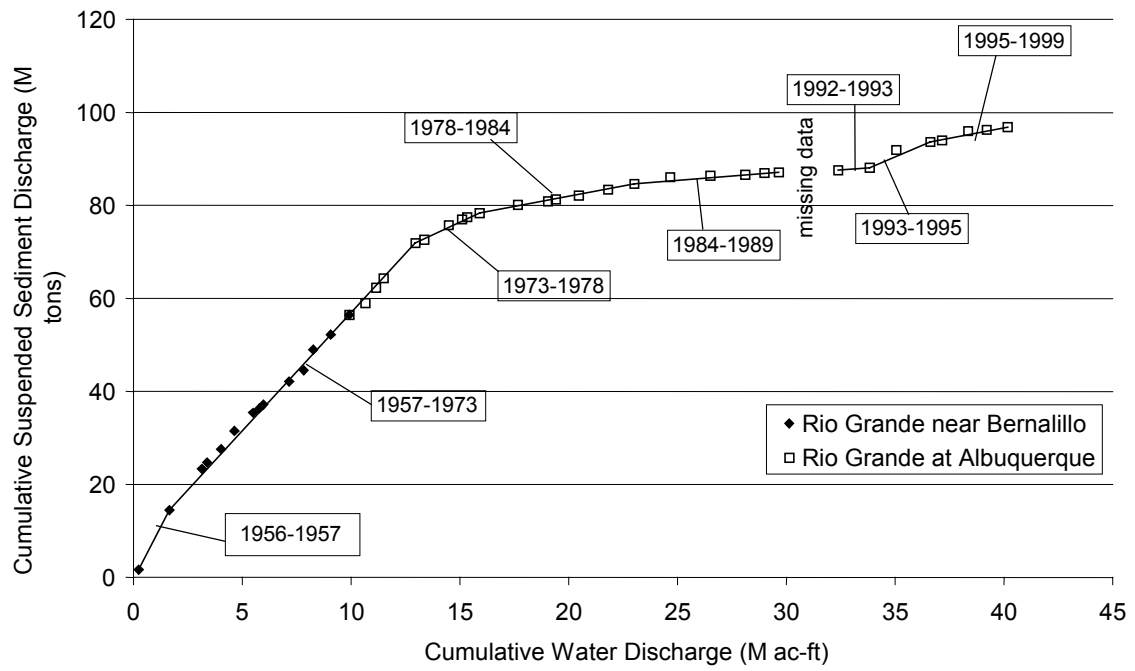


Figure H-3 Double mass curve for Bernardo and Albuquerque gages 1942-1999.

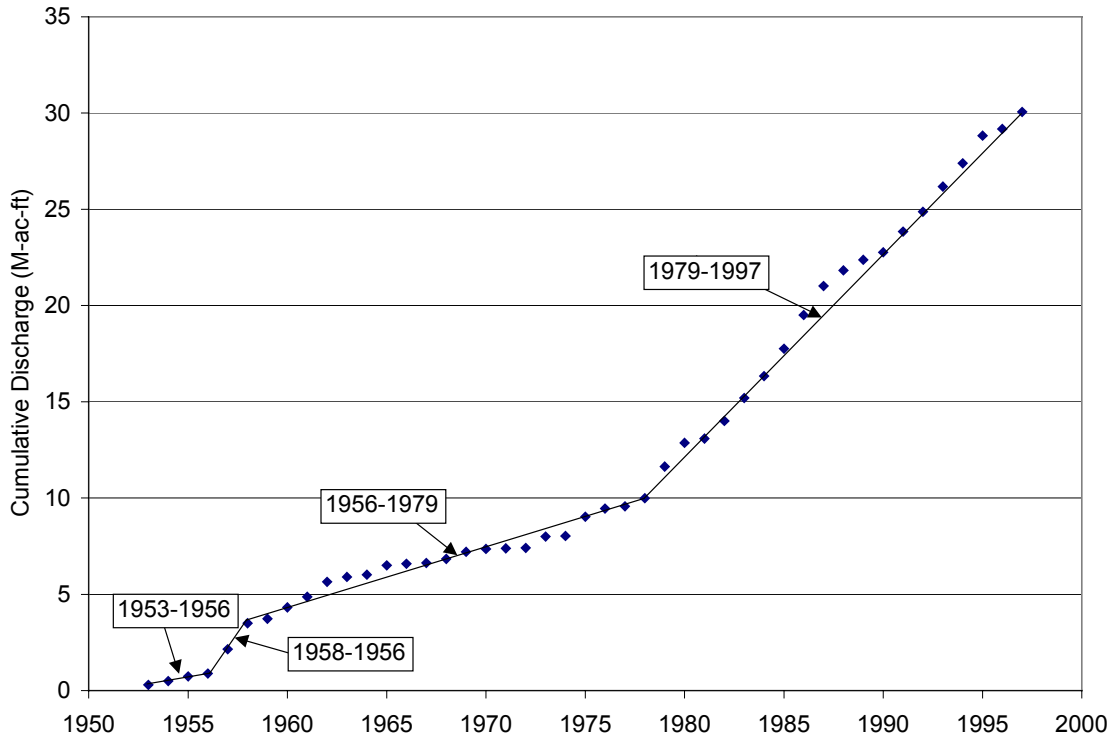


Figure H-4 Discharge mass curve for Bernardo gage 1953-1997.

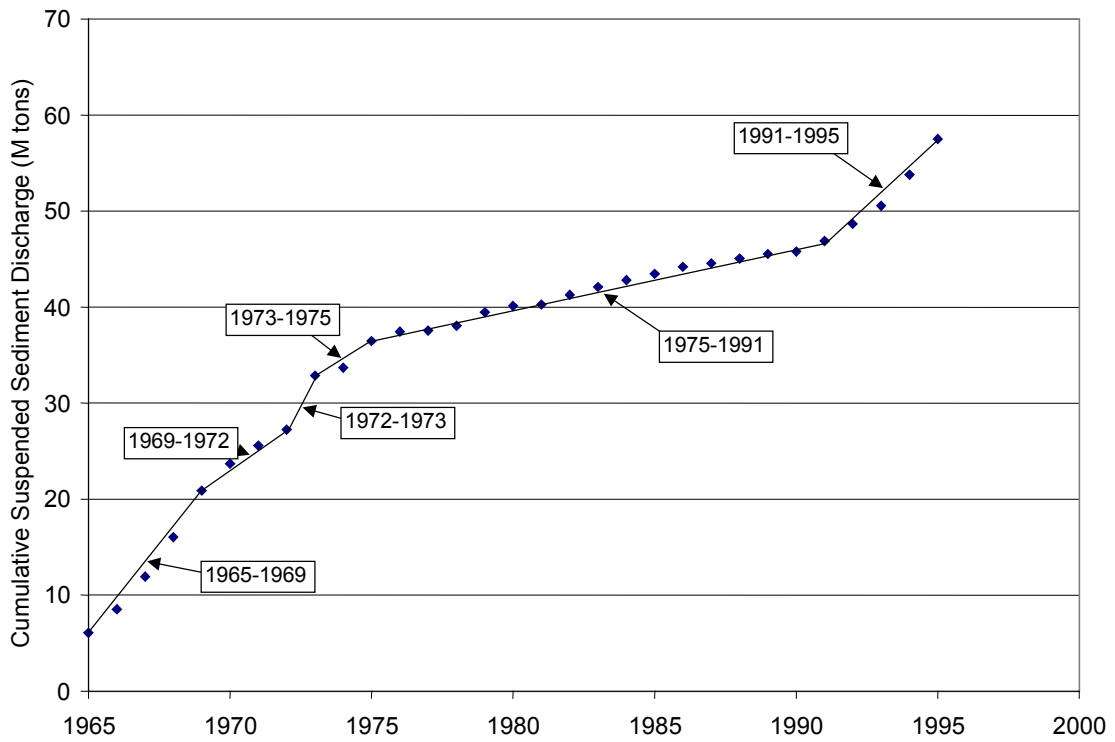


Figure H-5 Suspended Sediment mass curve for Bernardo gage 1965-1995.

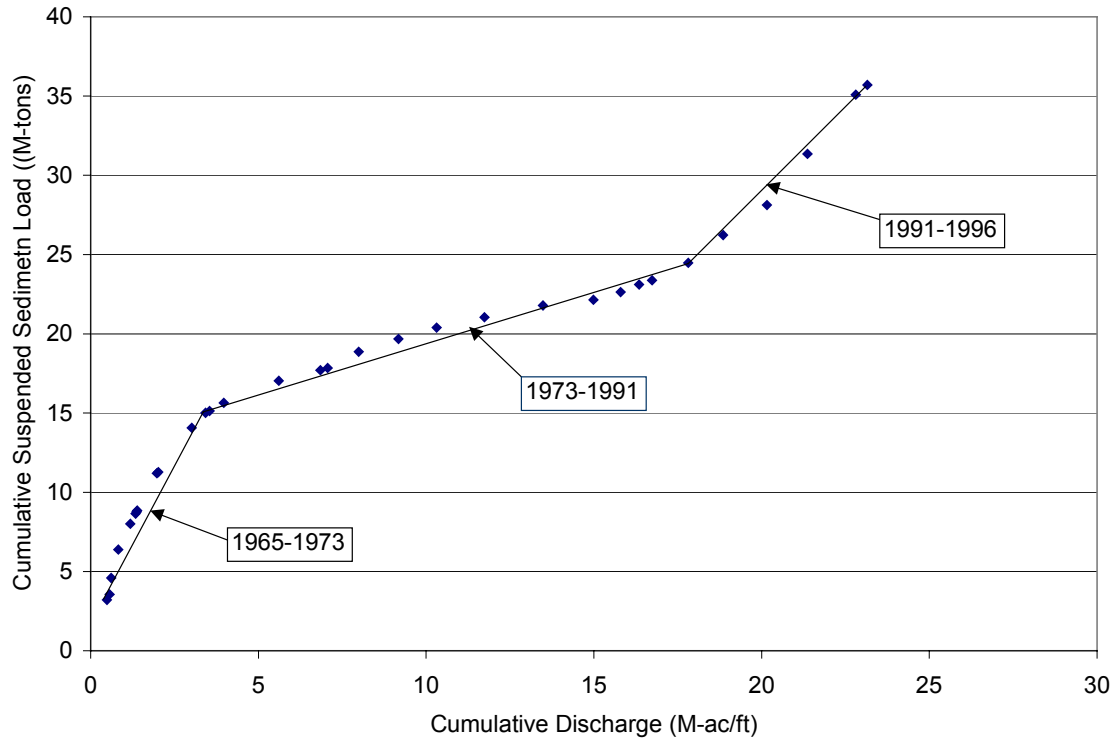


Figure H-6 Double mass curve for Bernardo gage 1965-1996.

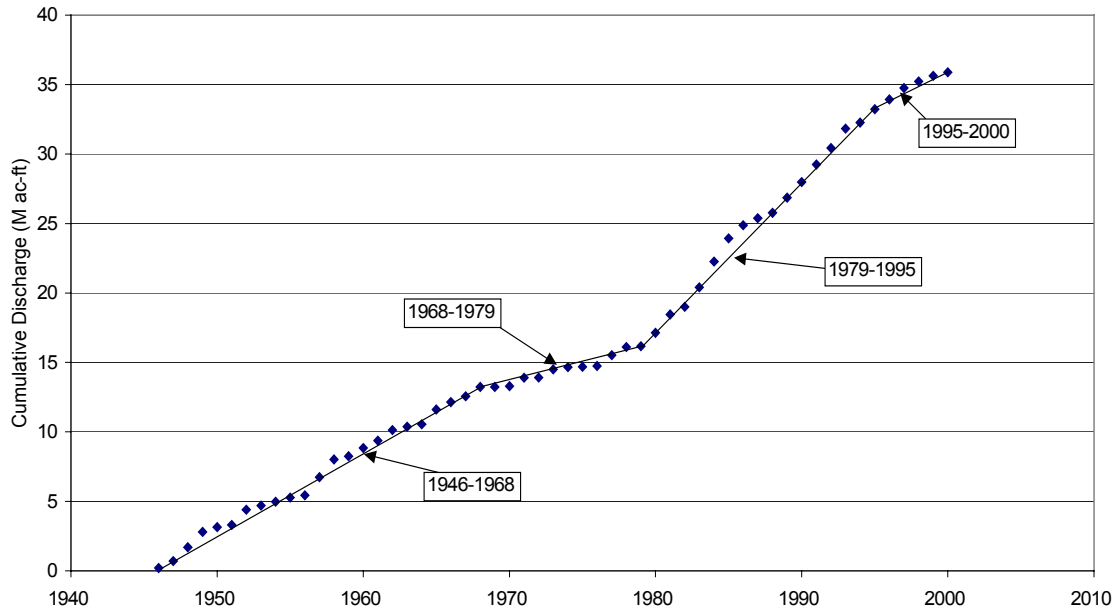


Figure H-7 Discharge mass curve for San Acacia gage 1946-2000.

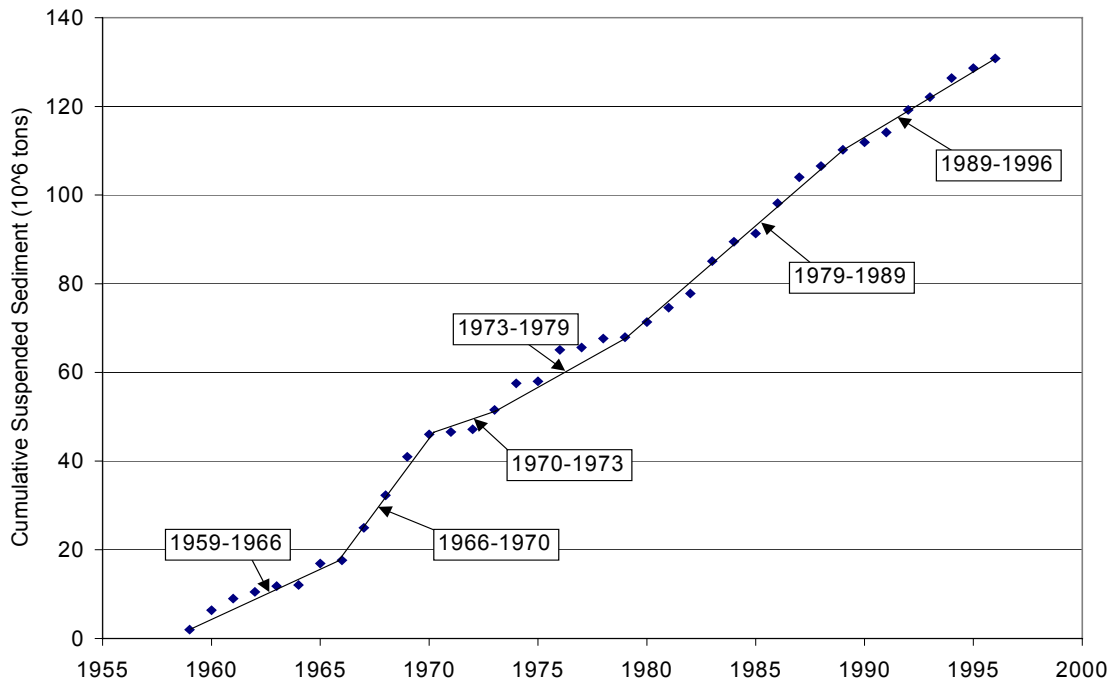


Figure H-8 Suspended Sediment mass curve for San Acacia gage 1959-1996.

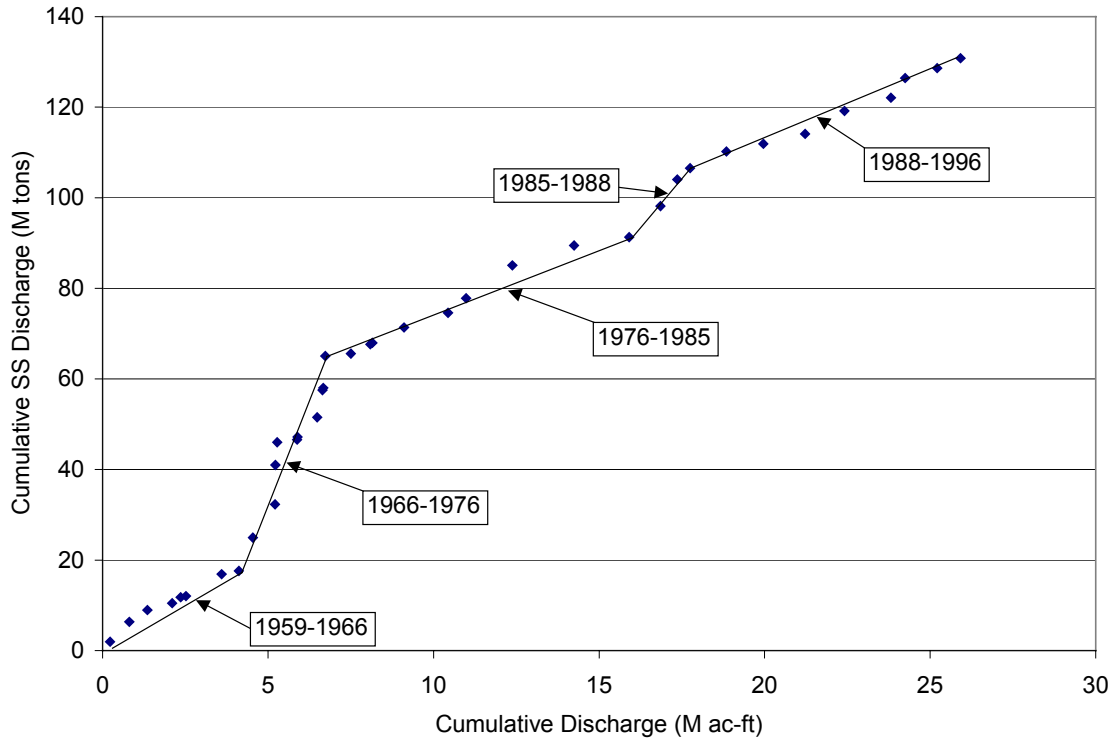


Figure H-9 Double mass curve for San Acacia gage 1959-1996

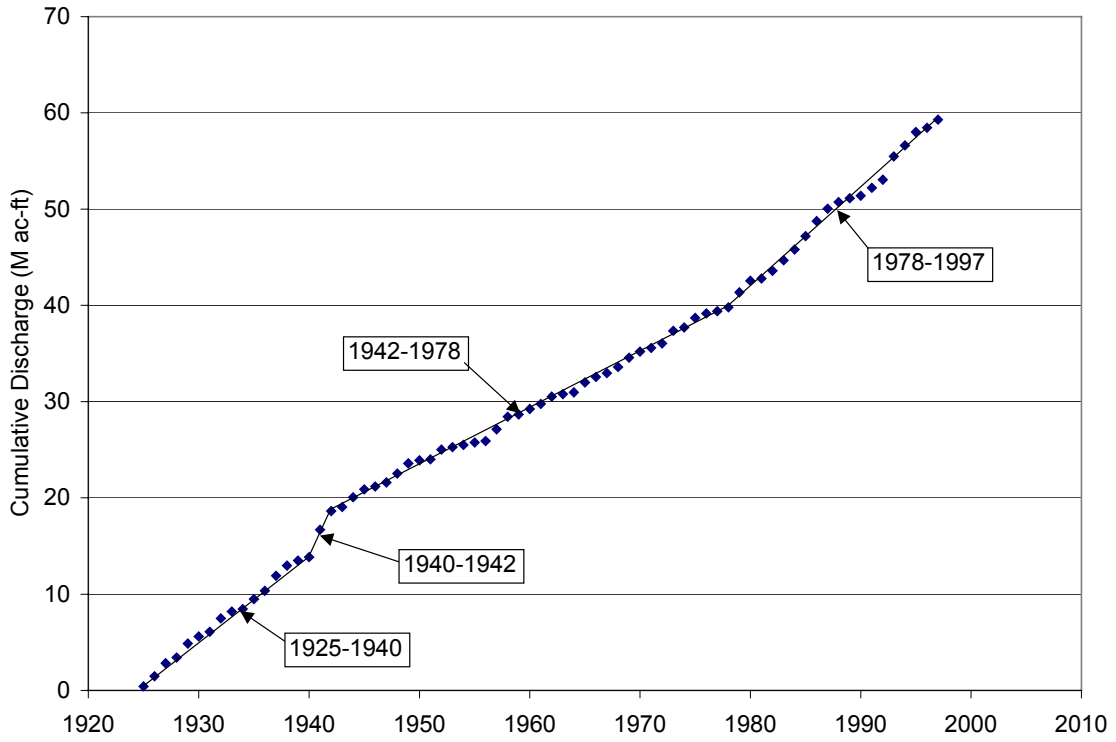


Figure H-10 Discharge mass curve for San Marcial gage 1925-1997.

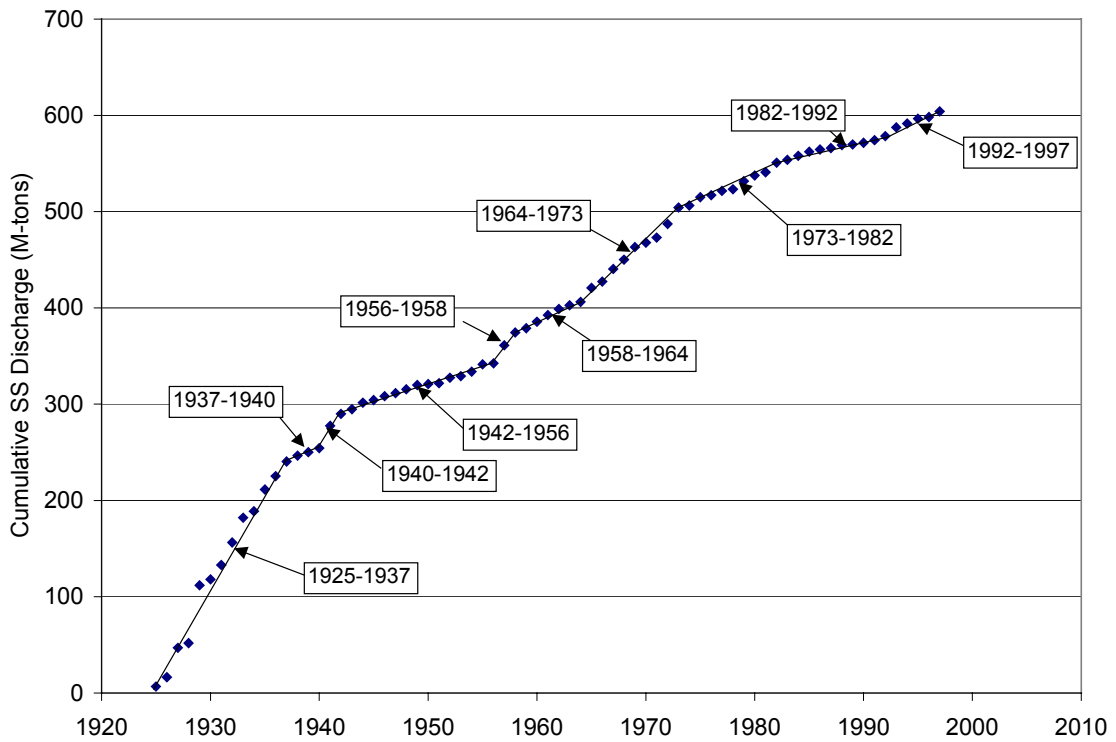


Figure H-11 Suspended Sediment mass curve for San Marcial Gage 1925-1997.

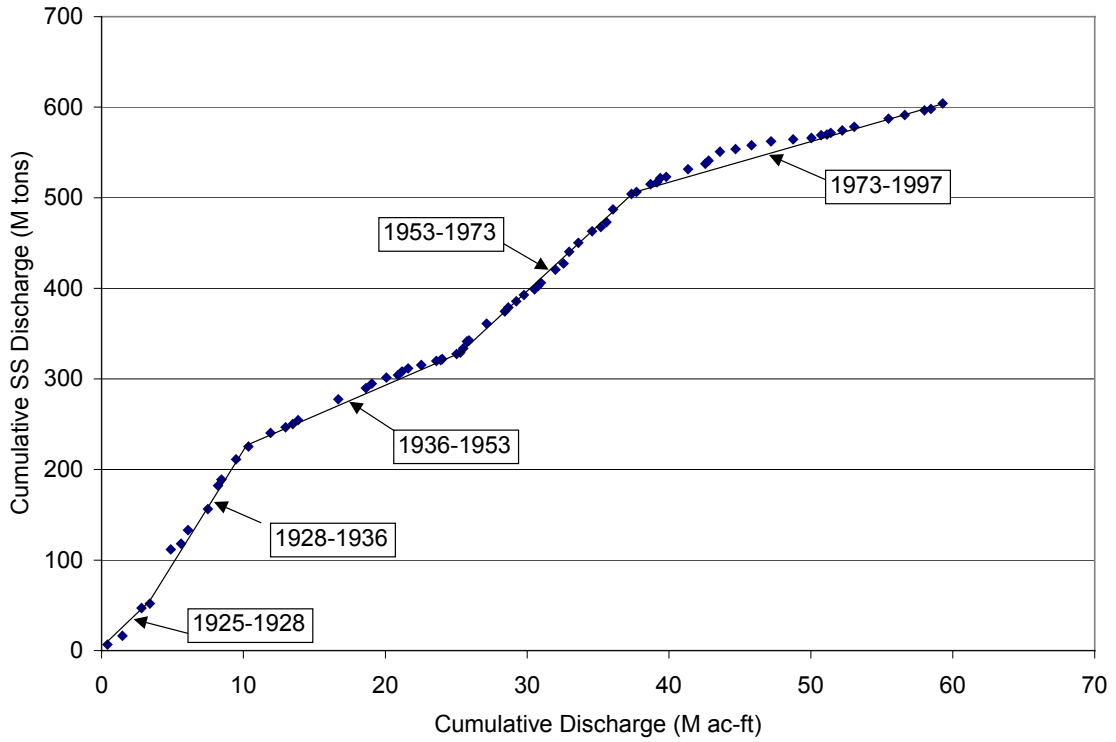


Figure H-12 Double mass curve for San Marcial 1925-1997.

Rio Puerco Mass Curve

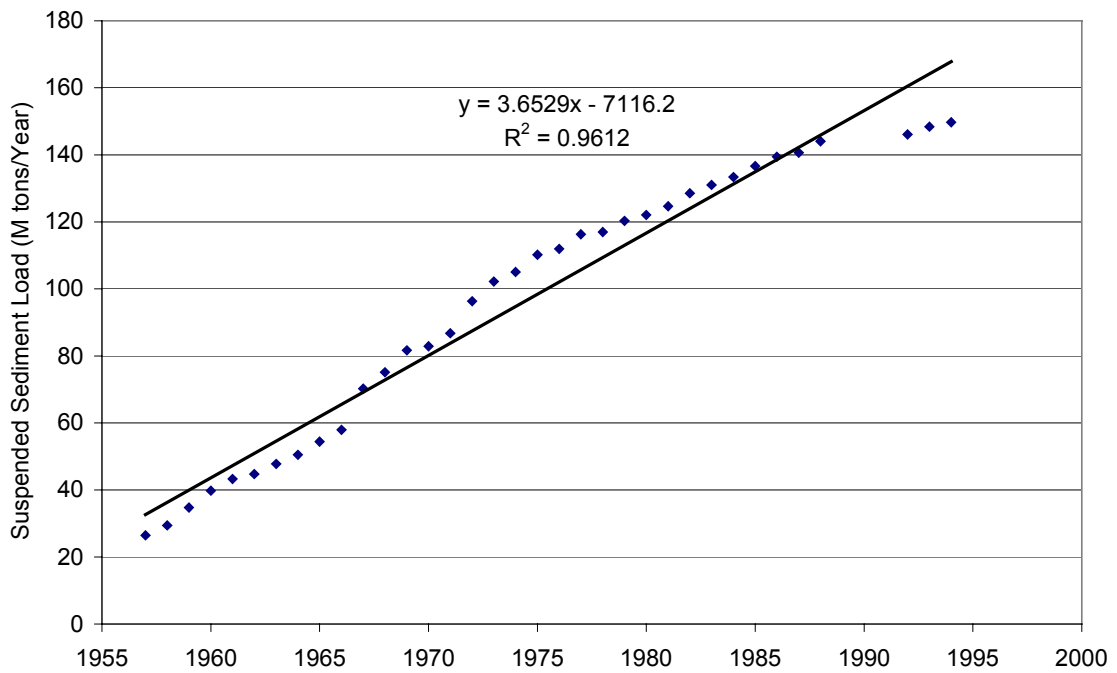


Figure H-13 Suspended Sediment mass curve for Rio Puerco.

**APPENDIX I:
BORAMEP Data**

Table I-1 BORAMEP data for the Bernallilo and Albuquerque Gages.

***		Discharge	Conc	Suspended	d65	d35	Temp	Total Load	Total Sand Load
Location	Date	(cfs)	(PPM)	Sample (tons/day)	(mm)	(mm)	F	(tons/day)	(>0.625mm)(tons/day)
08329500	11/18/1968	1660	3040	13625.28	0.2283956	0.1641583	42.8	23082.19698	19379.19846
08329500	1/14/1969	552	2080	3100.032	0.2449707	0.1984388	42.8	5326.284922	4635.929453
08329500	1/29/1969	1650	6620	29492.1	0.2748908	0.1924503	46.4	41708.32635	23358.03217
08329500	3/12/1969	588	1130	1793.988	0.2699435	0.2084625	35.6	2940.659954	2376.626873
08329500	4/1/1969	936	2560	6469.632	0.245243	0.2009602	50	8318.18251	5901.761154
08329500	4/9/1969	2170	2000	11718	0.2427011	0.1971741	53.6	49557.3342	44114.07361
08329500	5/21/1969	3490	1670	15736.41	0.2563857	0.2260761	69.8	27289.2986	23643.89587
08330000	5/8/1969	4570	3200	39484.8	0.3822299	0.2337722	51.8	50657.05994	40208.01529
08330000	5/21/1969	3610	2730	26609.31	0.3102903	0.2125029	59	37460.10312	31147.99933
08330000	5/28/1970	2620	1570	11106.18	0.2291439	0.1666765	68.9	23356.51577	18902.60425
08330000	11/23/1970	1950	3430	18058.95	0.225037	0.1673933	50.9	29939.42908	24474.38751
08330000	12/4/1970	1170	1370	4327.83	0.2436919	0.1716196	35.6	7925.473879	6263.926455
08330000	12/14/1970	812	1660	3639.384	0.3179974	0.2147517	33.8	5227.006616	4274.23504
08330000	1/18/1971	550	1270	1885.95	0.236488	0.2003858	53.6	2735.529003	2202.201671
08330000	2/1/1971	1020	1240	3414.96	0.2853616	0.2185397	48.2	6049.088116	4762.991116
08330000	2/16/1971	865	1220	2849.31	0.2628688	0.202773	56.3	4951.973145	4170.111843
08330000	3/29/1971	2130	3530	20301.03	0.3533304	0.2321067	65.3	31137.9902	20035.23886
08330000	4/12/1971	833	865	1945.472	0.2767929	0.2092648	59	3445.655799	2718.493232
08330000	4/26/1971	913	1080	2662.308	0.2489767	0.2108319	53.6	3767.94463	2187.841633
08330000	5/17/1971	640	502	867.456	0.2338491	0.1795128	64.4	1820.892881	1359.395567
08330000	6/18/1971	336	480	435.456	0.2775084	0.2092648	77.9	707.5470843	357.1079478
08330000	11/8/1971	1720	5020	23312.88	0.2729661	0.2011878	50	29086.89068	12079.77264
08330000	1/10/1972	657	2180	3867.102	0.2384897	0.1792972	60	6773.560059	5806.138458
08330000	1/24/1972	794	1580	3387.204	0.25	0.206214	43.7	5027.455564	3384.581442
08330000	2/7/1972	720	1450	2818.8	0.2372766	0.1645146	46.4	5658.785053	4187.286289
08330000	2/22/1972	1010	1860	5072.22	0.293396	0.2118524	47.3	7157.159966	4328.663452
08330000	3/6/1972	1090	2280	6710.04	0.2380181	0.1768114	59	11485.10745	8153.639617
08330000	3/30/1972	763	476	980.6076	0.3181935	0.2047156	46.4	1959.63724	1606.425019
08330000	4/10/1972	605	1150	1878.525	0.3051827	0.2184621	56.3	2653.030768	1802.299116
08330000	11/6/1972	1550	5290	22138.65	0.1637922	0.1064999	53.6	33152.38918	13134.87008
08330000	11/28/1972	1310	4740	16765.38	0.3798093	0.2337722	45.5	23263.83137	13600.3794

Table I-1 BORAMEP data for the Bernallilo and Albuquerque Gages.

***		Discharge	Conc	Suspended	d65	d35	Temp	Total Load	Total Sand Load
Location	Date	(cfs)	(PPM)	Sample (tons/day)	(mm)	(mm)	F	(tons/day)	(>0.625mm)(tons/day)
08330000	12/19/1972	700	2410	4554.9	0.2279149	0.1465642	36.5	6751.884415	3879.329765
08330000	1/2/1973	669	2080	3757.104	0.2360389	0.1737342	41	6947.258575	5130.465794
08330000	1/15/1973	683	1790	3300.939	0.2243504	0.1404602	42.8	5776.554027	3344.872546
08330000	1/29/1973	700	2140	4044.6	0.2391046	0.1885293	42.8	5308.603227	3213.350527
08330000	2/20/1973	925	2400	5994	0.2136812	0.1487477	47.3	9766.52684	7156.064468
08330000	3/2/1973	900	2170	5273.1	0.3051392	0.189056	56.3	7100.540039	3646.782348
08330000	3/19/1973	1130	2780	8481.78	0.2483769	0.1907277	44.6	12188.42117	8454.852104
08330000	4/9/1973	1360	2900	10648.8	0.2357896	0.1932997	59	15375.11099	10809.35883
08330000	4/23/1973	1660	3790	16986.78	0.3655881	0.2309451	58.1	25724.53667	18778.10117
08330000	4/30/1973	3540	5750	54958.5	0.2813236	0.2151019	59	68459.21227	39925.95775
08330000	7/30/1973	3270	2570	22690.53	0.377907	0.2325281	69.8	29587.74107	23188.06555
08330000	8/6/1973	2160	3550	20703.6	0.2635389	0.202773	70.7	25711.29932	17975.3114
08330000	8/13/1973	1720	2280	10588.32	0.377907	0.2311019	69.8	16515.4237	10924.0227
08330000	9/10/1973	2000	3850	20790	0.4438751	0.3283337	71.6	29234.3607	17544.16588
08330000	10/23/1973	543	575	843.0075	0.2897394	0.1991768	59	2107.8118	1520.538221
08330000	11/5/1973	861	772	1794.668	0.3017216	0.2209673	66.2	3300.258453	2629.286602
08330000	1/14/1974	1610	2920	12693.24	0.3261218	0.2306466	41	22012.12108	20296.77322
08330000	1/28/1974	1580	2310	9854.46	0.3146975	0.226174	46.4	17255.55504	16316.5161
08330000	2/11/1974	843	1120	2549.232	0.416228	0.2861538	41	5001.032585	4219.653328
08330000	2/25/1974	575	1310	2033.775	0.2861415	0.2085776	44.6	3764.451294	3581.936844
08330000	3/11/1974	713	1120	2156.112	0.3641349	0.2313425	46.4	3575.042035	2796.676892
08330000	3/25/1974	1160	1230	3852.36	0.4228872	0.2919927	60	6440.727458	5563.790873
08330000	4/15/1974	480	669	867.024	0.3424558	0.2343311	57.2	1391.385864	1008.801979
08330000	4/29/1974	850	819	1879.605	0.311334	0.2069651	66.2	3289.522625	2578.236824
08330000	6/3/1974	404	116	126.5328	0.3880361	0.24015	62.6	304.8105191	223.5272168
08330000	12/2/1974	455	604	742.014	0.4509247	0.2753775	43.7	1055.112643	525.3024093
08330000	2/3/1975	709	747	1429.982	0.219015	0.1671278	40.1	2595.055294	1335.317944
08330000	2/24/1975	703	578	1097.102	0.2386109	0.1860774	44.6	2825.547703	2013.067566
08330000	3/10/1975	1250	1350	4556.25	0.3394452	0.2343311	44.6	5652.679693	3102.112265
08330000	3/31/1975	682	624	1149.034	0.2115792	0.1504513	42.8	2115.603851	1332.69931
08330000	4/21/1975	1180	1210	3855.06	0.243087	0.212631	51.8	6776.811131	4768.606785

Table I-1 BORAMEP data for the Bernallilo and Albuquerque Gages.

***		Discharge	Conc	Suspended	d65	d35	Temp	Total Load	Total Sand Load
Location	Date	(cfs)	(PPM)	Sample (tons/day)	(mm)	(mm)	F	(tons/day)	(>0.625mm)(tons/day)
08330000	4/24/1975	4440	5780	69290.64	0.4077534	0.2801835	57.2	84356.1247	58404.55408
08330000	5/22/1975	4530	2050	25073.55	0.4029327	0.2313425	54.5	42313.16708	36873.78675
08330000	5/27/1975	4590	1390	17226.27	0.3345182	0.2299734	65.3	27585.18781	24662.76105
08330000	6/2/1975	4440	1910	22897.08	0.4774482	0.3247107	68	32841.9694	30285.18815
08330000	6/23/1975	3370	2270	20654.73	0.3706769	0.242394	82.4	30134.16444	21758.41334
08330000	7/7/1975	2880	1100	8553.6	0.4642857	0.25	68	14806.013	14003.6355
08330000	7/28/1975	1030	457	1270.917	0.3611214	0.2310185	77	2486.510901	2068.070723
08330000	8/4/1975	429	70	81.081	0.3051827	0.2184621	71.6	288.8530511	214.7550211
08330000	9/22/1975	554	587	878.0346	0.4315874	0.3117254	56.3	1217.855822	572.6053719
08330000	9/29/1975	270	130	94.77	0.4273624	0.2974955	73.4	187.1078503	136.3166363
08330000	11/21/1975	1580	733	3126.978	0.3185799	0.2147235	43.7	7194.262637	5776.020675
08330000	12/8/1975	1760	1100	5227.2	0.4556621	0.3324448	48.2	7869.724202	6320.875202
08330000	12/22/1975	1740	1810	8503.38	0.4138221	0.2811497	44.6	14131.37393	12554.55374
08330000	1/16/1976	1840	1910	9488.88	0.2457503	0.2179157	62.6	18062.54584	17029.56366
08330000	3/8/1976	876	363	858.5676	0.4304088	0.2887052	48.2	1603.080745	1399.228282
08330000	4/26/1976	1050	1110	3146.85	0.2924217	0.2221283	69.8	5494.228457	4860.249793
08330000	5/10/1976	3000	7430	60183	0.4747282	0.3078145	64.4	69097.33718	61813.00412
08330000	6/7/1976	1090	247	726.921	0.3731891	0.2410853	67.1	1504.5743	1148.993734
08330000	7/6/1976	481	71	92.2077	0.4158597	0.2766955	71.6	206.0010867	152.921566
08330000	10/4/1976	119	236	75.8268	0.4371935	0.2996985	65.3	115.0392899	49.04156631
08330000	1/17/1977	507	392	536.6088	0.3817908	0.2418997	39.2	1080.407797	807.4502468
08330000	1/31/1977	531	455	652.3335	0.3741116	0.2369183	48.2	1329.198401	800.2150215
08330000	2/28/1977	625	325	548.4375	0.376483	0.2412246	46.4	1039.116938	694.940722
08330000	3/14/1977	425	195	223.7625	0.3998315	0.2461963	52.7	399.4344549	196.5041265
08330000	3/28/1977	488	384	505.9584	0.3785891	0.2412246	45.5	892.6031197	482.8329934
08330000	5/9/1977	304	191	156.7728	0.3532609	0.2313425	64.4	342.6741231	188.6096328
08330000	5/16/1977	105	240	68.04	0.4273228	0.301942	61.7	125.9600258	64.60605243
08330000	6/20/1977	694	702	1315.408	0.3387102	0.2184493	71.6	1852.110299	678.0442899
08330000	9/6/1977	356	855	821.826	0.4309987	0.2838264	74.3	1186.183081	437.8734345
08330000	11/7/1977	346	861	804.3462	0.4388936	0.2902024	57.2	1040.018462	336.8736259
08330000	11/28/1977	325	317	278.1675	0.3231051	0.2190801	44.6	409.9476363	181.2168547

Table I-1 BORAMEP data for the Bernallilo and Albuquerque Gages.

***		Discharge	Conc	Suspended	d65	d35	Temp	Total Load	Total Sand Load
Location	Date	(cfs)	(PPM)	Sample (tons/day)	(mm)	(mm)	F	(tons/day)	(>0.625mm)(tons/day)
08330000	1/3/1978	508	371	508.8636	0.3563378	0.1888763	37.4	763.6789748	326.9293143
08330000	2/13/1978	604	396	645.7968	0.2761205	0.1899899	48.2	1458.066769	946.8718529
08330000	2/27/1978	498	657	883.4022	0.4020092	0.2654771	53.6	1263.03863	830.4247284
08330000	3/20/1978	496	388	519.6096	0.3886827	0.2393177	53.6	810.6210167	478.4942448
08330000	4/24/1978	329	696	618.2568	0.4234892	0.25	54.5	1175.201936	1016.480779
08330000	5/8/1978	1420	926	3550.284	0.4053826	0.2480432	61.7	5196.473002	3009.826419
08330000	5/22/1978	4260	4030	46353.06	0.3908937	0.2480432	64.4	66166.07867	52888.90967
08330000	5/30/1978	2520	943	6416.172	0.3611111	0.2326393	66.2	9649.063488	6745.029202
08330000	6/5/1978	2810	1080	8193.96	0.4205977	0.2869467	66.2	12691.92826	10007.45984
08330000	6/26/1978	1350	637	2321.865	1.264396	0.25	68	3785.857065	2964.767344
08330000	11/27/1978	1150	1720	5340.6	0.3496001	0.2289689	45.5	7221.441625	2740.639714
08330000	12/18/1978	858	797	1846.33	0.4025868	0.2437661	39.2	3245.959838	2629.323729
08330000	1/8/1979	720	381	740.664	0.3231511	0.2137939	39.2	1271.810514	721.7260799
08330000	1/22/1979	964	912	2373.754	0.3953113	0.2483168	39.2	3515.774938	1710.101048
08330000	2/5/1979	823	540	1199.934	0.3584676	0.2212454	35.6	2895.430191	2001.533882
08330000	2/26/1979	922	505	1257.147	0.3200093	0.223666	40.1	2341.186432	1574.398407
08330000	4/2/1979	1840	782	3884.976	0.3670139	0.2374945	50	7309.077564	6098.54668
08330000	4/23/1979	4980	2110	28371.06	0.459656	0.2762446	59	40945.13259	34565.35842
08330000	8/13/1979	588	514	816.0264	0.434836	0.279168	70.7	1443.581887	605.9767391
08330000	11/13/1979	1820	599	2943.486	0.3417722	0.2362538	47.3	6089.823624	5446.112076
08330000	12/3/1979	1680	1620	7348.32	0.2955199	0.2221283	40.1	10846.80438	10537.60057
08330000	12/17/1979	1650	561	2499.255	0.458095	0.2354222	41	5608.294238	5280.805743
08330000	1/14/1980	850	168	385.56	0.3472343	0.2362538	44.6	1095.792586	1014.107199
08330000	2/4/1980	1030	390	1084.59	0.4651141	0.3162571	48.2	2042.326414	1964.238798
08330000	2/19/1980	1020	182	501.228	0.4427252	0.3009235	45.5	1004.123821	837.7576735
08330000	4/7/1980	926	126	315.0252	0.4445651	0.3061773	51.8	610.1484052	514.274481
08330000	6/9/1980	6610	1520	27127.44	0.4709788	0.3279648	62.6	37243.47943	34760.97058
08330000	7/21/1980	638	108	186.0408	0.4798804	0.3598106	71.6	303.0816208	186.7171493
08330000	11/10/1980	1130	363	1107.513	0.434513	0.2457086	50	2180.877011	1621.174451
08330000	12/1/1980	1450	340	1331.1	0.4133801	0.2611549	44.6	2881.850947	2444.356291
08330000	12/15/1980	1260	281	955.962	0.4128432	0.2365945	45.5	2301.038253	1981.796616

Table I-1 BORAMEP data for the Bernallilo and Albuquerque Gages.

***		Discharge	Conc	Suspended	d65	d35	Temp	Total Load	Total Sand Load
Location	Date	(cfs)	(PPM)	Sample (tons/day)	(mm)	(mm)	F	(tons/day)	(>0.625mm)(tons/day)
08330000	1/12/1981	685	96	177.552	0.4509247	0.2753775	41	507.8834679	460.6037717
08330000	1/26/1981	633	85	145.2735	0.4213516	0.2670594	46.4	498.4537657	465.9616888
08330000	2/17/1981	1100	175	519.75	0.4036709	0.2383105	45.5	1471.251005	1339.034246
08330000	3/2/1981	1090	165	485.595	0.4369772	0.2563235	46.4	1231.231122	1068.904731
08330000	3/16/1981	623	98	164.8458	0.444172	0.2457086	50.9	368.1126128	294.154903
08330000	4/20/1981	641	68	117.6876	0.43388	0.2680507	62.6	368.7238737	303.7960487
08330000	6/22/1981	694	390	730.782	0.4374094	0.2683255	73.4	1898.533531	983.3201521
08330000	11/16/1981	753	561	1140.569	0.4687334	0.3321699	48.2	1608.555054	699.2717445
08330000	4/26/1982	1740	1660	7798.68	0.4083045	0.260875	53.6	12473.19175	11223.77879
08330000	5/3/1982	3350	1130	10220.85	0.3447024	0.2295453	59	15142.77167	9814.373749
08330000	5/24/1982	4280	898	10377.29	0.4897603	0.3687164	63.5	14973.97119	11294.657
08330000	6/7/1982	4570	678	8365.842	0.4408359	0.2956	56.3	14209.96409	11873.54311
08330000	7/7/1982	1100	167	495.99	0.4567911	0.3283166	69.8	808.4825575	615.9168379
08330000	7/26/1982	159	69	29.6217	0.4920723	0.3550137	75.2	37.33491698	13.8267211
08330000	11/1/1983	274	217	160.5366	0.4632231	0.3736412	63.5	259.6647849	137.3223853
08330000	1/3/1984	634	122	208.8396	0.4791167	0.3908334	36.5	378.2860218	333.3016315
08330000	3/13/1984	824	90	200.232	0.4427252	0.3009235	55.4	535.2874621	387.0454729
08330000	4/24/1984	4270	832	9592.128	0.3044356	0.2311995	60.8	16954.23686	13629.36845
08330000	5/8/1984	4440	905	10849.14	0.3692416	0.2427247	53.6	20227.97086	17269.39518
08330000	11/13/1984	509	103	141.5529	0.4959441	0.3564576	57.2	311.2094474	254.2710509
08330000	12/3/1984	878	134	317.6604	0.3231051	0.2168887	41	867.8689057	676.535608
08330000	1/21/1985	573	131	202.6701	0.4910657	0.3834502	40.1	329.9521623	255.3459382
08330000	3/4/1985	1490	2130	8568.99	0.4782952	0.3301387	39.2	11057.89247	9841.623063
08330000	3/18/1985	4200	1140	12927.6	0.4338821	0.2842678	47.3	21065.85368	15265.6324
08330000	5/15/1985	7170	434	8401.806	0.148851	0.09703705	59	20682.66656	15171.87457
08330000	7/1/1985	3280	1000	8856	0.3752209	0.2379316	51.8	16526.6494	15673.91417
08330000	2/4/1986	3250	387	3395.925	0.4648536	0.3828035	36.5	6362.410612	4987.638273
08330000	5/6/1986	2430	241	1581.201	0.4213516	0.2670594	59	4635.860086	4281.654917
08330000	6/3/1986	3440	387	3594.456	0.3812787	0.2486415	53.6	8938.773358	8328.027752
08330000	9/26/1988	894	256	617.9328	0.4489903	0.3257698	60	1542.816811	919.9211812
08330000	5/8/1990	1950	142	747.63	0.493867	0.2994196	61.7	3232.415964	2529.959421

Table I-1 BORAMEP data for the Bernallilo and Albuquerque Gages.

***		Discharge	Conc	Suspended	d65	d35	Temp	Total Load	Total Sand Load
Location	Date	(cfs)	(PPM)	Sample (tons/day)	(mm)	(mm)	F	(tons/day)	(>0.625mm)(tons/day)
08330000	10/31/1990	331	61	54.5157	0.4954006	0.3405844	61.7	100.151284	52.69974592
08330000	1/4/1991	712	122	234.5328	0.8540267	0.4782328	40.1	346.7039823	249.3228406
08330000	4/4/1991	1490	262	1054.026	0.4582878	0.333353	50	2293.261954	1840.837791
08330000	4/10/1991	2130	2160	12422.16	0.7635816	0.4875322	53.6	18267.56903	17012.80841
08330000	5/1/1991	3390	703	6434.559	0.4824271	0.406684	55.4	12817.69135	11166.28278
08330000	6/3/1991	3590	669	6484.617	0.4536933	0.3180822	60	12664.01431	11091.58511
08330000	7/2/1991	2470	300	2000.7	0.4769794	0.3585944	59	4521.630608	3105.587883
08330000	7/10/1991	401	218	236.0286	0.5657704	0.4011683	60	319.1474335	201.3227417
08330000	1/31/1992	911	156	383.7132	0.5621437	0.3410681	41	697.898761	529.4332306
08330000	6/1/1992	3850	868	9022.86	0.4701153	0.3600966	60	15248.1035	14118.73192
08330000	7/31/1992	801	1300	2811.51	0.8952668	0.4231853	74.3	4536.092767	4165.649041
08330000	8/31/1992	1070	343	990.927	0.4772217	0.3721547	70.7	1322.71435	484.1494699
08330000	11/30/1992	593	76	121.6836	0.5755462	0.3964203	38.3	180.9988094	131.5219303
08330000	8/13/1993	536	179	259.0488	0.6742307	0.4183733	68	382.638156	163.4680358
08330000	4/1/1994	1370	151	558.549	0.8863776	0.4761915	49.1	1126.217311	892.1734117
08330000	5/2/1994	3300	317	2824.47	0.7623398	0.4348658	60	6584.866603	5469.86941
08330000	6/27/1994	4860	382	5012.604	0.5278135	0.3813545	73.22	10674.32374	9590.030158
08330000	11/1/1994	688	549	1019.822	0.5	0.3878557	45.86	1548.009238	1233.509147
08330000	2/6/1995	956	116	299.4192	0.4953717	0.4096673	41	530.830737	439.0674923
08330000	5/5/1995	3980	641	6888.186	0.4953717	0.4096673	56.3	10512.62305	8486.534669
08330000	5/24/1995	6400	668	11543.04	0.5755462	0.4153775	62.6	18231.65268	15302.60434
08330000	6/6/1995	4960	682	9133.344	0.9028943	0.4837994	60	16643.3273	15303.51101
08330000	7/3/1995	5620	993	15067.78	0.4568817	0.3742835	61.7	18477.3476	16560.9234
08330000	9/8/1995	696	308	578.7936	0.7656847	0.4648295	68.9	1107.439393	807.47165
08330000	10/6/1995	660	60	106.92	0.5618008	0.3993418	58.28	285.1666347	215.5566341
08330000	11/3/1995	1120	153	462.672	0.4755008	0.3343296	51.8	1161.748845	811.8341723
08330000	12/5/1995	1130	102	311.202	0.7082434	0.4474442	60	815.1890793	705.8054428
08330000	2/13/1996	1520	147	603.288	0.4687334	0.3321699	41.18	1976.051725	1820.484632
08330000	3/8/1996	1290	158	550.314	0.4799128	0.340731	44.42	1770.133208	1522.661056
08330000	5/3/1996	471	367	466.7139	0.5565434	0.3799798	59.72	701.1652701	658.056082
08330000	6/20/1996	572	86	132.8184	0.5971807	0.3964203	66.56	253.4570755	163.6275924

Table I-1 BORAMEP data for the Bernallilo and Albuquerque Gages.

***		Discharge	Conc	Suspended	d65	d35	Temp	Total Load	Total Sand Load
Location	Date	(cfs)	(PPM)	Sample (tons/day)	(mm)	(mm)	F	(tons/day)	(>0.625mm)(tons/day)
08330000	10/28/1996	322	126	109.5444	1.109085	0.4626082	51.8	126.8786367	70.42037329
08330000	12/2/1996	619	854	1427.29	0.6450876	0.4000267	44.6	1843.510285	1743.943329
08330000	1/27/1997	1050	1570	4450.95	0.7534612	0.4474442	46.4	5526.501776	4937.308051
08330000	2/10/1997	868	125	292.95	0.7050005	0.4251294	41.9	477.1274852	321.9904461
08330000	3/5/1997	904	147	358.7976	0.5	0.330824	36.68	969.5771815	674.150088
08330000	4/4/1997	2090	1500	8464.5	0.4860373	0.3623811	50	12887.97966	10883.22514
08330000	5/9/1997	3230	1790	15610.59	0.4668022	0.3362793	60	20927.40892	16307.71333
08330000	6/3/1997	5040	1820	24766.56	0.7455746	0.443525	61.7	33314.52924	31056.25238
08330000	3/3/1998	894	99	238.9662	0.6012782	0.4237049	38.84	396.7546749	281.9894847
08330000	5/5/1998	3180	534	4584.924	0.4967538	0.3814555	56.3	8267.601783	6800.676856
08330000	6/3/1998	3540	2180	20836.44	0.6012782	0.409707	64.4	24618.50566	23567.40422
08330000	7/6/1998	533	191	274.8681	0.6012782	0.4237049	60	343.8544125	139.6345334
08330000	11/30/1998	954	547	1408.963	0.787165	0.4451863	42.8	2573.465578	2467.692491
08330000	2/2/1999	1100	216	641.52	0.5445523	0.4071758	42.8	1338.429981	1235.714565
08330000	2/25/1999	468	156	197.1216	0.7921362	0.4474442	43.7	509.7237399	477.0735133
08330000	3/29/1999	758	643	1315.964	0.6568995	0.4381603	55.4	2084.48371	2016.829703
08330000	4/27/1999	969	164	429.0732	0.6185527	0.427494	53.6	706.3167334	441.0725165
08330000	5/24/1999	4080	648	7138.368	0.5779406	0.3964203	59.9	13147.02308	11120.25375
08330000	9/17/1999	1080	152	443.232	0.7278816	0.4500343	66.2	774.7744946	438.8606762
08330000	11/9/2000	465	106	133.083	0.6396841	0.4250059	50	182.3287108	85.14989305
08330000	1/11/2001	608	69	113.2704	0.6849595	0.4403343	41	221.0449435	171.4555499

Table I-2 BORAMEP data for the Bernardo gage.

***		Discharge	Conc	Suspended	d65	d35	Temp	Total Load	Total Sand Load
Location	Date	(cfs)	(PPM)	Sample (tons/day)	(mm)	(mm)	F	(tons/day)	(>0.625mm)(tons/day)
08332010	4/8/1969	427	2660	3066.714	0.246373	0.2016122	53.6	3910.943483	1326.31521
08332010	4/17/1969	656	4290	7598.448	0.2767929	0.1996709	59	11503.7731	8126.398865
08332010	5/1/1969	739	3260	6504.678	0.197666	0.1347511	68	10314.02455	6928.147644
08332010	5/6/1969	3050	4770	39280.95	0.2307407	0.1863626	55.4	47838.12381	28521.85602
08332010	5/23/1969	2210	2310	13783.77	0.2048521	0.1402476	68	19749.0271	10528.47491
08332010	6/11/1969	2330	7560	47559.96	0.2265416	0.1821913	69.8	64322.62561	28976.18567
08332010	6/16/1969	3550	4510	43228.35	0.2316416	0.1909574	68	63172.01767	46251.10727
08332010	6/25/1969	279	938	706.5954	0.2299047	0.1839003	73.4	1068.633194	644.9545021
08332010	5/10/1973	3120	3510	29568.24	0.2326815	0.1789943	65.3	51051.54175	27611.84875
08332010	5/21/1973	6160	5130	85322.16	0.1562834	0.1056953	68.9	110038.6021	71214.43668
08332010	2/6/1975	665	947	1700.339	0.2222256	0.1762146	35.6	3083.91787	2046.895691
08332010	3/12/1975	1080	1060	3090.96	0.2282709	0.1931072	41	5151.69455	2898.650604
08332010	4/1/1975	585	458	723.411	0.3752962	0.2337722	48.2	1045.092659	429.4744455
08332010	6/11/1975	3380	1120	10221.12	0.2248106	0.1694038	63.5	15723.8916	11027.30713
08332010	7/3/1975	1790	444	2145.852	0.2351182	0.1843965	68	5030.234375	3645.351074
08332010	9/25/1975	406	729	799.1298	0.2162504	0.1641144	68	1425.721855	1045.608902
08332010	10/16/1975	130	80	28.08	0.3605522	0.2398351	50	83.32351398	50.37862492
08332010	10/30/1975	152	100	41.04	0.3779111	0.2486415	50.9	110.3035958	85.71901441
08332010	11/26/1975	2370	1800	11518.2	0.1838949	0.1164873	34.7	20783.29199	16238.05469
08332010	5/12/1976	2820	1360	10355.04	0.1091519	0.07605902	64.4	22127.74069	11865.04282
08332010	5/26/1976	1350	1120	4082.4	0.2185856	0.1744862	62.6	8371.462059	6877.927032
08332010	1/21/1977	514	362	502.3836	0.2468178	0.1899901	40.1	996.3720638	508.3493167
08332010	2/7/1977	550	560	831.6	0.4077534	0.2801835	46.4	1141.776801	587.1097327
08332010	5/19/1978	2800	1290	9752.4	0.155667	0.1090184	66.2	17482.02432	8592.727448
08332010	5/31/1978	2300	1010	6272.1	0.2087097	0.1497295	73.4	12099.66486	7400.678955
08332010	1/29/1979	543	1210	1773.981	0.1212551	0.1008667	41	3079.17635	1913.045727
08332010	5/17/1979	5770	831	12946.15	0.1135229	0.08185949	64.4	30547.06116	16135.80371
08332010	8/30/1979	311	554	465.1938	0.1766304	0.1008942	66.2	913.6855005	437.7716326
08332010	12/7/1979	1620	463	2025.162	0.2115792	0.1623439	35.6	5813.57604	4328.676239
08332010	12/20/1979	1740	612	2875.176	0.2100165	0.1580486	33.8	9432.569862	7817.71814
08332010	3/6/1980	1300	259	909.09	0.245243	0.2009602	51.8	1672.765076	966.0618858

Table I-2 BORAMEP data for the Bernardo gage.

***		Discharge	Conc	Suspended	d65	d35	Temp	Total Load	Total Sand Load
Location	Date	(cfs)	(PPM)	Sample (tons/day)	(mm)	(mm)	F	(tons/day)	(>0.625mm)(tons/day)
08332010	4/7/1980	547	103	152.1207	0.2325328	0.1935652	60.8	302.8199325	182.1143551
08332010	6/19/1980	5410	320	4674.24	0.1227664	0.09586255	69.8	12345.3954	7516.958389
08332010	7/17/1980	394	115	122.337	0.2282685	0.1850592	77	311.4888535	173.5747452
08332010	12/17/1981	613	553	915.2703	0.4183725	0.2865437	43.7	1376.825394	750.1195297
08332010	5/21/1982	3800	455	4668.3	0.1311368	0.08898123	64.4	11768.97119	7353.545166
08332010	1/9/1984	844	350	797.58	0.2689808	0.2109778	42.8	1525.423315	1228.324316
08332010	2/17/1984	757	82	167.5998	0.1100116	0.07130092	42.8	1029.289075	397.4422736
08332010	3/9/1984	372	94	94.4136	0.3830571	0.2486415	48.2	268.8208952	217.1306601
08332010	3/16/1984	543	161	236.0421	0.3360626	0.2354583	57.2	621.6361674	493.232252
08332010	5/10/1984	5120	1060	14653.44	0.248315	0.2162758	61.7	32783.43176	27247.35852
08332010	6/7/1984	7540	2370	48248.46	0.2332333	0.1918577	65.3	79868.00452	71289.8844
08332010	7/13/1984	115	89	27.6345	0.227488	0.1846467	78.8	97.59044057	59.254278
08332010	1/23/1985	707	320	610.848	0.3324357	0.2213009	41.9	1673.705141	1468.376054
08332010	5/7/1985	7810	326	6874.362	0.1900349	0.1218953	64.4	18014.66541	8606.571655
08332010	7/9/1985	4100	786	8701.02	0.1231865	0.1008061	76.1	18603.25049	12813.29053
08332010	12/5/1985	206	32	17.7984	0.2195267	0.1785962	44.6	71.64831281	50.66071439
08332010	1/21/1986	2600	251	1762.02	0.1917147	0.1297277	55.4	5752.841576	3253.210716
08332010	4/10/1986	2060	92	511.704	0.1228722	0.09708554	62.6	1779.367542	833.1694832
08332010	1/30/1989	894	519	1252.762	0.4362966	0.33357	32	1631.033612	1262.250195
08332010	3/16/1989	1370	616	2278.584	0.4347818	0.25	58.1	3946.042177	2466.30353
08332010	1/5/1990	685	190	351.405	0.461154	0.325015	53.6	514.9059536	259.2920925
08332010	3/21/1991	1180	197	627.642	0.3934844	0.2360284	50	1223.673286	552.5880806
08332010	4/9/1991	1140	172	529.416	0.2346658	0.1505601	55.4	1715.009621	965.1153946
08332010	5/10/1991	2310	354	2207.898	0.1766652	0.09222946	60.8	4894.211639	2595.822723
08332010	12/5/1991	1460	1550	6110.1	0.4126953	0.2114222	41	9987.886294	8719.108829
08332010	2/12/1992	1170	357	1127.763	0.2575139	0.163195	45.5	2611.784421	1889.093075
08332010	3/3/1992	1300	240	842.4	0.2343768	0.158596	50	3294.088142	2265.151131
08332010	6/17/1992	2670	1890	13625.01	0.3980545	0.2651454	75.2	16998.76482	16034.12731
08332010	7/20/1992	202	137	74.7198	0.4247939	0.3177119	84.2	110.604247	83.88394821
08332010	11/10/1992	646	354	617.4468	0.4379497	0.295027	49.1	1220.191108	957.7620609
08332010	1/6/1993	1350	1280	4665.6	0.2227008	0.1084481	42.8	8797.593386	6677.888796

Table I-2 BORAMEP data for the Bernardo gage.

***		Discharge	Conc	Suspended	d65	d35	Temp	Total Load	Total Sand Load
Location	Date	(cfs)	(PPM)	Sample (tons/day)	(mm)	(mm)	F	(tons/day)	(>0.625mm)(tons/day)
08332010	6/17/1993	3730	568	5720.328	0.4465775	0.3249771	69.8	8414.546152	7019.933237
08332010	11/22/1993	1250	564	1903.5	0.4378785	0.3178802	46.04	3234.85981	2596.537483
08332010	1/12/1994	1110	208	623.376	0.4316297	0.3074346	35.24	1286.107832	1024.460249
08332010	2/24/1994	1010	241	657.207	0.4189208	0.2614569	45.5	1177.002083	898.1544574
08332010	3/21/1994	1360	196	719.712	0.4295745	0.2731968	59.9	1192.040242	610.2455644
08332010	4/18/1994	2710	1640	11999.88	0.2820813	0.2125563	62.06	20297.39478	17887.87012
08332010	5/27/1994	6090	1400	23020.2	0.4573531	0.2988293	65.12	31798.0177	20875.10071
08332010	6/21/1994	4450	445	5346.675	0.4126953	0.2333576	72.5	10168.58377	8343.973543
08332010	7/18/1994	166	48	21.5136	0.4860373	0.3623811	83.84	35.94648237	21.46331281
08332010	9/22/1994	171	200	92.34	0.431659	0.3159372	73.22	99.9887942	25.05835902
08332010	10/21/1994	508	412	565.0992	0.4399709	0.3503045	58.28	678.6499237	198.7877105
08332010	4/18/1995	2840	629	4823.172	0.392632	0.2646859	54.14	7347.503464	4450.673141
08332010	5/18/1995	4830	1050	13693.05	0.2488991	0.208118	58.82	21948.97635	16346.74881
08332010	7/21/1995	4480	1240	14999.04	0.3840787	0.2416885	77	19804.62562	9449.844985
08332010	11/30/1995	1260	286	972.972	0.4664283	0.3453086	43.7	1412.59997	1065.271052
08332010	2/23/1996	1530	2260	9336.06	0.4664283	0.3453086	47.48	10675.39954	9916.998657
08332010	7/10/1996	448	5680	6870.528	0.410788	0.2610123	71.6	7595.189764	2474.06806
08332010	2/11/1997	932	430	1082.052	0.4133389	0.2664118	40.1	2364.608973	1148.845667
08332010	3/18/1997	727	620	1216.998	0.4059228	0.2607425	55.4	1701.815301	990.2866144
08332010	5/20/1997	4520	2090	25506.36	0.475667	0.3135555	66.2	33769.20909	27468.06507
08332010	6/24/1997	2060	429	2386.098	0.4206966	0.2915451	74.48	3113.763369	2192.419741
08332010	9/16/1997	746	963	1939.675	0.433663	0.316565	60	2479.4528	1502.587321
08332010	10/22/1997	2150	998	5793.39	0.4121641	0.2854109	58.46	9888.108044	7777.458874
08332010	11/18/1997	1610	418	1817.046	0.371742	0.2262201	45.14	2524.585459	1779.248972
08332010	12/16/1997	1170	537	1696.383	0.4036367	0.2606147	41.72	2901.411782	2611.033089
08332010	1/20/1998	940	833	2114.154	0.4081661	0.2555426	42.8	2606.07729	2397.917088
08332010	2/23/1998	1050	232	657.72	0.4405073	0.3143133	46.94	1032.428667	788.8588578
08332010	4/21/1998	974	313	823.1274	0.4251279	0.2969899	60	1796.149663	1529.451513
08332010	5/18/1998	3040	676	5548.608	0.3757398	0.242795	63.5	7555.222249	5363.276692
08332010	6/23/1998	301	71	57.7017	0.4460696	0.3291034	60	123.2475084	99.01888792
08332010	12/9/1998	855	291	671.7735	0.4020092	0.2654771	60	1003.325587	718.2727301

Table I-2 BORAMEP data for the Bernardo gage.

***		Discharge	Conc	Suspended	d65	d35	Temp	Total Load	Total Sand Load
Location	Date	(cfs)	(PPM)	Sample (tons/day)	(mm)	(mm)	F	(tons/day)	(>0.625mm)(tons/day)
08332010	1/7/1999	942	377	958.8618	0.4058694	0.2798814	43.7	1868.435081	1533.542259
08332010	4/22/1999	53	88	12.5928	0.3554962	0.2339599	60	18.45044983	10.57935655
08332010	6/15/1999	2130	1490	8568.99	0.4260226	0.3141625	60	24519.76471	23121.95538
08332010	10/26/1999	355	194	185.949	0.4206966	0.2915451	60.8	315.5892124	264.0706883
08332010	1/28/2000	998	269	724.8474	0.4788162	0.3684472	48.2	1074.537906	631.5974157
08332010	2/29/2000	865	295	688.9725	0.4423967	0.3192818	54.5	1126.343137	567.3957497
08332010	3/30/2000	550	82	121.77	0.4014404	0.2604913	65.84	293.5145964	198.8703856
08332010	4/10/2000	460	111	137.862	0.4145763	0.2902858	71.6	255.7443656	158.5747642
08332010	12/22/2000	499	284	382.6332	0.4025114	0.2444497	41	746.9203801	607.5359044
08332010	1/9/2001	544	179	262.9152	0.4547408	0.3365063	60	367.0405298	249.3574625
08332010	2/26/2001	810	204	446.148	0.4750731	0.3486083	60	743.9231812	475.8616577
08332010	5/30/2001	1510	287	1170.099	0.4054033	0.2467214	78.8	1966.121204	1322.564808
08332010	10/18/2001	94	49	12.4362	0.4351821	0.294475	60	15.49261954	6.381937057
08332010	12/20/2001	552	533	794.3832	0.4487414	0.302244	41.9	1264.434012	620.0337421

Table I-3 BORAMEP data for the San Acacia gage.

***		Discharge	Conc	Suspended	d65	d35	Temp	Total Load	Total Sand Load
Location	Date	(cfs)	(PPM)	Sample (tons/day)	(mm)	(mm)	F	(tons/day)	(>0.625mm)(tons/day)
08355000	4/15/1969	609	3490	5738.607	0.1926843	0.1274432	62.6	9241.760773	4996.638916
08354900	4/15/1969	609	3490	5738.607	0.1926843	0.1274432	62.6	9241.760773	4996.638916
08355000	6/16/1969	3480	10200	95839.2	0.2066255	0.1471363	68	108805.9919	34316.03584
08354900	6/16/1969	3480	10200	95839.2	0.2066255	0.1471363	68	108805.9919	34316.03584
08355000	6/5/1973	6000	4480	72576	0.104057	0.07153845	64.4	108775.668	36793.22461
08354900	6/5/1973	6000	4480	72576	0.104057	0.07153845	64.4	108775.668	36793.22461
08355000	7/3/1973	1820	1540	7567.56	0.2057465	0.1469329	75.2	10983.54556	5876.39859
08354900	7/3/1973	1820	1540	7567.56	0.2057465	0.1469329	75.2	10983.54556	5876.39859
08355000	11/6/1973	207	1630	911.007	0.2052904	0.1488611	53.6	1301.642986	690.4026523
08354900	11/6/1973	207	1630	911.007	0.2052904	0.1488611	53.6	1301.642986	690.4026523
08355000	5/6/1975	2250	1610	9780.75	0.1118599	0.07671823	50	16015.49335	5384.544434
08354900	5/6/1975	2250	1610	9780.75	0.1118599	0.07671823	50	16015.49335	5384.544434
08355000	5/29/1975	3160	1560	13309.92	0.1310002	0.09655906	57.2	22158.64355	10530.70728
08354900	5/29/1975	3160	1560	13309.92	0.1310002	0.09655906	57.2	22158.64355	10530.70728
08355000	7/1/1975	1640	555	2457.54	0.2016582	0.1375056	69.8	4931.730499	3456.761261
08354900	7/1/1975	1640	555	2457.54	0.2016582	0.1375056	69.8	4931.730499	3456.761261
08355000	9/30/1975	340	1650	1514.7	0.2173066	0.1664514	60.8	3608.589643	3039.117661
08354900	9/30/1975	340	1650	1514.7	0.2173066	0.1664514	60.8	3608.589643	3039.117661
08355000	1/27/1976	680	1660	3047.76	0.2473976	0.1997871	40.1	6518.740725	5608.596956
08354900	1/27/1976	680	1660	3047.76	0.2473976	0.1997871	40.1	6518.740725	5608.596956
08355000	2/9/1976	689	941	1750.542	0.2222256	0.1762146	54.5	3546.132126	2712.777283
08354900	2/9/1976	689	941	1750.542	0.2222256	0.1762146	54.5	3546.132126	2712.777283
08355000	2/23/1976	740	960	1918.08	0.2299689	0.1879786	48.2	4648.877586	3808.739586
08354900	2/23/1976	740	960	1918.08	0.2299689	0.1879786	48.2	4648.877586	3808.739586
08355000	3/2/1976	665	1400	2513.7	0.231083	0.1927142	50.9	5775.643188	5163.723816
08354900	3/2/1976	665	1400	2513.7	0.231083	0.1927142	50.9	5775.643188	5163.723816
08355000	3/30/1976	210	258	146.286	0.3898795	0.2598315	48.2	284.1856956	214.8409996
08354900	3/30/1976	210	258	146.286	0.3898795	0.2598315	48.2	284.1856956	214.8409996
08355000	5/10/1976	938	1800	4558.68	0.2228525	0.1745855	64.4	8167.544975	5609.147461
08354900	5/10/1976	938	1800	4558.68	0.2228525	0.1745855	64.4	8167.544975	5609.147461
08355000	5/24/1976	176	734	348.7968	0.2307636	0.1884131	77	680.0627556	482.7799768

Table I-3 BORAMEP data for the San Acacia gage.

***		Discharge	Conc	Suspended	d65	d35	Temp	Total Load	Total Sand Load
Location	Date	(cfs)	(PPM)	Sample (tons/day)	(mm)	(mm)	F	(tons/day)	(>0.625mm)(tons/day)
08354900	5/24/1976	176	734	348.7968	0.2307636	0.1884131	77	680.0627556	482.7799768
08355000	7/3/1980	1690	349	1592.487	0.1122476	0.08144244	77	4364.557621	1960.187504
08354900	7/3/1980	1690	349	1592.487	0.1122476	0.08144244	77	4364.557621	1960.187504
08355000	12/14/1981	805	1560	3390.66	0.1113695	0.07893547	46.4	8576.596649	4439.334473
08354900	12/14/1981	805	1560	3390.66	0.1113695	0.07893547	46.4	8576.596649	4439.334473
08355000	2/17/1982	758	763	1561.556	0.2330647	0.1982347	50	2687.33606	1343.267578
08354900	2/17/1982	758	763	1561.556	0.2330647	0.1982347	50	2687.33606	1343.267578
08355000	3/3/1982	777	2560	5370.624	0.2350684	0.1994948	51.8	7539.725311	3840.796692
08354900	3/3/1982	777	2560	5370.624	0.2350684	0.1994948	51.8	7539.725311	3840.796692
08355000	5/5/1982	4630	5210	65130.21	0.3917645	0.2430713	59	73487.19617	24838.92029
08354900	5/5/1982	4630	5210	65130.21	0.3917645	0.2430713	59	73487.19617	24838.92029
08355000	7/6/1982	1880	752	3817.152	0.2475072	0.2157136	70.7	7203.913589	5496.12233
08354900	7/6/1982	1880	752	3817.152	0.2475072	0.2157136	70.7	7203.913589	5496.12233
08355000	11/4/1983	456	3380	4161.456	0.2475028	0.1647423	57.2	7007.634935	3879.335016
08354900	11/4/1983	456	3380	4161.456	0.2475028	0.1647423	57.2	7007.634935	3879.335016
08355000	11/15/1983	683	1440	2655.504	0.2352245	0.1534558	47.3	5420.067841	3049.436378
08354900	11/15/1983	683	1440	2655.504	0.2352245	0.1534558	47.3	5420.067841	3049.436378
08355000	4/17/1984	2040	1550	8537.4	0.1214117	0.09519092	68	14778.62068	8441.875488
08354900	4/17/1984	2040	1550	8537.4	0.1214117	0.09519092	68	14778.62068	8441.875488
08355000	5/11/1984	3280	1850	16383.6	0.2200488	0.1592848	64.4	23858.12689	15881.5332
08354900	5/11/1984	3280	1850	16383.6	0.2200488	0.1592848	64.4	23858.12689	15881.5332
08355000	5/21/1984	5420	2330	34097.22	0.125	0.1018493	64.4	47808.81152	14933.56543
08354900	5/21/1984	5420	2330	34097.22	0.125	0.1018493	64.4	47808.81152	14933.56543
08355000	6/5/1984	5550	3340	50049.9	0.125	0.09939256	64.4	72450.20813	17708.66321
08354900	6/5/1984	5550	3340	50049.9	0.125	0.09939256	64.4	72450.20813	17708.66321
08355000	6/20/1984	1480	627	2505.492	0.1885065	0.1215357	73.4	4487.085617	2533.640671
08354900	6/20/1984	1480	627	2505.492	0.1885065	0.1215357	73.4	4487.085617	2533.640671
08355000	3/21/1985	4200	5140	58287.6	0.2491456	0.2168534	49.1	79839.86481	56344.55817
08354900	3/21/1985	4200	5140	58287.6	0.2491456	0.2168534	49.1	79839.86481	56344.55817
08355000	12/4/1985	379	349	357.1317	0.1344904	0.1005939	44.6	1560.171623	1142.927818
08354900	12/4/1985	379	349	357.1317	0.1344904	0.1005939	44.6	1560.171623	1142.927818

Table I-3 BORAMEP data for the San Acacia gage.

***		Discharge	Conc	Suspended	d65	d35	Temp	Total Load	Total Sand Load
Location	Date	(cfs)	(PPM)	Sample (tons/day)	(mm)	(mm)	F	(tons/day)	(>0.625mm)(tons/day)
08355000	2/19/1986	3810	714	7344.918	0.1117015	0.07155462	48.2	15538.42696	10399.99658
08354900	2/19/1986	3810	714	7344.918	0.1117015	0.07155462	48.2	15538.42696	10399.99658
08355000	3/4/1986	4350	441	5179.545	0.3166708	0.2069651	48.2	9663.426636	5421.569244
08354900	3/4/1986	4350	441	5179.545	0.3166708	0.2069651	48.2	9663.426636	5421.569244
08355000	11/6/1987	1320	3940	14042.16	0.239021	0.1928991	55.4	21023.96866	7944.646515
08354900	11/6/1987	1320	3940	14042.16	0.239021	0.1928991	55.4	21023.96866	7944.646515
08355000	11/21/1988	1230	2510	8335.71	0.2677295	0.2109778	60	15708.52161	13678.08984
08354900	11/21/1988	1230	2510	8335.71	0.2677295	0.2109778	60	15708.52161	13678.08984
08355000	1/4/1989	1100	1440	4276.8	0.2395584	0.1954167	42.8	10895.86987	10290.50702
08354900	1/4/1989	1100	1440	4276.8	0.2395584	0.1954167	42.8	10895.86987	10290.50702
08355000	2/2/1990	716	549	1061.327	0.25	0.2174472	40.1	1764.451971	1470.856573
08354900	2/2/1990	716	549	1061.327	0.25	0.2174472	40.1	1764.451971	1470.856573
08355000	4/4/1990	728	112	220.1472	0.2200248	0.1694841	58.1	779.0748215	535.2477036
08354900	4/4/1990	728	112	220.1472	0.2200248	0.1694841	58.1	779.0748215	535.2477036
08355000	5/2/1990	721	636	1238.101	0.2282308	0.1790411	49.1	2117.359146	1546.840347
08354900	5/2/1990	721	636	1238.101	0.2282308	0.1790411	49.1	2117.359146	1546.840347
08355000	10/16/1990	196	180	95.256	0.1453128	0.1047506	59.9	221.2374786	139.3975509
08354900	10/16/1990	196	180	95.256	0.1453128	0.1047506	59.9	221.2374786	139.3975509
08355000	12/20/1990	1340	393	1421.874	0.1415019	0.08569036	41.9	3630.929871	1683.623108
08354900	12/20/1990	1340	393	1421.874	0.1415019	0.08569036	41.9	3630.929871	1683.623108
08355000	1/31/1991	990	1930	5158.89	0.2340619	0.1923257	41	7668.276062	5415.171082
08354900	1/31/1991	990	1930	5158.89	0.2340619	0.1923257	41	7668.276062	5415.171082
08355000	5/22/1991	4260	2110	24269.22	0.2133135	0.0888636	62.6	32274.46815	17468.8069
08354900	5/22/1991	4260	2110	24269.22	0.2133135	0.0888636	62.6	32274.46815	17468.8069
08355000	12/16/1991	1670	2030	9153.27	0.1236448	0.07947254	40.1	14931.39907	7242.006618
08354900	12/16/1991	1670	2030	9153.27	0.1236448	0.07947254	40.1	14931.39907	7242.006618
08355000	2/21/1992	575	3070	4766.175	0.2294756	0.1938426	50	5689.294167	1353.111
08354900	2/21/1992	575	3070	4766.175	0.2294756	0.1938426	50	5689.294167	1353.111
08355000	6/18/1992	2050	219	1212.165	0.3617303	0.2277981	71.6	1930.983413	1081.939101
08354900	6/18/1992	2050	219	1212.165	0.3617303	0.2277981	71.6	1930.983413	1081.939101
08355000	9/17/1992	327	470	414.963	0.2286007	0.1687047	69.8	848.4961112	379.7923758

Table I-3 BORAMEP data for the San Acacia gage.

***		Discharge	Conc	Suspended	d65	d35	Temp	Total Load	Total Sand Load
Location	Date	(cfs)	(PPM)	Sample (tons/day)	(mm)	(mm)	F	(tons/day)	(>0.625mm)(tons/day)
08354900	9/17/1992	327	470	414.963	0.2286007	0.1687047	69.8	848.4961112	379.7923758
08355000	11/4/1992	941	2270	5767.389	0.23741	0.1898547	50	9063.334583	4856.697083
08354900	11/4/1992	941	2270	5767.389	0.23741	0.1898547	50	9063.334583	4856.697083
08355000	12/11/1992	1030	1170	3253.77	0.2955199	0.2253126	42.8	8000.716208	7032.437277
08354900	12/11/1992	1030	1170	3253.77	0.2955199	0.2253126	42.8	8000.716208	7032.437277
08355000	8/11/1993	351	734	695.6118	0.2481539	0.2241595	78.8	2022.818634	1612.78299
08354900	8/11/1993	351	734	695.6118	0.2481539	0.2241595	78.8	2022.818634	1612.78299
08355000	10/6/1993	153	166	68.5746	0.4456688	0.3015711	66.2	134.1185903	112.8295431
08354900	10/6/1993	153	166	68.5746	0.4456688	0.3015711	66.2	134.1185903	112.8295431
08355000	11/19/1993	1680	2820	12791.52	0.2565452	0.2095018	50	21343.84891	18410.85794
08354900	11/19/1993	1680	2820	12791.52	0.2565452	0.2095018	50	21343.84891	18410.85794
08355000	12/15/1993	1770	2720	12998.88	0.3291202	0.2234296	38.84	23157.12061	15094.56689
08354900	12/15/1993	1770	2720	12998.88	0.3291202	0.2234296	38.84	23157.12061	15094.56689
08355000	1/10/1994	1110	2010	6023.97	0.4821779	0.356072	39.2	8378.570108	8002.171304
08354900	1/10/1994	1110	2010	6023.97	0.4821779	0.356072	39.2	8378.570108	8002.171304
08355000	2/23/1994	1070	221	638.469	0.4676784	0.3502662	48.2	844.3283455	485.5983345
08354900	2/23/1994	1070	221	638.469	0.4676784	0.3502662	48.2	844.3283455	485.5983345
08355000	3/22/1994	1350	123	448.335	0.899033	0.3928709	55.22	787.1559975	484.8211587
08354900	3/22/1994	1350	123	448.335	0.899033	0.3928709	55.22	787.1559975	484.8211587
08355000	6/22/1994	4460	867	10440.41	0.3669419	0.2333576	77	16107.39228	13645.05073
08354900	6/22/1994	4460	867	10440.41	0.3669419	0.2333576	77	16107.39228	13645.05073
08355000	7/20/1994	138	100	37.26	0.2830039	0.1972834	74.84	123.5230071	95.673825
08354900	7/20/1994	138	100	37.26	0.2830039	0.1972834	74.84	123.5230071	95.673825
08355000	12/15/1994	1220	964	3175.416	0.3454108	0.2344248	41.54	6527.216866	5738.859749
08354900	12/15/1994	1220	964	3175.416	0.3454108	0.2344248	41.54	6527.216866	5738.859749
08355000	1/19/1995	1120	707	2137.968	0.4510194	0.3555282	36.5	3440.006658	2871.04096
08354900	1/19/1995	1120	707	2137.968	0.4510194	0.3555282	36.5	3440.006658	2871.04096
08355000	2/1/1995	1160	939	2940.948	0.3499756	0.2260162	44.6	6113.549769	3661.599573
08354900	2/1/1995	1160	939	2940.948	0.3499756	0.2260162	44.6	6113.549769	3661.599573
08355000	12/4/1995	1220	1810	5962.14	0.3824962	0.25	45.5	10897.33463	9930.230865
08354900	12/4/1995	1220	1810	5962.14	0.3824962	0.25	45.5	10897.33463	9930.230865

Table I-3 BORAMEP data for the San Acacia gage.

***		Discharge	Conc	Suspended	d65	d35	Temp	Total Load	Total Sand Load
Location	Date	(cfs)	(PPM)	Sample (tons/day)	(mm)	(mm)	F	(tons/day)	(>0.625mm)(tons/day)
08355000	1/10/1996	1200	506	1639.44	0.3265637	0.2082094	37.4	3711.114695	2948.228465
08354900	1/10/1996	1200	506	1639.44	0.3265637	0.2082094	37.4	3711.114695	2948.228465
08355000	2/22/1996	1380	836	3114.936	0.3817908	0.2384384	50.36	8576.95244	7720.818651
08354900	2/22/1996	1380	836	3114.936	0.3817908	0.2384384	50.36	8576.95244	7720.818651
08355000	11/13/1996	892	3080	7417.872	0.2998981	0.2127814	46.4	14076.81624	10661.33895
08354900	11/13/1996	892	3080	7417.872	0.2998981	0.2127814	46.4	14076.81624	10661.33895
08355000	12/17/1996	935	1820	4594.59	0.2694477	0.206007	39.2	10780.33462	9114.382347
08354900	12/17/1996	935	1820	4594.59	0.2694477	0.206007	39.2	10780.33462	9114.382347
08355000	1/16/1997	649	1410	2470.743	0.3999273	0.2831408	41.9	3744.267101	3049.783215
08354900	1/16/1997	649	1410	2470.743	0.3999273	0.2831408	41.9	3744.267101	3049.783215
08355000	2/11/1997	1010	714	1947.078	0.4457175	0.3331731	42.8	2602.094371	1120.133556
08354900	2/11/1997	1010	714	1947.078	0.4457175	0.3331731	42.8	2602.094371	1120.133556
08355000	3/18/1997	735	193	383.0085	0.6933774	0.4227812	52.7	501.1725452	275.2480914
08354900	3/18/1997	735	193	383.0085	0.6933774	0.4227812	52.7	501.1725452	275.2480914
08355000	6/24/1997	980	1790	4736.34	0.3764224	0.235587	71.06	7373.525213	6656.907171
08354900	6/24/1997	980	1790	4736.34	0.3764224	0.235587	71.06	7373.525213	6656.907171
08355000	8/19/1997	583	1770	2786.157	0.2325768	0.1701559	73.94	6762.389626	6201.697548
08354900	8/19/1997	583	1770	2786.157	0.2325768	0.1701559	73.94	6762.389626	6201.697548
08355000	9/16/1997	800	8220	17755.2	0.4540915	0.327438	53.6	19020.84522	4297.938848
08354900	9/16/1997	800	8220	17755.2	0.4540915	0.327438	53.6	19020.84522	4297.938848
08355000	10/22/1997	2210	1270	7578.09	0.4664801	0.2302632	56.3	10077.81219	6445.068539
08354900	10/22/1997	2210	1270	7578.09	0.4664801	0.2302632	56.3	10077.81219	6445.068539
08355000	11/18/1997	1780	1070	5142.42	0.3706179	0.2282013	42.62	10579.86982	9291.47724
08354900	11/18/1997	1780	1070	5142.42	0.3706179	0.2282013	42.62	10579.86982	9291.47724
08355000	12/16/1997	1250	560	1890	0.4493252	0.3427967	37.22	2769.683137	2265.062073
08354900	12/16/1997	1250	560	1890	0.4493252	0.3427967	37.22	2769.683137	2265.062073
08355000	2/23/1998	1170	703	2220.777	0.4860373	0.3623811	46.94	3680.030973	3239.741209
08354900	2/23/1998	1170	703	2220.777	0.4860373	0.3623811	46.94	3680.030973	3239.741209
08355000	5/18/1998	3460	1260	11770.92	2	0.1890807	60.8	14268.73253	5736.109852
08354900	5/18/1998	3460	1260	11770.92	2	0.1890807	60.8	14268.73253	5736.109852
08355000	10/5/1998	559	7270	10972.61	0.2352939	0.1418003	60.8	13421.68013	6067.663588

Table I-3 BORAMEP data for the San Acacia gage.

***		Discharge	Conc	Suspended	d65	d35	Temp	Total Load	Total Sand Load
Location	Date	(cfs)	(PPM)	Sample (tons/day)	(mm)	(mm)	F	(tons/day)	(>0.625mm)(tons/day)
08354900	10/5/1998	559	7270	10972.61	0.2352939	0.1418003	60.8	13421.68013	6067.663588
08355000	11/3/1998	1710	1280	5909.76	0.3785891	0.242394	57.2	10419.13111	8757.479009
08354900	11/3/1998	1710	1280	5909.76	0.3785891	0.242394	57.2	10419.13111	8757.479009
08355000	2/11/1999	1090	786	2313.198	0.4565371	0.3701185	60	3291.742018	2634.636183
08354900	2/11/1999	1090	786	2313.198	0.4565371	0.3701185	60	3291.742018	2634.636183
08355000	8/27/1999	1140	1940	5971.32	0.2930775	0.1640101	80.6	10115.62659	6817.352997
08354900	8/27/1999	1140	1940	5971.32	0.2930775	0.1640101	80.6	10115.62659	6817.352997
08355000	9/13/1999	609	669	1100.037	0.246965	0.1924329	60	1400.64965	757.9407796
08354900	9/13/1999	609	669	1100.037	0.246965	0.1924329	60	1400.64965	757.9407796
08355000	10/29/1999	390	33	34.749	1.593069	0.2700433	59	60.10043724	60.10043724
08354900	10/29/1999	390	33	34.749	1.593069	0.2700433	59	60.10043724	60.10043724
08355000	12/1/1999	1070	2070	5980.23	0.308995	0.2193806	44.6	9974.285889	9163.330322
08354900	12/1/1999	1070	2070	5980.23	0.308995	0.2193806	44.6	9974.285889	9163.330322
08355000	1/12/2000	881	1240	2949.588	0.482297	0.3745853	48.2	4644.625493	4131.334538
08354900	1/12/2000	881	1240	2949.588	0.482297	0.3745853	48.2	4644.625493	4131.334538
08355000	10/5/2000	306	94	77.6628	0.5246695	0.3489569	60	107.8464644	54.14242385
08354900	10/5/2000	306	94	77.6628	0.5246695	0.3489569	60	107.8464644	54.14242385
08355000	11/15/2000	668	625	1127.25	0.4747282	0.3078145	60	2103.112123	1592.480043
08354900	11/15/2000	668	625	1127.25	0.4747282	0.3078145	60	2103.112123	1592.480043
08355000	12/6/2000	792	2360	5046.624	0.4491737	0.3507387	60	6337.128711	5869.28133
08354900	12/6/2000	792	2360	5046.624	0.4491737	0.3507387	60	6337.128711	5869.28133
08355000	3/2/2001	876	1420	3358.584	0.5375025	0.4153751	60	3917.27366	3476.036661
08354900	3/2/2001	876	1420	3358.584	0.5375025	0.4153751	60	3917.27366	3476.036661
08355000	4/24/2001	702	217	411.3018	0.8922014	0.4500343	59.9	689.9023314	534.8287078
08354900	4/24/2001	702	217	411.3018	0.8922014	0.4500343	59.9	689.9023314	534.8287078
08355000	11/7/2001	546	2840	4186.728	0.2410087	0.2056931	61.7	7570.084682	6661.996334
08354900	11/7/2001	546	2840	4186.728	0.2410087	0.2056931	61.7	7570.084682	6661.996334
08355000	1/9/2002	701	544	1029.629	0.6110312	0.3879609	48.2	1322.640629	542.1917767
08354900	1/9/2002	701	544	1029.629	0.6110312	0.3879609	48.2	1322.640629	542.1917767
08355000	3/14/2002	197	266	141.4854	1.095533	0.4617374	54.5	229.7175689	153.8575988
08354900	3/14/2002	197	266	141.4854	1.095533	0.4617374	54.5	229.7175689	153.8575988

Table I-4 BORAMEP data for the San Marcial gage.

***		Discharge	Conc	Suspended	d65	d35	Temp	Total Load	Total Sand Load
Location	Date	(cfs)	(PPM)	Sample (tons/day)	(mm)	(mm)	F	(tons/day)	(>0.625mm)(tons/day)
08358400	10/1/1968	38	84	8.6184	0.2265416	0.1821913	66.2	13.40555917	5.357072072
08358400	10/16/1968	71	145	27.7965	0.2260274	0.1877661	59	36.13989781	10.01766919
08358300	11/25/1968	1420	6350	24345.9	0.2084719	0.1475615	48.2	31705.55817	20228.36188
08358300	12/2/1968	749	4840	9787.932	0.2082726	0.1453461	37.4	13634.02368	10324.03491
08358300	12/16/1968	661	2900	5175.63	0.2384848	0.1904143	35.6	7853.894827	6341.390356
08358300	1/6/1969	805	3800	8259.3	0.2325768	0.1701559	39.2	11859.72534	8729.534363
08358300	1/27/1969	928	2000	5011.2	0.2238221	0.176969	50	7992.478012	5700.532196
08358300	2/3/1969	854	5410	12474.38	0.2375365	0.1743042	39.2	16860.40003	12455.1592
08358300	3/3/1969	875	2920	6898.5	0.2148599	0.1576641	46.4	10670.1217	8559.122681
08358300	3/24/1969	607	3990	6539.211	0.2264259	0.1761977	48.2	8650.091125	4081.431
08358300	4/7/1969	1550	5820	24356.7	0.237991	0.1923424	57.2	28359.3399	14020.15155
08358300	4/21/1969	1600	3910	16891.2	0.2188576	0.1630812	64.4	21703.71579	14202.36017
08358300	5/19/1969	1850	4340	21678.3	0.2407422	0.1915867	68	25565.1106	14167.70306
08358300	6/9/1969	1940	3460	18123.48	0.2381121	0.1836278	71.6	22958.07184	15943.17615
08358300	6/23/1969	1770	3310	15818.49	0.193273	0.1298189	71.6	21409.4216	14433.49146
08358300	10/12/1970	289	2000	1560.6	0.2230348	0.1645517	48.2	2387.543812	1306.701111
08358300	11/12/1970	1900	7490	38423.7	0.2461634	0.199102	47.3	43228.44884	18735.6903
08358300	11/16/1970	1750	5580	26365.5	0.2473976	0.1997871	41.9	30686.03561	17041.24923
08358300	12/14/1970	1070	3170	9158.13	0.2344869	0.1819541	36.5	13091.43851	9658.517761
08358300	1/4/1971	930	1570	3942.27	0.2267299	0.1722458	32	6187.038475	4058.71048
08358300	1/18/1971	950	3230	8284.95	0.2365395	0.1692093	39.2	13388.76711	10732.40668
08358300	2/8/1971	986	3290	8758.638	0.2357492	0.1781438	33.8	13138.08237	10432.30164
08358300	2/16/1971	915	2380	5879.79	0.2451015	0.1868258	48.2	8809.833408	6418.402058
08358300	3/8/1971	640	1710	2954.88	0.2828852	0.2029478	43.7	4936.572124	3356.69337
08358300	3/23/1971	525	1290	1828.575	0.25	0.206214	51.8	3312.199228	2356.851282
08358300	5/4/1971	360	866	841.752	0.2200248	0.1694841	58.1	1779.044977	1358.056023
08358300	5/17/1971	255	615	423.4275	0.2489767	0.2108319	63.5	691.882611	496.4740036
08358300	1/16/1972	1040	3890	10923.12	0.1118132	0.08019479	41	18276.06136	7055.605881
08358300	3/6/1972	1020	2160	5948.64	0.1573194	0.1028894	55.4	9340.680634	3900.793915
08358300	11/13/1972	1340	12700	45948.6	0.1041038	0.06394286	48.2	59218.48309	25490.06073
08358300	11/27/1972	955	9570	24676.24	0.1122476	0.08144244	41	33414.22919	17895.55518

Table I-4 BORAMEP data for the San Marcial gage.

***		Discharge	Conc	Suspended	d65	d35	Temp	Total Load	Total Sand Load
Location	Date	(cfs)	(PPM)	Sample (tons/day)	(mm)	(mm)	F	(tons/day)	(>0.625mm)(tons/day)
08358300	1/29/1973	698	2370	4466.502	0.2568952	0.2069385	39.2	5718.685615	2565.93122
08358300	7/16/1973	1690	2910	13278.33	0.2340291	0.1838704	71.6	18340.07211	12896
08358300	1/7/1974	1400	2440	9223.2	0.1192449	0.0896486	39.2	14447.65669	10249.32576
08358300	1/21/1974	1400	1540	5821.2	0.2351182	0.1843965	42.8	8728.011978	6316.177917
08358300	2/25/1974	854	760	1752.408	0.2219376	0.1641669	42.8	3119.598351	2167.695129
08358300	3/24/1975	530	1990	2847.69	0.244149	0.2003283	66.2	3569.333382	1598.965218
08358300	3/31/1975	740	1340	2677.32	0.3079757	0.2047156	43.7	3995.304901	1945.038727
08358300	6/16/1975	788	873	1857.395	0.2322667	0.180924	71.6	3259.506683	1809.169281
08358300	10/20/1975	143	158	61.0038	0.1949397	0.1299157	61.7	234.7465048	184.2999487
08358300	11/17/1975	1430	4660	17992.26	0.1174688	0.08433217	46.4	25881.54242	17761.49936
08358400	2/24/1976	720	1020	1982.88	0.2376185	0.1943283	50	4009.440172	3089.459948
08358400	8/17/1976	106	1170	334.854	0.2196879	0.1768526	73.4	501.4551239	386.1280155
08358400	10/13/1976	180	558	271.188	0.2322667	0.180924	57.2	496.2165483	306.1632808
08358400	12/13/1976	570	1880	2893.32	0.2376185	0.1943283	40.1	4132.247802	2617.578178
08358400	12/22/1976	835	2530	5703.885	0.2488237	0.2055128	41	7274.529317	3041.396596
08358400	1/17/1977	439	1070	1268.271	0.2201985	0.1714834	39.2	2547.848473	1928.473595
08358400	2/15/1977	584	1470	2317.896	0.2290382	0.1915112	47.3	4697.911087	3769.193039
08358400	3/1/1977	650	1220	2141.1	0.2224318	0.1838325	50	4412.827087	3397.645409
08358400	3/15/1977	360	848	824.256	0.2366908	0.1938069	57.2	1266.418022	665.2837448
08358400	4/18/1977	136	169	62.0568	0.3334661	0.2123381	56.3	101.0002929	47.06257355
08358400	10/19/1977	83	619	138.7179	0.2312097	0.1804321	50	212.7235155	96.13390636
08358400	2/16/1978	666	3390	6095.898	0.1949397	0.1299157	33.8	10451.93591	7855.642075
08358400	3/7/1978	723	7980	15577.76	0.2032695	0.1463567	53.6	19141.66234	5251.967148
08358400	5/17/1978	1940	3220	16866.36	0.1853384	0.1151186	68	24051.11006	10582.51143
08358400	6/2/1978	1830	1730	8547.93	0.1990273	0.1325727	71.6	13965.28003	6465.960754
08358400	6/29/1978	977	555	1464.035	0.2201985	0.1714834	59	3096.616966	2033.105194
08358400	5/29/1979	6100	8850	145759.5	0.1014673	0.06997034	66.2	203613.7988	63516.1875
08358400	7/6/1979	4910	1840	24392.88	0.1944183	0.1274943	66.2	33478.37402	15198.48944
08358400	9/11/1979	86	133	30.8826	0.2332333	0.1918577	66.2	60.10170887	39.54065464
08358400	12/4/1979	1540	1040	4324.32	0.1749878	0.1095653	37.4	10074.24948	7183.381622
08358400	1/3/1980	820	1140	2523.96	0.191067	0.1273952	33.8	5852.294201	4193.242611

Table I-4 BORAMEP data for the San Marcial gage.

***		Discharge	Conc	Suspended	d65	d35	Temp	Total Load	Total Sand Load
Location	Date	(cfs)	(PPM)	Sample (tons/day)	(mm)	(mm)	F	(tons/day)	(>0.625mm)(tons/day)
08358400	2/4/1980	1030	524	1457.244	0.1843613	0.1226033	48.2	4126.993378	3203.819386
08358400	3/3/1980	1370	3050	11281.95	0.2034993	0.1503347	41	16645.37232	8296.918648
08358400	5/14/1980	5420	3680	53853.12	0.2003562	0.13505	64.4	66652.0047	25064.20642
08358400	10/15/1980	112	346	104.6304	0.2212139	0.1738426	57.2	139.8352404	66.6948843
08358400	12/2/1980	1370	1100	4068.9	0.2119242	0.1606075	46.4	7295.554718	4387.966553
08358400	1/5/1981	1320	935	3332.34	0.1994684	0.1393801	44.6	8699.299171	6943.354065
08358400	1/20/1981	766	1120	2316.384	0.1684358	0.1082172	39.2	6482.568176	5363.161316
08358400	2/2/1981	650	339	594.945	0.2465846	0.2041755	44.6	1398.830338	1008.700272
08358400	2/19/1981	933	1300	3274.83	0.1915286	0.1240216	51.8	7432.354176	6249.627258
08358400	3/17/1981	649	1080	1892.484	0.2301312	0.1901012	54.5	3396.863022	2544.855713
08358400	4/14/1981	76	94	19.2888	0.2298939	0.1859167	55.4	31.22394729	21.34777236
08358400	1/5/1982	394	3130	3329.694	0.1976699	0.1300727	35.6	5379.91362	2751.904495
08358400	5/6/1982	4310	11000	128007	0.2298939	0.1859167	59	152231.7735	75347.95931
08358400	7/1/1982	2580	4380	30511.08	0.204527	0.1445691	68	41494.53293	28412.72369
08358300	11/2/1983	189	254	129.6162	0.225265	0.1834691	58.1	372.789634	292.5233605
08358400	11/14/1983	371	4050	4056.885	0.1897823	0.1241584	51.8	5110.001133	1161.956303
08358300	1/4/1984	818	1520	3357.072	0.2312097	0.1804321	43.7	4892.844354	3706.920281
08358300	3/15/1984	610	3340	5500.98	0.2265607	0.1920612	55.4	6750.845612	2200.607269
08358300	5/9/1984	1430	1960	7567.56	0.2181921	0.1724664	64.4	9471.400711	4732.117096
08358400	5/25/1984	4940	1430	19073.34	0.191717	0.09951159	68	35198.04533	23569.04192
08358400	6/4/1984	5150	3180	44217.9	0.117426	0.09746163	63.5	69345.4823	34664.27441
08358300	7/11/1984	505	478	651.753	0.2846496	0.2100961	71.6	858.7843784	679.0143588
08358300	11/15/1984	720	2420	4704.48	0.2312097	0.1804321	49.1	6641.286316	4796.291809
08358300	1/25/1985	807	1250	2723.625	0.2406501	0.2006146	42.8	4049.966078	3066.99678
08358400	3/19/1985	3190	9490	81737.37	0.2259871	0.183852	50	96211.96564	38568.52716
08358400	5/17/1985	6300	4590	78075.9	0.2096346	0.1499629	62.6	98696.95532	55183.94556
08358400	7/17/1985	2600	1810	12706.2	0.1906394	0.1240216	74.3	21326.86757	16450.0773
08358300	5/3/1990	571	540	832.518	0.1855864	0.1150027	51.8	1677.378769	660.9375458
08358300	6/5/1990	297	172	137.9268	0.2298768	0.1598963	71.6	199.0165062	100.0295449
08358400	11/15/1991	1230	2440	8103.24	0.1842086	0.1061086	50	14287.52469	7339.386597
08358300	12/20/1991	332	95	85.158	0.1867825	0.1181269	51.8	300.5290943	100.0564685

Table I-4 BORAMEP data for the San Marcial gage.

***		Discharge	Conc	Suspended	d65	d35	Temp	Total Load	Total Sand Load
Location	Date	(cfs)	(PPM)	Sample (tons/day)	(mm)	(mm)	F	(tons/day)	(>0.625mm)(tons/day)
08358400	1/3/1992	868	1460	3421.656	0.2846221	0.2015356	34.7	6743.254036	5081.617577
08358300	1/21/1992	280	66	49.896	0.4437566	0.3444254	51.8	86.85192925	63.41686875
08358400	1/22/1992	830	1630	3652.83	0.2260274	0.1877661	34.7	7482.517632	6040.315826
08358400	5/5/1992	4580	2920	36108.72	0.2158149	0.1537173	62.6	54056.16423	34443.7758
08358300	6/18/1992	376	211	214.2072	0.1167464	0.06598338	65.3	395.3792007	178.075978
08358300	10/6/1992	328	214	189.5184	0.4351057	0.3369123	64.4	255.5266094	119.8933392
08358300	1/7/1993	250	67	45.225	0.4687603	0.3765452	43.7	70.73962009	41.9862765
08358400	1/7/1993	897	3110	7532.109	0.239162	0.1974367	42.8	10468.57296	4373.808367
08358300	2/5/1993	242	190	124.146	0.4783239	0.3948734	43.7	168.9874327	112.2977316
08358400	2/5/1993	807	1120	2440.368	0.2247085	0.110386	43.7	6171.016357	3225.45343
08358400	3/9/1993	738	3290	6555.654	0.2341633	0.1966944	53.6	7642.389033	3022.824
08358400	4/26/1993	2870	2120	16427.88	0.2201985	0.1714834	60	23648.39783	15316.05127
08358400	6/25/1993	3210	1640	14213.88	0.2132379	0.15914	73.4	20850.02979	13281.20087
08358300	11/19/1993	256	283	195.6096	0.4777876	0.3991123	53.6	301.1127104	273.1794905
08358300	12/14/1993	270	66	48.114	0.4877681	0.4100119	47.84	86.06068015	64.0421865
08358400	1/11/1994	754	1330	2707.614	0.1734352	0.08134415	37.22	6365.412636	4590.120522
08358300	2/23/1994	248	55	36.828	0.4953717	0.4096673	48.74	58.65646747	37.25878146
08358400	2/23/1994	750	1540	3118.5	0.224589	0.1733844	38.84	5694.652802	4404.009979
08358400	3/23/1994	905	1300	3176.55	0.2126022	0.150707	58.1	5656.623657	3614.869385
08358300	4/20/1994	352	294	279.4176	0.484157	0.4077629	59	346.6791958	222.5529217
08358400	4/20/1994	2380	2560	16450.56	0.2259871	0.183852	63.68	25583.20947	17993.07959
08358300	5/17/1994	526	528	749.8656	0.4648384	0.3786335	63.86	1067.77846	703.1215992
08358400	5/18/1994	4760	1810	23262.12	0.2301857	0.1799548	61.34	31540.36621	15668.73926
08358400	11/17/1994	1320	5360	19103.04	0.2200488	0.1592848	43.16	26439.31433	8726.884155
08358400	11/14/1996	483	1170	1525.797	0.2379476	0.1879508	46.4	2138.921875	1084.992554
08358400	12/18/1996	467	833	1050.33	0.2853616	0.2085776	32	1776.762406	1193.011612
08358400	2/12/1997	730	660	1300.86	0.2401001	0.197982	42.8	3211.234985	2552.415405
08358400	3/19/1997	389	1540	1617.462	0.2220218	0.1742092	52.7	2329.130894	1184.026646
08358400	8/20/1997	280	847	640.332	0.2324268	0.1914018	77	990.9243546	351.119545
08358400	10/23/1997	2060	3340	18577.08	0.1999977	0.1326543	53.6	31346.80786	19592.74829
08358400	11/19/1997	1560	2030	8550.36	0.2238221	0.176969	40.82	15350.50006	11313.17218

Table I-4 BORAMEP data for the San Marcial gage.

***		Discharge	Conc	Suspended	d65	d35	Temp	Total Load	Total Sand Load
Location	Date	(cfs)	(PPM)	Sample (tons/day)	(mm)	(mm)	F	(tons/day)	(>0.625mm)(tons/day)
08358400	12/15/1997	996	1360	3657.312	0.2334301	0.187775	60	6279.037415	4667.172302
08358400	1/21/1998	808	1290	2814.264	0.2300014	0.1819166	40.64	5738.577576	4476.141174
08358400	2/24/1998	897	1220	2954.718	0.2344532	0.1775963	60	5436.926636	4368.918945
08358400	3/25/1998	984	1190	3161.592	0.2364348	0.1980705	60	5800.859894	3941.733795
08358400	5/19/1998	2690	2330	16922.79	0.1965282	0.1240216	62.6	28963.89064	18851.7173
08358400	1/11/1999	770	1820	3783.78	0.2307636	0.1884131	41.9	4638893.095	4629555.031
08358400	2/24/1999	662	1120	2001.888	0.2183536	0.1687897	60	4158.850525	3152.18222
08358400	6/16/1999	1530	1490	6155.19	0.2312097	0.1804321	74.3	9636.564835	6121.418396
08358400	11/29/1999	813	2610	5729.211	0.2435955	0.1861399	46.22	12215.35774	10086.69763
08358400	12/29/1999	587	1140	1806.786	0.2622737	0.2186865	41	2733.137792	1768.129216
08358400	10/4/2000	113	252	76.8852	0.2460881	0.2089736	60	108.7675789	33.88356093
08358400	11/28/2000	439	872	1033.582	0.3233967	0.2339462	60	1581.423211	1002.00554
08358400	2/27/2001	619	1320	2206.116	0.2685402	0.2135866	50	3362.676948	2594.993178
08358400	4/25/2001	415	680	761.94	0.2238221	0.176969	62.6	1168.489571	669.0925369
08358400	5/21/2001	1660	1730	7753.86	0.2410087	0.2056931	69.8	9975.243439	3755.687531
08358400	12/3/2001	395	1070	1141.155	0.2457986	0.2061959	43.7	1399.592643	483.9002597

APPENDIX J:
Total and Sand Load Rating Curves

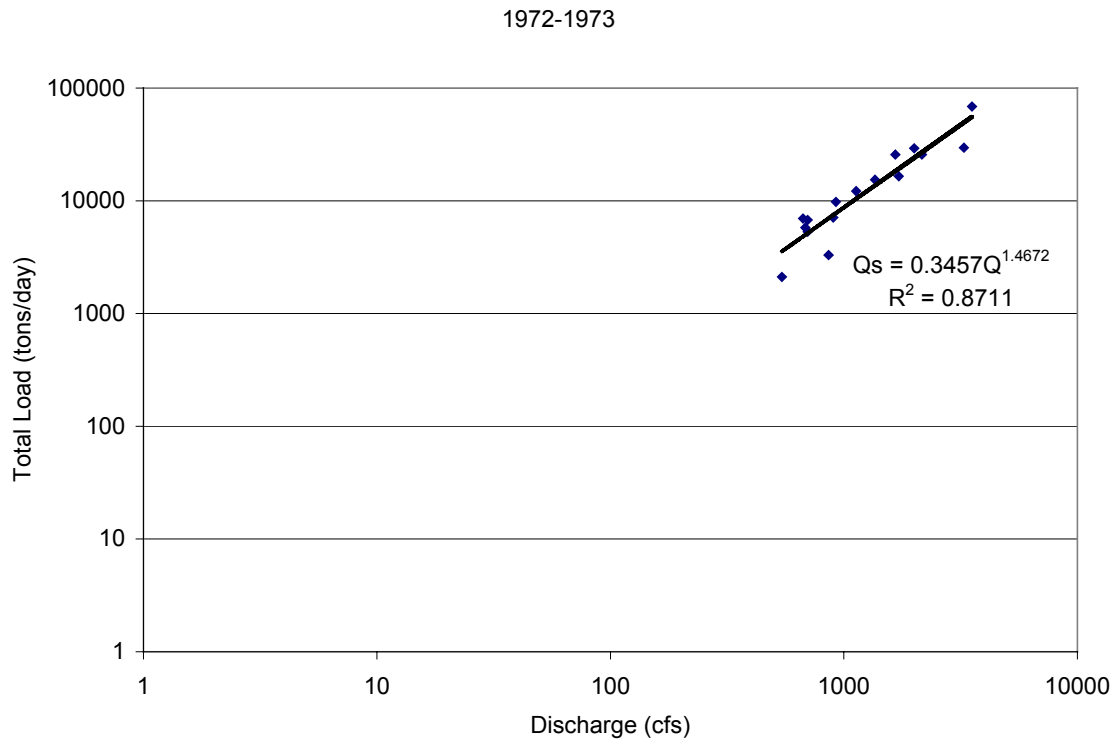
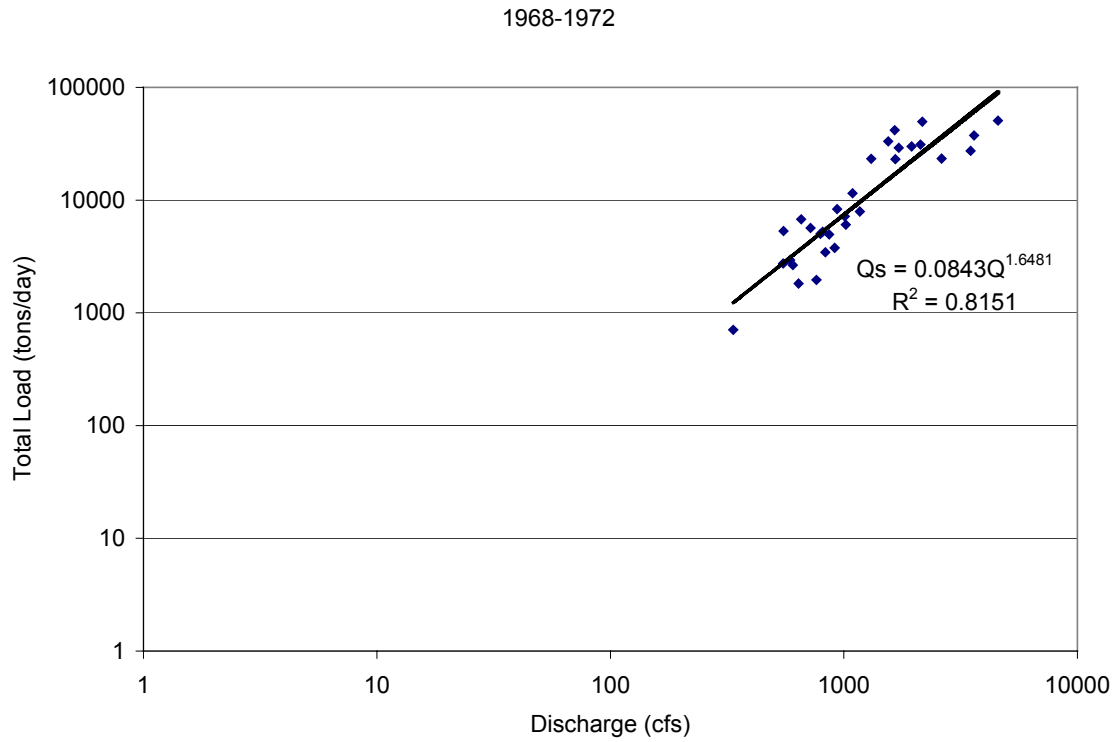


Figure J-1 Total load rating curves for the Albuquerque Gage 1968-1973.

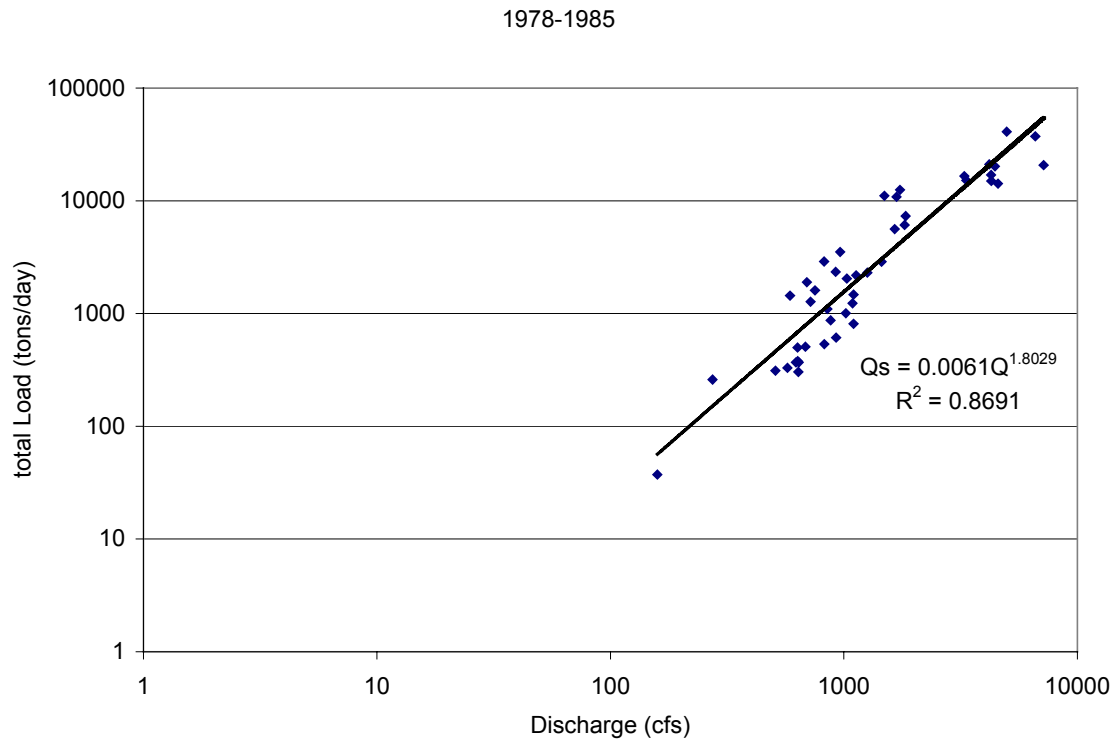
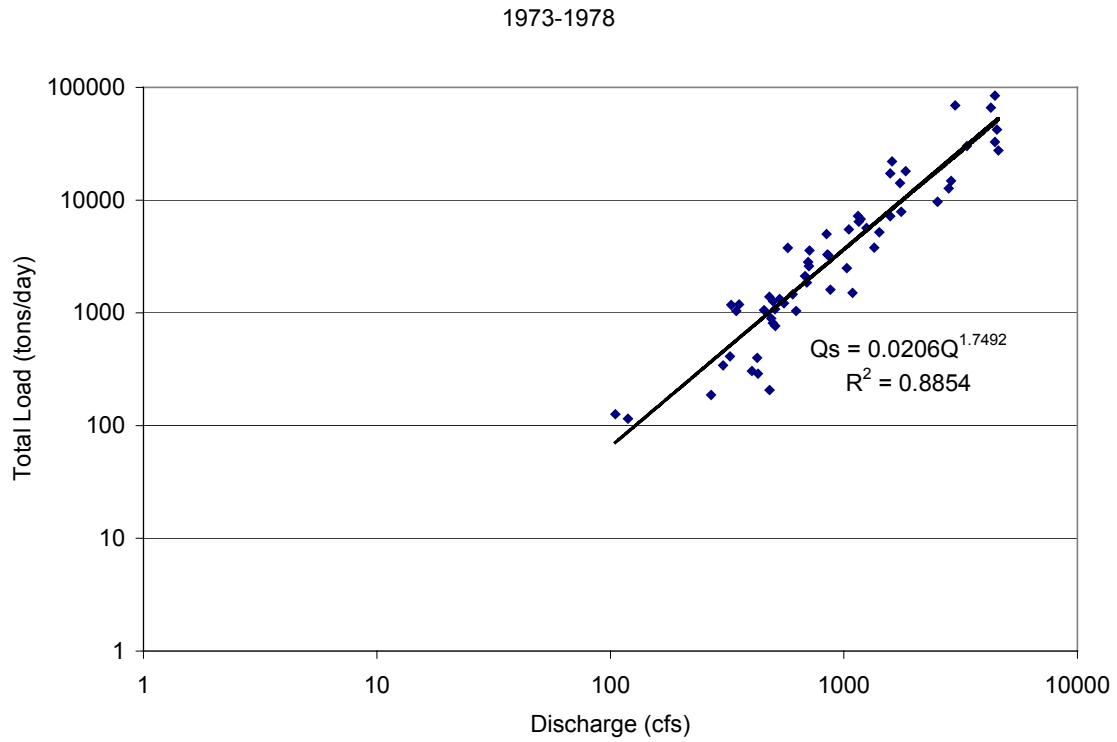


Figure J-2 Total load rating curves for the Albuquerque Gage 1973-1985.

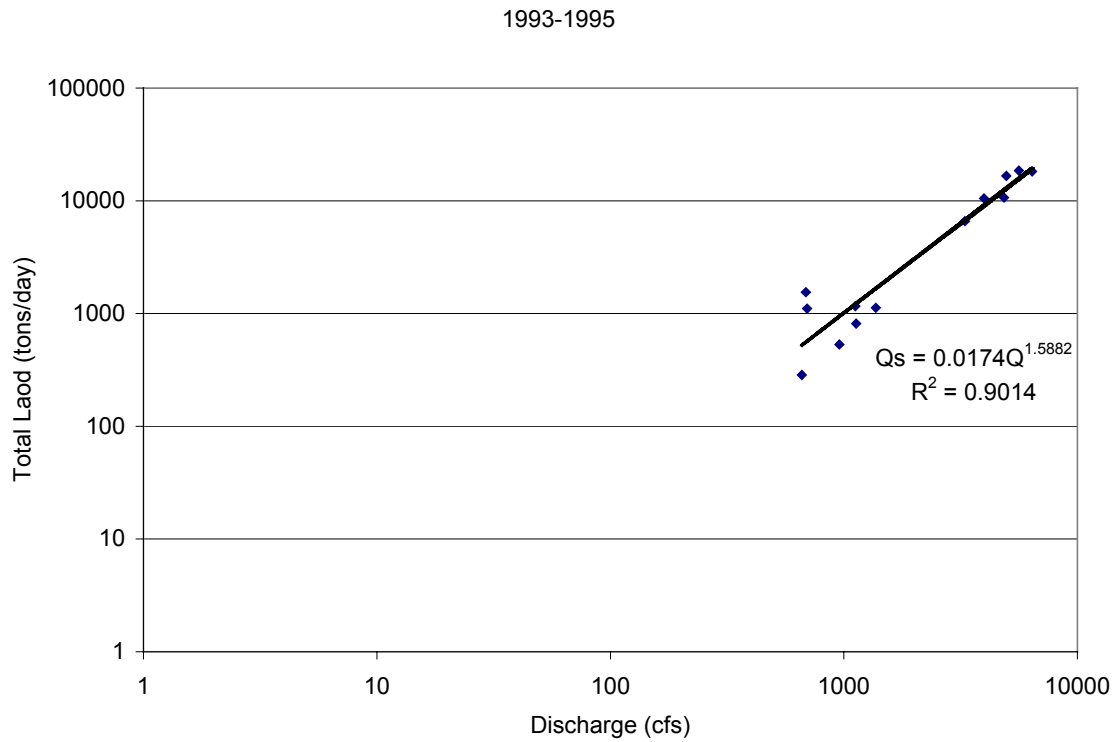
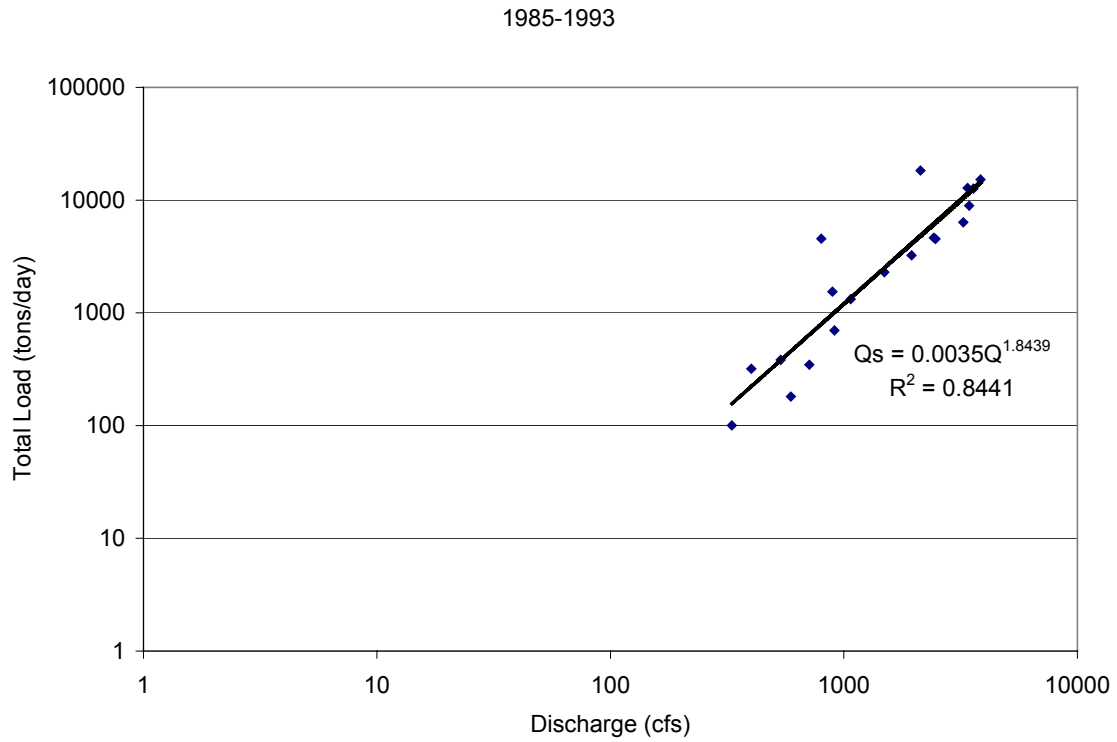


Figure J-3 Total load rating curves for the Albuquerque Gage 1985-1995.

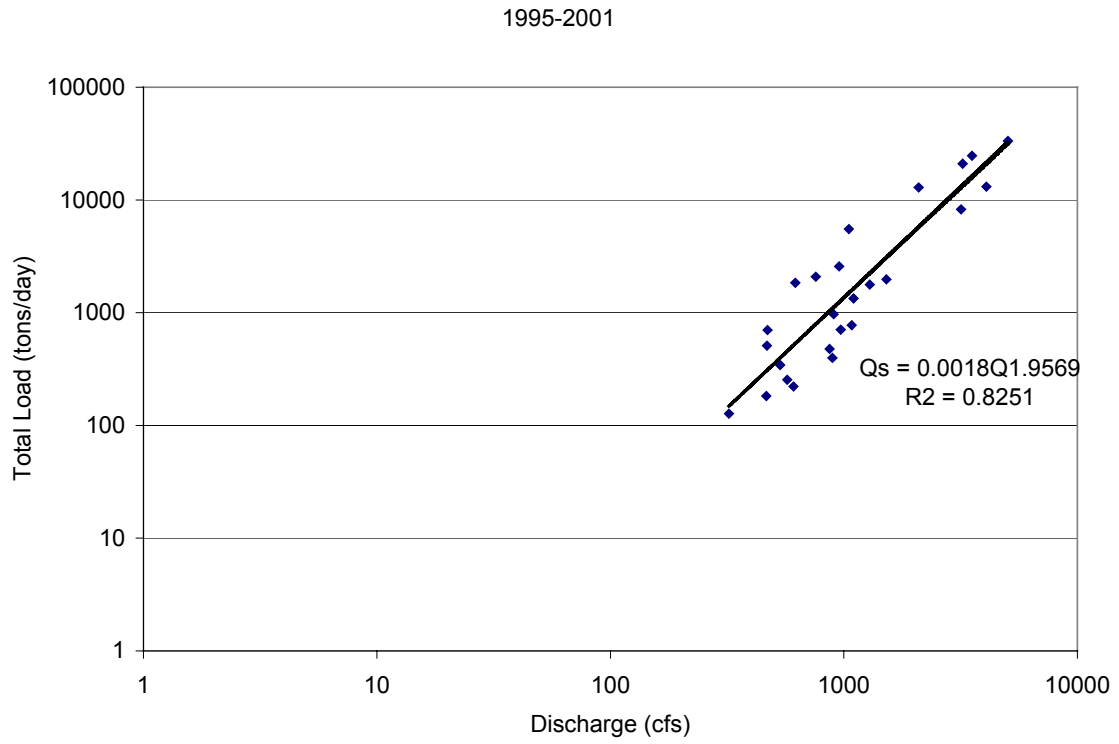


Figure J-4 Total load rating curves for the Albuquerque Gage 1995-2001.

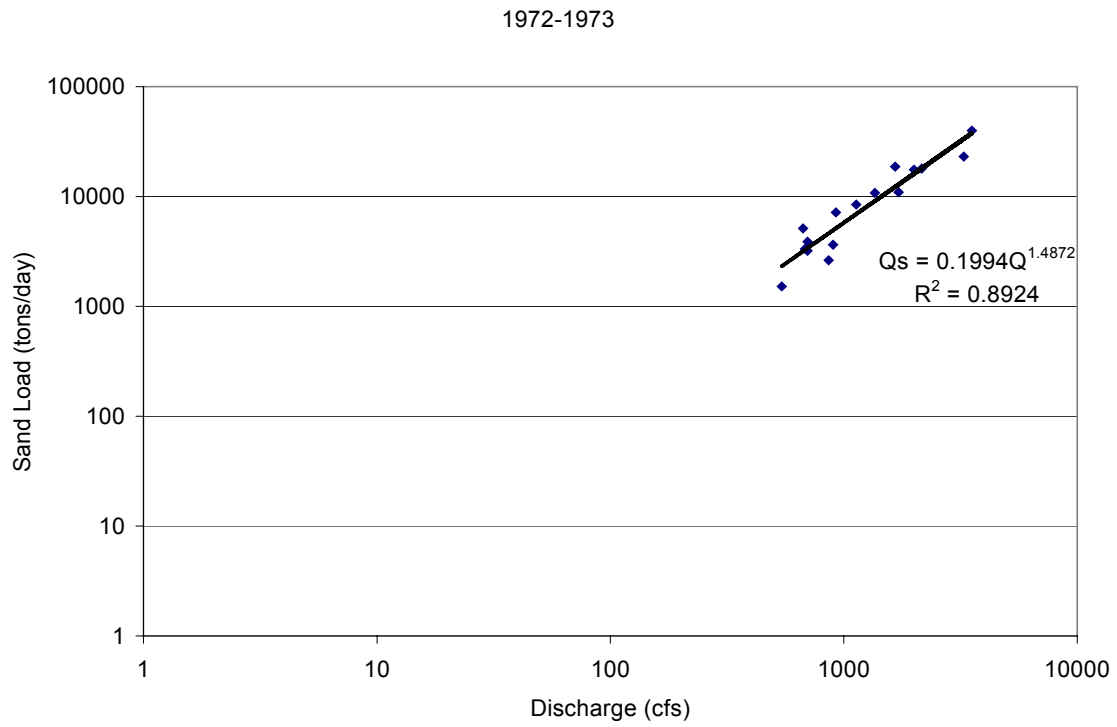
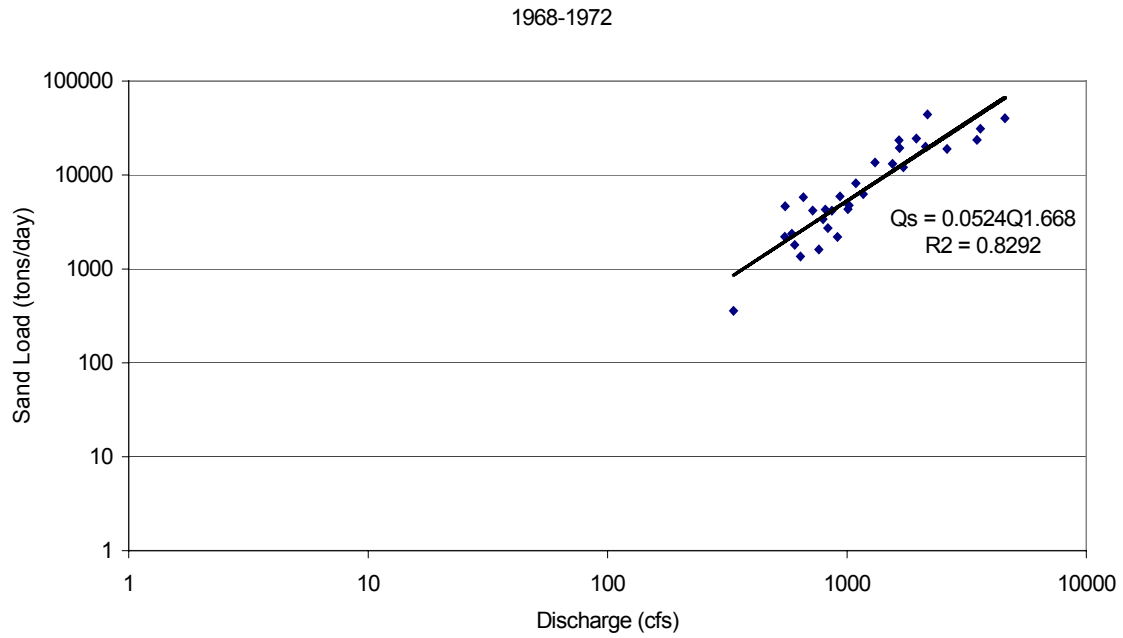


Figure J-5 Sand load rating curves for the Albuquerque Gage 1968-1973.

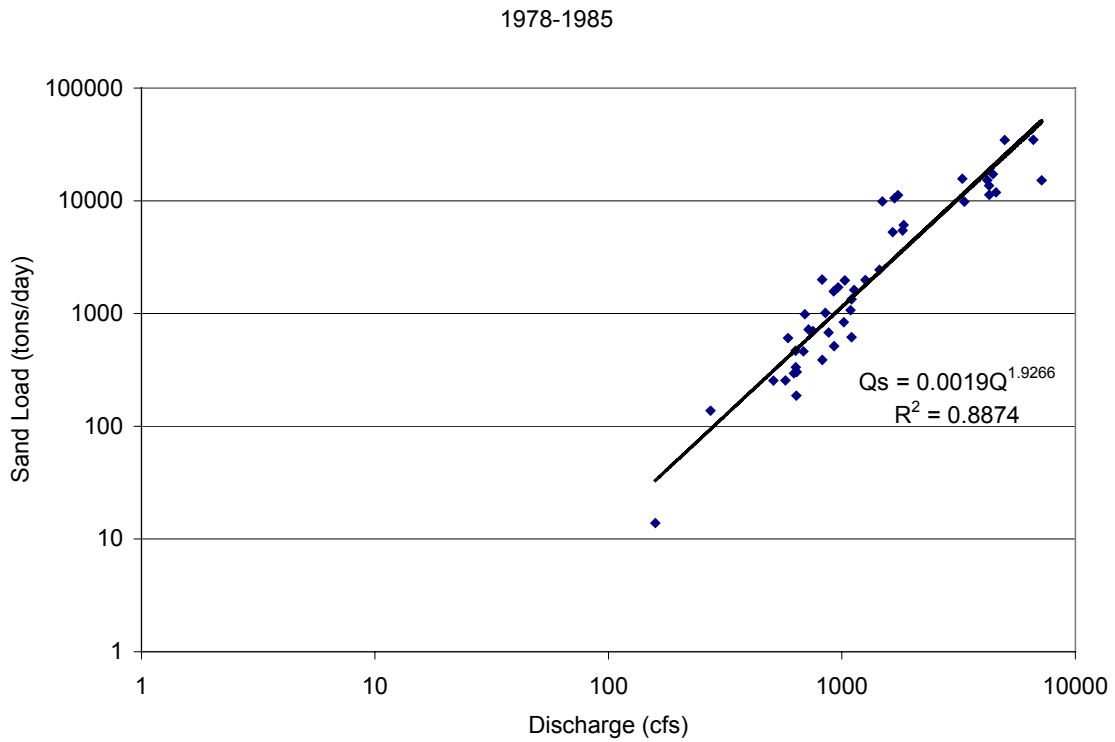
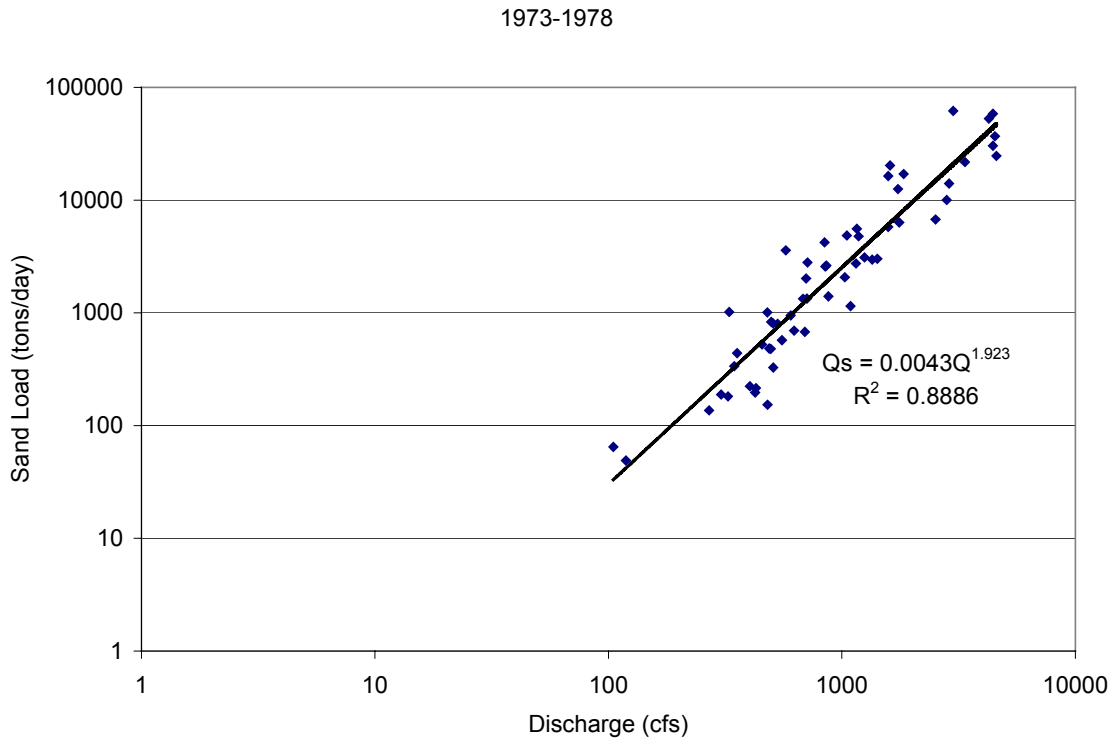


Figure J-6 Sand load rating curves for the Albuquerque Gage 1973-1985.

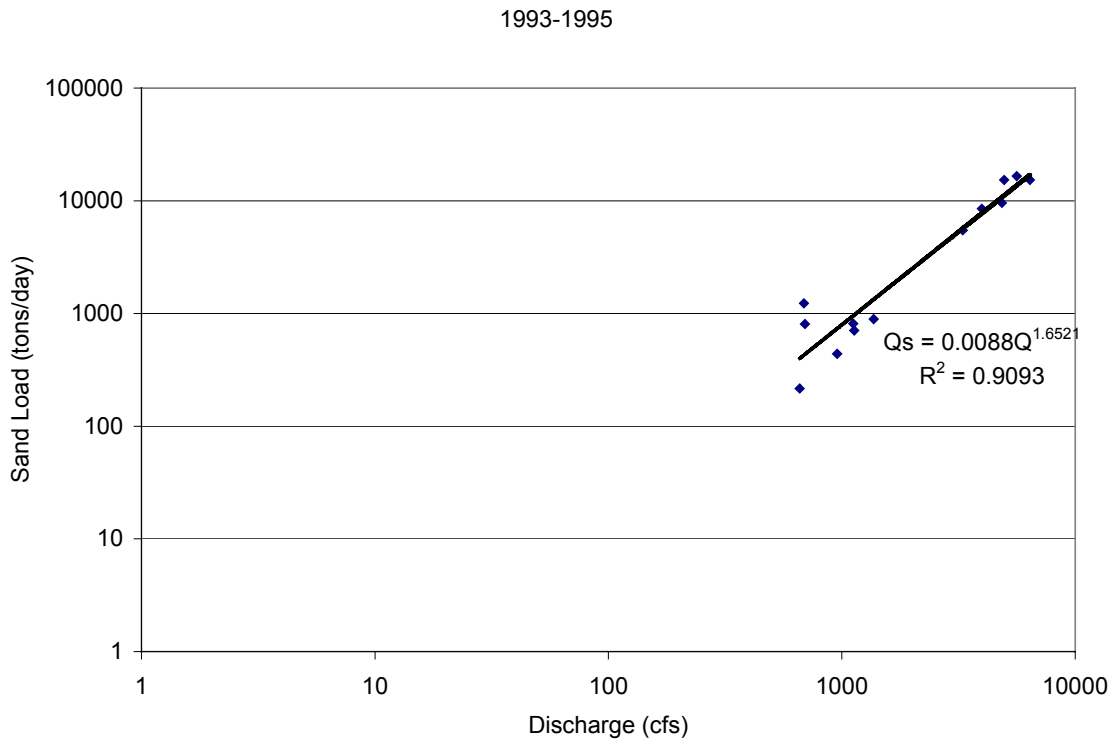
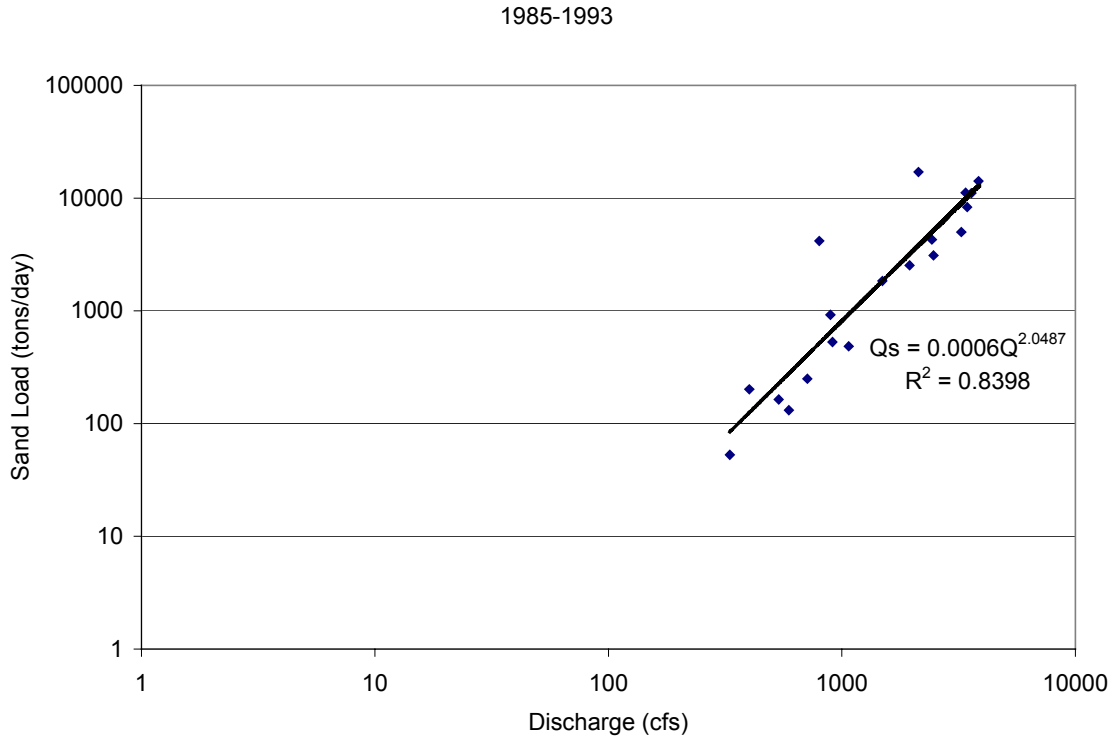


Figure J-7 Sand load rating curves for the Albuquerque Gage 1985-1995.

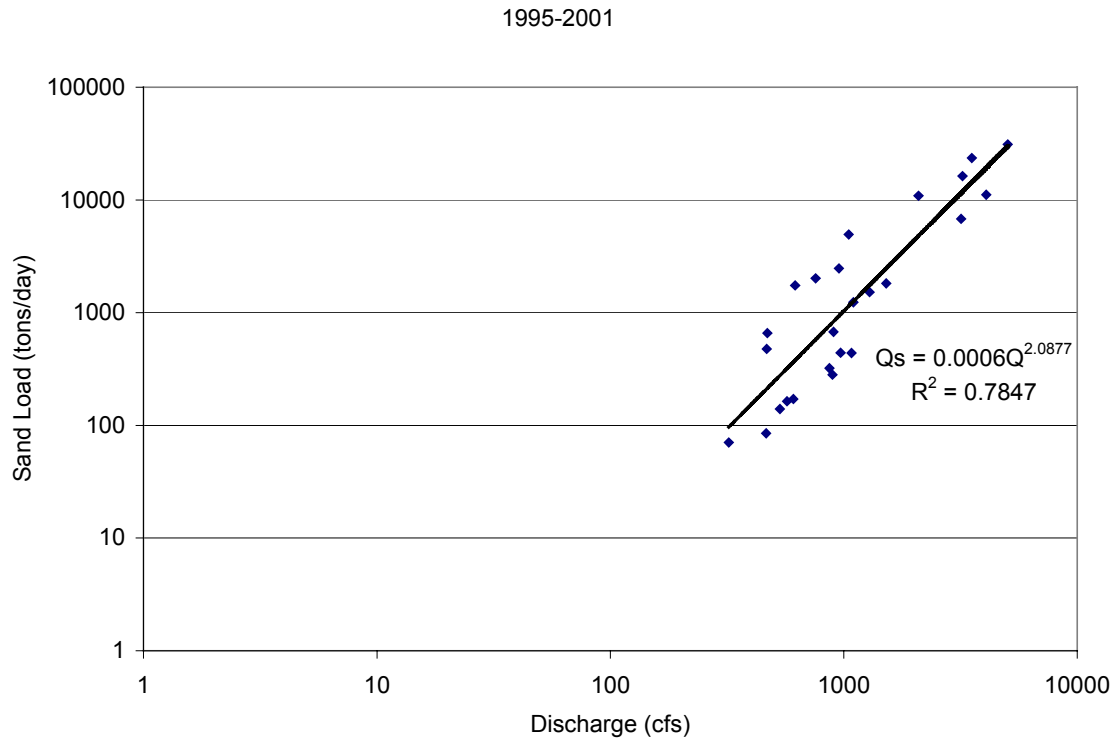


Figure J-8 Sand load rating curves for the Albuquerque Gage 1995-2001.

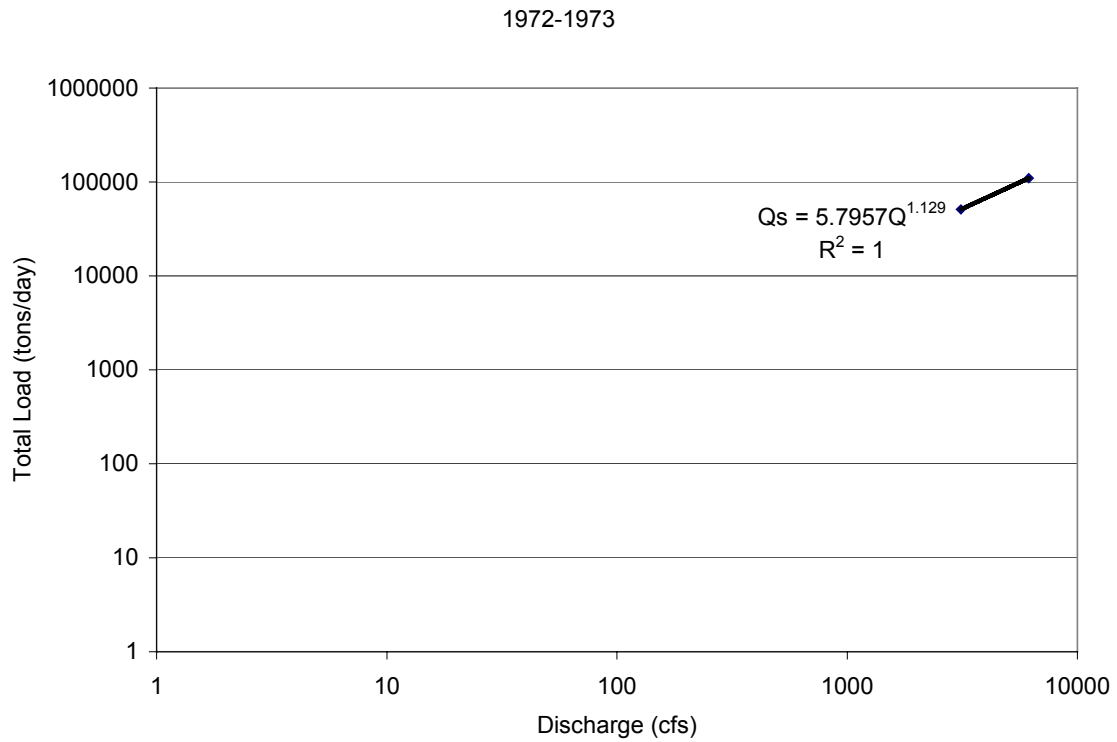
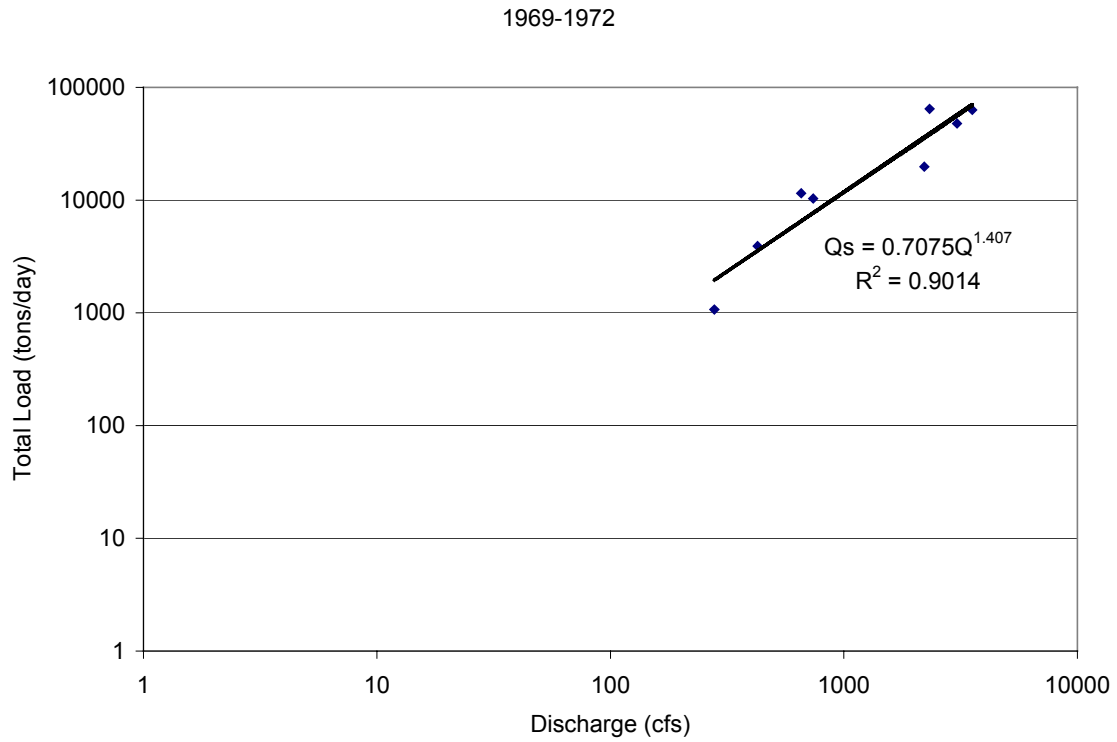


Figure J-9 Total load rating curves for the Bernardo Gage 1968-1973.

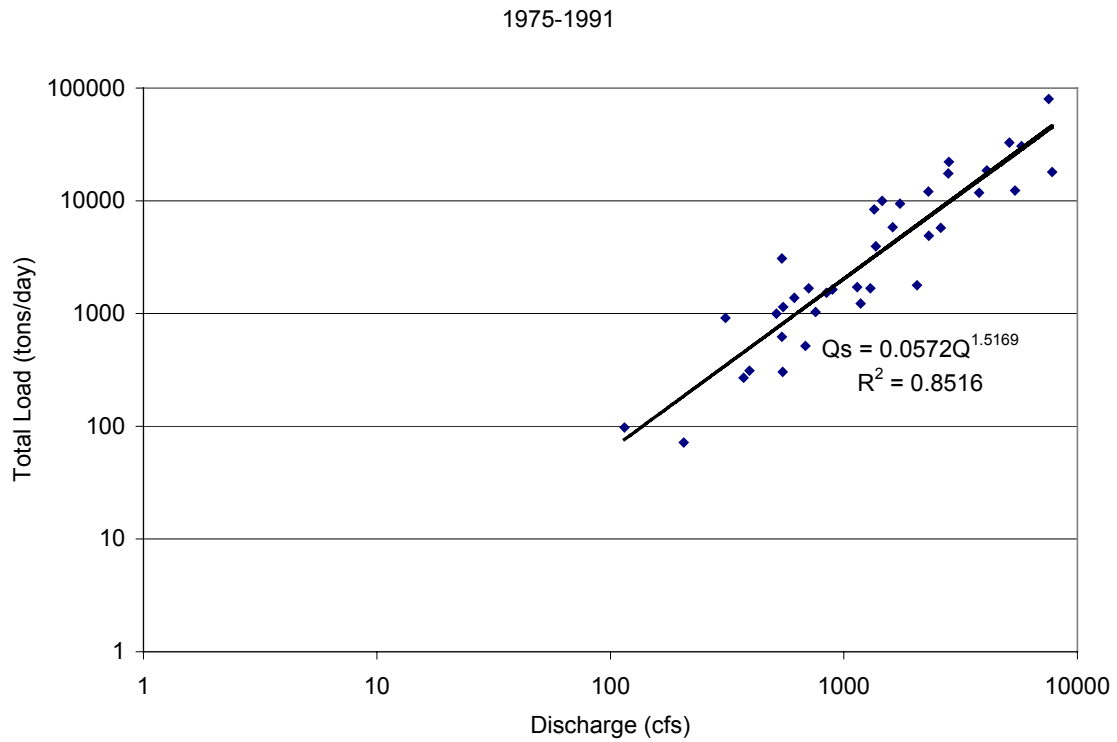
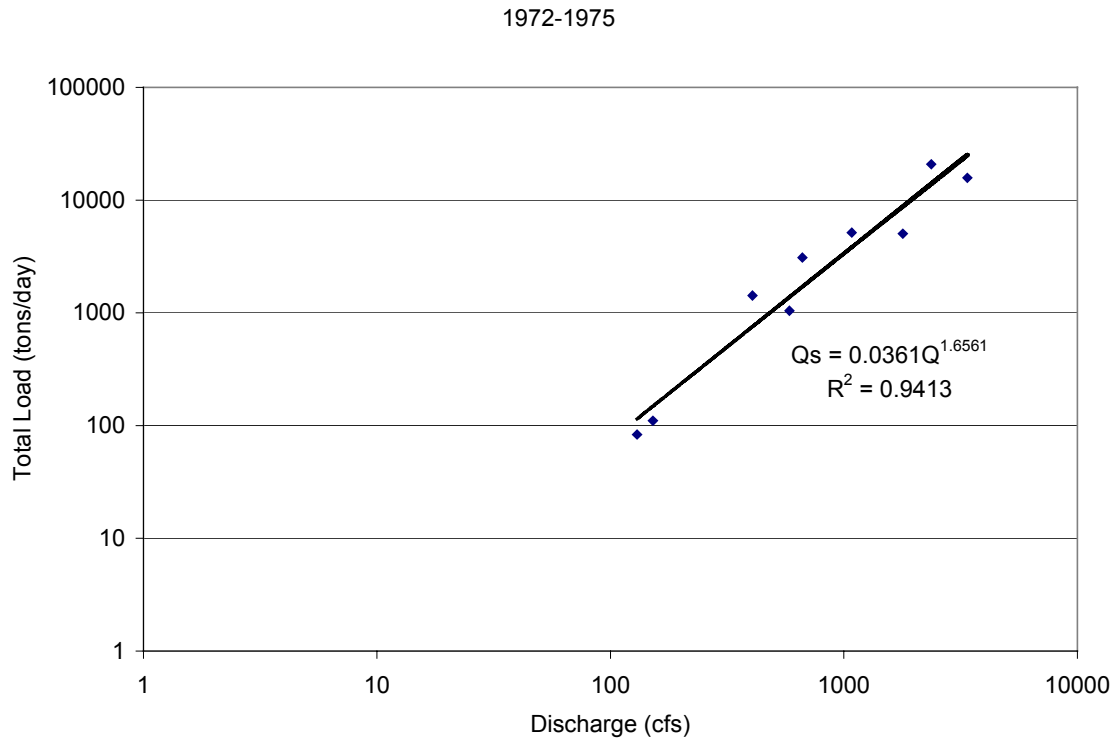


Figure J-10 Total load rating curves for the Bernardo Gage 1973-1991.

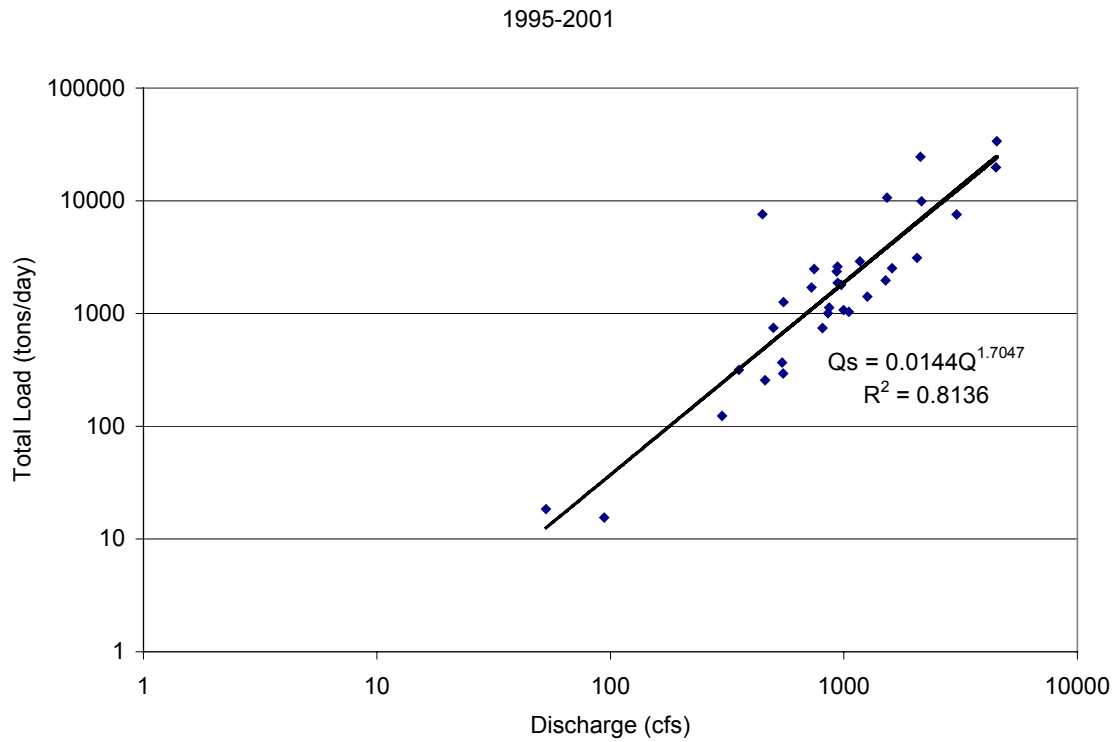
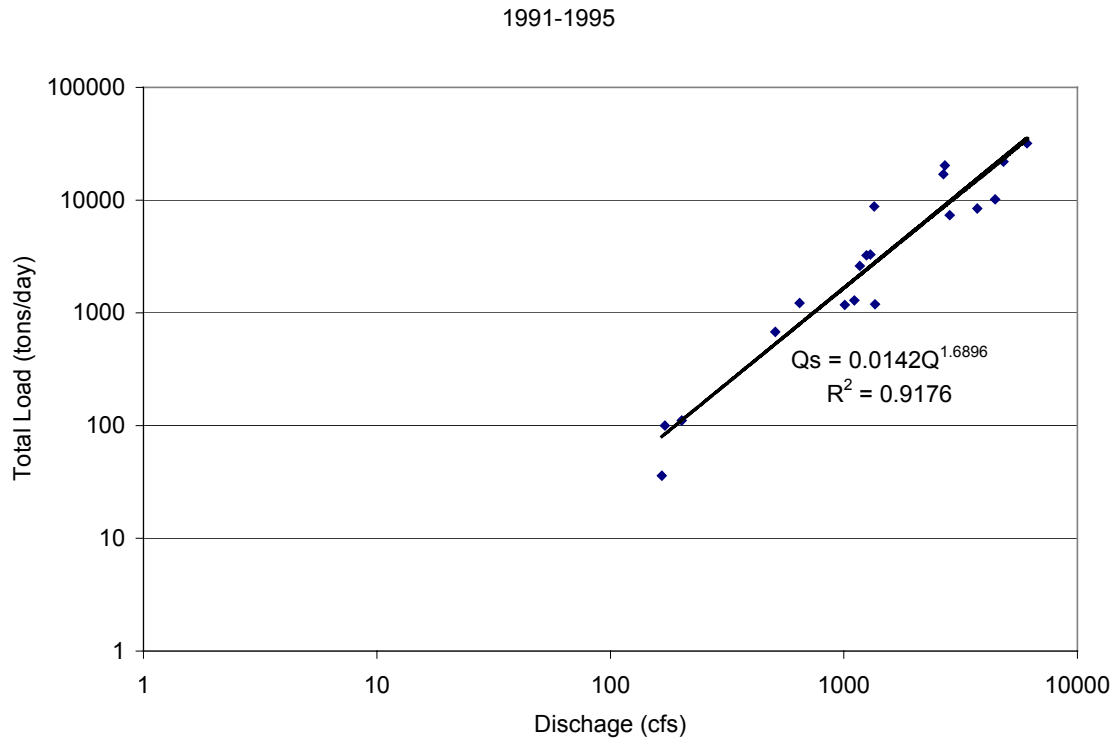


Figure J-11 Total load rating curves for the Bernardo Gage 1991-2001.

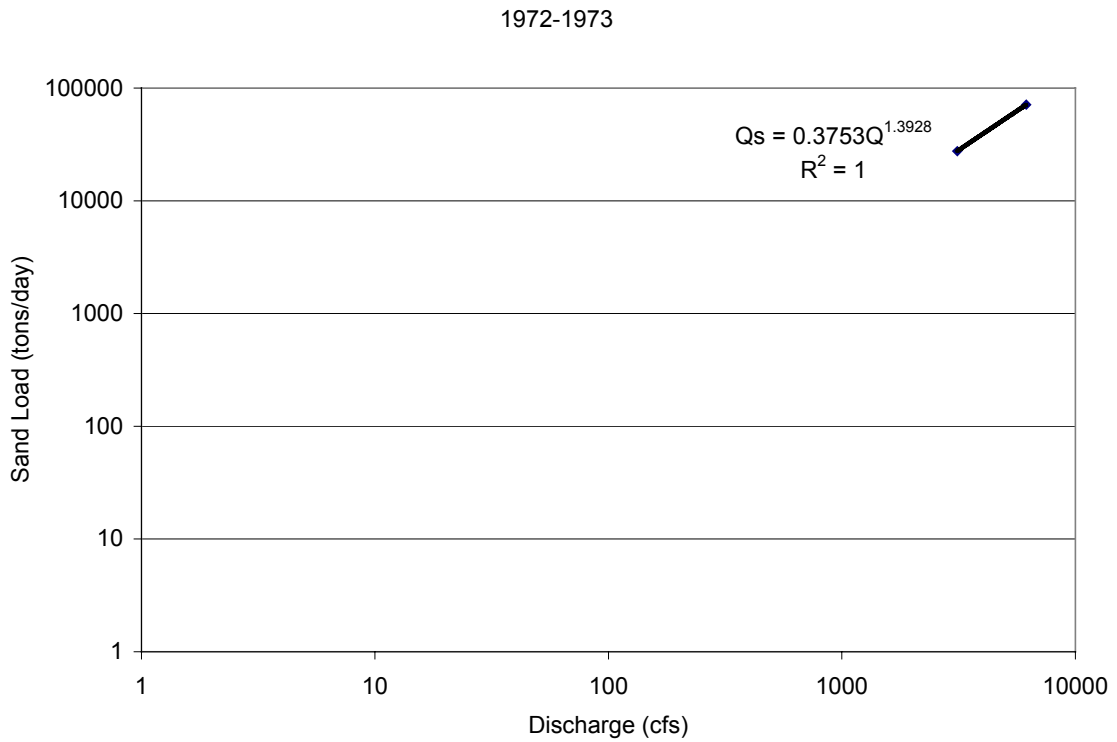
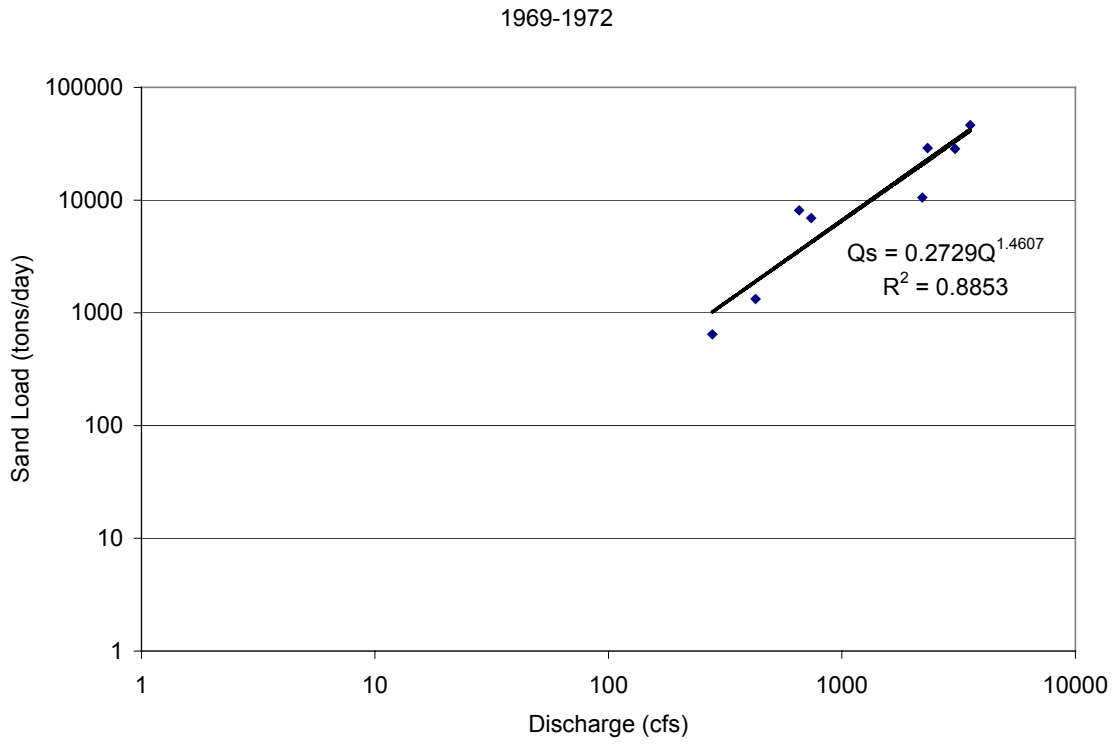


Figure J-12 Sand load rating curves for the Bernardo Gage 1968-1973.

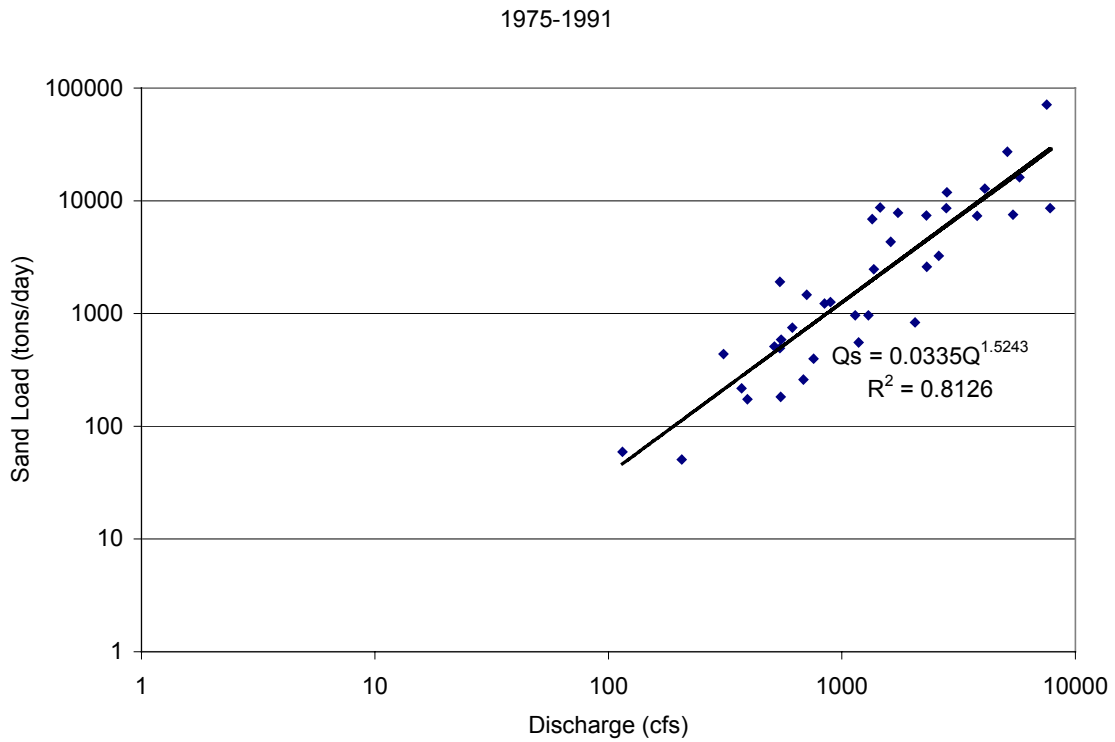
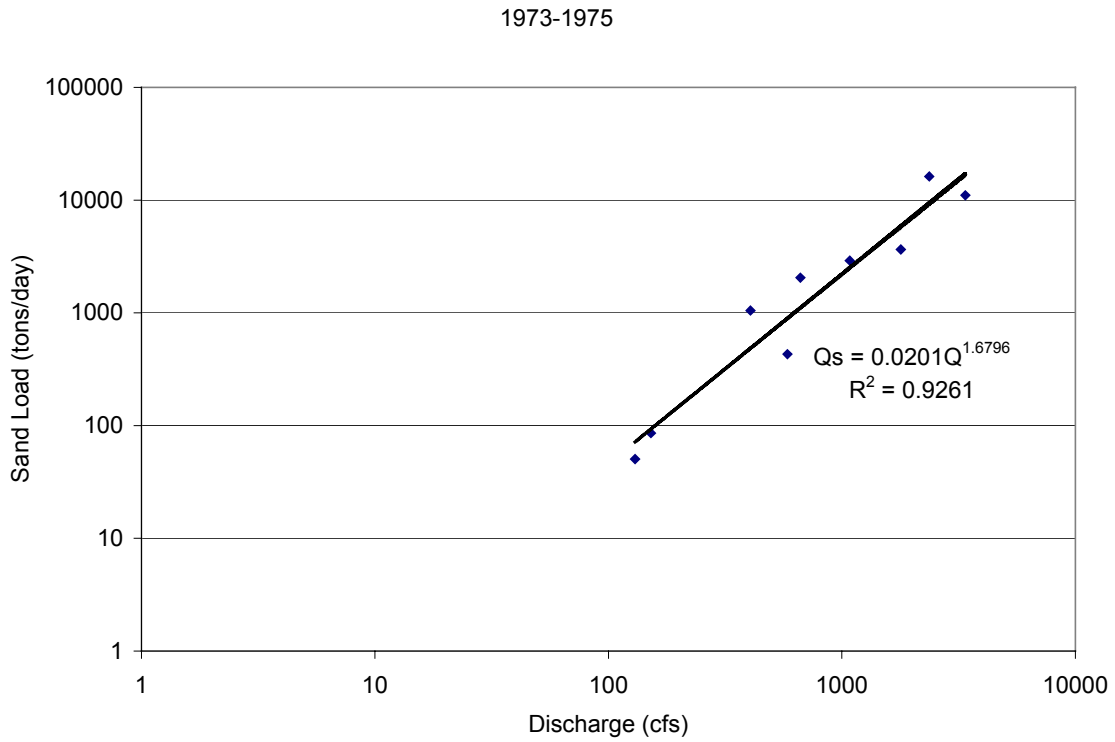


Figure J-13 Sand load rating curves for the Bernardo Gage 1973-1991.

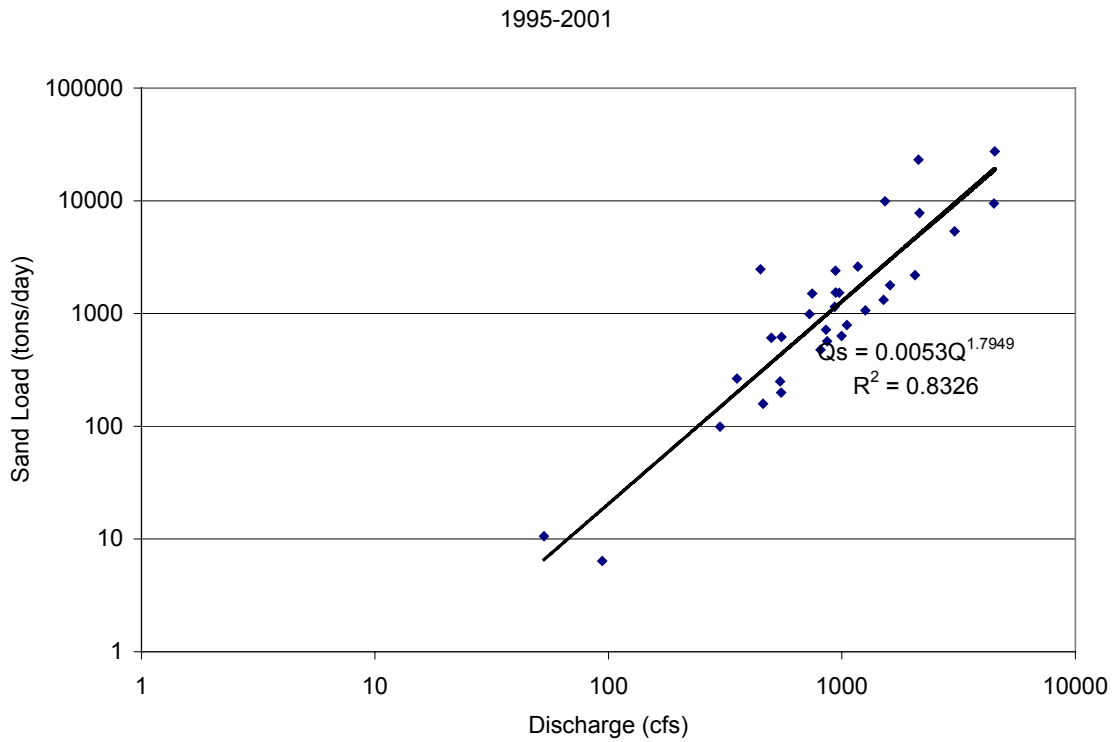
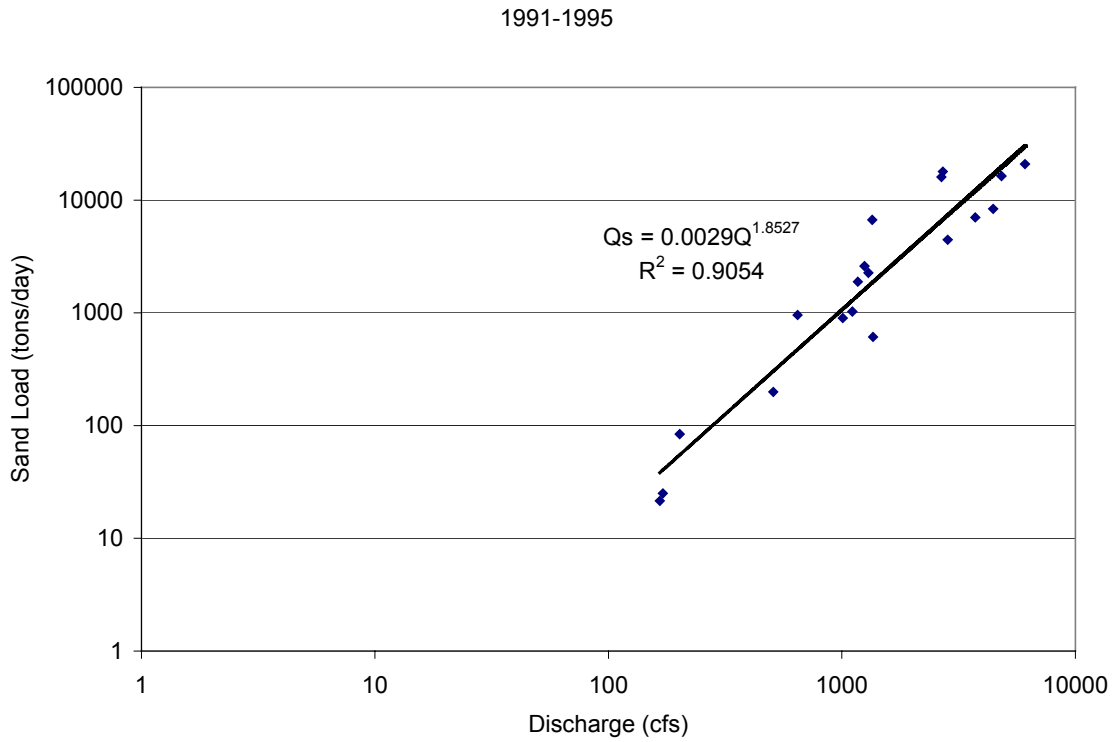


Figure J-14 Sand load rating curves for the Bernardo Gage 1991-2001.

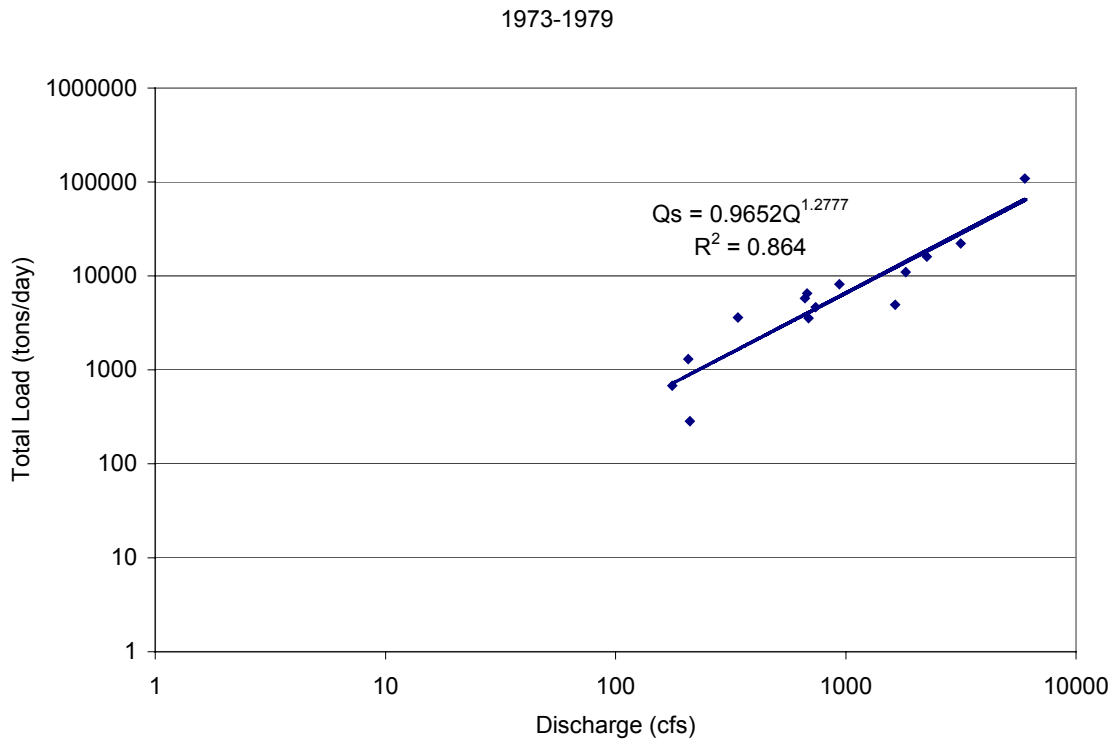
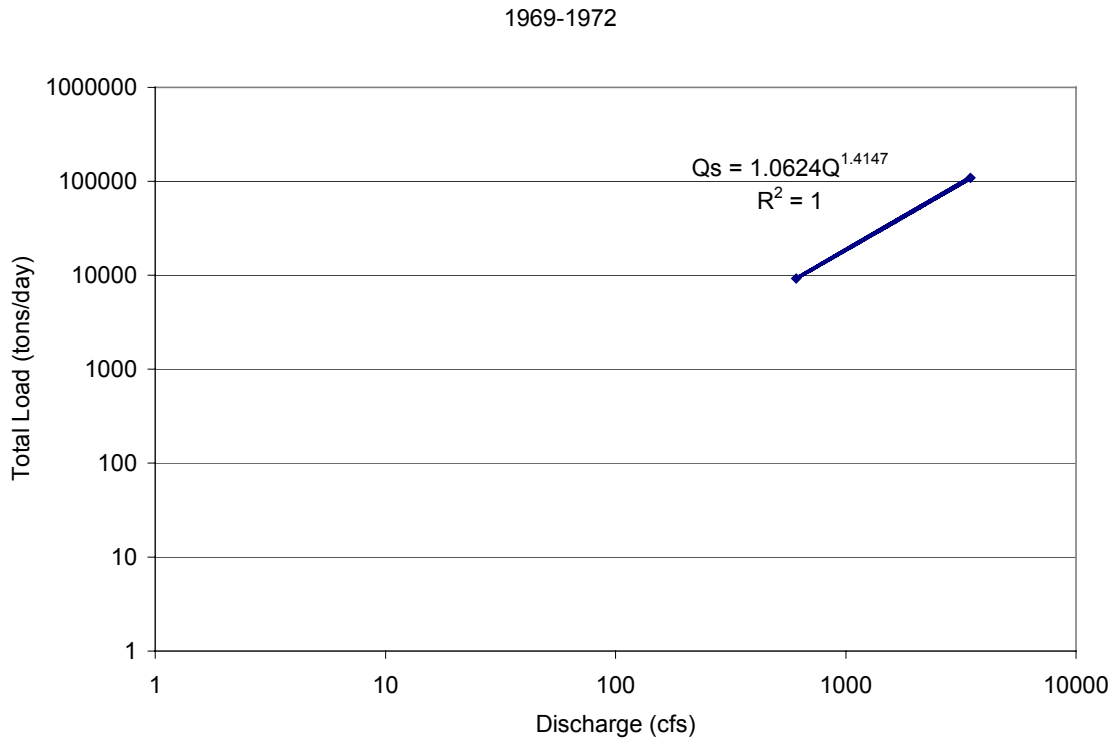


Figure J-15 Total load rating curves for the San Acacia Gage 1969-1979.

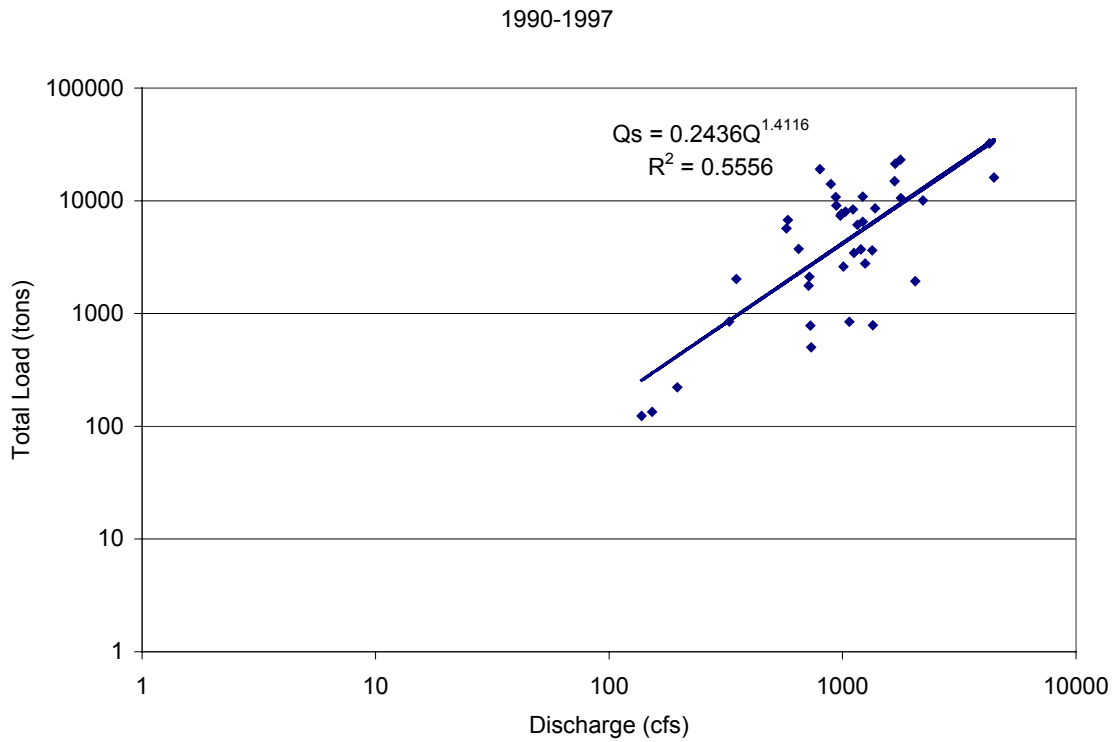
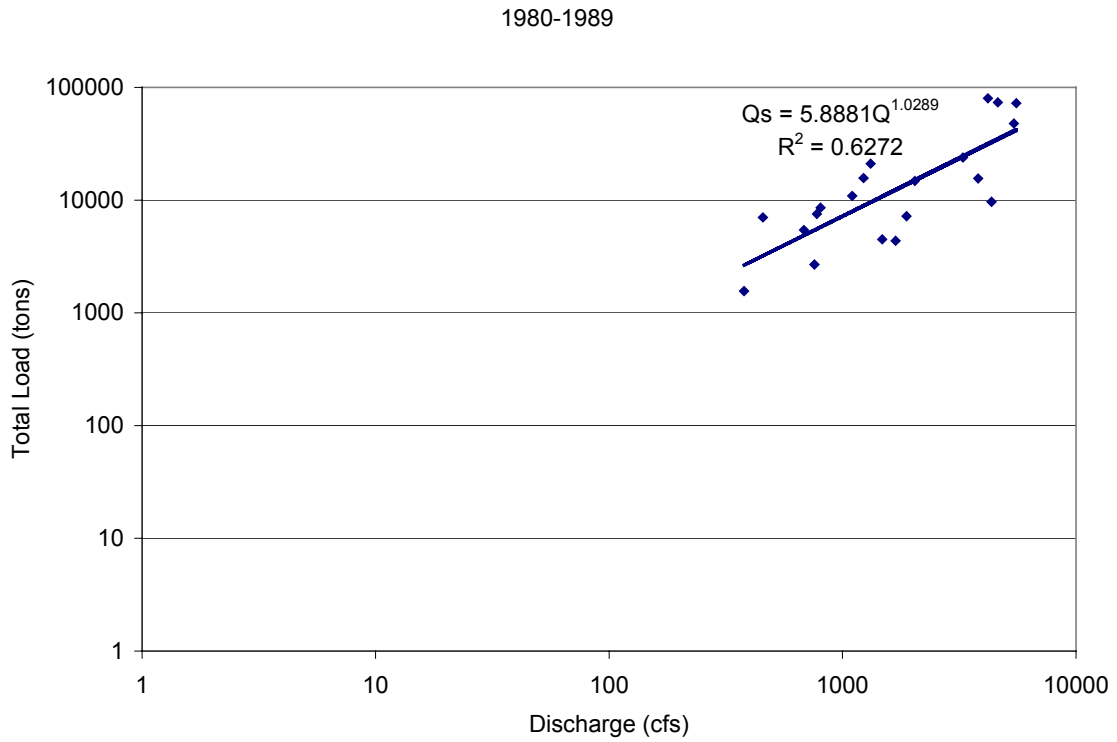


Figure J-16 Total load rating curves for the San Acacia Gage 1979-1997.

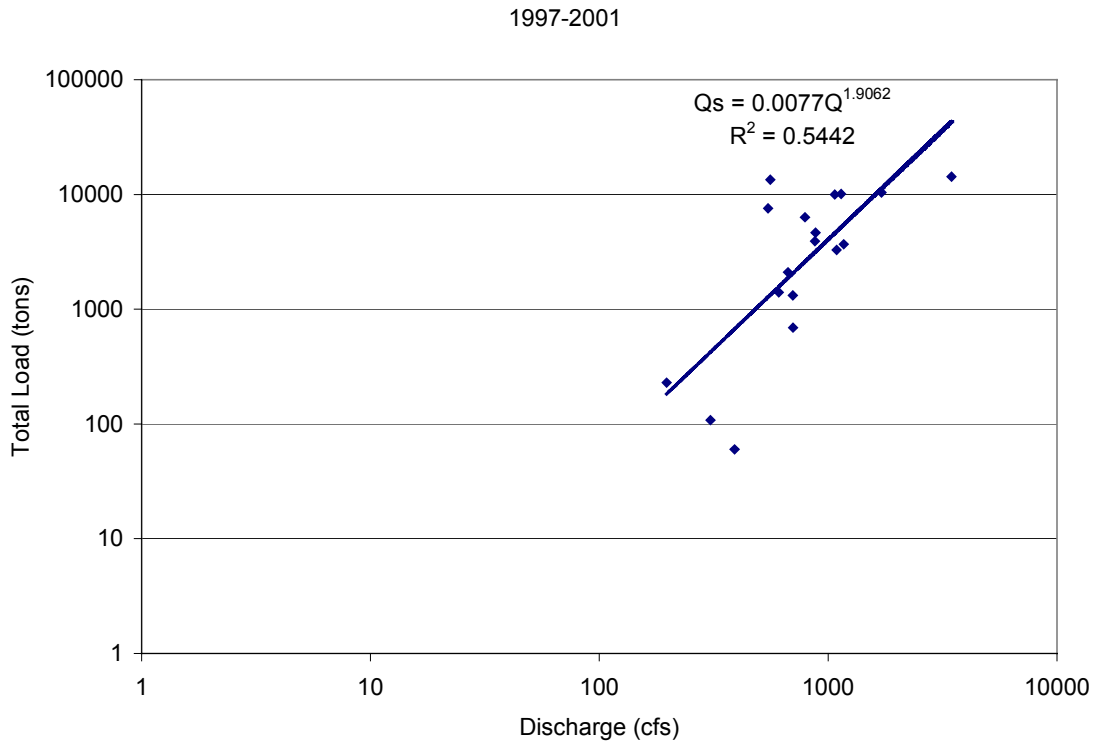


Figure J-17 Total load rating curves for the San Acacia Gage 1997-2001.

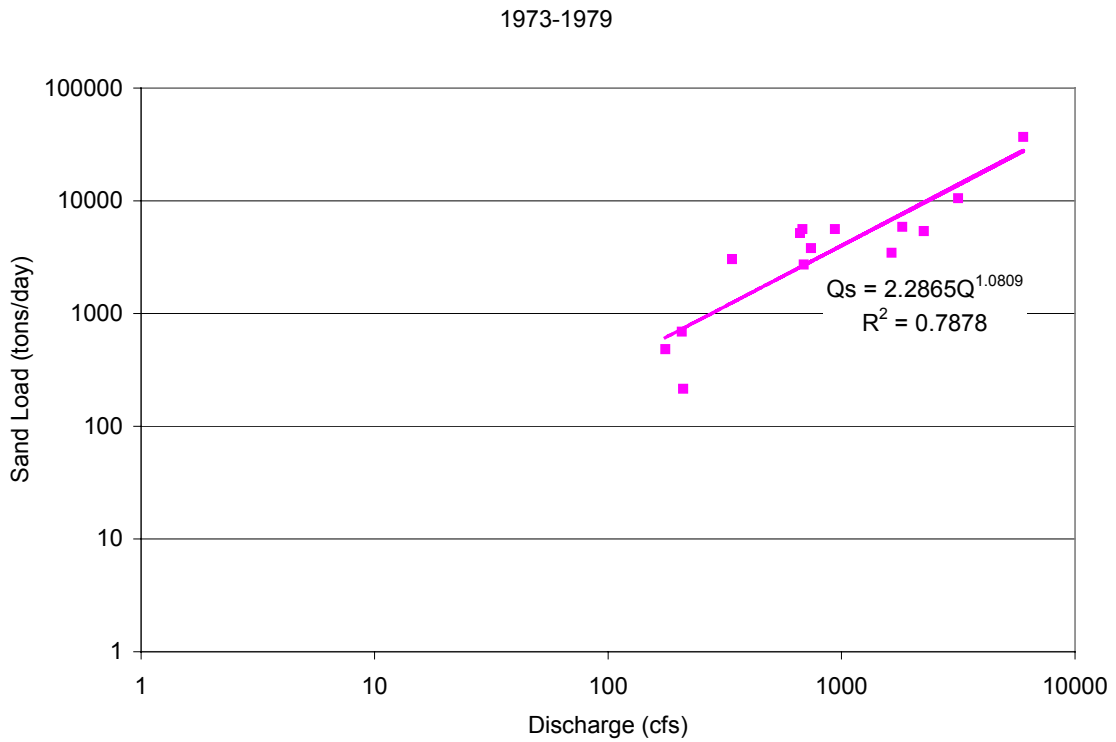
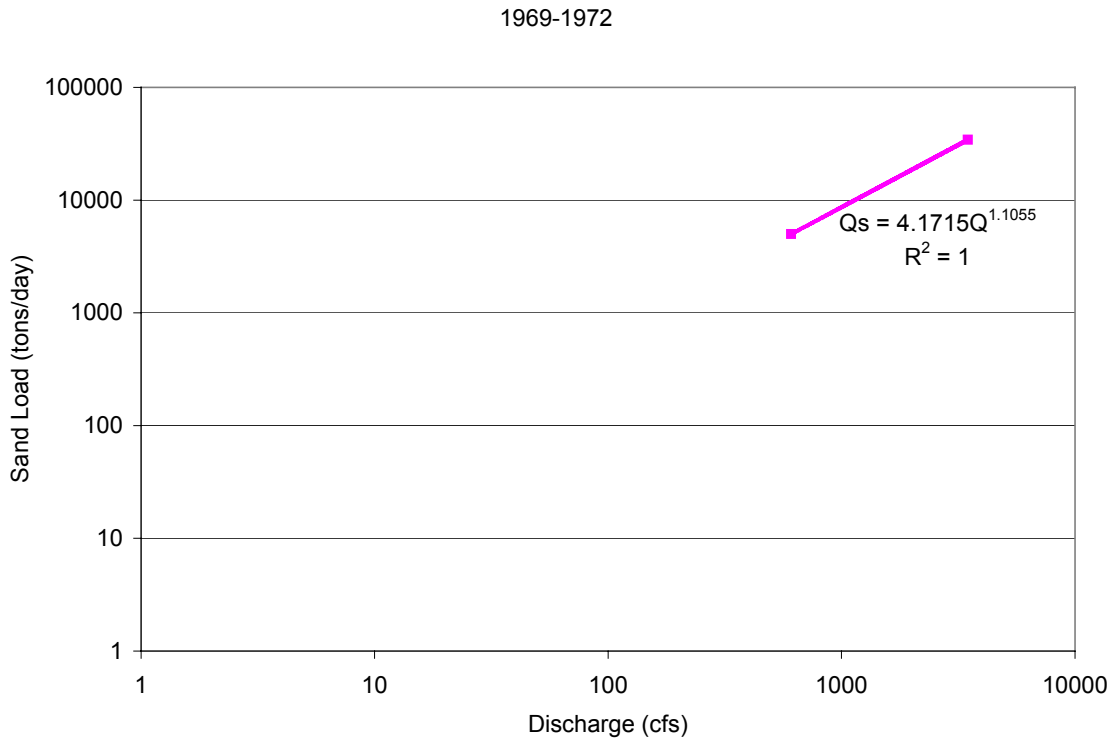


Figure J-18 Sand load rating curves for the San Acacia Gage 1969-1979.

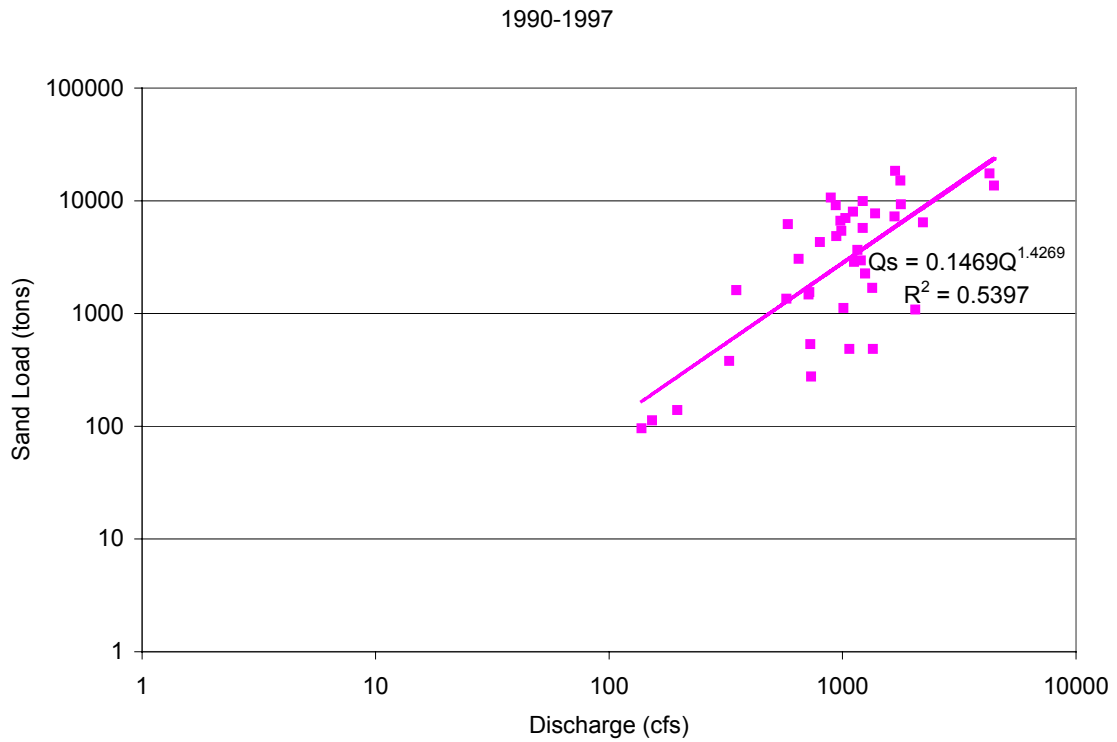
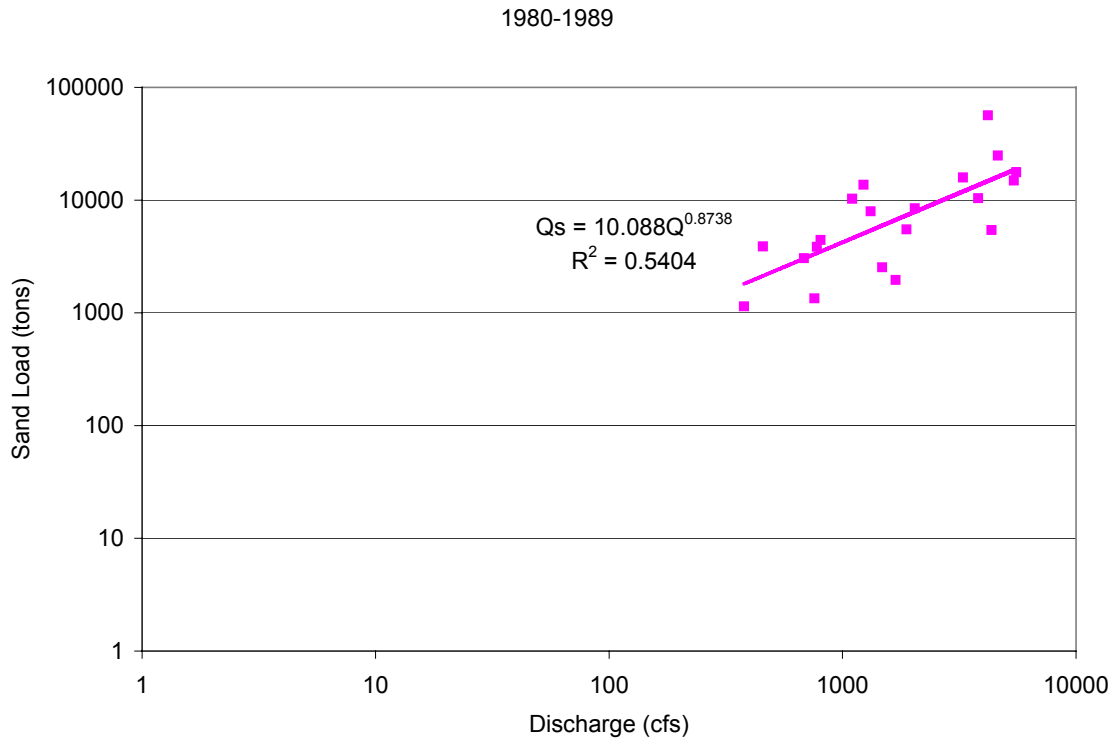


Figure J-19 Sand load rating curves for the San Acacia Gage 1979-1997.

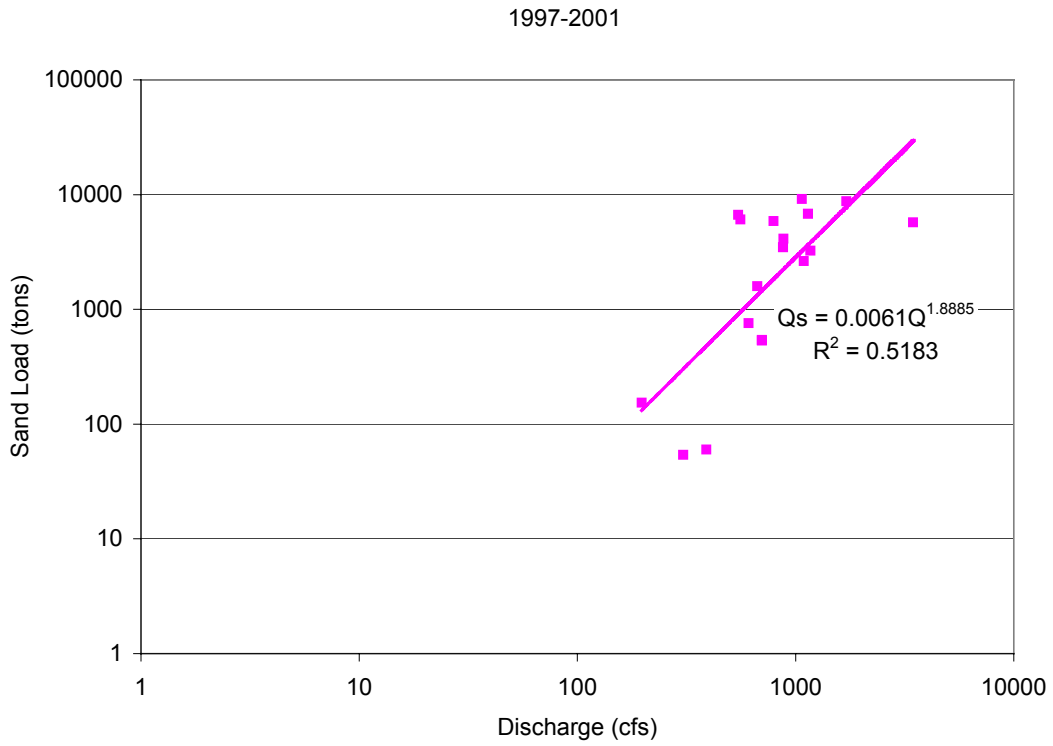
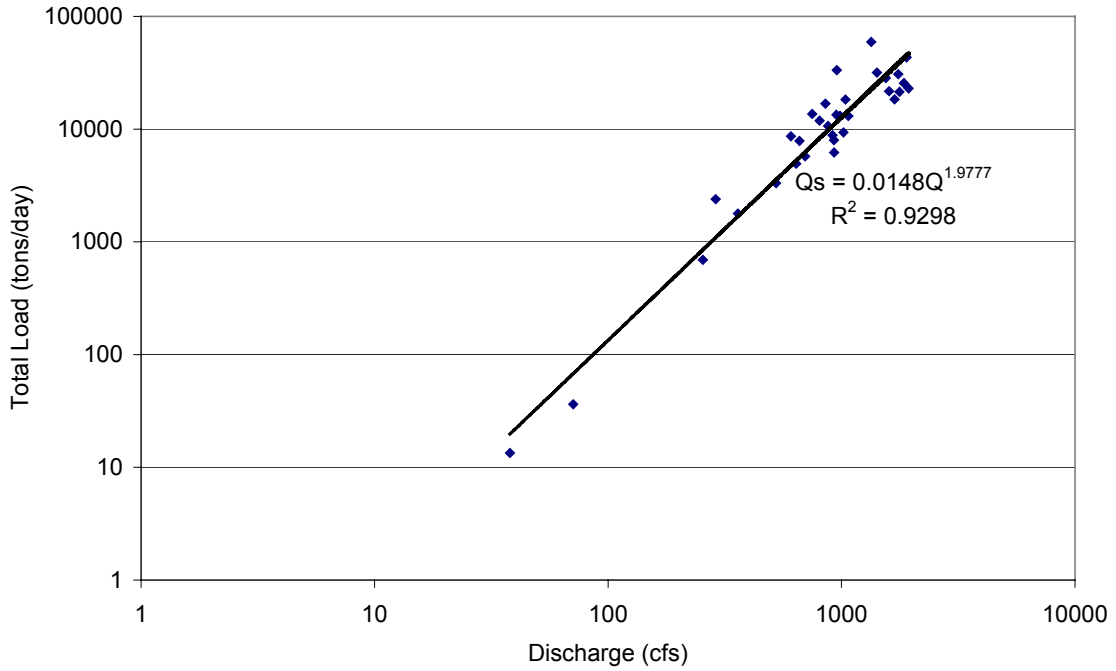


Figure J-20 Sand load rating curves for the San Acacia Gage 1997-2001.

FW+CC 1968-1973



FW+CC 1973-1982

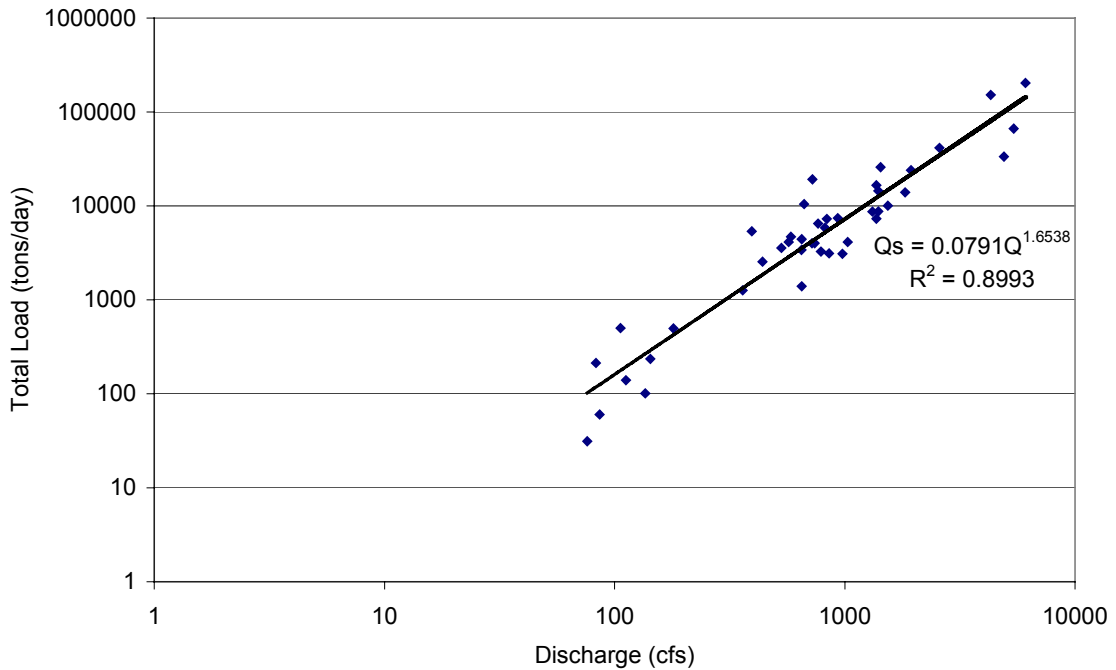
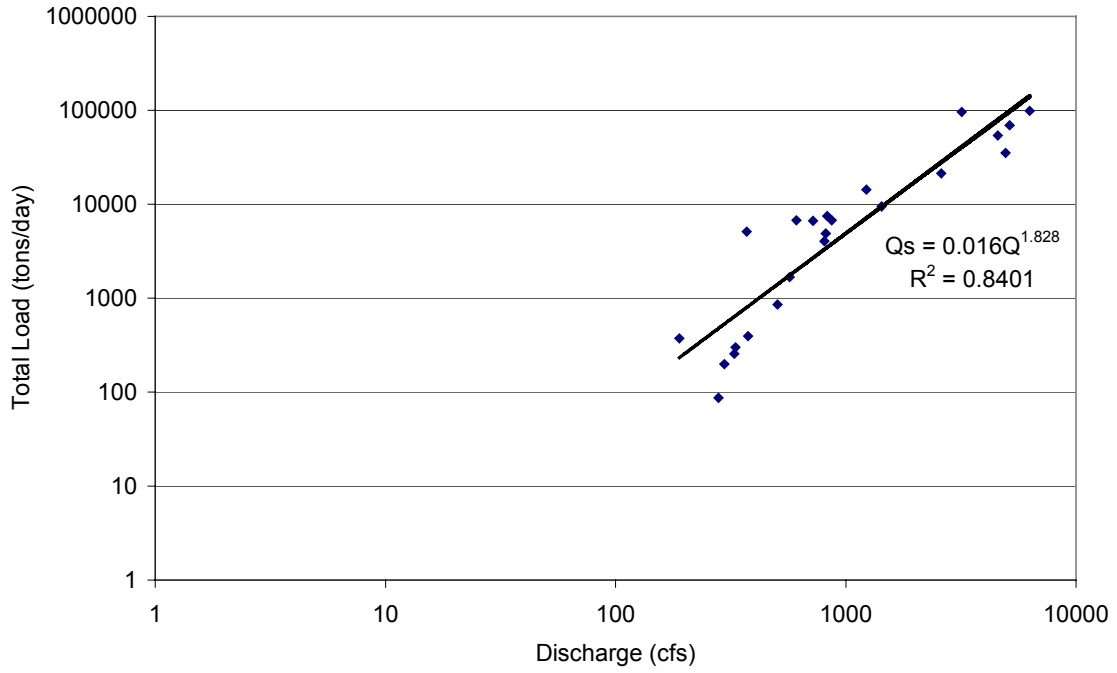


Figure J-21 Total load rating curves for the San Marcial Gage 1968-1982

FW+CC 1982-1992



FW+CC 1992-1997

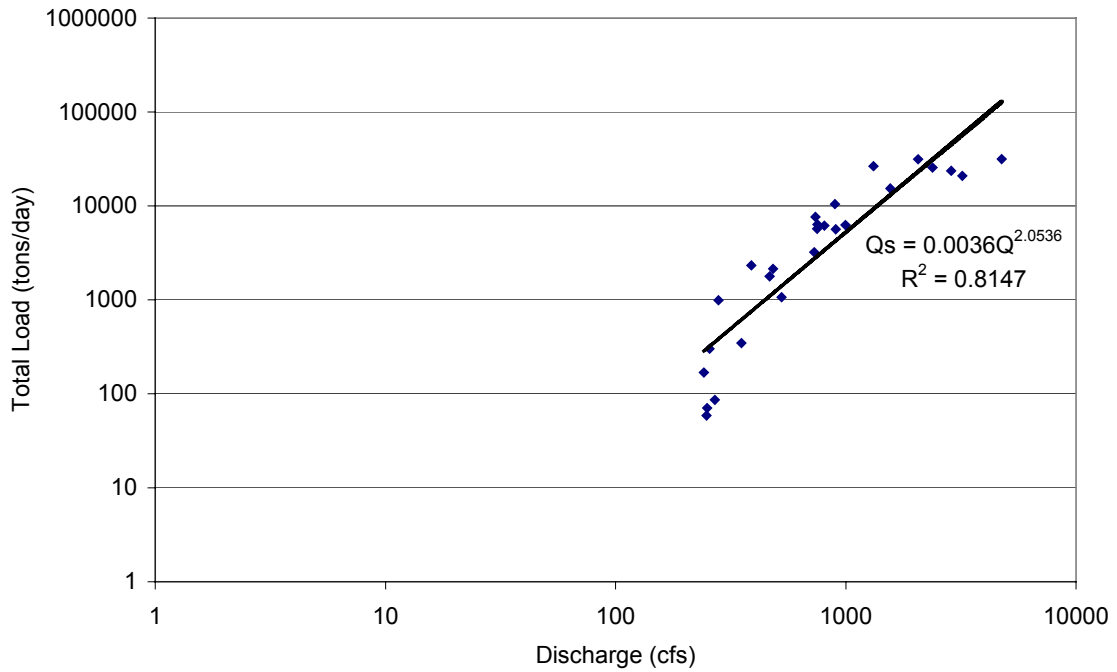


Figure J-22 Total load rating curves for the San Marcial Gage 1982-1997

FW+CC 1997-2001

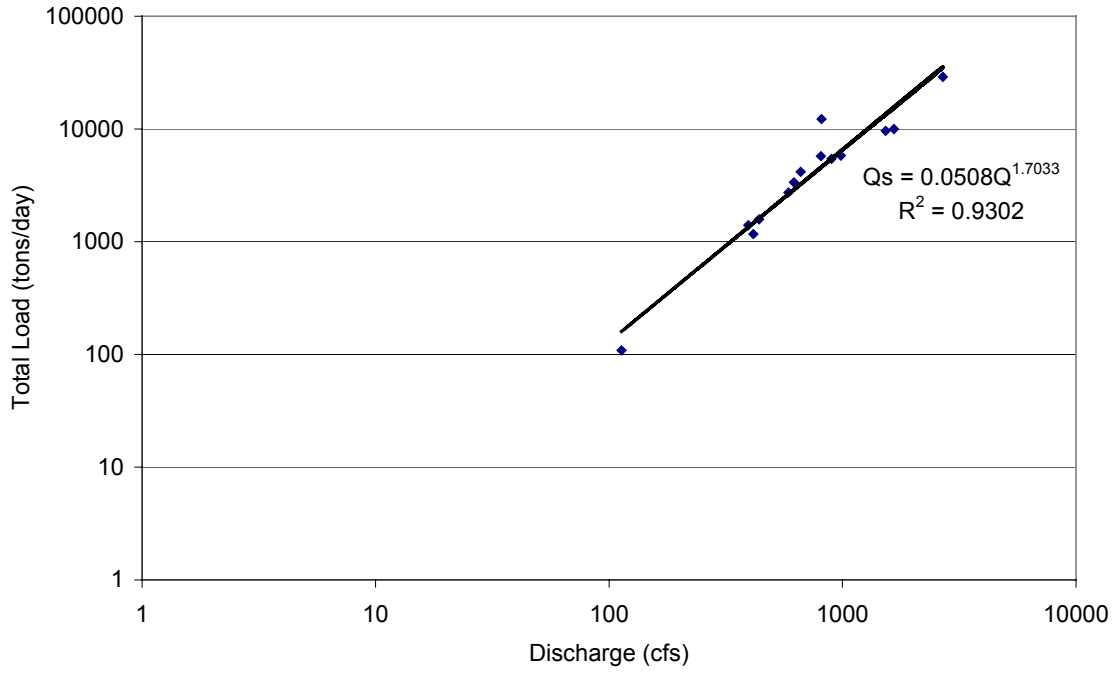
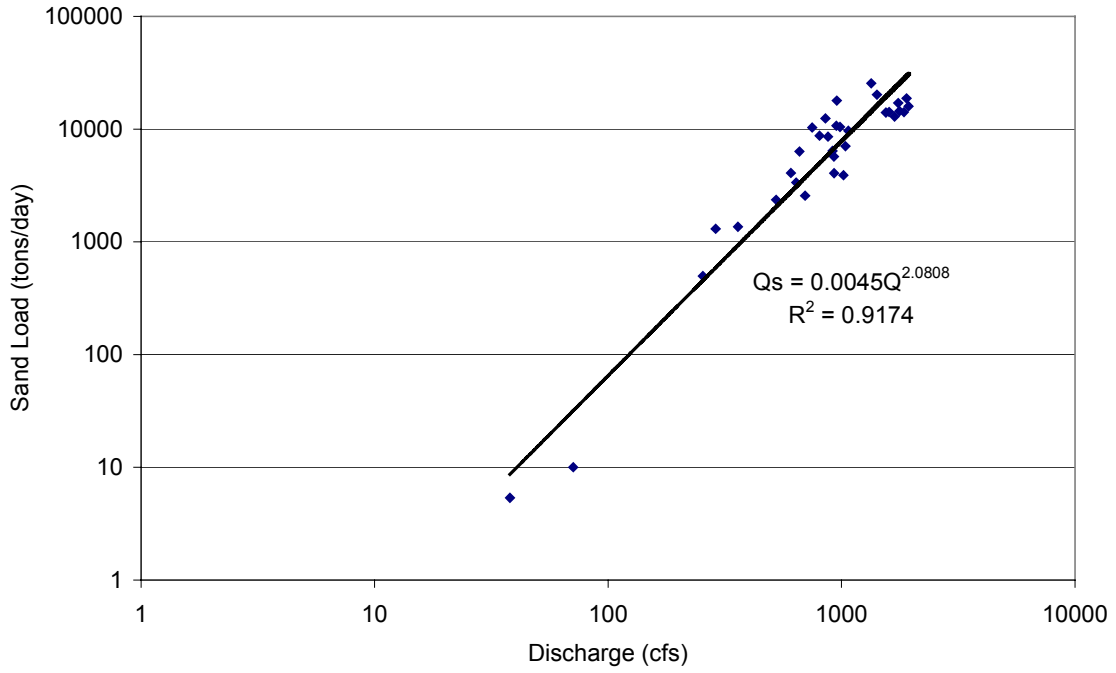


Figure J-23 Total load rating curves for the San Marcial Gage 1997-2001

FW+CC 1968-1973



FW+CC 1973-1982

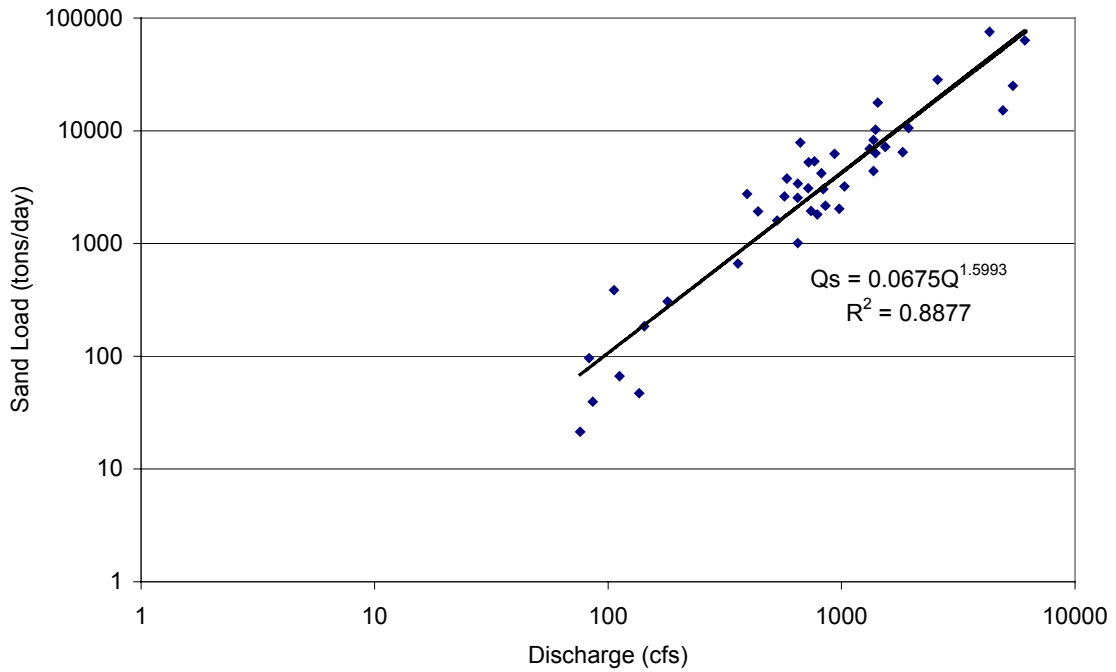
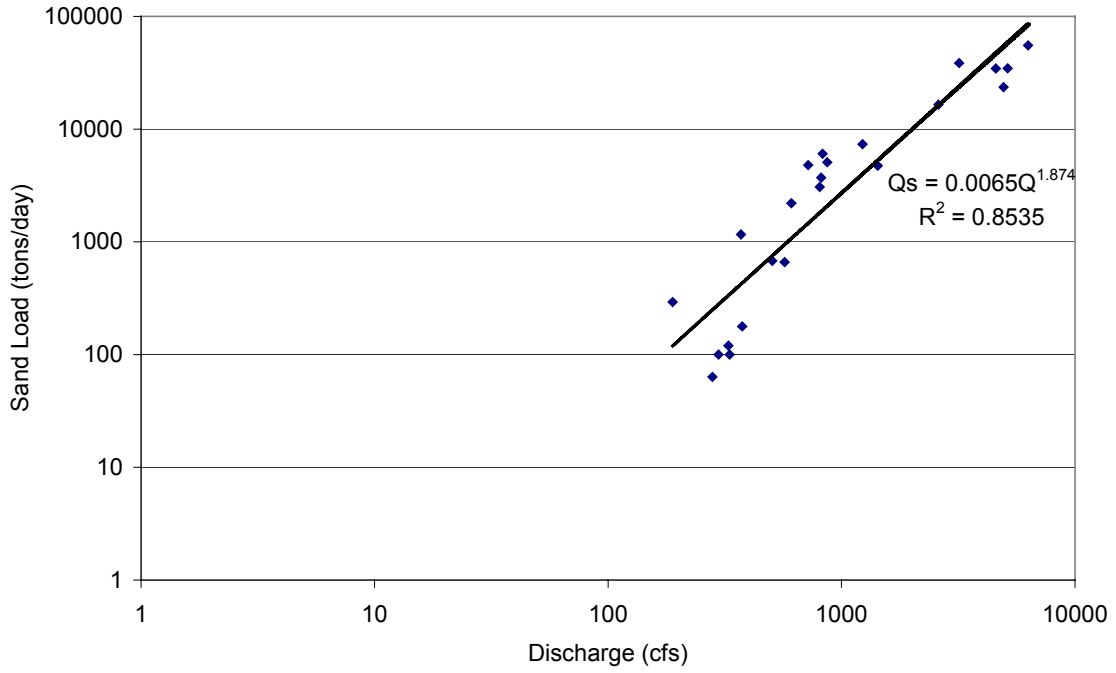


Figure J-24 Sand load rating curves for the San Marcial Gage 1968-1982

FW+CC 1982-1992



FW+CC 1992-1997

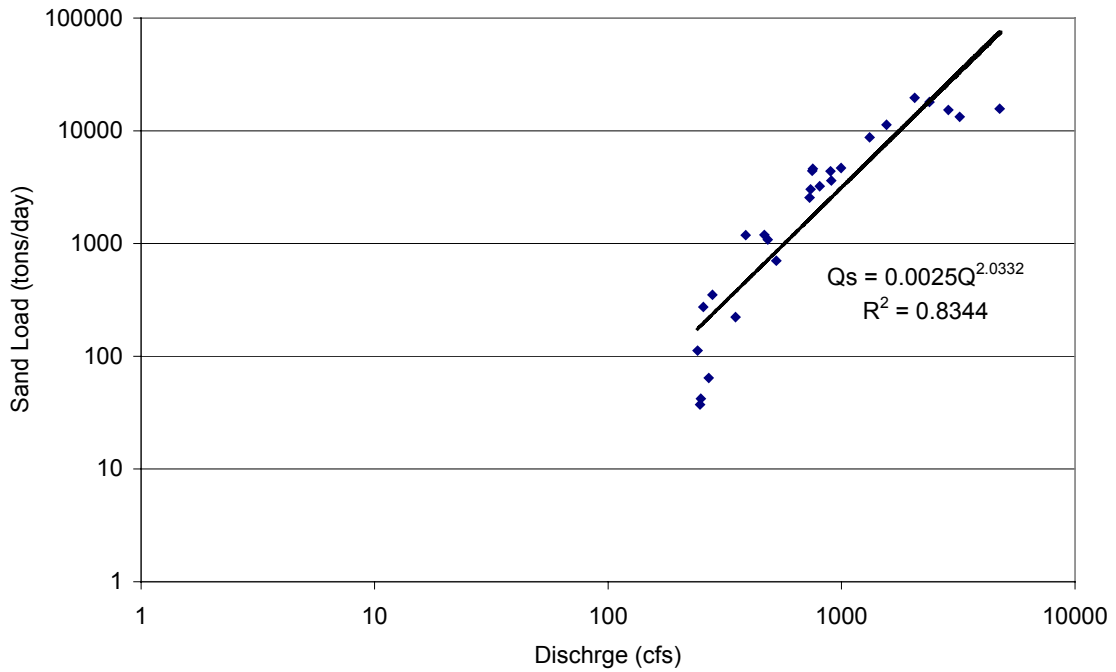


Figure J-25 Sand load rating curves for the San Marcial Gage 1982-1997

FW+CC 1997-2001

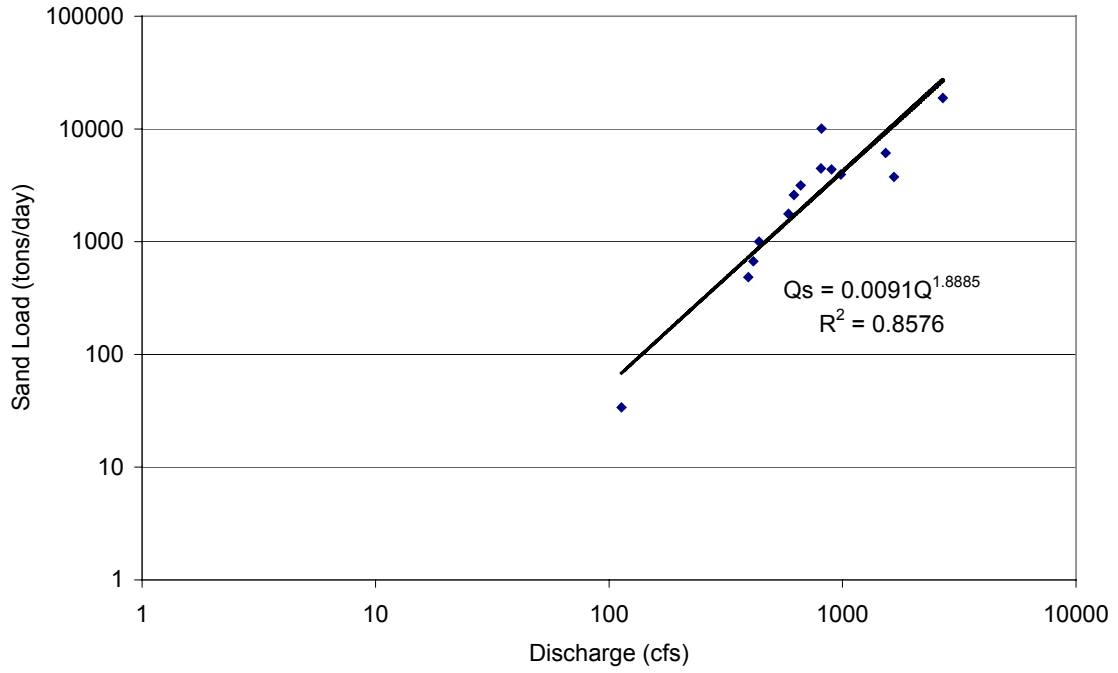


Figure J-26 Sand load rating curves for the San Marcial Gage 1997-2001